

Copyright © 1991, by the author(s).  
All rights reserved.

Permission to make digital or hard copies of all or part of this work for personal or classroom use is granted without fee provided that copies are not made or distributed for profit or commercial advantage and that copies bear this notice and the full citation on the first page. To copy otherwise, to republish, to post on servers or to redistribute to lists, requires prior specific permission.

**CONTROL OF A CLASS OF INTERCONNECTED  
NONLINEAR DYNAMICAL SYSTEMS: THE  
PLATOON PROBLEM**

by

Shahab Eddin Sheikholeslam

Memorandum No. UCB/ERL M91/115

25 November 1991

*cover sheet*

**CONTROL OF A CLASS OF INTERCONNECTED  
NONLINEAR DYNAMICAL SYSTEMS: THE  
PLATOON PROBLEM**

by

Shahab Eddin Sheikholeslam

Memorandum No. UCB/ERL M91/115

25 November 1991

**ELECTRONICS RESEARCH LABORATORY**

College of Engineering  
University of California, Berkeley  
94720

TITLE PAGE

**CONTROL OF A CLASS OF INTERCONNECTED  
NONLINEAR DYNAMICAL SYSTEMS: THE  
PLATOON PROBLEM**

by

**Shahab Eddin Sheikholeslam**

**Memorandum No. UCB/ERL M91/115**

**25 November 1991**

**ELECTRONICS RESEARCH LABORATORY**

**College of Engineering  
University of California, Berkeley  
94720**

# Control of a Class of Interconnected Nonlinear Dynamical Systems: The Platoon Problem

by

Shahab Eddin Sheikholeslam

## Abstract

This dissertation presents a system-level study of control laws for a platoon of *non-identical* vehicles on intelligent vehicle highway systems (IVHS); the platoon problem arises as follows: the productivity of a lane of a freeway is  $\rho v$ , the number of vehicles per hour, where  $\rho$  denotes the density and  $v$  denotes the speed. By law  $v$  is bounded; hence, to increase the productivity of one lane we need to increase  $\rho$ . Our objective is to investigate the possibility of using automatic control to reduce the distance between successive vehicles in a lane. Then, motivated by this application, it is shown that *decentralized* control laws can be designed for a general class of interconnected nonlinear dynamical systems.

Chapter 2 of this system study advances the art of automatic longitudinal control for a platoon of vehicles on a straight lane of highway in the sense that a) it considers *longer* platoons composed of *non-identical* vehicles; b) it uses nonlinear models and nonlinear control laws; c) the longitudinal control laws take advantage of communication possibilities not available in the recent past. This study proposes *decentralized* control laws for a platoon of closely-spaced *non-identical* vehicles traveling at high speeds along a straight lane of highway. In addition, chapter 3 of this study proposes longitudinal control laws for the platoon in the event of loss of communication between the lead vehicle and the other vehicles in the platoon. Comparison with the full communication case shows that, in case of loss of communication between the lead vehicle and the other vehicles, the performance of the longitudinal control laws degrades; but, this degradation is not catastrophic.

In chapter 4, this study considers the problem of *combined* longitudinal and lateral control of a platoon of non-identical vehicles and proposes *nonlinear* control laws for this platoon of vehicles *accelerating on a curved* lane of highway. These control laws are based

on *nonlinear* models of vehicles' *combined* longitudinal and lateral dynamics. Simulation results show that the proposed control laws perform well, for roads with suitably large radius of curvature, under nominal operation. One of the contributions of this dissertation is the origination of preliminary study of *combined* longitudinal and lateral control laws for a platoon of vehicles.

Motivated by the above application, in chapters 5 and 6 we address the problem of decentralized control of a class of interconnected nonlinear dynamical systems. It is shown that *under general qualitative conditions imposed on the interconnected nonlinear dynamical subsystems* as in the platoon control problem, appropriate dynamical behavior for the overall system can be achieved *using only decentralized control*. Furthermore, we design *decentralized adaptive* control laws for this class of interconnected nonlinear dynamical systems; in fact, we have stated sufficient conditions on the inputs and the parameter errors under which we can design suitable *decentralized* control laws for the interconnection of nonlinear dynamical systems under consideration. From a control designer's view point, the *decentralization* reduces the computation cost while increasing the reliability and the flexibility of the system; furthermore, the *adaptation* improves the *robustness* of the system.

To implement the proposed control laws, a number of experiments should be performed; in addition, a number of studies have to be done to analyze the effects of disturbances (such as wind gusts, road irregularities, etc...) and modeling errors (in engine dynamic model, tire dynamic model, etc...) on the performance of these control laws.

The contributions of this dissertation are twofold: from an application view point, this study advances the art of automatic control of a platoon of closely-spaced vehicles traveling at high speeds on an automated lane of a highway; from a theoretical view point, this study originates techniques for analysis and design of *decentralized* control laws for a general class of nonlinear dynamical systems.




---

Charles A. Desoer, Thesis Committee Chair

# Contents

<b>List of Figures</b>	<b>vi</b>
<b>1 Introduction</b>	<b>1</b>
<b>I Control of a Platoon of Vehicles on Automated Highways</b>	<b>6</b>
<b>2 Longitudinal Control of a Platoon of Vehicles</b>	<b>7</b>
2.1 Introduction . . . . .	7
2.2 Platoon Configuration . . . . .	8
2.3 Vehicle Model . . . . .	9
2.4 Exact Linearization of Vehicle Dynamics . . . . .	10
2.5 Platoon Dynamics . . . . .	11
2.5.1 Proposed control law . . . . .	11
2.5.2 Implementation Issues . . . . .	13
2.5.3 First vehicle dynamics . . . . .	13
2.5.4 Second vehicle dynamics . . . . .	14
2.5.5 $i$ -th vehicle dynamics ( $i = 3, 4, \dots$ ) . . . . .	15
2.5.6 Design considerations . . . . .	16
2.6 Simulation Results . . . . .	17
2.6.1 Nominal system . . . . .	19
2.6.2 Control laws not conditioned on vehicle loading . . . . .	20
2.6.3 Control laws not conditioned on vehicle loading, including communication delays . . . . .	20
2.6.4 Control laws not conditioned on vehicle loading, including communication delays and measurement noise . . . . .	21
2.7 Conclusion . . . . .	22
2.8 Appendix: A Reduced Order Observer-Based Identifier for Identifying the Mass of a Vehicle . . . . .	22
2.8.1 Mass Identifier . . . . .	23
2.8.2 Simulation Results . . . . .	24
2.8.3 Summary . . . . .	25

<b>3 Longitudinal Control of a Platoon of Vehicles with no Communication of Lead Vehicle Information</b>	<b>40</b>
3.1 Introduction . . . . .	40
3.2 Proposed control laws and Platoon dynamics . . . . .	41
3.3 Design of the proposed control laws . . . . .	44
3.4 Simulation Results . . . . .	48
3.5 Conclusion . . . . .	49
<b>4 Combined Longitudinal and Lateral Control of a Platoon of Vehicles</b>	<b>60</b>
4.1 Introduction . . . . .	60
4.2 Notation . . . . .	61
4.3 Kinematics . . . . .	63
4.4 Dynamics . . . . .	67
4.5 Control laws . . . . .	70
4.6 Implementation issues . . . . .	74
4.7 Simulation Results . . . . .	75
4.8 Conclusions . . . . .	78
4.9 Appendix . . . . .	78
<b>II Decentralized Control of a Class of Interconnected Nonlinear Dynamical Systems</b>	<b>91</b>
<b>5 Control of Interconnected Nonlinear Dynamical Systems:the platoon problem</b>	<b>92</b>
5.1 Introduction . . . . .	92
5.2 Problem motivation . . . . .	93
5.3 Problem formulation . . . . .	95
5.4 Main result . . . . .	97
<b>6 Indirect Adaptive Control of a Class of Interconnected Nonlinear Dynamical Systems</b>	<b>103</b>
6.1 Introduction . . . . .	103
6.2 Problem Description . . . . .	104
6.2.1 Longitudinal Dynamics of a Platoon . . . . .	104
6.2.2 Lateral Dynamics of a Vehicle . . . . .	105
6.2.3 Control Laws . . . . .	105
6.3 Problem Formulation . . . . .	107
6.3.1 Interconnection of the Nonlinear Dynamical Systems with Parameter Uncertainty . . . . .	108
6.3.2 Indirect Adaptive Control of the Interconnection . . . . .	109
6.4 Main Results . . . . .	110
6.4.1 Stability of a nonlinear dynamical system with slowly- varying inputs and small parameter errors . . . . .	111

6.4.2 Control of an interconnection of nonlinear dynamical systems with slowly-varying inputs and small parameter errors . . . . .	113
6.5 Conclusion . . . . .	116
6.6 Appendix . . . . .	116
<b>7 Conclusion</b>	<b>130</b>
<b>References</b>	<b>132</b>

# List of Figures

2.1	Platoon of 4 vehicles . . . . .	26
2.2	Simplified model of the $i$ -th vehicle in the platoon . . . . .	26
2.3	Linearized model of the $i$ -th vehicle with control input $c_i, i = 1, 2, \dots$ . . . . .	27
2.4	Platoon Configuration under the proposed control law for a platoon of 4 vehicles . . . . .	27
2.5	Block diagram for a platoon of linearized vehicle models . . . . .	28
2.6	Lead vehicle's velocity profile ( $v_l$ ) . . . . .	28
2.7	$\Delta_1, \Delta_2, \Delta_3, \Delta_5, \Delta_9, \Delta_{13}$ , and $\Delta_{15}$ vs. $t$ : nominal system . . . . .	29
2.8	$a_l, \ddot{x}_1, \ddot{x}_2, \ddot{x}_3, \ddot{x}_5, \ddot{x}_9, \ddot{x}_{13}$ , and $\ddot{x}_{15}$ vs. $t$ : nominal system . . . . .	30
2.9	$\Delta_1, \Delta_2, \Delta_3, \Delta_5, \Delta_9, \Delta_{13}$ , and $\Delta_{15}$ vs. $t$ : mass variations . . . . .	31
2.10	$a_l, \ddot{x}_1, \ddot{x}_2, \ddot{x}_3, \ddot{x}_5, \ddot{x}_9, \ddot{x}_{13}$ , and $\ddot{x}_{15}$ vs. $t$ : mass variations . . . . .	32
2.11	$\Delta_1, \Delta_2, \Delta_3, \Delta_5, \Delta_9, \Delta_{13}$ , and $\Delta_{15}$ vs. $t$ : mass variations, and with communication delay in transmitting lead vehicle's velocity ( $v_l$ ), acceleration ( $a_l$ ), and in successive vehicle deviations ( $\Delta, \dot{\Delta}$ , and $\ddot{\Delta}$ ) . . . . .	33
2.12	$a_l, \ddot{x}_1, \ddot{x}_2, \ddot{x}_3, \ddot{x}_5, \ddot{x}_9, \ddot{x}_{13}$ , and $\ddot{x}_{15}$ vs. $t$ : mass variations, and with communication delay in transmitting lead vehicle's velocity ( $v_l$ ), acceleration ( $a_l$ ), and in successive vehicle deviations ( $\Delta, \dot{\Delta}$ , and $\ddot{\Delta}$ ) . . . . .	34
2.13	$\Delta_1, \Delta_2, \Delta_3, \Delta_5, \Delta_9, \Delta_{13}$ , and $\Delta_{15}$ vs. $t$ : mass variations, and with noisy measurement of $\Delta$ and with communication delay in transmitting lead vehicle's velocity ( $v_l$ ), acceleration ( $a_l$ ), and in successive vehicle deviations ( $\Delta, \dot{\Delta}$ , and $\ddot{\Delta}$ ) . . . . .	35
2.14	$a_l, \ddot{x}_1, \ddot{x}_2, \ddot{x}_3, \ddot{x}_5, \ddot{x}_9, \ddot{x}_{13}$ , and $\ddot{x}_{15}$ vs. $t$ : mass variations, and with noisy measurement of $\Delta$ and with communication delay in transmitting lead vehicle's velocity ( $v_l$ ), acceleration ( $a_l$ ), and in successive vehicle deviations ( $\Delta, \dot{\Delta}$ , and $\ddot{\Delta}$ ) . . . . .	36
2.15	Mass identifier's performance for Daihatsu Charade CLS . . . . .	37
2.16	Mass identifier's performance for Buick Regal . . . . .	38
2.17	Mass identifier's performance for BMW 750 iL . . . . .	39
3.1	A platoon of vehicles on a straight lane of highway . . . . .	51
3.2	Linearized model of the $i$ -th vehicle with control input $c_i, i = 1, 2, \dots, N$ . . . . .	51
3.3	Block diagram for a platoon of linearized vehicle models . . . . .	52
3.4	$ \hat{h}_{\text{initial}}(j\omega) ,  \hat{h}_{\text{final}}(j\omega) $ , and $ \hat{h}_{\text{target}}(j\omega) $ vs. $\omega$ . . . . .	52

3.5	$h_{\text{initial}}(t)$ , $h_{\text{final}}(t)$ , and $h_{\text{target}}(t)$ vs. $t$ . . . . .	53
3.6	$ \hat{g}_{\text{initial}}(j\omega) $ , $ \hat{g}_{\text{final}}(j\omega) $ , and $ \hat{g}_{\text{target}}(j\omega) $ vs. $\omega$ . . . . .	54
3.7	$g_{\text{initial}}(t)$ , $g_{\text{final}}(t)$ , and $g_{\text{target}}(t)$ vs. $t$ . . . . .	55
3.8	lead vehicle's velocity time-profile: $v_l(t)$ vs. $t$ . . . . .	56
3.9	lead vehicle's acceleration time-profile: $a_l(t)$ vs. $t$ . . . . .	57
3.10	$\Delta_1, \Delta_2, \Delta_3, \Delta_5, \Delta_9, \Delta_{13}$ , and $\Delta_{15}$ vs. $t$ : nominal case . . . . .	58
3.11	$\ddot{x}_1, \ddot{x}_2, \ddot{x}_3, \ddot{x}_5, \ddot{x}_9, \ddot{x}_{13}$ , and $\ddot{x}_{15}$ vs. $t$ : nominal case . . . . .	59
4.1	relevant quantities for the lateral dynamics of the $i$ -th vehicle. . . . .	81
4.2	relevant quantities for the longitudinal dynamics of the $(i - 1)$ -th and the $i$ -th vehicles in a platoon: $i = 1, 2, \dots, N$ . . . . .	82
4.3	The body frame of the $i$ -th vehicle. . . . .	83
4.4	Bicycle model for the $i$ -th vehicle in a platoon: $i = 1, 2, \dots, N$ . . . . .	84
4.5	plot of the lane center $\mathcal{L}$ and its derivatives: $\hat{y}(\cdot), \hat{y}'(\cdot), \hat{y}''(\cdot)$ , and $\hat{y}'''(\cdot)$ vs. $x$ . . . . .	85
4.6	the lead vehicle's throttle input: $u_0$ vs. $t$ . . . . .	86
4.7	components of acceleration of the $i$ -th vehicle: $a_F$ vs. $t$ and $a_S$ vs. $t$ , for $i = 0, 1, \dots, 5$ ; the solid curves represent $a_{F0}$ and $a_{S0}$ , respectively. (SI units) . . . . .	87
4.8	yaw angle of the $i$ -th vehicle and the corresponding angle on the lane center: $\epsilon_i$ vs. $t$ and $\epsilon_{di}$ vs. $t$ , for $i = 1, 5$ ; the solid curve represents $\epsilon_1$ . . . . .	88
4.9	$\Delta_{i,\text{lat}}$ vs. $t$ , for $i = 1, 2, \dots, 5$ . . . . .	89
4.10	$\Delta_{i-1,i}$ vs. $t$ , for $i = 1, 2, \dots, 5$ . . . . .	90
6.1	The interconnection of nonlinear dynamical systems with no parameter uncertainties . . . . .	127
6.2	The interconnection of nonlinear dynamical systems with parameter uncertainties; each dynamical system is <i>locally</i> controlled by an indirect adaptive controller. For brevity, we have used $\bar{u}_1(\hat{\theta}_1) := \bar{u}_1(\zeta_1, u, \hat{\theta}_1)$ and for $k = 2, 3, \dots, N$ , $\bar{u}_k(\hat{\theta}_k) := \bar{u}_k(\zeta_k, \zeta_{k-1}, u, \hat{\theta}_k)$ . . . . .	127
6.3	Indirect adaptive control of the first dynamical system . . . . .	128
6.4	Indirect adaptive control of the $k$ -th dynamical system ( $k = 2, 3, \dots, N$ ) . . . . .	129

# Chapter 1

## Introduction

This dissertation consists of two parts: in part I, we present a system-level study for automatic control of a platoon of vehicles on intelligent vehicle highway systems (IVHS); then, motivated by the control problem for a platoon of vehicles, in part II, we present a theoretical investigation in the analysis and design of decentralized controllers for a class of interconnected nonlinear dynamical systems.

Part I is organized as follows: in Chapter 2, we present a preliminary system study of a longitudinal control law for a platoon of *non-identical* vehicles using a simplified *nonlinear* model for the vehicle dynamics. The study in this chapter advances the art of automatic longitudinal control for a platoon of vehicles in the sense that it considers *longer* platoons composed of *non-identical* vehicles; furthermore, the longitudinal control laws presented in this chapter take advantage of communication possibilities not available in the recent past. In Chapter 3, we consider the problem of longitudinal control of a platoon of vehicles on a straight lane of highway and propose control laws in the event of loss of communication between the lead vehicle and the other vehicles in the platoon. The contribution of this chapter is to show that, in case of loss of communication between the lead vehicle and the other vehicles, the performance of the longitudinal control laws degrades; but, this degradation is not catastrophic. In Chapter 4, we present for the first time *combined* longitudinal and lateral control laws for a platoon of non-identical vehicles *accelerating* on a *curved* lane of highway. These control laws are based on *nonlinear* models of vehicles' *combined* longitudinal and lateral dynamics. Simulation results show that the proposed control laws perform well, for roads with suitably large radius of curvature, under nominal operation.

Part II is organized as follows: in Chapter 5, we consider the class of interconnected nonlinear dynamical systems suggested by the above platoon control problem. Under general qualitative conditions imposed on the nonlinear dynamical subsystems in the interconnection, we can obtain appropriate dynamical behavior for the overall system *using only decentralized control*. Considering the class of interconnected nonlinear dynamical systems suggested by the problem of combined longitudinal and lateral control of a platoon of vehicles on automated highways, in Chapter 6, we propose a *decentralized indirect adaptive* control scheme for this class of interconnected nonlinear systems. Then, we state precise conditions on the inputs, on the uncertain parameters, and on the dynamics of the nonlinear plants under which it is possible to attain the design objectives by using *decentralized, nonlinear, adaptive* control laws. The methods used in the analysis of the proposed nonlinear adaptive control laws in this chapter may be applied for studying other classes of interconnected nonlinear dynamical systems.

Finally, in Chapter 7, we summarize the results of previous chapters and discuss some directions for future research in improving the robustness of the proposed nonlinear control laws.

#### **Contributions of the thesis and relations to previous work**

This dissertation makes two types of contributions: a) practical contributions in advancing the art of automatic control of a platoon of closely-spaced, *non-identical* vehicles traveling at high speeds on a straight or curved lane of a freeway; note that our control laws are based on *nonlinear* models of vehicles' *combined* longitudinal and lateral dynamics; b) motivated by the platoon control problem, we propose *decentralized* control laws for a class of interconnected nonlinear dynamical systems; we demonstrate that *under general qualitative conditions imposed on the interconnected nonlinear dynamical subsystems* under consideration, appropriate dynamical behavior of the overall system can be achieved *using only decentralized control*; furthermore, we propose *decentralized, adaptive* control laws for this class of interconnected nonlinear dynamical systems to improve the *robustness* of the system.

Much effort has been spent on various control laws for *longitudinal* control of a platoon of vehicles [5],[6],[8],[12], [11],[16],[33] and lateral control of a vehicle [1],[30]. The contributions of this dissertation in advancing the art of automatic control of a platoon of vehicles traveling on a lane of freeway are as follows:

- (1) We use simplified *nonlinear* models for the vehicle longitudinal dynamics. In contrast to all the vehicle dynamics' models used in [49],[50],[5], and [6], our model includes two nonlinearities: the aerodynamic drag; the velocity-dependent engine time constant. Chiu, Stupp, and Brown used a linear engine/vehicle dynamics including a linearized approximation to aerodynamic drag [6].
- (2) We propose longitudinal control laws for a platoon of *non-identical* vehicles. Previous studies assumed that a platoon consists of identical vehicles [49], [50],[11],[5],[6].
- (3) Our analysis of our longitudinal control laws establish that, through the appropriate choice of design parameters, deviations in the successive vehicle spacings decrease from the front to the back of the platoon as a result of lead vehicle's acceleration from its initial steady-state velocity to its final steady-state velocity; hence, our longitudinal control laws prevent such *slinky-type effect* to propagate from the front to the end of the platoon. Previous work never addressed this slinky-type effect. Furthermore, simulation results show that our longitudinal control laws perform better than the control laws proposed in [49],[50],[51],[5], [6] for *longer* platoons.
- (4) Our longitudinal control law for the  $i$ -th vehicle in the platoon differs from the control laws in the literature by using the *lead vehicle's acceleration* in the  $i$ -th vehicle's control law. This additional input is realistic because of the technological progress in inter-vehicle communications. The addition of this input to the  $i$ -th vehicle's control law provides another degree of freedom in design; this turns out to be crucial in controlling the slinky-effect. Shladover had used lead vehicle's velocity [49] and second order time- derivative of the  $i$ -th vehicle's spacing error [50] in the  $i$ -th vehicle's control laws. Caudill and Garrard used a proportional-plus-integral control on the relative velocity error and proportional-integral-derivative control on the spacing error between successive vehicles [5]; they did not use the lead vehicle's velocity and acceleration in their longitudinal control laws. Chiu, Stupp, and Brown proposed control laws, for each vehicle, which depend only on the state of that vehicle and the state of the preceding vehicle [6].
- (5) Our control laws are based on *nonlinear* models of vehicles' *combined* longitudinal and lateral dynamics. Previous studies separated the problem of longitudinal control of a platoon of vehicles from the lateral control of each vehicle within the platoon: in the

case of longitudinal control of a platoon of vehicles, these studies proposed control laws for a platoon of vehicles traveling on a *straight* lane of a highway [49],[50]; in the case of lateral control of a vehicle, these studies proposed control laws based on a *linear* model of vehicle's lateral dynamics with the assumption that the vehicle's speed remains *constant* on a *curved* lane of highway [30]. These studies neglected the nonlinear coupling between the lateral dynamics and the longitudinal dynamics. In this dissertation, we demonstrate the performance of our *nonlinear* control laws for a platoon of vehicles *accelerating* on a lane of a highway whose center line is a sinusoid.

Motivated by the platoon control problem, we propose *decentralized* control laws for a class of interconnected nonlinear dynamical systems. The contributions of this dissertation in designing *decentralized* controllers for this class of interconnected dynamical systems are as follows:

- (1) We demonstrate that *under general qualitative conditions imposed on the interconnected nonlinear dynamical subsystems* under consideration, appropriate dynamical behavior for the overall system can be achieved *using only decentralized control*.
- (2) In the control of interconnected dynamical systems there are two important features:  
a) the graph of the interconnection and b) the time-scale separation of dynamics (in the present case, these time scales are that of the given dynamical subsystems and that of the controllers). We show that, by designing *decentralized* controllers whose dynamics are much faster than the dynamics of the subsystems, the deviations of each dynamical subsystem's state ( $\zeta_k$  for  $k = 1, 2, \dots, N$ ) from its respective equilibrium state ( $\zeta_e$ ) remain bounded for a slowly-varying input ( $u$ ); furthermore, if after some time  $T$ , the vector input  $u(t)$  becomes constant, then the peak value of these deviations *monotonically decreases as  $k$  increases* (i.e., no slinky-effect).
- (3) We propose *decentralized, nonlinear, adaptive* control laws for this class of interconnected nonlinear dynamical systems; in fact, we show that under sufficiently slowly-varying inputs ( $u$ ), and sufficiently small parameter errors ( $\phi_k$  for  $k = 1, 2, \dots, N$ ) in each dynamical subsystem, if the state of each dynamical system is initially sufficiently close to its corresponding equilibrium state, then the deviations of each dynamical subsystem's state ( $\zeta_k$  for  $k = 1, 2, \dots, N$ ) from its respective equilibrium state ( $\zeta_e$ ) remain bounded; furthermore, by suitable design of *decentralized* control laws, the peak de-

viation of each dynamical subsystem's state from its equilibrium state *monotonically* decreases as  $k$  increases. Note that the control laws are *decentralized* and *adaptive*; hence, a) the *decentralization* reduces the computation cost while increasing the *reliability* and the *flexibility* of the system; b) the *adaptation* improves the *robustness* of the system.

## **Part I**

# **Control of a Platoon of Vehicles on Automated Highways**

## Chapter 2

# Longitudinal Control of a Platoon of Vehicles

This chapter presents a preliminary system study of a longitudinal control law for a platoon of *non-identical* vehicles using a simplified *non-linear* model for the vehicle dynamics. This study advances the art of automatic longitudinal control for a platoon of vehicles in the sense that it considers *longer* platoons composed of *non-identical* vehicles; furthermore, the longitudinal control laws presented in this study take advantage of communication possibilities not available in the recent past.

We assume that for  $i = 1, 2, \dots$  vehicle  $i$  knows at all times  $v_i$  and  $a_i$  (the velocity and acceleration of the lead vehicle) in addition to the distance between vehicle  $i$  and the preceding vehicle,  $i - 1$ . A control law is developed and is tested on a simulation of a platoon of 16 vehicles where the lead vehicle increases its velocity at a rate of  $3 \text{ m.sec}^{-2}$ ; it is shown that the distance between successive vehicles does not change by more than  $0.12 \text{ m}$  in spite of variations in the masses of the vehicles (from the nominal), of communication delay and of noise in measurements.

### 2.1 Introduction

Much effort has been spent on various control laws for longitudinal control of a platoon of vehicles [5],[6],[8],[12], [11],[16],[33]. A more detailed discussion of previous work is to be found in section 2.5.1. The contribution of this chapter is to establish the feasibility of designing longitudinal control laws for a platoon of *non-identical* vehicles, using a *non-linear*

model to represent the vehicle dynamics and taking advantage of high-speed communication.

This system study does not examine various effects such as details of engine dynamics, dynamics of tires, wind gusts, road irregularities, and fuel economy. A number of studies are being pursued which take into account more realistic models for engine and transmission dynamics [25]; in addition, various measurement devices including ultrasonic sensors, radar, and infrared sensors are being evaluated.

The basic concepts of this study are: using exact linearization methods [18],[28],[36] to linearize and normalize the input-output behavior of each vehicle in the platoon; taking advantage of high-speed communication [59] to improve the longitudinal control of a platoon of vehicles.

To examine the behavior of a platoon of vehicles caused by a change in the lead vehicle's velocity, we ran simulations for platoons consisting of 16 non-identical vehicles. For the nominal case, these simulations show that, by appropriate choice of control law coefficients for each vehicle in the platoon, the deviations in vehicle spacings from their respective steady-state values do not get magnified from the front to the end of the platoon. An important feature of the design is that such deviations do not exhibit oscillatory time-behavior and their time-variations are well within passengers' comfort limits [15].

## 2.2 Platoon Configuration

Figure 2.1 shows the assumed platoon configuration for a platoon of 4 vehicles. The platoon is assumed to move from left to right in a straight line. The position of the  $i$ -th vehicle's rear bumper with respect to a fixed reference point  $O$  on the roadside is denoted by  $x_i$ . The position of the lead vehicle's rear bumper with respect to the same fixed reference point  $O$  is denoted by  $x_l$ . Each vehicle is assigned a slot of length  $L$  along the road. As shown,  $\Delta_i$  is the deviation of the  $i$ -th vehicle position from its assigned position. The subscript  $i$  is used because  $\Delta_i$  is measured by the sensors located in the  $i$ -th vehicle.

Given the platoon configuration in Figure 2.1, elementary geometry shows that:  
for  $i = 2, 3, \dots$

$$\Delta_i(t) := x_{i-1}(t) - x_i(t) - L. \quad (2.1)$$

The corresponding kinematic equation for the lead vehicle and the first vehicle are as follows:

$$\Delta_1(t) := x_l(t) - x_1(t) - L. \quad (2.2)$$

We assume that  $\Delta_i$  is measured in vehicle  $i$  and, together with its first and second derivatives, is used in the  $i$ -th vehicle's control law. We assume that for each vehicle in the platoon the lead vehicle's velocity ( $v_l$ ) and acceleration ( $a_l$ ) are known.(This requires a communication link from lead vehicle to each vehicle of the platoon.)

## 2.3 Vehicle Model

In this study we assume that the road surface is horizontal, there is no wind gust, and all the vehicles travel in the same direction at all times. Figure 2.2 shows the simplified vehicle model of the  $i$ -th vehicle in the platoon; the block ( $K_{di}(\dot{x}_i)^2$ ) specifies the force due to the air resistance, where  $K_{di}$  denotes  $\rho A_i C_{di}/2$ ,  $\rho$  denotes the specific mass of air,  $A_i$  denotes the cross-sectional area of the  $i$ -th vehicle, and  $C_{di}$  denotes the  $i$ -th vehicle's drag coefficient; the constant  $d_{mi}$  denotes the mechanical drag of the  $i$ -th vehicle (the value of  $d_{mi}$  can be estimated from coast-down tests on the vehicles);  $m_i$  denotes the  $i$ -th vehicle's mass;  $u_i$  denotes the throttle input to the  $i$ -th vehicle's engine;  $F_i$  denotes the force produced by the  $i$ -th vehicle's engine. The summing node at the bottom of Figure 2.2 represents Newton's second law for the  $i$ -th vehicle, namely

$$m_i \ddot{x}_i = F_i - K_{di} \dot{x}_i^2 - d_{mi}. \quad (2.3)$$

The engine dynamics is described by a nonlinear differential equation, namely,

$$\dot{F}_i = -\frac{F_i}{\tau_i(\dot{x}_i)} + \frac{u_i}{\tau_i(\dot{x}_i)} \quad (2.4)$$

where  $\tau_i(\dot{x}_i)$  denotes the  $i$ -th vehicle's engine time-constant when the  $i$ -th vehicle is traveling with a speed equal to  $\dot{x}_i$ .

The simple model used to describe the engine dynamics (2.4) has proven to be useful for preliminary system-level studies in longitudinal control of a platoon of vehicles [5], [6],[49],[50]. As a consequence, we do not use complex engine models which take into account factors such as ambient temperature, engine temperature, altitude, condition of spark plugs, transmission dynamics, etc...

## 2.4 Exact Linearization of Vehicle Dynamics

In the following section we will use exact linearization methods [18, sec. 4.2, pages 156–159], [28],[36] to linearize the input-output behavior of each vehicle in the platoon.

**Analysis** In the following we consider exclusively the simplified model (2.3) and (2.4). From (2.3) we obtain

$$F_i = m_i \ddot{x}_i + K_{di} \dot{x}_i^2 + d_{mi}. \quad (2.5)$$

Substituting the expression for  $F_i$  from (2.5) in (2.4) gives

$$\dot{F}_i = -\frac{1}{\tau_i(\dot{x}_i)} \left[ m_i \ddot{x}_i + K_{di} \dot{x}_i^2 + d_{mi} \right] + \frac{u_i}{\tau_i(\dot{x}_i)}. \quad (2.6)$$

Differentiating both sides of (2.3) with respect to time and substituting the expression for  $\dot{F}_i$  from (2.6) we get

$$\ddot{x}_i = -2 \frac{K_{di}}{m_i} \dot{x}_i \ddot{x}_i - \frac{1}{\tau_i(\dot{x}_i)} \left[ \ddot{x}_i + \frac{K_{di}}{m_i} \dot{x}_i^2 + \frac{d_{mi}}{m_i} \right] + \frac{u_i}{m_i \tau_i(\dot{x}_i)}. \quad (2.7)$$

**Linearizing state feedback** The expression in (2.7) is of the form

$$\ddot{x}_i = b_i(\dot{x}_i, \ddot{x}_i) + a_i(\dot{x}_i) u_i \quad (2.8)$$

where

$$b_i(\dot{x}_i, \ddot{x}_i) := -2 \frac{K_{di}}{m_i} \dot{x}_i \ddot{x}_i - \frac{1}{\tau_i(\dot{x}_i)} \left( \ddot{x}_i + \frac{K_{di}}{m_i} \dot{x}_i^2 + \frac{d_{mi}}{m_i} \right) \quad (2.9)$$

and

$$a_i(\dot{x}_i) := \frac{1}{m_i \tau_i(\dot{x}_i)}. \quad (2.10)$$

To linearize the  $i$ -th vehicle's nonlinear dynamics, we create an exogeneous input  $c_i$  which is related to the  $i$ -th vehicle throttle input,  $u_i$ , by the following equation

$$u_i = \frac{1}{a_i(\dot{x}_i)} [c_i - b_i(\dot{x}_i, \ddot{x}_i)]. \quad (2.11)$$

This equation describes a nonlinear state feedback applied to the  $i$ -th vehicle's dynamics (2.8).

Substituting (2.11) into (2.8) gives a system of *linear* differential equations representing the dynamics of the  $i$ -th vehicle after linearization by state feedback, namely, for  $i = 1, 2, \dots$

$$\frac{d}{dt}x_i = \dot{x}_i \quad (2.12)$$

$$\frac{d}{dt}\dot{x}_i = \ddot{x}_i \quad (2.13)$$

$$\frac{d}{dt}\ddot{x}_i = c_i. \quad (2.14)$$

Note that the new input  $c_i$  appears in equation (2.11).

**Remark** The nonlinear state feedback law (2.11) has achieved two objectives:

1. It linearized the  $i$ -th vehicle dynamics;
2. It achieves closed-loop dynamics that are independent of  $m_i$ ,  $d_{mi}$ ,  $K_{di}$ , and  $\tau_i(\dot{x}_i)$ ; i.e., the resulting dynamics of the vehicles are independent of their particular characteristics.

**Implementation Issues** To compute the linearizing state feedback (2.11), we need to be able to compute the values of the functions  $b_i(.,.)$  and  $a_i(.)$ . From (2.9) and (2.10), this requires sensors to measure the velocity of the  $i$ -th vehicle ( $\dot{x}_i$ ) and the acceleration of the  $i$ -th vehicle ( $\ddot{x}_i$ ). At the present time, group discussions are being held [29] to determine the most suitable sensor technology for measuring  $\dot{x}_i$  and  $\ddot{x}_i$  in terms of the projected cost and measurement accuracy. In addition, we need to be able to estimate the mass of the  $i$ -th vehicle ( $m_i$ ) and the  $i$ -th vehicle's mechanical drag ( $d_{mi}$ ). An adaptive identifier for estimating the mass of a vehicle is presented in [37]. (see Appendix) Estimates of the mechanical drag can be obtained from coast-down tests done on the highway. We assume that we know the data regarding engine time constant (the function  $\tau_i(.)$ ), and the vehicle's aerodynamic characteristics ( $K_{di} := \rho A_i C_{di}/2$ ).

## 2.5 Platoon Dynamics

In the sequel we will use the linearized vehicle model given in (2.12)-(2.14) for analyzing the platoon dynamics.

### 2.5.1 Proposed control law

Figure 2.3 shows the linearized model of the  $i$ -th vehicle with control input  $c_i$ . We propose the following linear control law for longitudinal control of vehicles: for the first linearized

vehicle model the control law is

$$c_1 := c_{p1}\Delta_1(t) + c_{v1}\dot{\Delta}_1(t) + c_{a1}\ddot{\Delta}_1(t) + k_{v1}[v_l(t) - v_l(0-)] + k_{a1}a_l(t) \quad (2.15)$$

where  $v_l(0-)$  denotes the steady-state value of the lead vehicle's velocity ( $v_l$ ); for linearized vehicle models 2, 3, ... the control law is

$$c_i := c_p\Delta_i(t) + c_v\dot{\Delta}_i(t) + c_a\ddot{\Delta}_i(t) + k_v[v_l(t) - v_i(t)] + k_a[a_l(t) - a_i(t)] \quad (2.16)$$

where  $c_{p1}, c_{v1}, c_{a1}, k_{v1}, k_{a1}, c_p, c_v, c_a, k_v$ , and  $k_a$  are design constants. Note that the control law for the first vehicle differs from the control law for all the other vehicles in the two rightmost terms in (2.15). This is due to the fact that for the first vehicle  $v_l - v_1 = \dot{\Delta}_1$  and  $a_l - a_1 = \ddot{\Delta}_1$  which are already a part of the first vehicle's control law; whereas, for vehicle  $i$  ( $i = 2, 3, \dots$ )  $v_l - v_i = \dot{\Delta}_1 + \dots + \dot{\Delta}_i$  and  $a_l - a_i = \ddot{\Delta}_1 + \dots + \ddot{\Delta}_i$ .

Comparison of our control law (2.16) for the  $i$ -th vehicle with the control laws in the literature shows that using the lead vehicle's acceleration ( $a_l$ ) in the  $i$ -th vehicle's control law is the new addition to the  $i$ -th vehicle's control laws considered in the literature. This addition to the  $i$ -th vehicle's control law provides additional degrees of freedom in designing the transfer functions relevant to the longitudinal control of a platoon of vehicles. It is intuitively clear that if each vehicle knew the lead vehicle's acceleration, platoon maintains a tighter formation than if each vehicle only measured the distance between it and the preceding vehicle. In contrast to all the vehicle dynamics' models used in the papers discussed below, our model includes two nonlinearities: the aerodynamic drag; the velocity dependent engine time constant. Shladover had used lead vehicle's velocity ( $v_l$ ) [49] and  $\ddot{\Delta}_i$  [50] in the  $i$ -th vehicle's control law. Caudill and Garrard used a proportional-plus-integral control on the relative velocity error and proportional-integral- derivative control on the spacing error between successive vehicles [5]; they did not use the lead vehicle's velocity ( $v_l$ ) and acceleration ( $a_l$ ) in their longitudinal control laws. Chiu, Stupp, and Brown used a linear engine/vehicle dynamics including a linearized approximation to aerodynamic drag [6]; in their approach to longitudinal control of a platoon of vehicles operating under nominal conditions they essentially proposed control laws, for each vehicle, which depend only on the state of that vehicle and the state of the preceding vehicle.

### 2.5.2 Implementation Issues

Figure 2.4 shows the platoon configuration under the proposed control law for a platoon of 4 vehicles: the lead vehicle's velocity ( $v_l$ ) and acceleration ( $a_l$ ) are transmitted to all the vehicles within the platoon. In addition, sensors on each vehicle, say  $i$ , measure the deviation of the  $i$ -th vehicle from its assigned position, namely  $\Delta_i$ . Computation of the first and the second order time derivatives of the  $i$ -th vehicle's deviation from its assigned position, namely  $\dot{\Delta}_i$  and  $\ddot{\Delta}_i$ , can be done in two different ways:

1. Communication of the  $(i-1)$ -st vehicle's velocity ( $\dot{x}_{i-1}$ ) and acceleration ( $\ddot{x}_{i-1}$ ) to the  $i$ -th vehicle. Obtaining the  $i$ -th vehicle's velocity ( $\dot{x}_i$ ) and acceleration ( $\ddot{x}_i$ ) from the sensors on the  $i$ -th vehicle, then the computer in this vehicle estimates  $\dot{\Delta}_i$  ( $:= \dot{x}_{i-1} - \dot{x}_i$ ) and  $\ddot{\Delta}_i$  ( $:= \ddot{x}_{i-1} - \ddot{x}_i$ ) for use in the  $i$ -th vehicle's control law.
2. Direct estimation of  $\dot{\Delta}_i$  and  $\ddot{\Delta}_i$  using the measured values for  $\Delta_i$ .

The communication of the position, velocity, and acceleration information is unidirectional: from the lead vehicle to each vehicle in the platoon. Communication speed and processing of the measured data should be fast compared to the time constants of the vehicle dynamics. Preliminary studies in [59] suggest that such a requirement is feasible with the present communication and data processing technology. Experiments are being conducted to develop an infrared link operating at a rate of 80000 bits/sec which would allow communicating roughly one packet of 100 bits per millisecond. It should be kept in mind that safety considerations will require a communication system within the platoon [14].

### 2.5.3 First vehicle dynamics

**Initial Conditions** Throughout the study of the platoon dynamics we assume the following: for all  $t < 0$ , the platoon is in steady-state; for  $t < 0$ ,  $\dot{x}_i(t) = \dot{x}_l(t) = v_0$ ,  $\Delta_i(t) = \dot{\Delta}_i(t) = \ddot{\Delta}_i(t) = 0$ . Let  $w_l$  denote the increment of velocity of the lead vehicle from its steady-state value ( $v_0$ ). Thus  $w_l(t) := v_l(t) - v_0$ .

The linear control law (2.15) applied to the linearized model results in the differential equation (2.18) relating  $\Delta_1$  to  $w_l$ : differentiating both sides of (2.2) three times with respect to the time variable and using the expression for  $\ddot{x}_1$  from (2.14) we obtain

$$\ddot{\Delta}_1(t) = \ddot{x}_l(t) - c_1(t). \quad (2.17)$$

Substituting (2.15) in (2.17) we obtain

$$\ddot{\Delta}_1(t) = \ddot{x}_l(t) - [c_{p1}\Delta_1(t) + c_{v1}\dot{\Delta}_1(t) + c_{a1}\ddot{\Delta}_1(t) + k_{v1}w_l(t) + k_{a1}a_l(t)]. \quad (2.18)$$

Taking Laplace transforms we obtain

$$\begin{aligned} & \left\{ s^3 + c_{a1}s^2 + c_{v1}s + c_{p1} \right\} \hat{\Delta}_1(s) \\ &= \left\{ s^2 - k_{a1}s - k_{v1} \right\} \hat{w}_l(s) \end{aligned} \quad (2.19)$$

where we use the symbol “^” to distinguish Laplace transforms from the corresponding time-domain functions.

Thus:

$$\hat{h}_{\Delta_1 w_l}(s) = \frac{s^2 - k_{a1}s - k_{v1}}{s^3 + c_{a1}s^2 + c_{v1}s + c_{p1}}. \quad (2.20)$$

Equation (2.20) is the first basic design equation. From (2.20), we note that the addition of the lead vehicle's acceleration ( $a_l$ ) to the control law for the first vehicle (2.15) allows us to *independently* select all the zeros and all the poles of  $\hat{h}_{\Delta_1 w_l}$  by choosing the design parameters  $c_{a1}, c_{v1}, c_{p1}, k_{a1}$ , and  $k_{v1}$ . It is crucial to note that *the selection of zeros and poles are independent of one another*.

#### 2.5.4 Second vehicle dynamics

The linear control law (2.16) applied to the linearized model results in the differential equation (2.22) relating  $\Delta_2$  to  $\Delta_1$  and  $w_l$ .

From (2.14) we obtain

$$\ddot{\Delta}_2(t) = c_1(t) - c_2(t). \quad (2.21)$$

Substituting in (2.21) the control laws for the first and the second vehicles, namely (2.15) and (2.16), we obtain

$$\begin{aligned}
\ddot{\Delta}_2(t) &= (c_{p1}\Delta_1(t) + c_{v1}\dot{\Delta}_1(t) + c_{a1}\ddot{\Delta}_1(t) + k_{v1}w_l(t) + k_{a1}a_l(t)) \\
&- (c_p\Delta_2(t) + c_v\dot{\Delta}_2(t) + c_a\ddot{\Delta}_2(t)) \\
&- (k_v[v_l(t) - v_2(t)] + k_a[a_l(t) - a_2(t)]).
\end{aligned} \tag{2.22}$$

Taking Laplace transforms we obtain

$$\begin{aligned}
&\left\{ s^3 + (c_a + k_a)s^2 + (c_v + k_v)s + c_p \right\} \hat{\Delta}_2(s) \\
&= \left\{ (c_{a1} - k_a)s^2 + (c_{v1} - k_v)s + c_{p1} \right\} \hat{\Delta}_1(s) \\
&\quad + \{k_{a1}s + k_{v1}\} \hat{w}_l(s)
\end{aligned} \tag{2.23}$$

Thus:

$$\hat{h}_{\Delta_2\Delta_1}(s) = \frac{(c_{a1} - k_a)s^2 + (c_{v1} - k_v)s + c_{p1}}{s^3 + (c_a + k_a)s^2 + (c_v + k_v)s + c_p}. \tag{2.24}$$

From (2.23), we note that in addition to the transfer function from  $\Delta_1$  to  $\Delta_2$  there is a transfer function from  $w_l$  to  $\Delta_2$ ; it differs from  $\hat{h}_{\Delta_2\Delta_1}$  by its numerator which is  $k_{a1}s + k_{v1}$ .

### 2.5.5 $i$ -th vehicle dynamics ( $i = 3, 4, \dots$ )

The linear control law (2.16) applied to the linearized model results in the differential equation (2.26) relating  $\Delta_i$  to  $\Delta_{i-1}$ .

From (2.14) we obtain

$$\ddot{\Delta}_i(t) = c_{i-1}(t) - c_i(t). \tag{2.25}$$

Substituting the expressions for the proposed linear control laws for the  $(i-1)$ -st and the  $i$ -th vehicles from (2.16) in (2.25) we obtain

$$\begin{aligned}
\ddot{\Delta}_i(t) &= c_p\Delta_{i-1}(t) + c_v\dot{\Delta}_{i-1}(t) + c_a\ddot{\Delta}_{i-1}(t) \\
&+ k_v[v_l(t) - v_{i-1}(t)] + k_a[a_l(t) - a_{i-1}(t)] \\
&- c_p\Delta_i(t) - c_v\dot{\Delta}_i(t) - c_a\ddot{\Delta}_i(t) \\
&- k_v[v_l(t) - v_i(t)] - k_a[a_l(t) - a_i(t)].
\end{aligned} \tag{2.26}$$

Taking Laplace transforms we obtain

$$\begin{aligned} & \left\{ s^3 + (c_a + k_a)s^2 + (c_v + k_v)s + c_p \right\} \hat{\Delta}_i(s) \\ = & \left\{ c_a s^2 + c_v s + c_p \right\} \hat{\Delta}_{i-1}(s). \end{aligned} \quad (2.27)$$

From (2.27), we obtain for  $i = 3, 4, \dots$

$$\hat{g}(s) := \hat{h}_{\Delta_i \Delta_{i-1}}(s) = \frac{c_a s^2 + c_v s + c_p}{s^3 + (c_a + k_a)s^2 + (c_v + k_v)s + c_p}. \quad (2.28)$$

Let

$$\chi(s) := s^3 + (c_a + k_a)s^2 + (c_v + k_v)s + c_p. \quad (2.29)$$

Equation (2.28) is the second basic design equation. From (2.28), we note that the addition of the lead vehicle's acceleration ( $a_l$ ) to the control law for the  $i$ -th vehicle (for  $i = 3, 4, \dots$ ) (2.16) allows us to *independently* select the poles of  $\hat{g}(s)$  (by choosing the appropriate design parameters  $(c_a + k_a)$ ,  $(c_v + k_v)$ , and  $c_p$ ) and the zeros of  $\hat{g}(s)$  (by choosing the appropriate  $c_a$  and  $c_v$ ).

Furthermore, let us set  $c_{a1} = c_a + k_a$ ,  $c_{v1} = c_v + k_v$ , and  $c_{p1} = c_p$ ; then equation (2.20) shows that  $\hat{h}_{\Delta_1 w_l}(s)$  has the same poles as  $\hat{g}(s)$ , and equation (2.24) shows that  $\hat{h}_{\Delta_2 \Delta_1}(s)$  has the same poles as  $\hat{g}(s)$ ; in other words, with these choices  $\hat{g}(s)$ ,  $\hat{h}_{\Delta_1 w_l}(s)$ , and  $\hat{h}_{\Delta_2 \Delta_1}(s)$  have  $\chi(s)$  as denominator polynomial.

## 2.5.6 Design considerations

We use the block diagram in Figure 2.5 for analyzing the platoon. Some consideration of Figure 2.5 suggests the main design objectives for the longitudinal control law: from (2.19), (2.23), and (2.27), we have for  $i = 2, 3, \dots$

$$\hat{h}_{\Delta_i w_l} = (\hat{g}(s))^{i-2} \left[ \hat{h}_{\Delta_1 w_l}(s) \hat{g}(s) + \frac{k_{v1} + k_{a1}s}{\chi(s)} \right]. \quad (2.30)$$

1. Since the perturbations in  $\Delta_i$  due to changes ( $w_l$ ) in the lead vehicle's velocity from its steady-state value should not get magnified from one vehicle to the next as one goes down the platoon, we require that  $|\hat{g}(j\omega)| < 1$  for all  $\omega > 0$  and  $\omega \mapsto |\hat{g}(j\omega)|$  to be a strictly decreasing function of  $\omega$  for  $\omega > 0$ .

2. Since the inverse Laplace transform of  $[\hat{g}(s)]^2$  is the convolution of the impulse response of  $\hat{g}(s)$  with itself (i.e.,  $(g * g)(t)$ ), to avoid oscillatory behavior down the platoon it is desirable to have  $g(t) > 0$  for all  $t$ .

The design parameters have been chosen to satisfy these two requirements.

## 2.6 Simulation Results

To examine the behavior of a platoon of non-identical vehicles under the above control laws, we ran simulations for platoons consisting of 3 different types of vehicles using the System Build software package within MATRIXx. We ran simulations for platoons of 4 and 16 vehicles. In all the simulations conducted, all the vehicles were assumed to be initially traveling at the steady-state velocity of  $v_0 = 17.9 \text{ m.sec}^{-1}$  (i.e., 40 m.p.h.). Beginning at time  $t = 0 \text{ sec}$ , the lead vehicle's velocity was increased from its steady-state value of  $17.9 \text{ m.sec}^{-1}$  until it reached its final value of  $29.9 \text{ m.sec}^{-1}$  (i.e., 67 m.p.h.).

Figure 2.6 shows the lead vehicle's velocity as a function of time: the curve  $v_l(t)$  corresponds to a maximum jerk of  $2.0 \text{ m.sec}^{-3}$  and peak acceleration of  $3.0 \text{ m.sec}^{-2}$  (i.e., roughly  $0.3g$ ).

Simulations were run on a platoon of vehicles assuming different types of physical uncertainties

- Nominal system. Having exact knowledge of all the relevant parameters for applying exact linearization method (2.9)-(2.11) for all of the vehicles within the platoon; assuming no communication delays in transmitting the lead vehicle's velocity ( $v_l$ ) and acceleration ( $a_l$ ); assuming no communication delays in using  $\Delta_i$  in the  $i$ -th vehicle's control law (2.15)-(2.16) for  $i = 1, 2, \dots$ ; assuming no noise in the measurement of  $\Delta_i$  for  $i = 1, 2, \dots$
- Control laws not conditioned on vehicle loading. Allowing variations in the  $i$ -th vehicle's mass ( $m_i$ ) due to passengers' mass and luggage. The value of the mass parameter used for applying exact linearization method (2.9)-(2.11) is the vehicle's curb mass. All the assumptions regarding communication delays and measurement noise are identical to the nominal system. Note that for vehicles with larger variations in vehicle's mass, one could use a push button device by which the driver punches in the number of vehicle occupants; but this is not assumed here.

- Control laws not conditioned on vehicle loading, including communication delays. Allowing variations in the  $i$ -th vehicle's mass ( $m_i$ ) due to passengers' mass and luggage. The value of the mass parameter used for applying exact linearization method (2.9)-(2.11) is the vehicle's curb mass. We assume a constant communication delay in transmitting the lead vehicle's velocity ( $v_l$ ) and acceleration ( $a_l$ ) between any two successive vehicles following the lead vehicle; a constant communication delay in using  $\Delta_i$ ,  $\dot{\Delta}_i$ , and  $\ddot{\Delta}_i$  in the  $i$ -th vehicle's control law (2.15)-(2.16) for  $i = 1, 2, \dots$ ; and no noise in the measurement of  $\Delta_i$  for  $i = 1, 2, \dots$
- Control laws not conditioned on vehicle loading, including communication delays and noisy measurement. Allowing variations in the  $i$ -th vehicle's mass ( $m_i$ ) due to passengers' mass and luggage. The value of the mass parameter used for applying exact linearization method (2.9)-(2.11) is the vehicle's curb mass. We assume a constant communication delay in transmitting the lead vehicle's velocity ( $v_l$ ) and acceleration ( $a_l$ ) between any two successive vehicles following the lead vehicle; a constant communication delay in using  $\Delta_i$ ,  $\dot{\Delta}_i$ , and  $\ddot{\Delta}_i$  in the  $i$ -th vehicle's control law (2.15)-(2.16) for  $i = 1, 2, \dots$ ; and additive Gaussian noise in the measurement of  $\Delta_i$  for  $i = 1, 2, \dots$

The following types of vehicles with their relevant parameters were used in the simulations

- Daihatsu Charade CLS- curb mass= 916 kg (i.e., 2015 lbs.); cross-sectional area ( $A$ )= 1.9  $m^2$ ; drag coefficient ( $C_d$ )= 0.35 (i.e.,  $K_d = 0.44 \text{ kg.m}^{-1}$ ); engine time constant ( $\tau$ )= 0.2 sec.
- Buick Regal Custom- curb mass= 1464 kg (i.e., 3220 lbs.); cross-sectional area ( $A$ )= 2.2  $m^2$ ; drag coefficient ( $C_d$ )= 0.35 (i.e.,  $K_d = 0.49 \text{ kg.m}^{-1}$ ); engine time constant ( $\tau$ )= 0.25 sec.
- BMW 750iL- curb mass= 1925 kg (i.e., 4235 lbs.); cross-sectional area ( $A$ )= 2.25  $m^2$ ; drag coefficient ( $C_d$ )= 0.35 (i.e.,  $K_d = 0.51 \text{ kg.m}^{-1}$ ); engine time constant ( $\tau$ )= 0.2 sec.

The order in which the above vehicles followed the lead vehicle was as follows: Daihatsu Charade CLS followed by Buick Regal Custom followed by BMW 750iL followed by Daihatsu Charade CLS and so on.

The number of passengers in each vehicle and their respective masses were as follows:

- Daihatsu Charade CLS- 3 passengers each with a mass of 91 kg
- Buick Regal Custom- 2 passengers each with a mass of 64 kg
- BMW 750iL- 4 passengers with the following masses (in kg): 45, 45, 91, 59.

The following values were chosen for the relevant parameters in the simulation:

$$c_{a1} = 15, c_{v1} = 74, c_{p1} = 120, k_{a1} = -3.03, k_{v1} = -0.05$$

$$c_a = 5, c_v = 49, c_p = 120, k_a = 10, k_v = 25.$$

Using the above values for the parameters, we obtain

$$\hat{h}_{\Delta_1 w_l}(s) = \frac{(s + 3.01)(s + 0.017)}{(s + 4)(s + 5)(s + 6)}$$

$$\hat{h}_{\Delta_2 w_l}(s) = \frac{s(1.97s^3 + 18.65s^2 + 43.75s - 1.25)}{[(s + 4)(s + 5)(s + 6)]^2}$$

$$\hat{g}(s) = \frac{5(s + 4.9)^2}{(s + 4)(s + 5)(s + 6)}.$$

Note that the above design parameters were selected so as to satisfy the design considerations discussed in section 2.5.6.

### 2.6.1 Nominal system

Figure 2.7 shows the deviations of the first, second, third, fifth, ninth, thirteenth, and fifteenth vehicles from their pre-assigned positions due to the lead vehicle's velocity profile shown in Figure 2.6.

Figure 2.8 shows the lead, first, second, third, fifth, ninth, thirteenth, and fifteenth vehicle's acceleration profiles due to the lead vehicle's velocity profile shown in Figure 2.6 for the nominal system.

Simulation results show that the deviations of the vehicles from their pre-assigned positions do not exceed 0.08 m (i.e., less than 4 inches) and decrease to values which are less than 0.01 m. The acceleration profiles of the vehicles in the platoon are within the range of acceptable comfort limits and are almost identical to the lead vehicle's acceleration

$(a_l)$ . Note that the spacing deviation of the first vehicle ( $\Delta_1$ ) is so much worse than all the other such deviations. This is partly due to the filtering effect from  $\Delta_1$  to  $\Delta_2, \Delta_3, \dots$  (as seen from the block diagram in Figure 2.5).

### 2.6.2 Control laws not conditioned on vehicle loading

Differences between the actual vehicle mass and the curb mass values assumed in deriving the control gains range from 8% to 23%. Figures 2.9 and 2.10 show the simulation results in this case: the deviations of the vehicles from their pre-assigned positions do not exceed 0.11  $m$  (i.e., 4 inches) and decrease to values which are less than 0.01  $m$ . Such deviations do not exhibit any oscillatory behavior. The acceleration profiles of the vehicles in the platoon are within the range of acceptable comfort limits and are almost identical to the lead vehicle's acceleration ( $a_l$ ).

If this study were not a *preliminary system* study but aimed at a detailed control system design, we would use a) a much more elaborate model for the vehicle dynamics which would include, in particular, the dynamics of tires, transmission, engine, etc..., b) a model for the actuator dynamics including at least saturation and time constants. We would also develop a detailed *design* for the controller. In particular, we would incorporate a robustness analysis for the mass perturbations and use constrained optimization algorithms [31] to compute the maximum allowable mass perturbations.

Our objective in this *preliminary system* study is to establish that the performance of the longitudinal control laws, in the case of differences between the actual vehicle mass and the curb mass values, is acceptable. To improve the robustness of the control laws with respect to the mass parameter, we propose a mass identifier in section 2.8.

### 2.6.3 Control laws not conditioned on vehicle loading, including communication delays

To evaluate the performance of the proposed control laws allowing variations in vehicles' masses as before and including communication delays, we chose the delay in communicating the lead vehicle's velocity ( $v_l$ ) and acceleration ( $a_l$ ) to the first vehicle in the platoon to be 20 msec; we chose the delay in communicating the lead vehicle's velocity ( $v_l$ ) and acceleration ( $a_l$ ) between any two successive vehicles in the platoon to be 6 msec; we chose the communication delay in using  $\Delta, \dot{\Delta}$ , and  $\ddot{\Delta}$  to be 6 msec. Recalling that the infrared

link can transmit roughly one packet per millisecond, a delay of 20 msec corresponds to the loss of 20 consecutive packets. Similarly, a delay of 6 msec corresponds to the loss of 6 consecutive packets. Under the present state of the art in communication technology, the above number of lost consecutive packets are quite high; hence, the above communication delays are quite stiff.

Figures 2.11 and 2.12 show the simulation results for the control laws not conditioned on vehicle loading and including the above communication delays: the deviations of the vehicles from their pre-assigned positions do not exceed 0.11 m (i.e., 4 inches) and decrease to values which are less than 0.01 m, but are noticeably worse than in the case without communication delays. The acceleration profiles of the vehicles in the platoon are within the range of acceptable comfort limits and are almost identical to the lead vehicle's acceleration ( $a_l$ ).

#### 2.6.4 Control laws not conditioned on vehicle loading, including communication delays and measurement noise

To evaluate the performance of the proposed control laws allowing variations in vehicles' masses and including communication delays as before with measurement noise, we chose the value of  $\Delta_i$  used in the  $i$ -th vehicle's control law (2.15)- (2.16) to be the sum of the actual measured value of  $\Delta_i$  delayed by 6 msec and some Gaussian noise with zero mean and standard deviation ( $\sigma$ ) of 0.05 m. Noting that the distance between two successive vehicles is assumed to be 1 m in this application, such measurement noise is quite stiff: most of the noise samples are within 3 times the standard deviation which corresponds to 0.15 m (or 15% error in measuring successive vehicle spacings).

Figures 2.13 and 2.14 show the simulation results for this case: the deviations of the vehicles from their pre-assigned positions do not exceed 0.11 m (i.e., 4 inches) and decrease to values which are less than 0.01 m. The acceleration profiles of the vehicles in the platoon are within the range of acceptable comfort limits and are almost identical to the lead vehicle's acceleration ( $a_l$ ). Note that the non-smooth variations in  $\Delta$  and  $\dot{x}$  are a result of injecting uncorrelated samples of noise at intervals of 3 msec whereas the linear controller's time constant is on the order of 1/6 sec; thus, the system does not have enough time to react smoothly to such fast varying inputs.

## 2.7 Conclusion

We have shown that it is feasible to design longitudinal control laws for a platoon of closely-spaced *non-identical* vehicles traveling at high speeds along a straight lane of highway. These control laws take advantage of high-speed communication capabilities not available in the recent past.

We have shown that for the nominal case through the appropriate choice of design parameters, deviations in the successive vehicle spacings do not get magnified from the front to the back of a platoon of non-identical vehicles as a result of lead vehicle's acceleration from its initial steady-state velocity( $v_0$ ) to its final steady-state velocity; however, such deviations are noticeably worse with delays in communication. Furthermore, for the nominal case, the deviations in the successive vehicle spacings do not exhibit any oscillatory time-behavior.

Simulation results show that the exact linearization method used performs well in the presence of variations in the vehicle's mass (from 8% to 23%), including communication delays and measurement noise; the magnitude of the successive vehicle spacings is well within 0.12 m for a platoon of 16 vehicles and the acceleration profiles of the vehicles in the platoon are within the range of acceptable comfort limits.

This preliminary study is by no means complete because it does not examine various effects such as details of engine dynamics, transmission dynamics, dynamics of tires, wind gusts, road profile, etc... A number of studies are being pursued to address issues like longitudinal control of a platoon of vehicles on curved lanes, appropriate sensor technologies, and detailed models for engine dynamics and tire forces.

## 2.8 Appendix: A Reduced Order Observer-Based Identifier for Identifying the Mass of a Vehicle

In this section, we present an identifier for identifying the mass of a vehicle using a nonlinear model for the vehicle dynamics. Taking advantage of the specific model for the vehicle dynamics, a reduced order observer-based identifier is proposed and tested on simulations of three different types of vehicles with various passenger and luggage loadings. These simulation results show that the proposed identifier accurately identifies the mass 3 seconds after the vehicle has accelerated from its steady-state velocity.

The mass identifier proposed will be a useful option as part of each vehicle's control system

for control of a platoon of vehicles on automated highways.

### 2.8.1 Mass Identifier

The mass identifier is very similar to the observer-based identifier proposed in [54, sec. 2.1, page 3].

**Notation** In the sequel we will adopt the following notations:

$\vec{x}_i := (x_i, \dot{x}_i, \ddot{x}_i)^T$ , where  $v^T$  denotes the transpose of the vector  $v$ .

**Vehicle Model** In the following we consider exclusively the simplified model (2.3) and (2.4). We write the engine/vehicle dynamics of the  $i$ -th vehicle as follows: (for  $i = 1, 2, \dots$ )

$$\dot{\vec{x}}_i = f_{0i}(\vec{x}_i) + \theta_i^*[f_{1i}(\vec{x}_i) + g_i(\vec{x}_i)u_i] \quad (2.31)$$

where

$$f_{0i}(\vec{x}_i) := f_{0i}(x_i, \dot{x}_i, \ddot{x}_i) = (\dot{x}_i, \ddot{x}_i, -\frac{\ddot{x}_i}{\tau_i(\dot{x}_i)})^T, \quad (2.32)$$

$$f_{1i}(\vec{x}_i) := f_{1i}(x_i, \dot{x}_i, \ddot{x}_i) = (0, 0, -\frac{K_d \dot{x}_i^2}{\tau_i(\dot{x}_i)} - \frac{d_{mi}}{\tau_i(\dot{x}_i)} - 2K_d \dot{x}_i \ddot{x}_i)^T, \quad (2.33)$$

$$g_i(\vec{x}_i) := g_i(x_i, \dot{x}_i, \ddot{x}_i) = (0, 0, \frac{1}{\tau_i(\dot{x}_i)})^T, \quad (2.34)$$

and  $\theta_i^* := \frac{1}{m_i}$ . Note that  $\theta_i^*$  is the unknown parameter.

We assume that  $f_{0i}(\cdot)$ ,  $f_{1i}(\cdot)$ , and  $g_i(\cdot)$  are known functions and that we can measure the velocity ( $\dot{x}_i$ ) and the acceleration ( $\ddot{x}_i$ ) of the  $i$ -th vehicle.

**Regressor** From the right hand side of (2.31), we denote the regressor to be the expression in the bracket as follows:

$$w_i(\vec{x}_i, u_i) := f_{1i}(\vec{x}_i) + g_i(\vec{x}_i)u_i. \quad (2.35)$$

**Observer** Since the first two components of  $f_{1i}(\cdot)$  and  $g_i(\cdot)$  are zero, we propose a reduced order observer based on the third component of the regressor (2.35) as follows:

Denote the third component of the regressor ( $w_i$ ) by  $w_{3i}$ . From (2.33) and (2.34) we note that

$$w_{3i}(\vec{x}_i, u_i) = [-\frac{K_d \dot{x}_i^2}{\tau_i(\dot{x}_i)} - \frac{d_{mi}}{\tau_i(\dot{x}_i)} - 2K_d \dot{x}_i \ddot{x}_i] + [\frac{1}{\tau_i(\dot{x}_i)}]u_i. \quad (2.36)$$

Denoting the observer's state by  $(\hat{x}_i, \hat{\theta}_i)^T$ , we propose the following reduced order observer-based identifier

$$\frac{d}{dt}\hat{x}_i = -\sigma(\hat{x}_i - \ddot{x}_i) + f_{03i}(\vec{x}_i) + w_{3i}(\vec{x}_i, u_i)\hat{\theta}_i$$

$$\frac{d}{dt} \hat{\theta}_i = -p \frac{w_{3i}(\tilde{x}_i, u_i)}{1 + w_{3i}^2(\tilde{x}_i, u_i)} (\hat{x}_i - \tilde{x}_i) \quad (2.37)$$

where  $f_{03i}(\tilde{x}_i) := -\frac{\tilde{x}_i}{\tau_i(\tilde{x}_i)}$  (i.e., the third component of  $f_{0i}$ ),  $\sigma > 0$ , and  $p > 0$ .

The choice of the positive constants  $\sigma$  and  $p$  depends on the particular model. The stability of the observer is established by standard Lyapunov arguments [54, sec. 2.1, theorem 2.1, page 4]. The convergence of the parameter estimate ( $\hat{\theta}_i$ ) to the true value ( $\theta_i^*$ ) is established by standard sufficiently richness condition on the regressor ( $w_{3i}$ ) [35].

Note that in (2.37) we have used a normalized parameter update law. In this application, normalization of the regressor  $w_{3i}$  provides desirable parameter convergence for the identifier and does not exhibit any bursting phenomenon as seen in the update law with no normalization of the regressor  $w_{3i}$ .

### 2.8.2 Simulation Results

To examine the performance of the mass identifier, simulations were run for three different types of vehicles with various passenger and luggage loadings using the System Build software package within MATRIXx. In all the simulations conducted, vehicles were assumed to be initially traveling at the steady-state velocity of  $11 \text{ m.sec}^{-1}$  (i.e., 25 m.p.h.). Beginning at time  $t = 0 \text{ sec}$ , the vehicle's velocity was increased from its steady-state value of  $11 \text{ m.sec}^{-1}$  until it reached its final value. Each vehicle's acceleration increased linearly during the first second of the maneuver until it reached its peak value.

The following types of vehicles with their relevant parameters were used in the simulations

- Daihatsu Charade CLS- curb mass= 2015 lbs. (i.e., 916 kg); cross-sectional area ( $A$ )=  $1.9 \text{ m}^2$ ; drag coefficient ( $C_d$ )= 0.35 (i.e.,  $K_d = 0.44 \text{ kg.m}^{-1}$ ); engine time constant ( $\tau$ )= 0.2 sec.
- Buick Regal Custom- curb mass= 3220 lbs. (i.e., 1464 kg); cross-sectional area ( $A$ )=  $2.2 \text{ m}^2$ ; drag coefficient ( $C_d$ )= 0.35 (i.e.,  $K_d = 0.49 \text{ kg.m}^{-1}$ ); engine time constant ( $\tau$ )= 0.25 sec.
- BMW 750iL- curb mass= 4000 lbs. (i.e., 1820 kg); cross-sectional area ( $A$ )=  $2.25 \text{ m}^2$ ; drag coefficient ( $C_d$ )= 0.35 (i.e.,  $K_d = 0.51 \text{ kg.m}^{-1}$ ); engine time constant ( $\tau$ )= 0.2 sec.

Each vehicle's respective mass with passenger and luggage loading were as follows:

- Daihatsu Charade CLS- 1136 kg
- Buick Regal Custom- 1613 kg
- BMW 750iL- 2222 kg.

The values of the parameters  $\sigma$  and  $p$  were chosen as follows:

$$\sigma = 10$$

$$p = 16.$$

Figures 2.15, 2.16, and 2.17 show the performance of the mass identifier for the three different types of vehicles with the above passenger and luggage loadings.

These simulation results show that the mass identifier accurately identifies each vehicle's respective mass three seconds after the start of each vehicle's acceleration. In addition to the mass estimate (mass in  $kg$ ) for each vehicle, we have plotted each vehicle's respective engine input ( $u_i$  in  $N$ ), identifier error ( $e_i := \hat{x}_i - \ddot{x}_i$  in  $m.sec^{-2}$ ), and rate of change of the parameter estimate ( $\dot{\hat{\theta}}_i$  in  $kg^{-1}.sec^{-1}$ ). Note that in each case the identifier error ( $e_i$ ) and the rate of change of the parameter estimate ( $\dot{\hat{\theta}}_i$ ) converge to values close to zero within three seconds of the start of the respective vehicle's acceleration.

### 2.8.3 Summary

We have proposed a mass identifier for identifying the mass of a vehicle. The identifier consists of a normalized parameter update law. Simulation results for three different types of vehicles with various passenger and luggage loadings show that the identifier accurately estimates the mass of each respective vehicle three seconds after the start of each respective vehicle's acceleration.

The mass identifier can be used as a useful option as part of each vehicle's control system for control of a platoon of vehicles on automated highways.

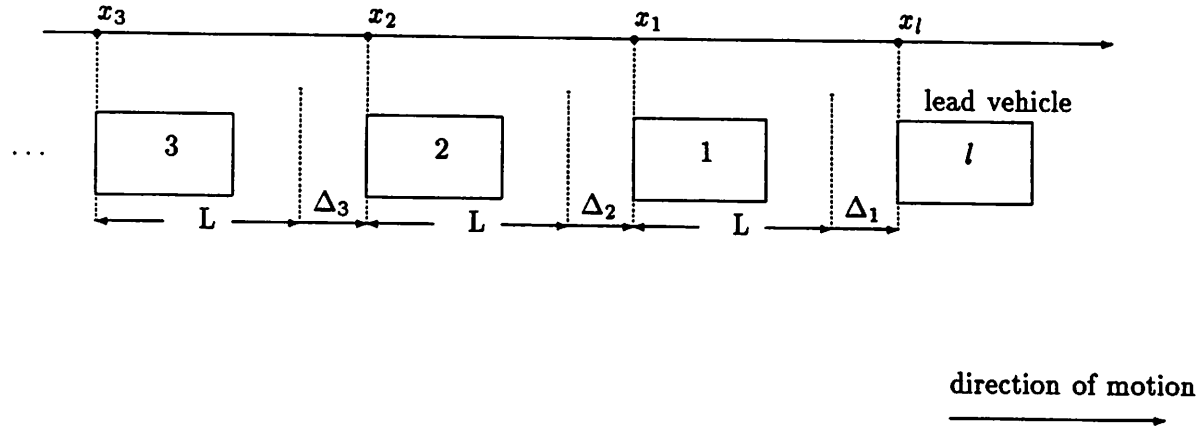
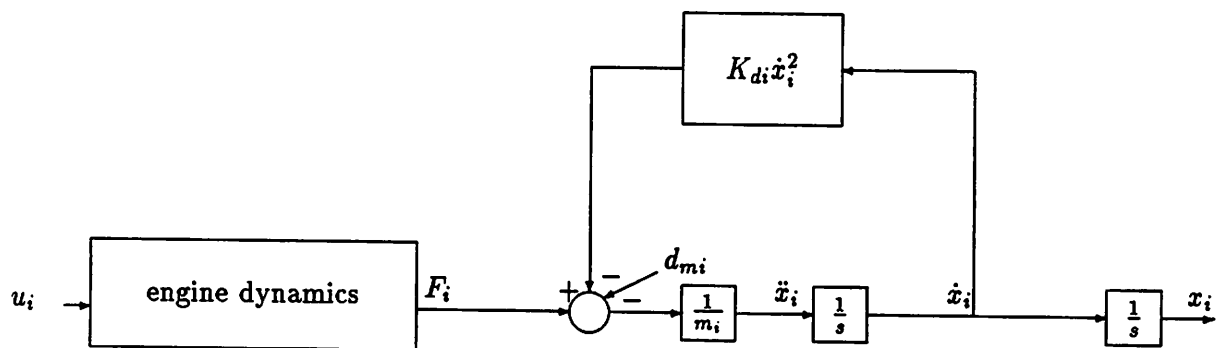


Figure 2.1: Platoon of 4 vehicles

Figure 2.2: Simplified model of the  $i$ -th vehicle in the platoon

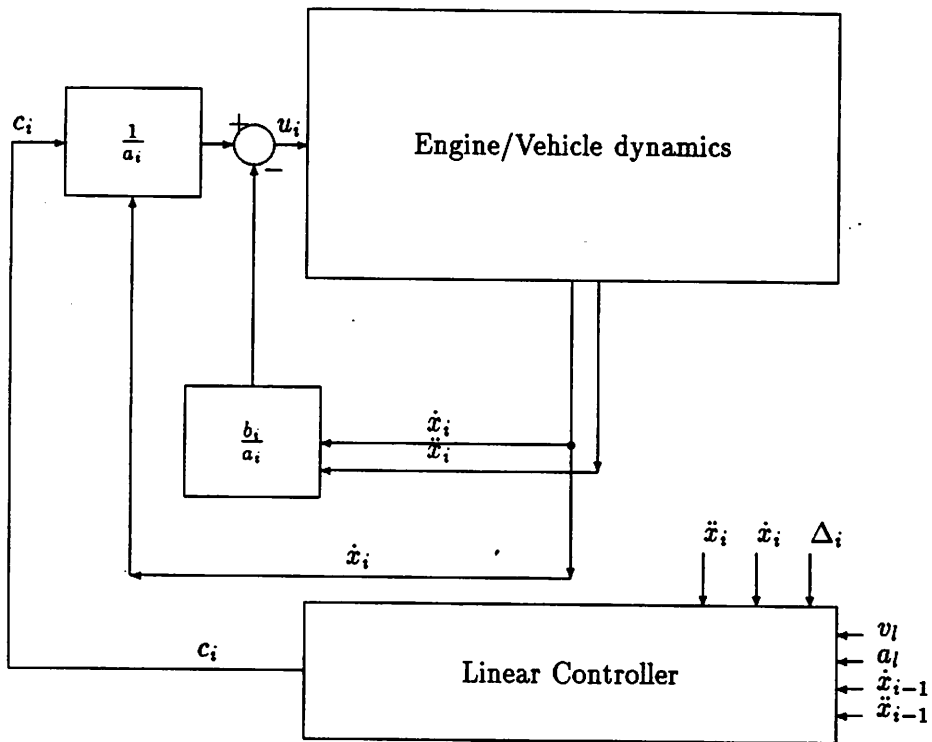


Figure 2.3: Linearized model of the  $i$ -th vehicle with control input  $c_i$ ,  $i = 1, 2, \dots$

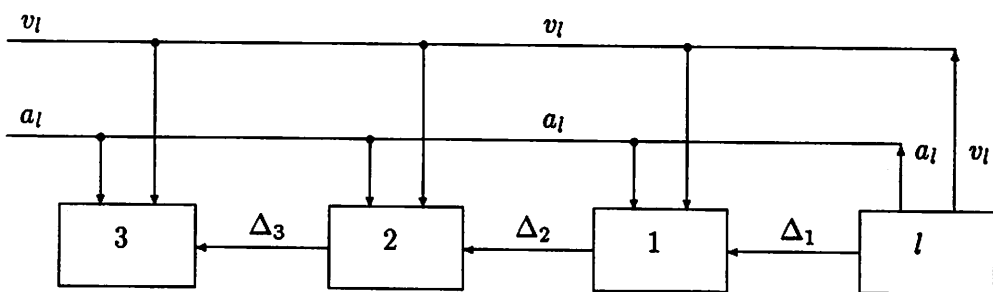


Figure 2.4: Platoon Configuration under the proposed control law for a platoon of 4 vehicles

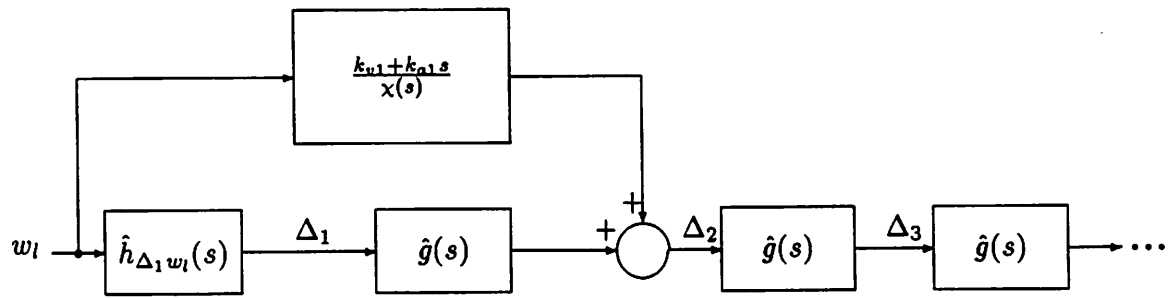


Figure 2.5: Block diagram for a platoon of linearized vehicle models

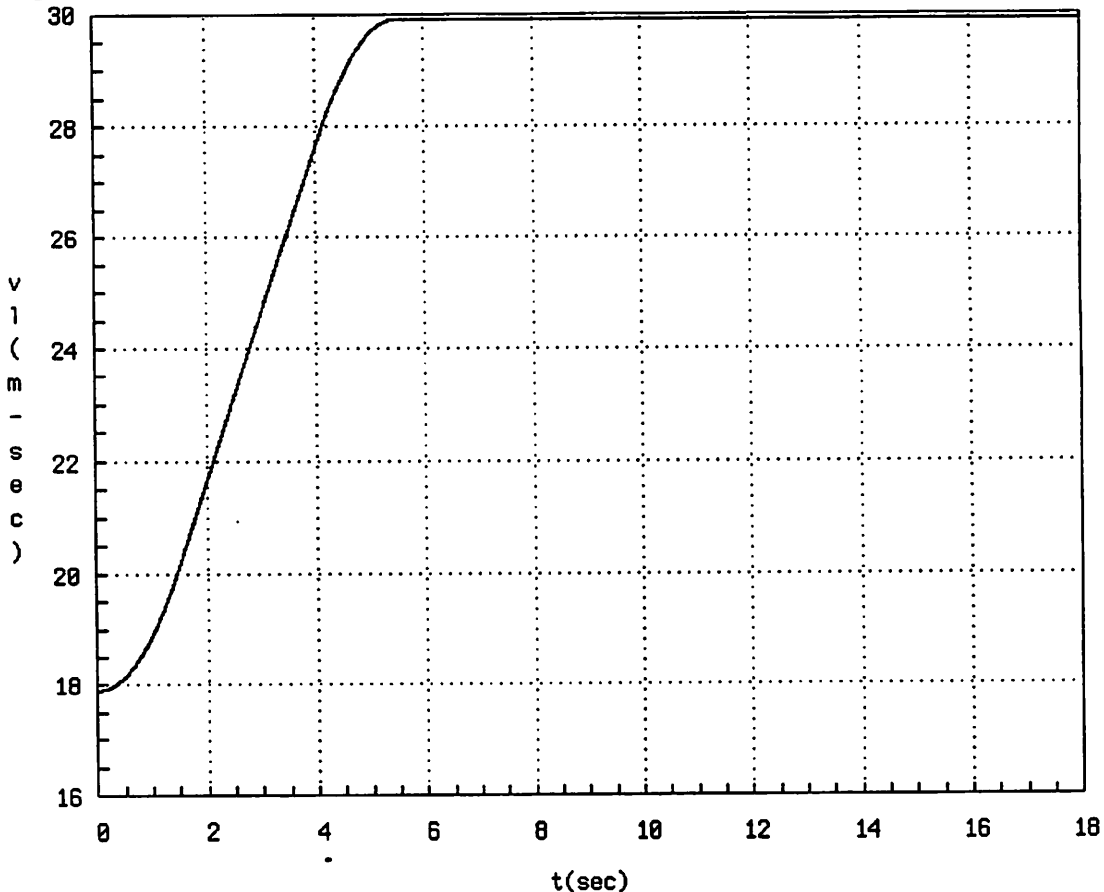


Figure 2.6: Lead vehicle's velocity profile ( $v_l$ )

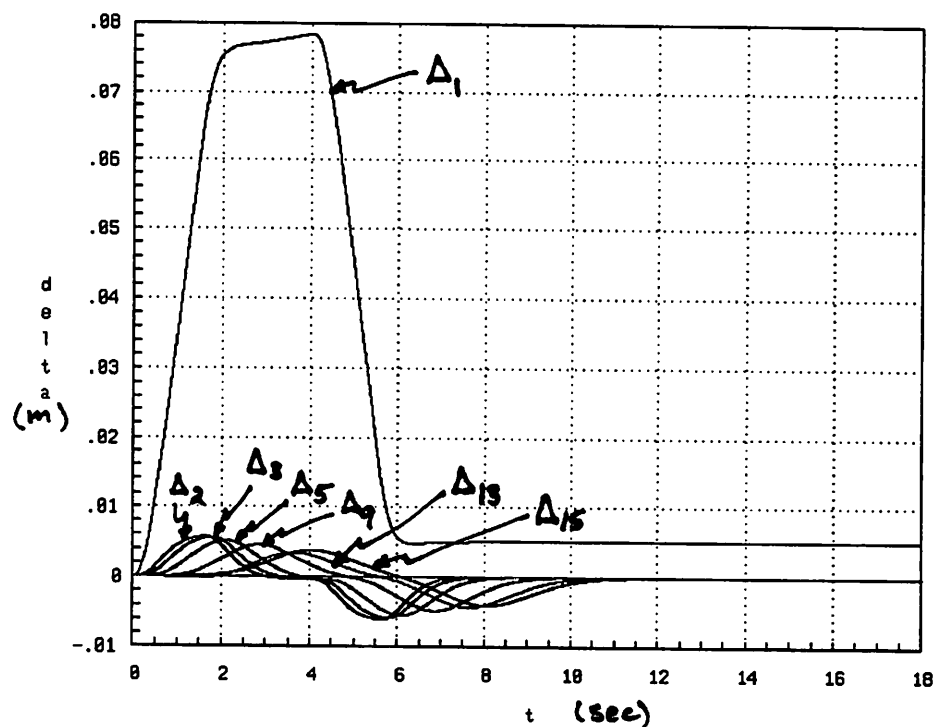


Figure 2.7:  $\Delta_1, \Delta_2, \Delta_3, \Delta_5, \Delta_9, \Delta_{13}$ , and  $\Delta_{15}$  vs.  $t$ : nominal system

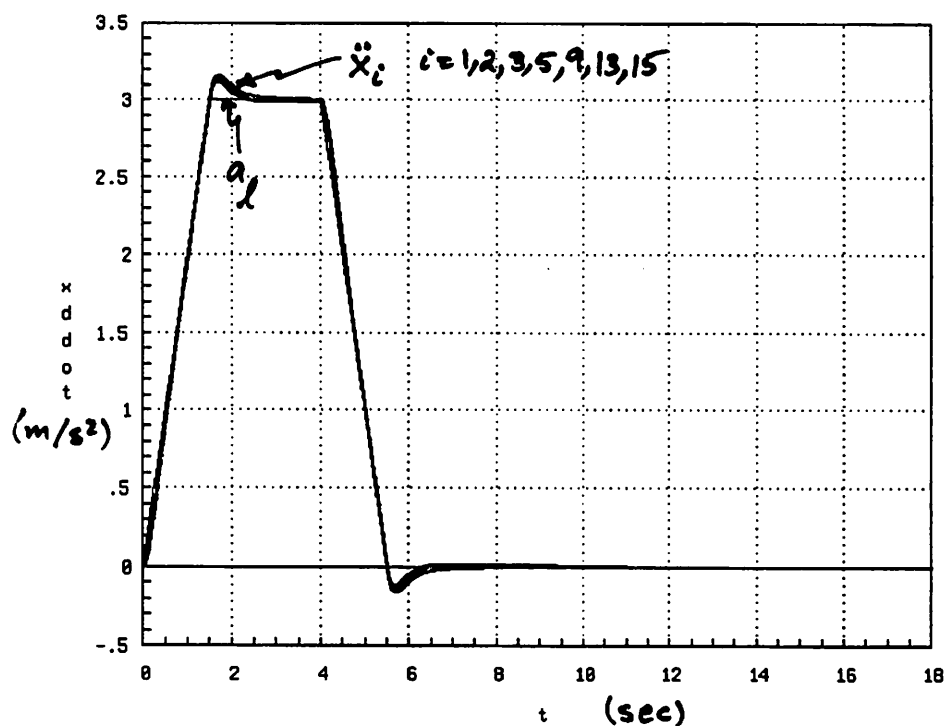


Figure 2.8:  $a_l, \ddot{x}_1, \ddot{x}_2, \ddot{x}_3, \ddot{x}_5, \ddot{x}_9, \ddot{x}_{13}$ , and  $\ddot{x}_{15}$  vs.  $t$ : nominal system

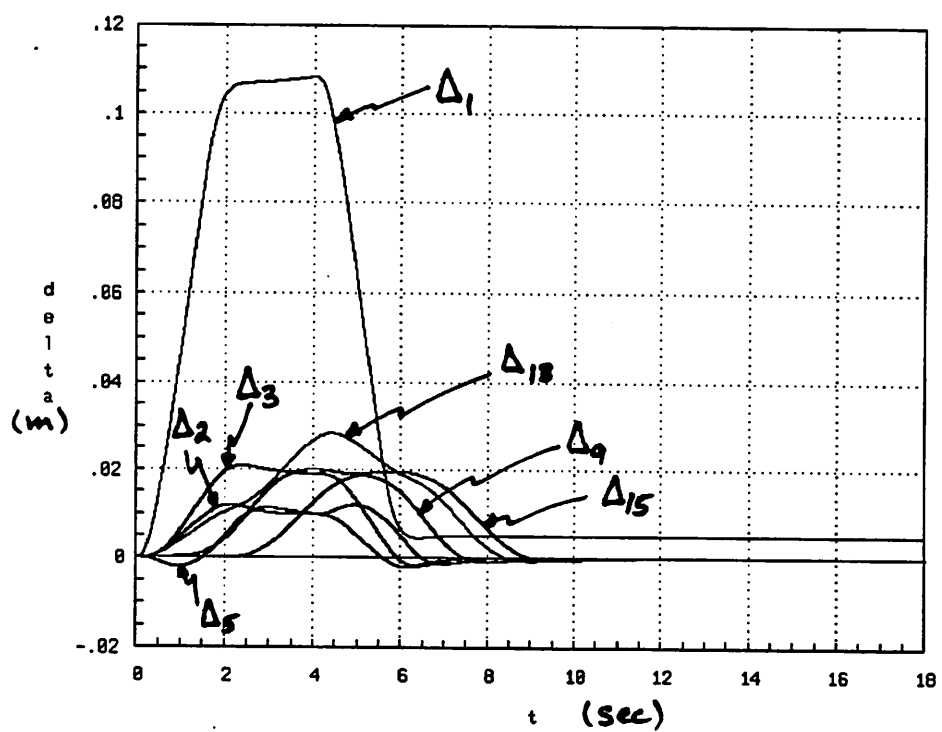


Figure 2.9:  $\Delta_1, \Delta_2, \Delta_3, \Delta_5, \Delta_9, \Delta_{13}$ , and  $\Delta_{15}$  vs.  $t$ : mass variations

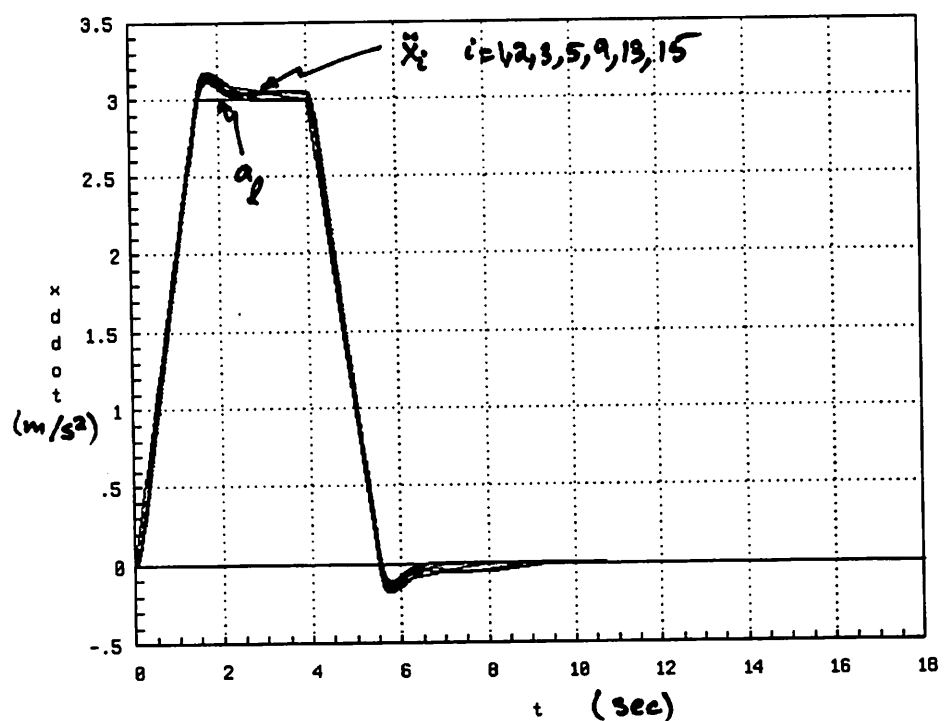


Figure 2.10:  $a_l, \ddot{x}_1, \ddot{x}_2, \ddot{x}_3, \ddot{x}_5, \ddot{x}_9, \ddot{x}_{13}$ , and  $\ddot{x}_{15}$  vs.  $t$ : mass variations

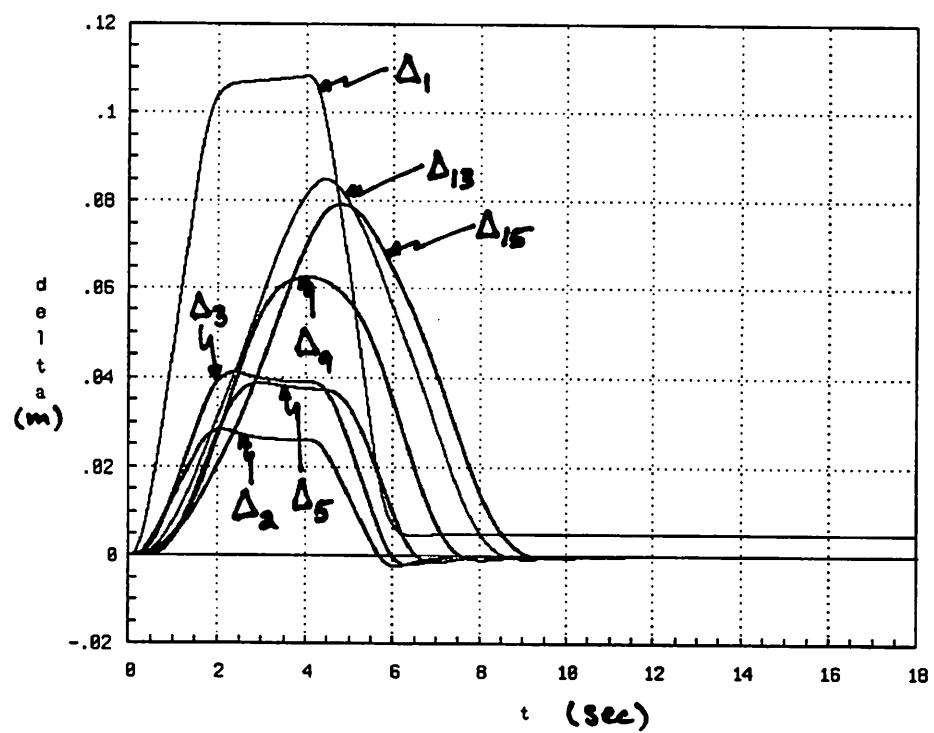


Figure 2.11:  $\Delta_1, \Delta_2, \Delta_3, \Delta_5, \Delta_9, \Delta_{13}$ , and  $\Delta_{15}$  vs.  $t$ : mass variations, and with communication delay in transmitting lead vehicle's velocity ( $v_l$ ), acceleration ( $a_l$ ), and in successive vehicle deviations ( $\Delta$ ,  $\dot{\Delta}$ , and  $\ddot{\Delta}$ )

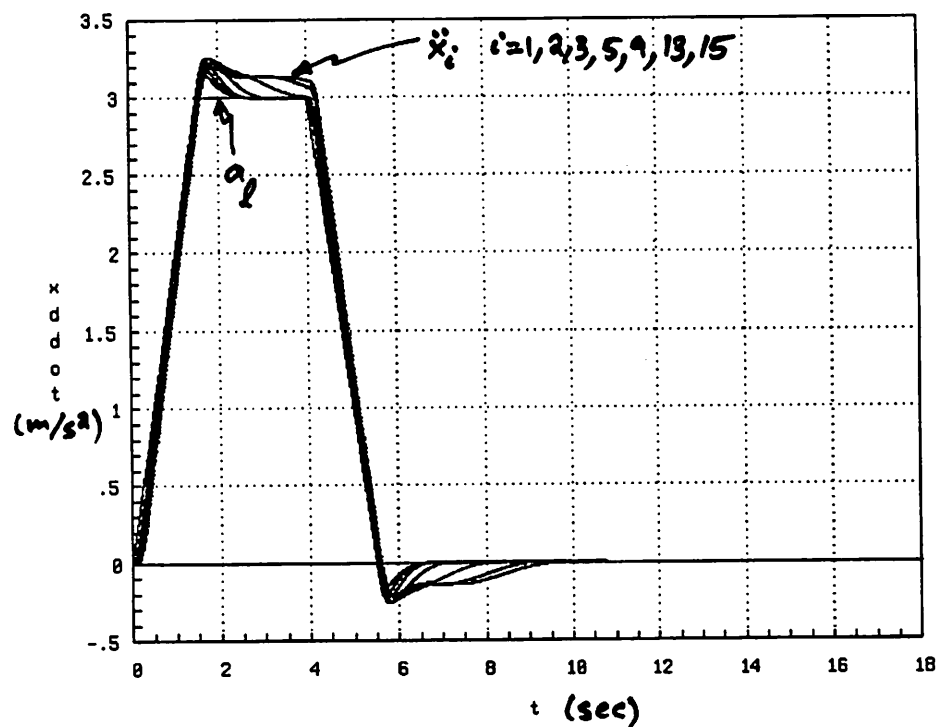


Figure 2.12:  $a_l, \ddot{x}_1, \ddot{x}_2, \ddot{x}_3, \ddot{x}_5, \ddot{x}_9, \ddot{x}_{13}$ , and  $\ddot{x}_{15}$  vs.  $t$ : mass variations, and with communication delay in transmitting lead vehicle's velocity ( $v_l$ ), acceleration ( $a_l$ ), and in successive vehicle deviations ( $\Delta$ ,  $\dot{\Delta}$ , and  $\ddot{\Delta}$ )

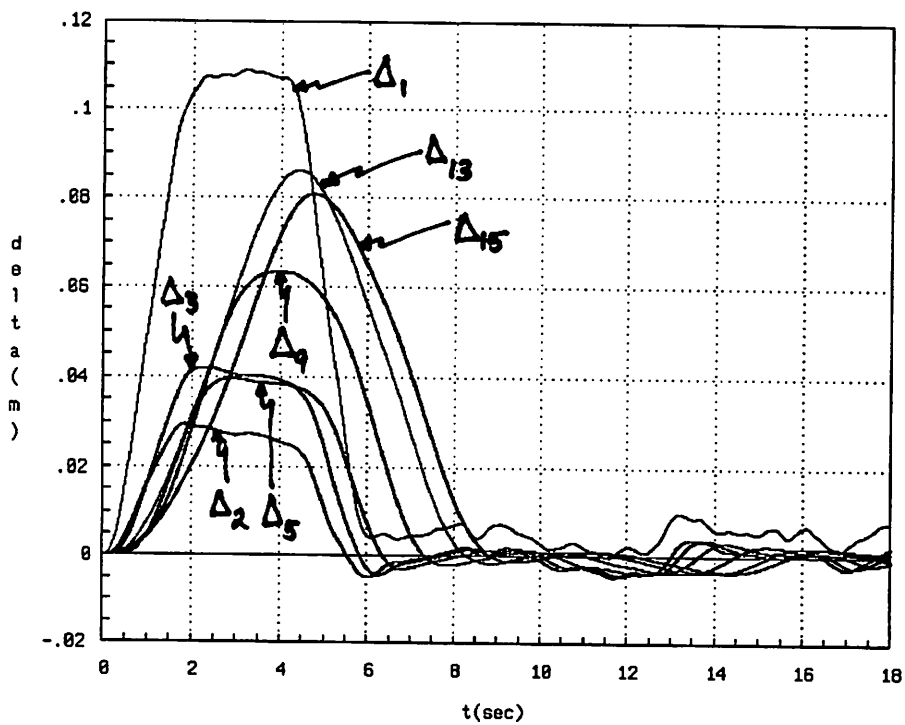


Figure 2.13:  $\Delta_1, \Delta_2, \Delta_3, \Delta_5, \Delta_9, \Delta_{13}$ , and  $\Delta_{15}$  vs.  $t$ : mass variations, and with noisy measurement of  $\Delta$  and with communication delay in transmitting lead vehicle's velocity ( $v_l$ ), acceleration ( $a_l$ ), and in successive vehicle deviations ( $\Delta$ ,  $\dot{\Delta}$ , and  $\ddot{\Delta}$ )

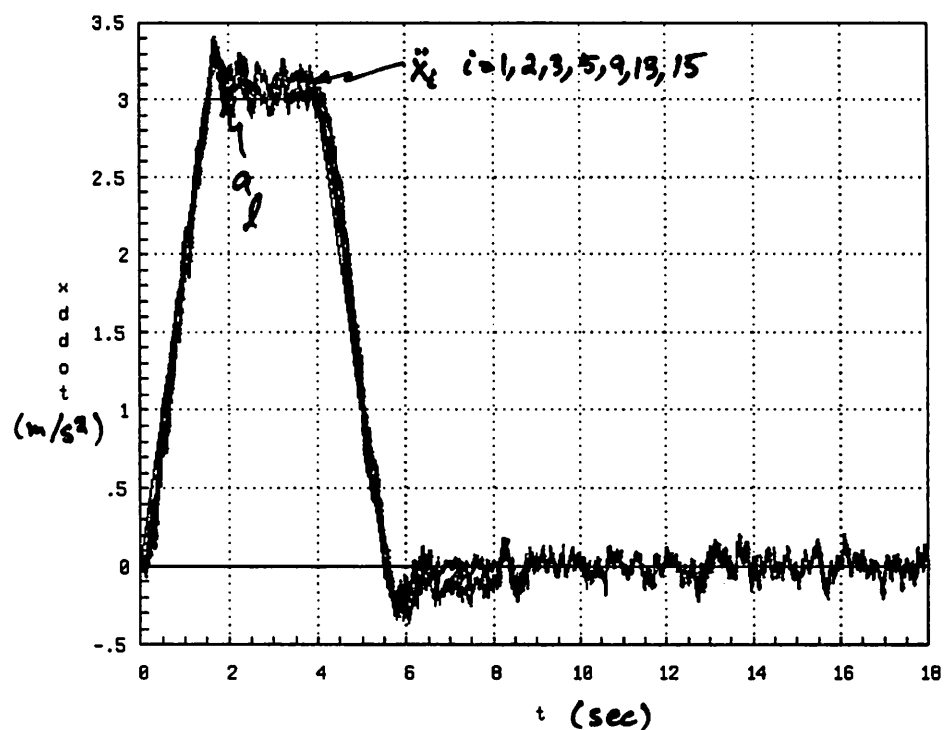


Figure 2.14:  $a_l$ ,  $\ddot{x}_1$ ,  $\ddot{x}_2$ ,  $\ddot{x}_3$ ,  $\ddot{x}_5$ ,  $\ddot{x}_9$ ,  $\ddot{x}_{13}$ , and  $\ddot{x}_{15}$  vs.  $t$ : mass variations, and with noisy measurement of  $\Delta$  and with communication delay in transmitting lead vehicle's velocity ( $v_l$ ), acceleration ( $a_l$ ), and in successive vehicle deviations ( $\Delta$ ,  $\dot{\Delta}$ , and  $\ddot{\Delta}$ )

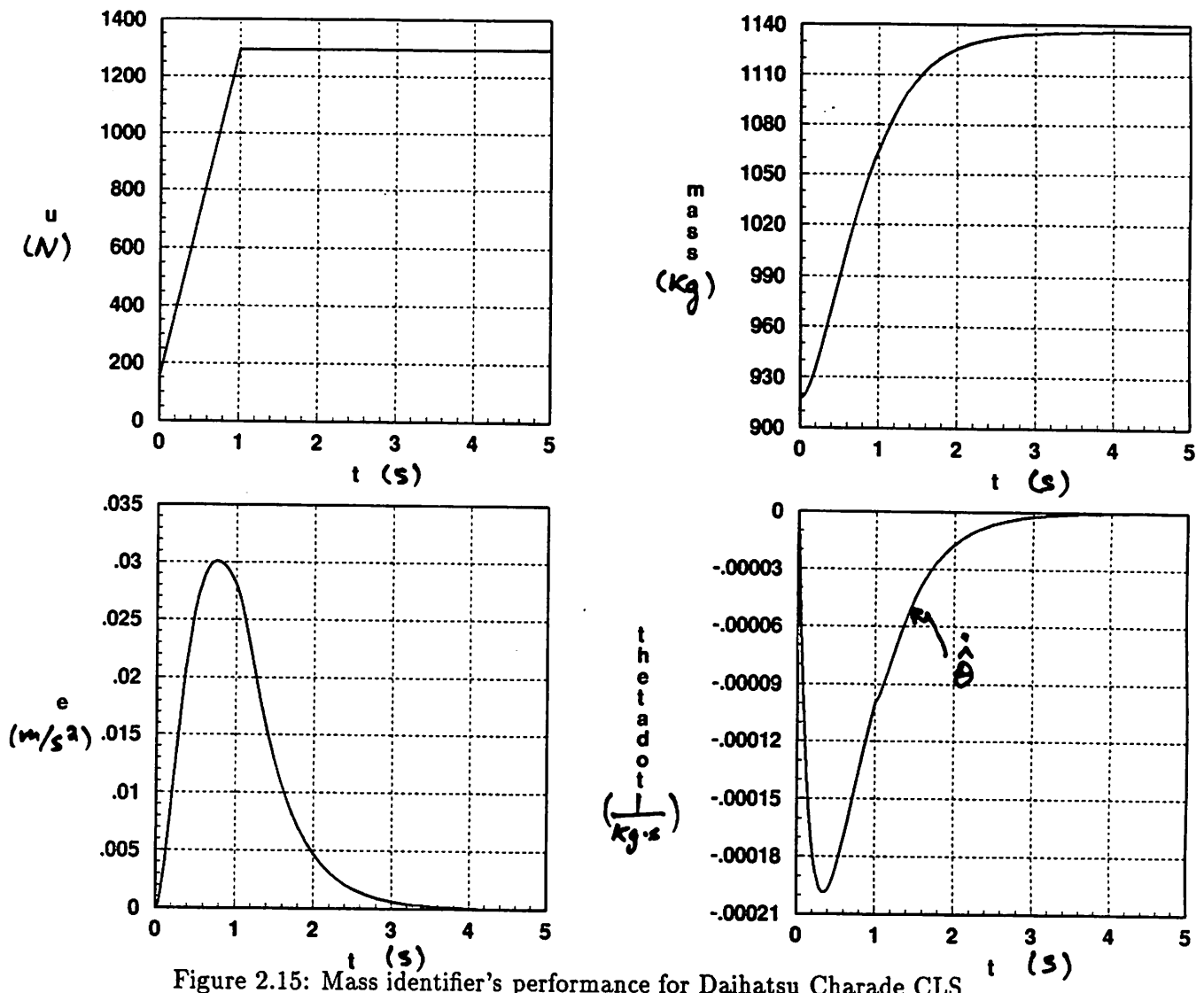
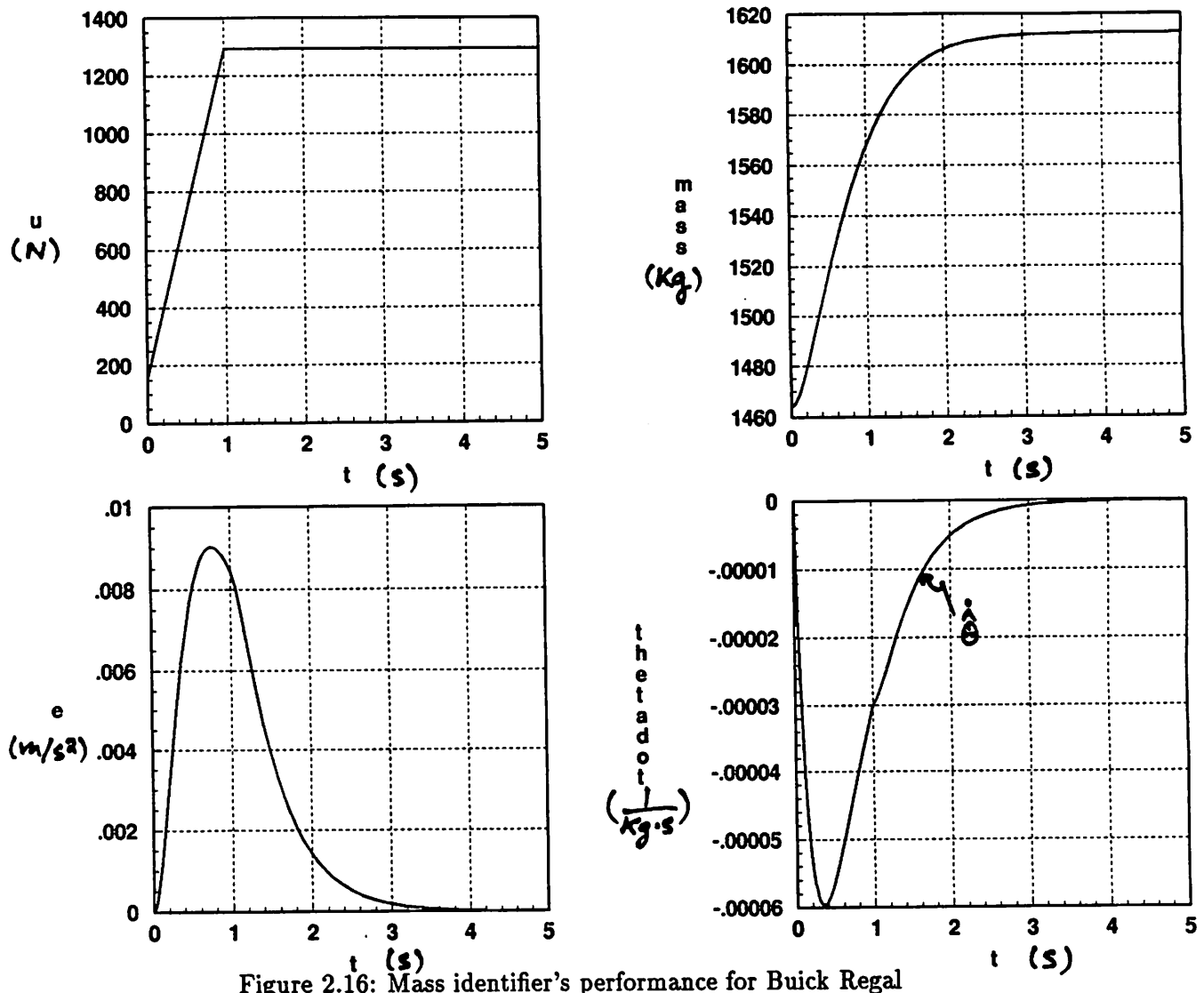


Figure 2.15: Mass identifier's performance for Daihatsu Charade CLS



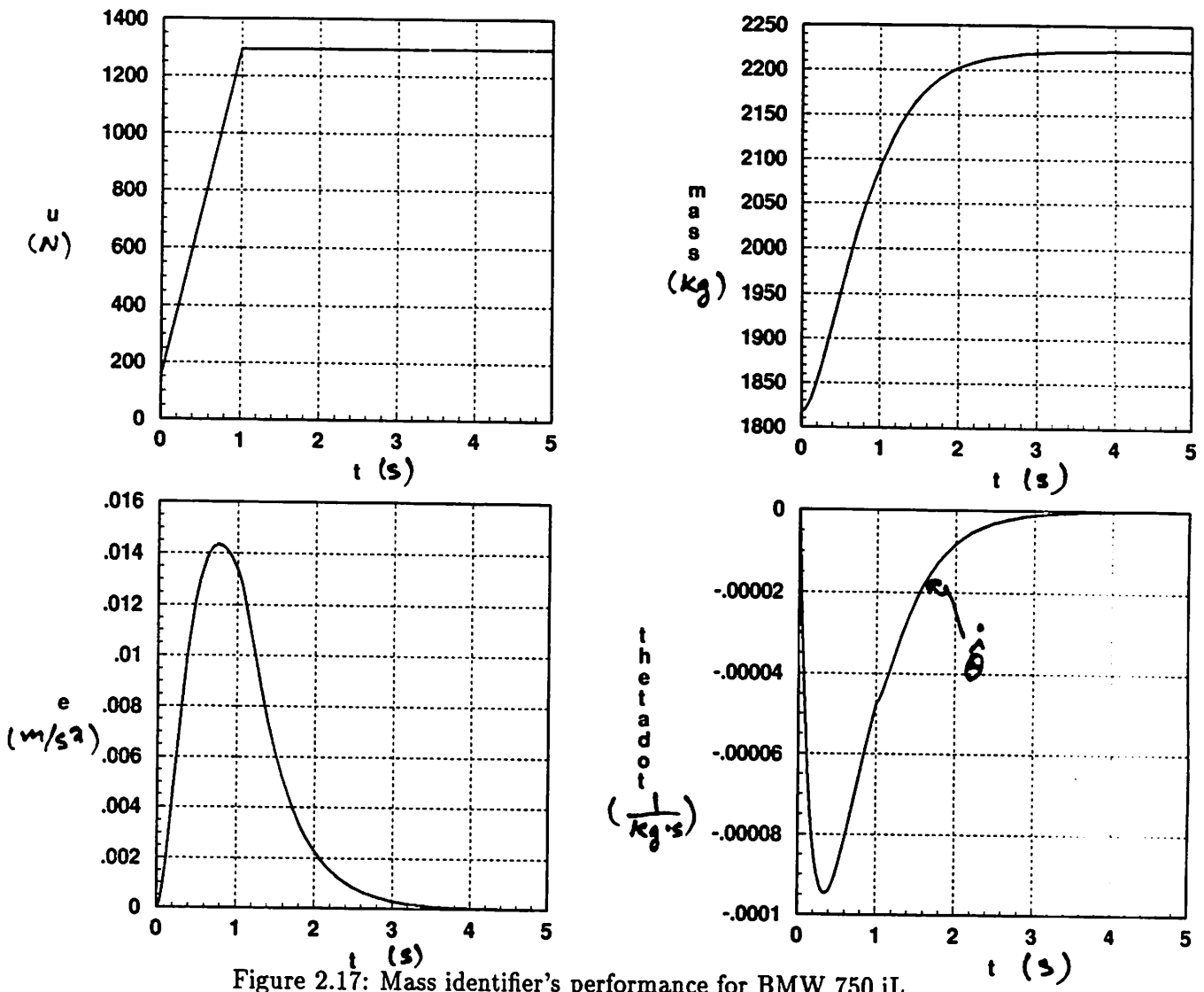


Figure 2.17: Mass identifier's performance for BMW 750 iL

## Chapter 3

# Longitudinal Control of a Platoon of Vehicles with no Communication of Lead Vehicle Information

This chapter considers the problem of longitudinal control of a platoon of automotive vehicles on a straight lane of a highway and proposes control laws in the event of loss of communication between the lead vehicle and the other vehicles in a platoon. After discussing the main design objectives for the proposed control laws, we obtain longitudinal control laws for a platoon of vehicles which do not use any communication from the lead vehicle to the other vehicles in the platoon. Comparison between these control laws and the control laws, in chapter 2, which use such a communication link to transmit lead-vehicle information to the other vehicles in a platoon shows that, in case of loss of communication between the lead vehicle and the other vehicles, the performance of the longitudinal control laws degrades; but, this degradation is not catastrophic.

### 3.1 Introduction

Traffic congestion is a global problem. One method to increase traffic flow is to decrease inter-vehicular spacings, thus forming a platoon of vehicles traveling at high speed. One

way to achieve this objective is to automatically control the dynamics of vehicles within a platoon. The concept of automatically-controlled platoon of vehicles with the corresponding sensor, actuator, and communication requirements are discussed in [51],[48, and references therein]. Much work has been done in the study of longitudinal control of a platoon of vehicles on automated guideway transit systems [5],[6],[11],[12] [16],[33],[49],[51]. The problem of longitudinal control of *longer* platoons of *non-identical* vehicles was presented in chapter 2, [47] and [41]. A platoon consists of a lead vehicle followed by vehicles  $1, 2, \dots, N$ .

In chapter 2, longitudinal control laws for each vehicle in the platoon, say the  $i$ -th vehicle, use the lead vehicle's velocity ( $v_l$ ) and acceleration ( $a_l$ ) in addition to the preceding vehicle's velocity ( $v_{i-1}$ ), acceleration ( $a_{i-1}$ ), and the distance between vehicle  $i$  and the preceding vehicle,  $i - 1$ . In these papers, the lead vehicle's velocity ( $v_l$ ) and acceleration ( $a_l$ ) are transmitted to each vehicle in the platoon via a communication link. From a system point of view, an important question is: what is the loss of performance if communication from the lead vehicle to the other vehicles is lost? The purpose of this chapter is to evaluate the performance of longitudinal control laws with *no communication of lead vehicle information*.

The organization of this chapter is as follows: in section 3.2, after giving a brief review of vehicle model and exact linearization and normalization of vehicle dynamics [47],[41], we propose a longitudinal control law which uses no lead vehicle information and present the resulting platoon dynamics; in section 3.3, we present design considerations for the proposed control laws; in section 3.4, we present the simulation results for a platoon of vehicles under these control laws and compare the performance of these laws with those which require communication of lead vehicle information [47],[41]; in section 3.5, we discuss some of the trade-offs involved in using the proposed control laws.

### 3.2 Proposed control laws and Platoon dynamics

In this section, we review the vehicle model and the exact linearization of vehicles' longitudinal dynamics [47],[41]. Then, we propose longitudinal control laws which do not require communication of the lead vehicle's velocity ( $v_l$ ) and acceleration ( $a_l$ ) to each vehicle in the platoon. Using the proposed control laws, we obtain a block diagram for analyzing the platoon dynamics.

We consider a platoon of  $N$  vehicles following a lead vehicle on a straight lane of

highway [47],[41] (see Figure 3.1): each vehicle in the platoon is assigned a slot of length  $L$ ; the abscissa of the rear bumper of the  $i$ -th vehicle with respect to a fixed point O on the road is denoted by  $x_i$ ; for  $i = 1, 2, \dots, N$ ,  $\Delta_i$  denotes the deviation of the  $i$ -th vehicle's position from its assigned position. Hence, we have

$$\Delta_1 := x_1 - x_1 - L$$

and for  $i = 2, 3, \dots, N$ ,

$$\Delta_i := x_{i-1} - x_i - L.$$

**Vehicle model**[47],[41] The longitudinal dynamics of the  $i$ -th vehicle in the platoon is modelled as follows: (for  $i = 1, 2, \dots, N$ )

$$\dot{F}_i = -\frac{F_i}{\tau_i(\dot{x}_i)} + \frac{u_i}{\tau_i(\dot{x}_i)} \quad (3.1)$$

$$m_i \ddot{x}_i = F_i - K_{di} \dot{x}_i^2 - d_{mi} \quad (3.2)$$

where  $F_i$  denotes the driving force produced by the  $i$ -th vehicle's engine;  $m_i$  denotes the mass of the  $i$ -th vehicle;  $\tau_i(\cdot)$  denotes the engine time lag for the  $i$ -th vehicle;  $u_i$  denotes the throttle command input to the  $i$ -th vehicle's engine;  $K_{di}$  denotes the aerodynamic drag coefficient for the  $i$ -th vehicle; and  $d_{mi}$  denotes the  $i$ -th vehicle's mechanical drag. Equation (3.1) represents the  $i$ -th vehicle's engine dynamics and equation (3.2) represents Newton's second law applied to the  $i$ -th vehicle modelled as a particle of mass  $m_i$ .

This simple model used to describe the engine dynamics (3.1) has proved to be useful for preliminary system-level studies in longitudinal control of a platoon of vehicles [5], [6],[49],[51].

**Exact linearization of vehicle longitudinal dynamics** [47],[41] In the sequel, we use exact linearization methods [18], [36] to *linearize* and *normalize* the input-output behavior of each vehicle in the platoon. Differentiating both sides of (3.2) with respect to time and substituting the expression for  $\dot{F}_i$  in terms of  $\dot{x}_i$  and  $\ddot{x}_i$  from equations (3.1)- (3.2) we obtain: (for  $i = 1, 2, \dots, N$ )

$$\ddot{x}_i = b_i(\dot{x}_i, \ddot{x}_i) + a_i(\dot{x}_i)u_i \quad (3.3)$$

where

$$b_i(\dot{x}_i, \ddot{x}_i) = -\frac{1}{\tau_i(\dot{x}_i)} \left[ \ddot{x}_i + \frac{K_{di}}{m_i} \dot{x}_i^2 + \frac{d_{mi}}{m_i} \right] - \frac{2K_{di}}{m_i} \dot{x}_i \ddot{x}_i \quad (3.4)$$

and

$$a_i(\dot{x}_i) = \frac{1}{m_i \tau_i(\dot{x}_i)}. \quad (3.5)$$

We propose the following control law: (for  $i = 1, 2, \dots, N$ )

$$u_i(\dot{x}_i, \ddot{x}_i) = \frac{1}{a_i(\dot{x}_i)} [-b_i(\dot{x}_i, \ddot{x}_i) + c_i] \quad (3.6)$$

where  $c_i$  is an exogenous input to the  $i$ -th vehicle dynamics.

Substituting the expression for  $u_i$  from (3.6) into (3.3) we obtain: (for  $i = 1, 2, \dots, N$ )

$$\ddot{x}_i = c_i. \quad (3.7)$$

Note that the control law (3.6) has achieved two objectives: a) it has linearized the input-output behavior of the  $i$ -th vehicle's dynamics, and b) it has resulted in dynamics, for each vehicle, which are independent of the vehicle's particular characteristics (e.g., mass of the vehicle, engine time lag, etc...).

**Control laws** We propose the following linear control laws for the linearized vehicle model (3.7): for the first linearized vehicle model the control law is

$$\begin{aligned} c_1 &:= c_p \Delta_1(t) + c_v \dot{\Delta}_1(t) + c_a \ddot{\Delta}_1(t) + k_v [v_l(t) - v_l(0-)] \\ &+ k_a a_l(t) \end{aligned} \quad (3.8)$$

where  $v_l(0-)$  denotes the steady-state value of the lead vehicle's velocity ( $v_l$ ); for the  $i$ -th linearized vehicle model ( $i = 2, 3, \dots, N$ ) the control law is

$$\begin{aligned} c_i &:= c_p \Delta_i(t) + c_v \dot{\Delta}_i(t) + c_a \ddot{\Delta}_i(t) + k_v [v_{i-1}(t) - v_{i-1}(0-)] \\ &+ k_a a_{i-1}(t) \end{aligned} \quad (3.9)$$

where  $v_{i-1}(0-)$  denotes the steady-state value of the  $(i-1)$ -th vehicle's velocity and  $c_p, c_v, c_a, k_v$ , and  $k_a$  are design constants. Figure 3.2 shows the linearized model of the  $i$ -th vehicle with the proposed control laws  $c_i$ .

Note that the control law (3.8) for the first vehicle uses the lead vehicle's velocity ( $v_l$ ) and acceleration ( $a_l$ ); these quantities are obtained in the first vehicle by measuring  $\dot{\Delta}_1, \ddot{\Delta}_1, \dot{x}_1, \ddot{x}_1$  and using the relations  $v_l = \dot{x}_1 + \dot{\Delta}_1$  and  $a_l = \ddot{x}_1 + \ddot{\Delta}_1$ .

**Platoon Dynamics** Let  $w_l(t)$  denote the deviation of the lead vehicle's velocity from its steady-state value at time  $t$  (i.e.,  $w_l(t) := v_l(t) - v_l(0-)$ ). Then, using the proposed control laws (3.8)-(3.9) for the linearized vehicle models, we obtain the block diagram in Figure 3.3 where:

$$\hat{h}_{\Delta_1 w_l}(s) := \frac{s^2 - k_a s - k_v}{s^3 + c_a s^2 + c_v s + c_p} \quad (3.10)$$

and for  $i = 2, 3, \dots, N$ ,

$$\hat{g}(s) := \hat{h}_{\Delta_i \Delta_{i-1}}(s) = \frac{(c_a + k_a)s^2 + (c_v + k_v)s + c_p}{s^3 + c_a s^2 + c_v s + c_p}. \quad (3.11)$$

In (3.10) and (3.11) we have used the symbol “ $\hat{\cdot}$ ” to distinguish Laplace transforms from the corresponding time-domain functions. Thus,  $\hat{h}_{ab}(\cdot)$  denotes the transfer function from  $b$  to  $a$ .

In the next section, we use the block diagram in Figure 3.3 to analyze the platoon dynamics.

### 3.3 Design of the proposed control laws

In this section, we discuss the main design objectives for the longitudinal control laws and propose a design suitable for this preliminary system study.

**Design Considerations** Some consideration of Figure 3.3 suggests the main design objectives for the longitudinal control laws:

1. Stability requires that  $\hat{h}_{\Delta_1 w_l}$  and  $\hat{g}$  have all their poles in the open left half-plane of the  $s$ -plane.
2.  $\hat{h}_{\Delta_1 w_l}$  should be designed so that the deviation of the first vehicle from its assigned position (i.e.,  $\Delta_1$ ) remains small as a result of a change in the velocity of the lead vehicle( $w_l$ ); in addition, it is desirable to have the deviation of the  $i$ -th vehicle (for  $i = 1, 2, \dots, N$ ) asymptotically approach zero (i.e.,  $\Delta_i(t) \rightarrow 0$  as  $t \rightarrow \infty$ ), at the end of a maneuver.
3. Since the magnitude of  $\Delta_i$  (for  $i = 1, 2, \dots, N$ ) due to changes ( $w_l$ ) in the lead vehicle's velocity from its steady-state value should not increase from one vehicle to the next as one goes down the platoon, we require that  $|\hat{g}(j\omega)| < 1$  for all  $\omega > 0$ , (to avoid a slinky-type effect).

4. Since the inverse Laplace transform of  $[\hat{g}(s)]^2$  is the convolution of the impulse response of  $\hat{g}(s)$  with itself (i.e.,  $(g * g)(t)$ ), to avoid oscillatory behavior down the platoon it is desirable to have  $g(t) > 0$  for all  $t > 0$ .

From Figure 3.3 we note that for  $i = 1, 2, \dots, N$

$$\hat{\Delta}_i(s) = \hat{h}_{\Delta_1 w_i}(s)[\hat{g}(s)]^{i-1} \hat{w}_i(s). \quad (3.12)$$

Suppose the lead vehicle reaches its final steady-state value at time  $t_f$ . We can write: for  $t > 0$ ,

$$w_i(t) = [v_i(t_f) - v_i(0-)] + \tilde{w}_i(t) \quad (3.13)$$

where  $\tilde{w}_i(t) = 0$  for all  $t > t_f$ .

Taking Laplace transforms of both sides of (3.13) we obtain

$$\hat{w}_i(s) = \frac{v_i(t_f) - v_i(0-)}{s} + \hat{\tilde{w}}_i(s). \quad (3.14)$$

Substituting (3.14) into (3.12) and using the final value theorem, we obtain (for  $i = 1, 2, \dots, N$ )

$$\lim_{t \rightarrow \infty} \Delta_i(t) = \lim_{s \rightarrow 0} s \hat{h}_{\Delta_1 w_i}(s) [\hat{g}(s)]^{i-1} \left[ \frac{v_i(t_f) - v_i(0-)}{s} + \hat{\tilde{w}}_i(s) \right]. \quad (3.15)$$

Since  $\hat{g}(0) = 1$  from (3.11) and  $\hat{\tilde{w}}_i(0) = \int_0^{t_f} \tilde{w}_i(t) dt < \infty$ , from (3.15) we obtain (for  $i = 1, 2, \dots, N$ )

$$\lim_{t \rightarrow \infty} \Delta_i(t) = \hat{h}_{\Delta_1 w_i}(0) [v_i(t_f) - v_i(0-)]. \quad (3.16)$$

We choose  $k_v = 0$  so that from (3.10) and (3.16) we obtain  $\lim_{t \rightarrow \infty} \Delta_i(t) = 0$  for  $i = 1, 2, \dots, N$ .

**Design of  $\hat{h}_{\Delta_1 w_i}$  and  $\hat{g}$**  Having chosen  $k_v = 0$ , we still need to design parameters  $k_a, c_a, c_v$ , and  $c_p$ . We choose the design vector ( $q$ ) as follows

$$q := [\alpha, \beta, p, k_a]^T \quad (3.17)$$

where

$$\begin{aligned} c_a &= -\alpha - p \\ c_v &= \alpha p + \beta \\ c_p &= -\beta p. \end{aligned} \quad (3.18)$$

From (3.10),(3.11), and (3.18) we write the design transfer functions as follows:

$$\hat{h}_{\Delta_1 w_l}(s, q) = \frac{s^2 - k_a s}{(s^2 - \alpha s + \beta)(s - p)} \quad (3.19)$$

$$\hat{g}(s, q) = \frac{(-\alpha - p + k_a)s^2 + (\alpha p + \beta)s - \beta p}{(s^2 - \alpha s + \beta)(s - p)}. \quad (3.20)$$

From (3.19)-(3.20) we note that

$$s\hat{h}_{\Delta_1 w_l}(s, q) + \hat{g}(s, q) = 1 \quad (3.21)$$

for all  $s \in C$  and for all  $q \in R^4$ ; hence, we cannot design  $\hat{h}_{\Delta_1 w_l}(s, q)$  and  $\hat{g}(s, q)$  independently. Thus, we choose target transfer functions

$$\hat{h}_{target}(s) = \frac{s^2}{(s + 4)(s + 5)(s + 6)} \quad (3.22)$$

$$\hat{g}_{target}(s) = \frac{5s^2 + 49s + 120}{(s + 4)(s + 5)(s + 6)} \quad (3.23)$$

which are based on the design considerations above and on our work in [47],[41]. Next, we formulate a design strategy based on steepest descent ideas.

We propose to obtain a  $q^*$  suitable for our problem by considering the following optimization problem:

$$\min_{q \in R_S^4} f^0(q) \quad (3.24)$$

where  $R_S^4 := \{q \in R^4 | \hat{h}_{\Delta_1 w_l}(s, q) \text{ and } \hat{g}(s, q) \text{ stable transfer functions}\}$  and

$$\begin{aligned} f^0(q) &:= \sum_{k=1}^n w_k^h \left[ |\hat{h}_{\Delta_1 w_l}(j\omega_k, q)|^2 - |\hat{h}_{target}(j\omega_k)|^2 \right] \\ &+ \sum_{k=1}^n w_k^g \left[ |\hat{g}(j\omega_k, q)|^2 - |\hat{g}_{target}(j\omega_k)|^2 \right]. \end{aligned} \quad (3.25)$$

Equation (3.25) represents a weighted quadratic cost function with  $w_k^h$  and  $w_k^g$  (for  $k = 1, 2, \dots, n$ ) denoting the appropriate weights and  $n$  chosen appropriately to include all frequencies of interest: since most of the energy of  $w_l(\cdot)$  is between 0 rad.sec<sup>-1</sup> and 3 rad.sec<sup>-1</sup>,  $w_k^h$  and  $w_k^g$  (for  $\omega_k$  between these frequencies) were chosen to be much larger than the corresponding weights ( $w_k^h$  and  $w_k^g$ ) for frequencies between 3 rad.sec<sup>-1</sup> and 6 rad.sec<sup>-1</sup>; to decrease the effect of higher frequency signals on the designed control laws,

$w_k^h$  and  $w_k^g$  (for  $\omega_k$  greater than 6 rad.sec $^{-1}$ ) were chosen large enough so that the magnitude of the frequency response of the designed transfer functions closely approximated the corresponding magnitude of the frequency response of the target transfer functions.

The constrained optimization problem (3.24)-(3.25) does not take into account all the design considerations appropriate for our problem: in the course of the descent procedure we take into account these additional engineering considerations by adjusting the weighting factors. If this study were not a *preliminary study* but aimed at a detailed control system design, we would use a) a much more elaborate model for the vehicle dynamics which would include, in particular, the dynamics of tires, transmission, engine, etc..., b) a model for the actuator dynamics including at least saturation and time constants. We would also develop a detailed *design* for the controller. In particular, we would incorporate a number of design constraints due to actuator saturation limits, regions of stability of the transfer functions in the open left-half plane, regions of constraints for the zero locations of the design transfer functions, etc... In such controller design, we would use constrained optimization algorithms and semi-infinite optimization methods discussed in [31, algorithm 6.3 with Armijo step size rule (6.31a)-(6.31b), pp.81-2].

Our objective in this *preliminary study* is to establish that, in case of loss of communication between the lead vehicle and the other vehicles, the performance of the longitudinal control laws degrades; but, this degradation is acceptable. To accomplish this objective, we a) use simple nonlinear vehicle/engine dynamics, b) formulate some of the system-level design considerations into a cost function, and c) obtain a suitable design by using a descent-type algorithm. (see e.g., [31, and references therein])

Using the above approach, we obtain the following final design transfer functions:

$$\hat{h}_{final}(s) = \frac{s^2 + 5.15s}{(s + 1.71)(s + 4.93)(s + 10.92)} \quad (3.26)$$

$$\hat{g}_{final}(s) = \frac{12.42s^2 + 80.96s + 91.99}{(s + 1.71)(s + 4.93)(s + 10.92)}; \quad (3.27)$$

the corresponding values of the design variables are

$$[c_p, c_v, c_a, k_v, k_a] = [91.99, 80.96, 17.56, 0, -5.15]. \quad (3.28)$$

Denote  $\hat{h}_{initial}(s) := \hat{h}_{\Delta_1 w_i}(s, q_0)$  and  $\hat{g}_{initial}(s) := \hat{g}(s, q_0)$  where  $q_0$  is the initial design vector  $q_0 = [-9, 20, -6, -3]^T$ . Figures 3.4 and 3.6 show the magnitudes of frequency response of  $\omega \mapsto \hat{h}_{initial}(j\omega)$ ,  $\omega \mapsto \hat{h}_{final}(j\omega)$ ,  $\omega \mapsto \hat{h}_{target}(j\omega)$ ,  $\omega \mapsto \hat{g}_{initial}(j\omega)$ ,

$\omega \mapsto \hat{g}_{final}(j\omega)$ , and  $\omega \mapsto \hat{g}_{target}(j\omega)$ . The corresponding impulse responses are shown in Figures 3.5 and 3.7.

### 3.4 Simulation Results

To examine the performance of (3.8)-(3.9) with the design constants (3.28), we ran simulations for platoons consisting of 3 different types of vehicles. Within each platoon, 15 vehicles ( $N = 15$ ) followed a lead vehicle. In all the simulations conducted, all the vehicles are assumed to be initially traveling at the steady-state velocity of  $v_0 = 17.9 \text{ m.sec}^{-1}$  (i.e., 40 m.p.h.). Beginning at time  $t = 0 \text{ sec}$ , the lead vehicle's velocity increases from its steady-state value of  $17.9 \text{ m.sec}^{-1}$  until it reaches its final value of  $21.9 \text{ m.sec}^{-1}$  (i.e., 50 m.p.h.); the maximum jerk and the peak acceleration values, corresponding to this velocity time-profile, were  $0.5 \text{ m.sec}^{-3}$  and  $1 \text{ m.sec}^{-2}$ , respectively (see Figures 3.8 and 3.9).

Figures 3.10 and 3.11 show the simulation results for the nominal case:

- the deviations of the vehicles from their assigned positions (i.e.,  $\Delta_i$  for  $i = 1, 2, \dots, 15$ ) are less than  $0.08 \text{ m}$ .
- These deviations decrease to zero reasonably fast and do not exhibit too much oscillatory behavior.
- The peak values of these deviations *increase* from one vehicle to the next as one goes down the platoon. This is due to the fact that  $|\hat{g}_{final}(j\omega)| \geq 1$  for  $\omega$  between  $0 \text{ rad.sec}^{-1}$  and  $6 \text{ rad.sec}^{-1}$ .
- The acceleration curves show that the peak magnitude of vehicle accelerations increase from one vehicle to the next as one goes down the platoon. The peak values of these accelerations remain within  $1.5 \text{ m.sec}^{-2}$ .

In comparison to chapter 2, [47],[41], the peak value of the lead vehicle's acceleration ( $a_l$ ) is  $1 \text{ m.sec}^{-2}$ ; whereas, in chapter 2,[47],[41], this peak value was  $3 \text{ m.sec}^{-2}$ : the maneuver considered here was chosen to be gentler because otherwise the acceleration demands on the tail vehicle of the platoon were excessive.

In contrast to chapter 2, the deviations of the vehicles from their assigned positions (i.e.,  $\Delta_i$  for  $i = 1, 2, \dots, 15$ ) increase from one vehicle to the next under the control laws

(3.8)- (3.9); however, the peak values of these deviations are within acceptable performance limits and these deviations do not exhibit too much oscillatory behavior.

Since under the control laws (3.8)- (3.9), the  $i$ -th vehicle in the platoon (for  $i = 2, 3, \dots, 15$ ) does not require the lead vehicle's velocity ( $v_l$ ) and acceleration ( $a_l$ ) for computing its control input ( $c_i$ ), the longitudinal control scheme presented here does not necessitate the need for a communication system; hence, the implementation of this longitudinal control scheme is less expensive than the one presented in chapter 2. The performance of the longitudinal control scheme in chapter 2,[47],[41] degrades slightly due to communication delays in transmitting the lead vehicle information; in contrast, control laws (3.8)-(3.9) do not depend on transmission of the lead vehicle information to each vehicle in the platoon.

The exact linearization method is based on exact knowledge of vehicle / engine parameters. We ran simulations to evaluate the robustness of the control laws (3.8)-(3.9) with the design constants (3.28); namely, robustness with respect to each vehicle's mass variations and measurement noise. The mass variations ranged from 8% to 23% of each vehicle's mass. The value of  $\Delta_i$  (for  $i = 1, 2, \dots, 15$ ) used in the  $i$ -the vehicle's control laws (3.8)-(3.9) was the sum of the actual measured value of  $\Delta_i$  and some Gaussian noise with zero mean and standard deviation ( $\sigma$ ) of 0.05 m. Based on these simulations, the deviations of the vehicles from their respective positions were larger than the respective deviations in the nominal case; however, such deviations were within acceptable performance limits.

### 3.5 Conclusion

In contrast to previous work in chapter 2, [47],[41] this chapter considers longitudinal control laws for a platoon of vehicles which do not use any communication of lead vehicle information.

Comparison with the full communication case, presented in chapter 2, [47],[41], shows that using control laws (3.8)-(3.9): the deviations in vehicle spacings from their assigned positions increase from one vehicle to the next as one goes down the platoon; furthermore, the acceleration demands on the tail vehicle of the platoon are much larger than the respective demands under the control laws in chapter 2,[47],[41]. On the other hand, the longitudinal control scheme presented here does not require communication of lead vehicle information; hence, it is less expensive than the corresponding scheme in chapter

2,[47],[41] and cannot suffer from any degradation due to communication delays.

At present system designers are inclined to view the communication system within the platoon to be indispensable for safety, entrainment and detrainment maneuvers. This study shows that in case the communication breaks down, the control laws proposed in this chapter can be used as an alternative means to control the longitudinal dynamics of a platoon of vehicles.

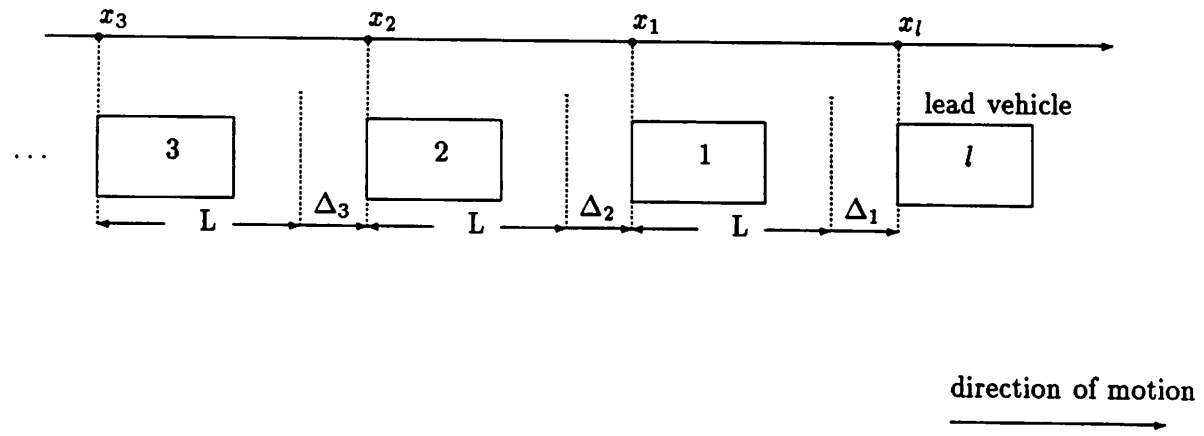


Figure 3.1: A platoon of vehicles on a straight lane of highway

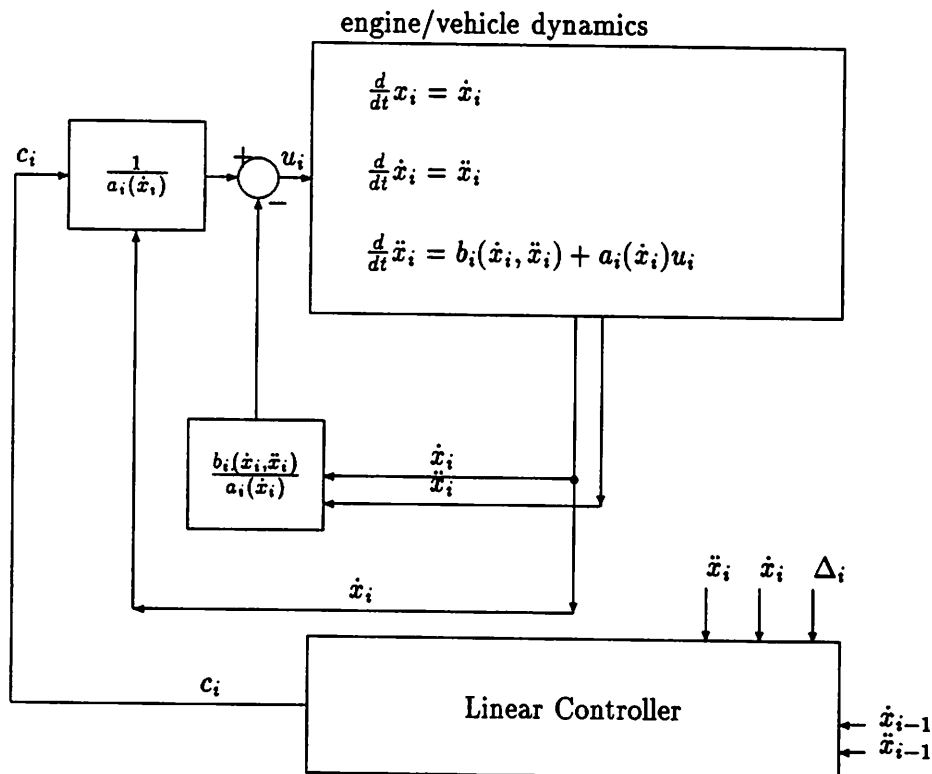


Figure 3.2: Linearized model of the  $i$ -th vehicle with control input  $c_i, i = 1, 2, \dots, N$

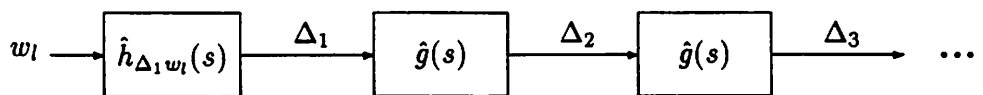


Figure 3.3: Block diagram for a platoon of linearized vehicle models

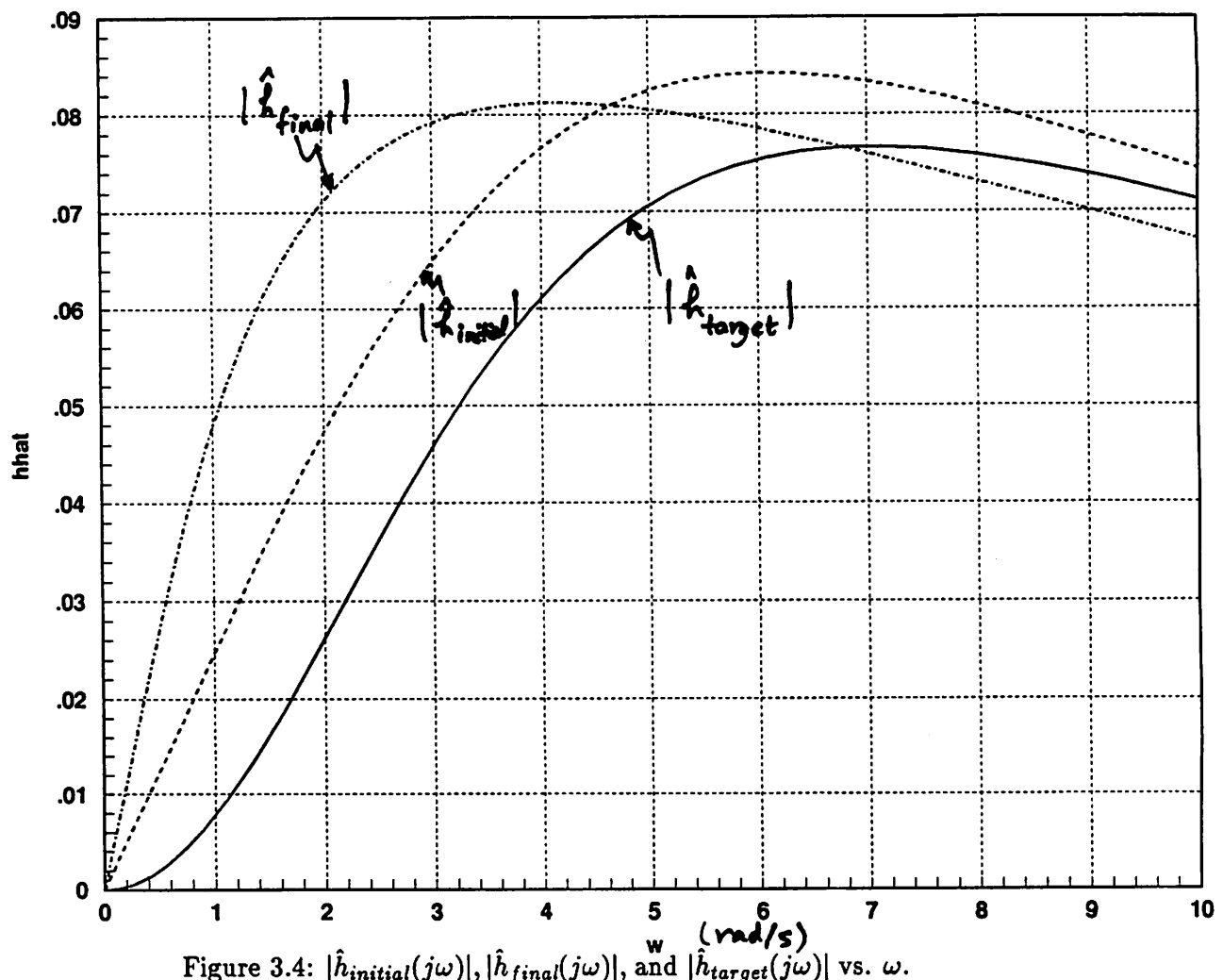


Figure 3.4:  $|\hat{h}_{initial}(j\omega)|$ ,  $|\hat{h}_{final}(j\omega)|$ , and  $|\hat{h}_{target}(j\omega)|$  vs.  $\omega$ .

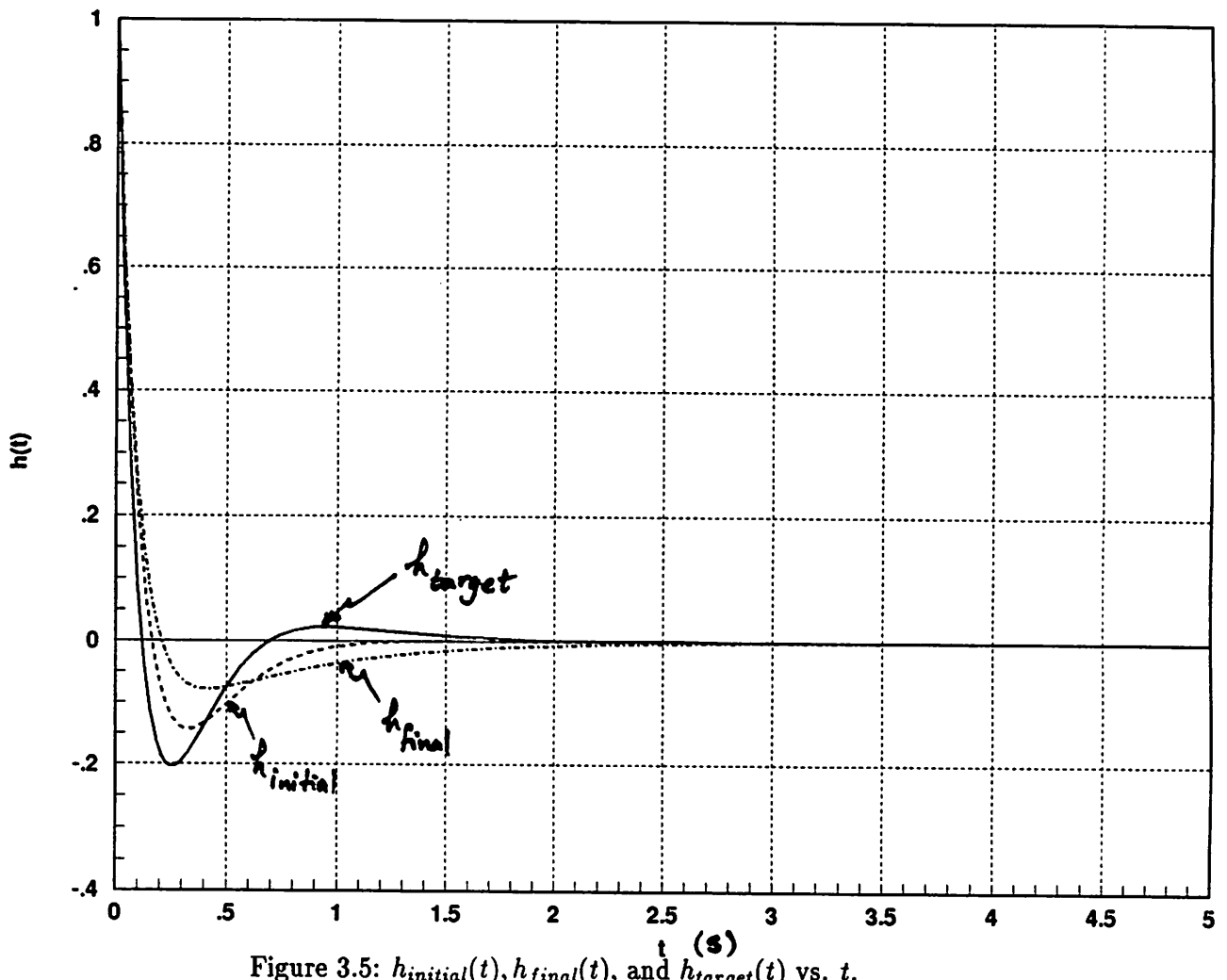


Figure 3.5:  $h_{initial}(t)$ ,  $h_{final}(t)$ , and  $h_{target}(t)$  vs.  $t$ .

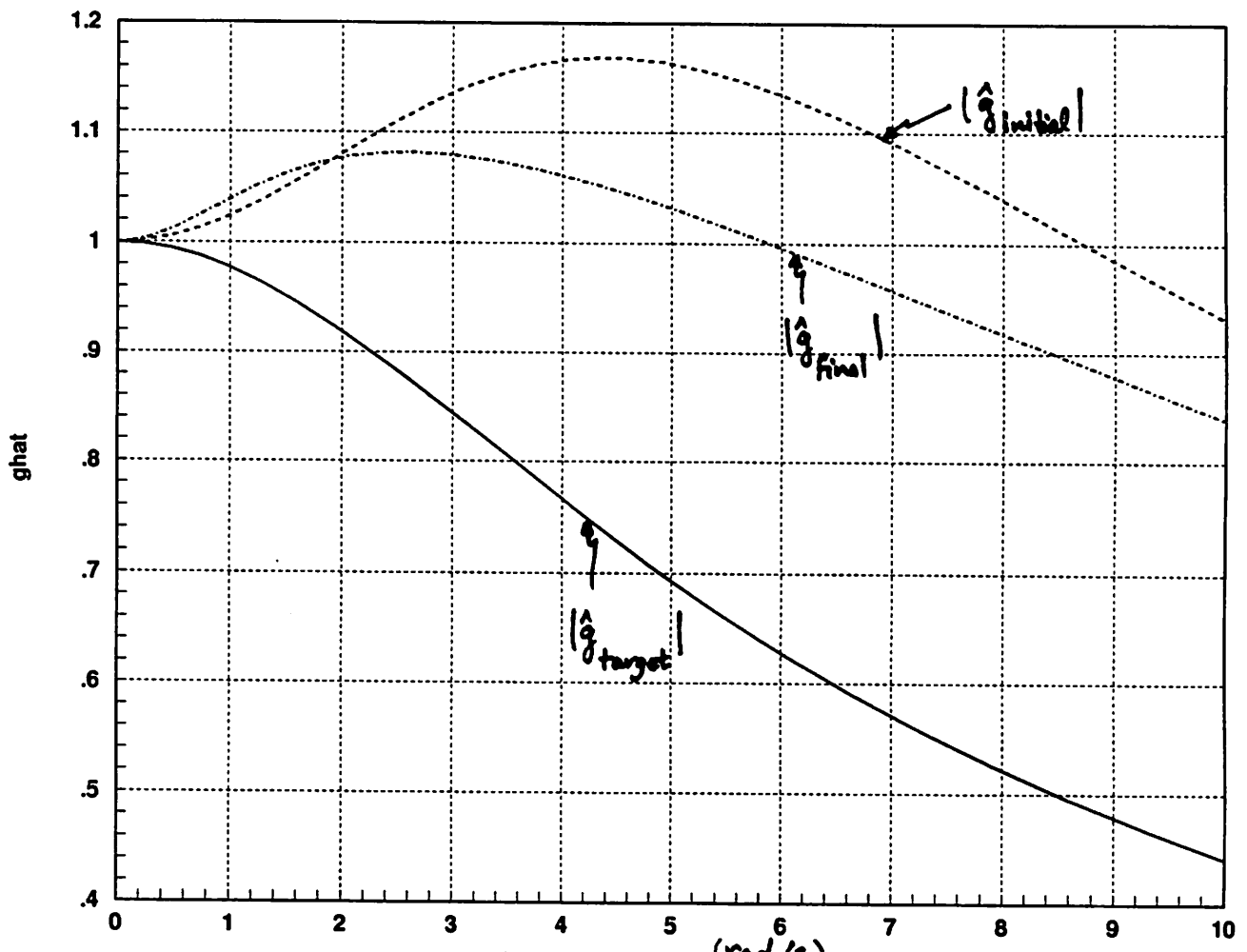
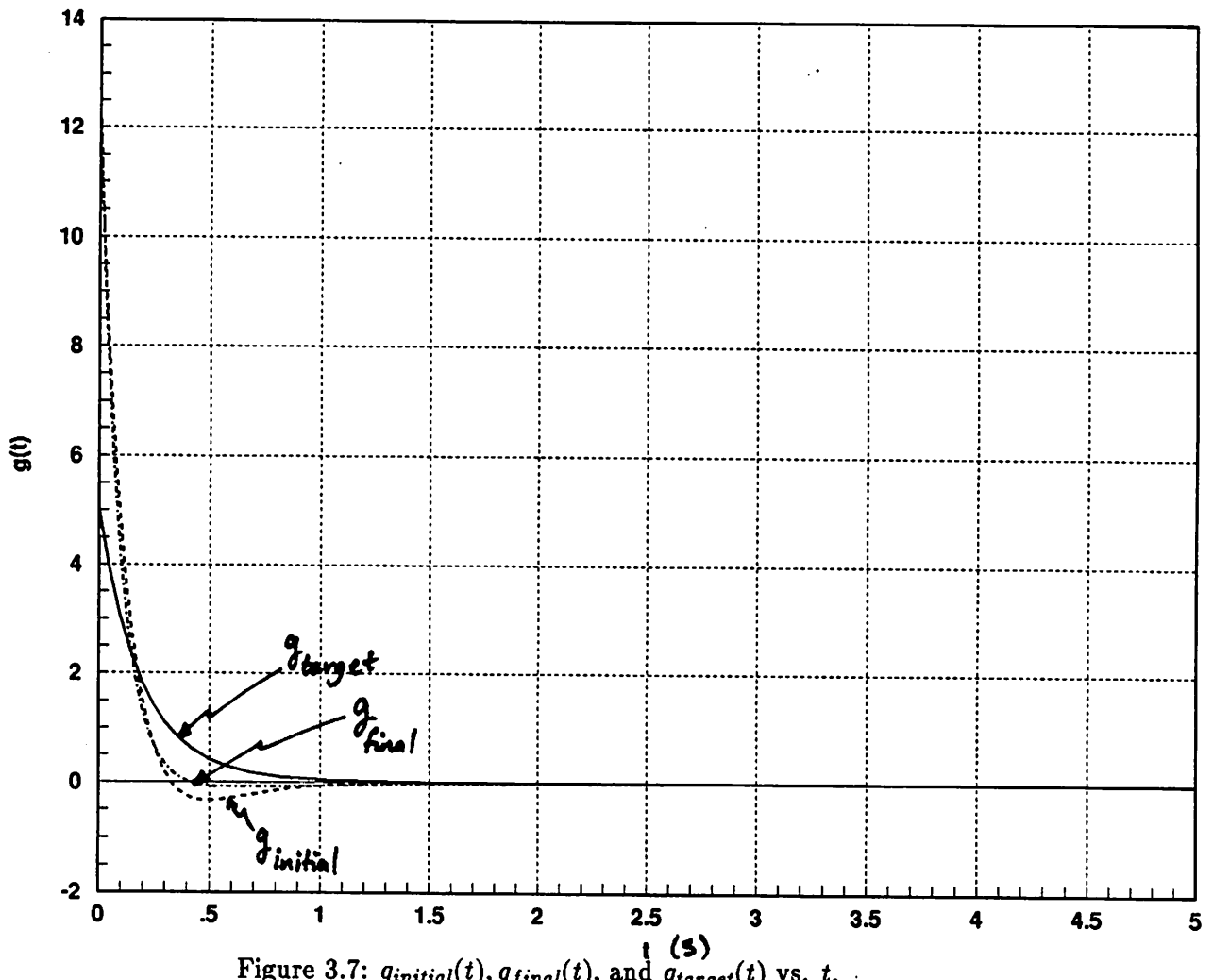
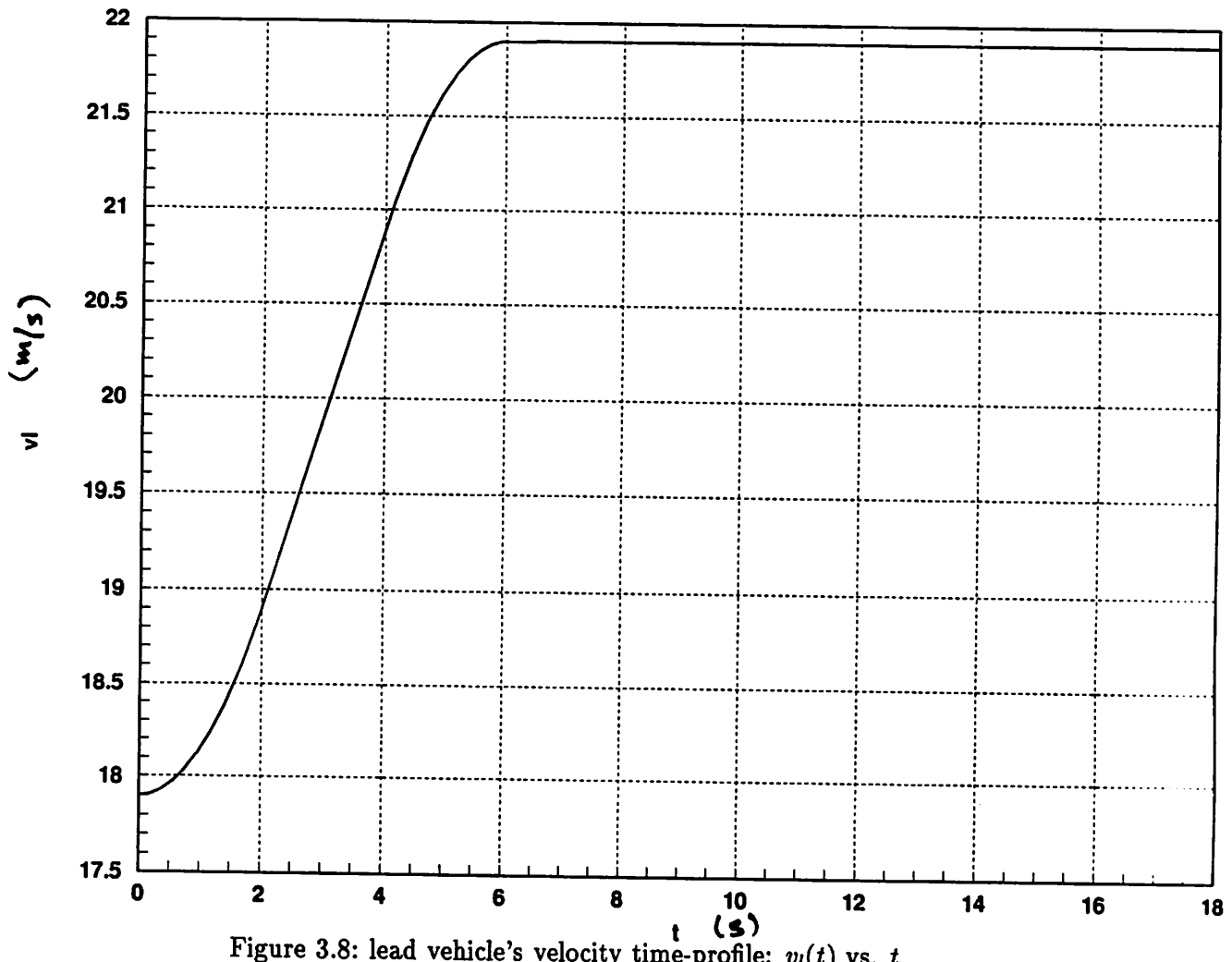
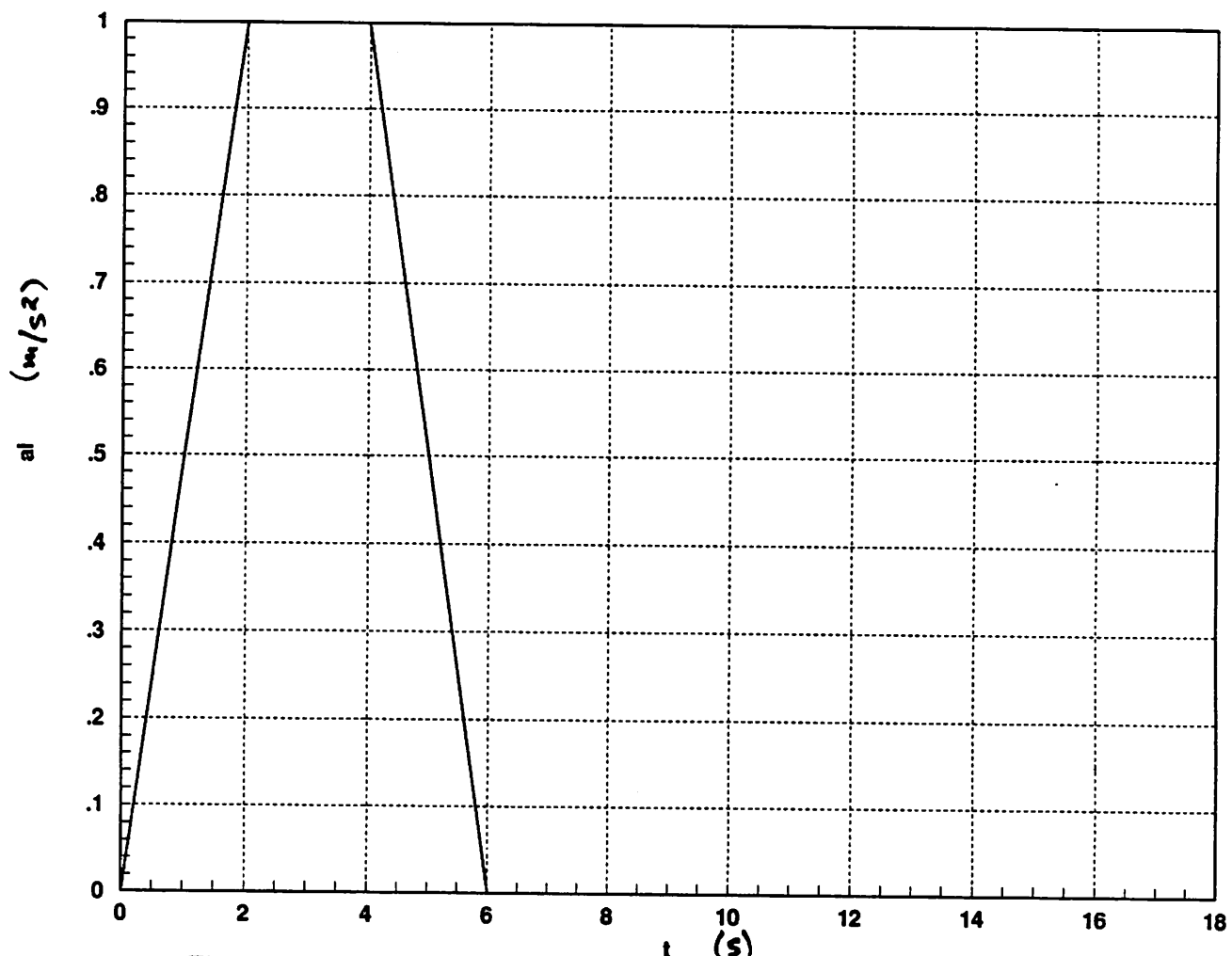


Figure 3.6:  $|\hat{g}_{\text{initial}}(j\omega)|$ ,  $|\hat{g}_{\text{final}}(j\omega)|$ , and  $|\hat{g}_{\text{target}}(j\omega)|$  vs.  $\omega$ .







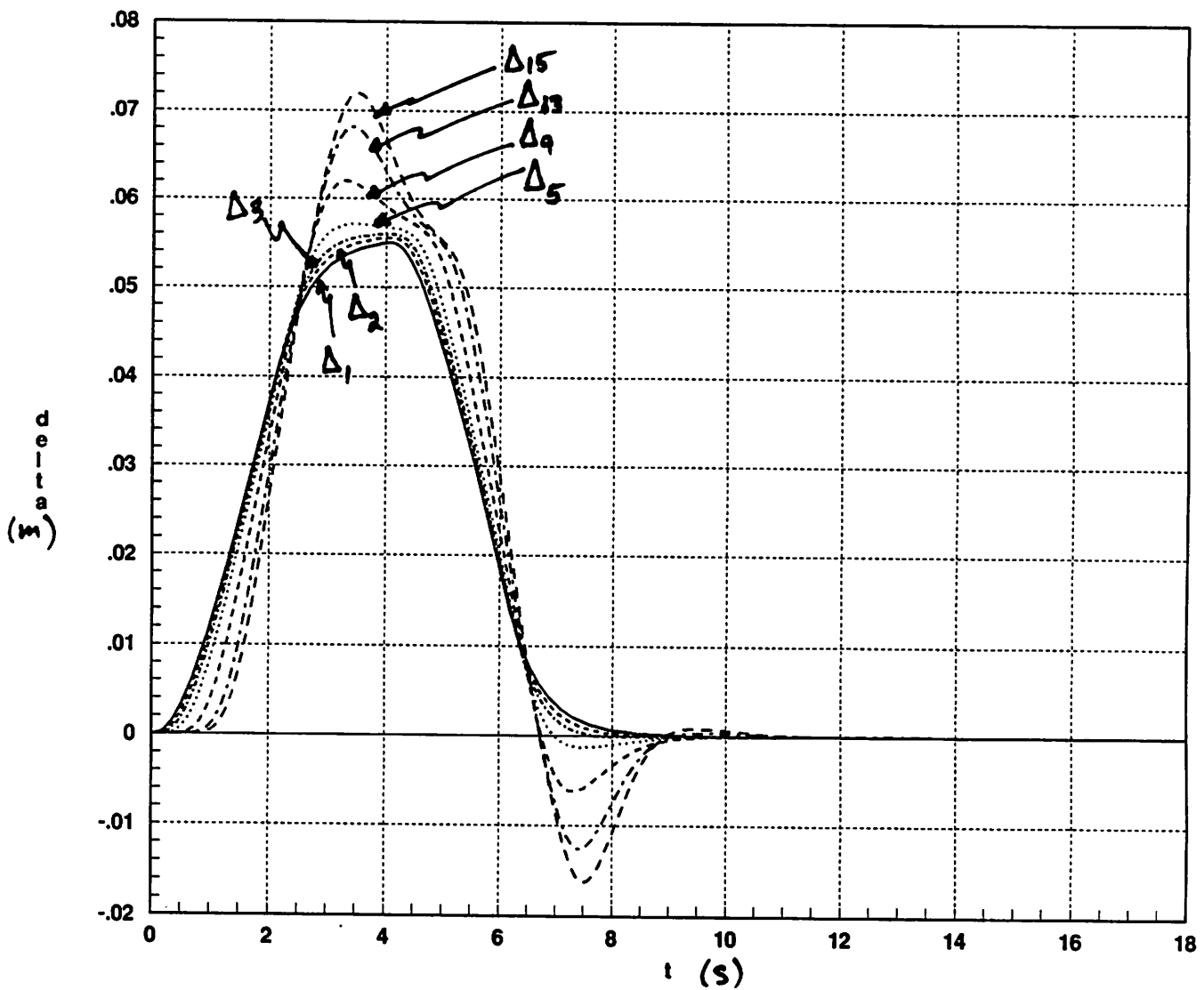


Figure 3.10:  $\Delta_1, \Delta_2, \Delta_3, \Delta_5, \Delta_9, \Delta_{13}$ , and  $\Delta_{15}$  vs.  $t$ : nominal case

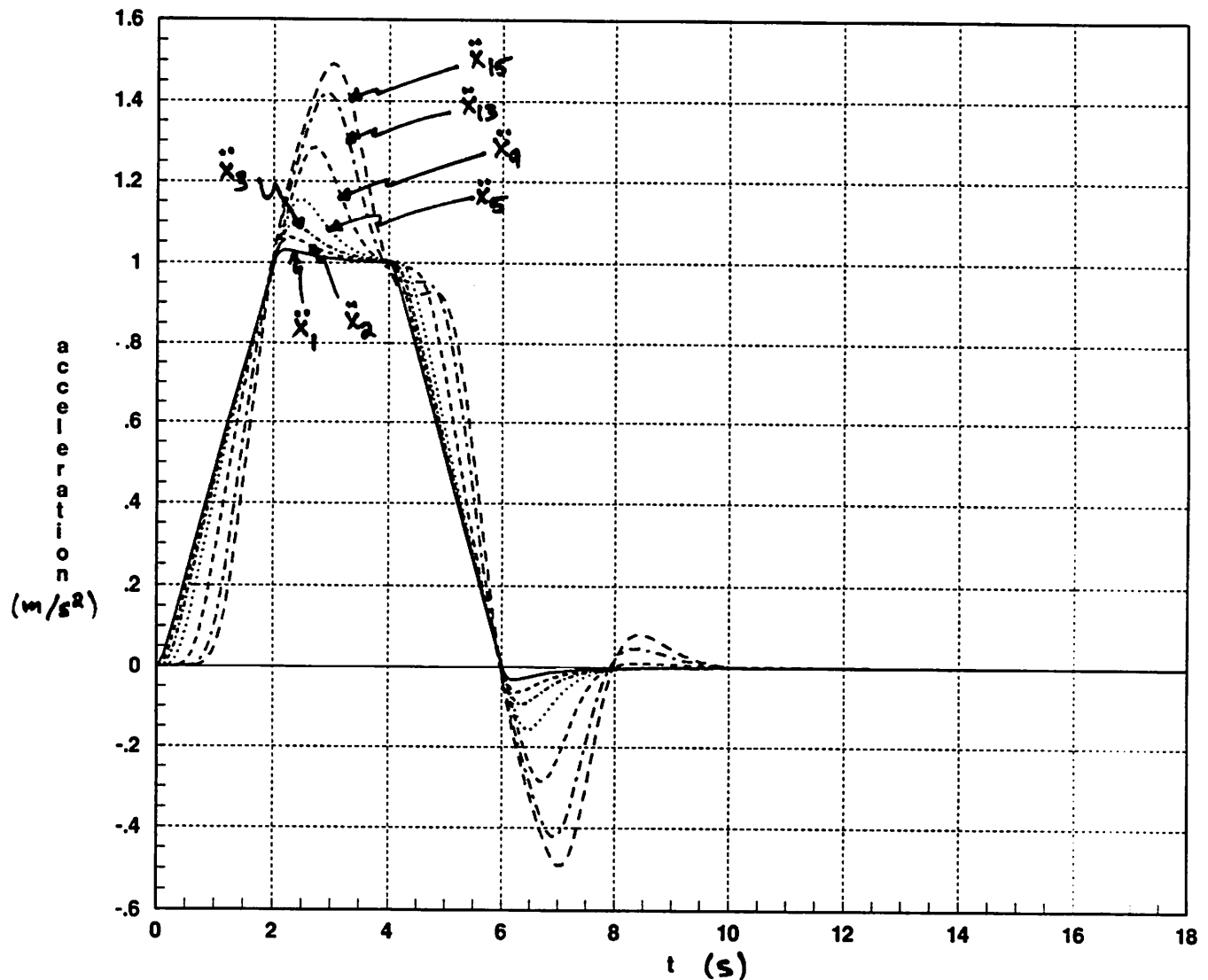


Figure 3.11:  $\ddot{x}_1, \ddot{x}_2, \ddot{x}_3, \ddot{x}_5, \ddot{x}_9, \ddot{x}_{13}$ , and  $\ddot{x}_{15}$  vs.  $t$ : nominal case

## Chapter 4

# Combined Longitudinal and Lateral Control of a Platoon of Vehicles

### 4.1 Introduction

In recent years, a number of studies have been done on intelligent vehicle highway systems (IVHS) [41],[46], [13],[30],[51]. One direction of such studies is to investigate the feasibility of using automatic control techniques to increase the throughput of vehicles in a lane of a highway: more precisely, the goal is to use automatic control to reduce the distance between successive vehicles.

This chapter considers the problem of combined *longitudinal* and *lateral* control of a platoon of vehicles on automated highways. A platoon consists of  $N$  *non-identical* vehicles following a lead vehicle. Previous studies separated the problem of longitudinal control of a platoon of vehicles from the lateral control of each vehicle within the platoon: in the case of longitudinal control of a platoon of vehicles, these studies showed that suitable control laws, as in chapter 2, can be designed for a platoon of 16 vehicles traveling on a *straight* lane of a highway [41],[46],[47]; in the case of lateral control of a vehicle, these studies proposed control laws based on a *linear* model of vehicle's lateral dynamics with the assumption that the vehicle's speed remains *constant* on a *curved* lane of highway [30]. In the present system-level study, we propose *nonlinear* control laws for a platoon of non-identical vehicles

accelerating on a *curved* lane of highway. These control laws are based on *nonlinear* models of vehicles' *combined* longitudinal and lateral dynamics.

The organization of the chapter is as follows: section 4.2 summarizes the notation; in section 4.3, we derive the kinematic equations for the  $i$ -th vehicle ( $i = 1, 2, \dots, N$ ) in a platoon; in section 4.4, we describe the dynamic equations representing the  $i$ -th vehicle's engine and steering actuator dynamics (for  $i = 1, 2, \dots, N$ ) and then derive the equations of motion for the  $i$ -th vehicle's center of mass; in section 4.5, using both the kinematic and the dynamic equations for the  $i$ -th vehicle, we propose a lateral control law for this vehicle and longitudinal control laws for the platoon; the implementation issues regarding the needed sensors, estimators, guidance system, and communication link are discussed in section 4.6; in section 4.7, we show the simulation results for a platoon of 5 vehicles following a lead vehicle, accelerating on a curved lane of a highway, under the proposed control laws; and finally, in section 4.8, we conclude the chapter by giving a plan for further improving the robustness of the proposed control laws under parameter uncertainties.

## 4.2 Notation

Figures 4.1, 4.2, 4.3, and 4.4 show the relevant quantities for the lateral dynamics of the  $i$ -th vehicle in a platoon, the longitudinal dynamics for the  $(i - 1)$ -th and the  $i$ -th vehicles in a platoon, the body frame of the  $i$ -th vehicle in a platoon, and the bicycle model for the  $i$ -th vehicle in a platoon, (for  $i = 1, 2, \dots, N$ ), respectively:

- $(O, x, y)$  a fixed inertial frame in the plane.
- $\mathcal{L}$  lane center (a smooth curve in the plane).
- $\hat{e}_{F_i}, \hat{e}_{S_i}, \hat{e}_{Z_i}$  unit vectors along the longitudinal axis of the  $i$ -th vehicle, the transversal axis of the  $i$ -th vehicle, and the vertical axis through the  $i$ -th vehicle's center of mass;  $(\hat{e}_{F_i}, \hat{e}_{S_i}, \hat{e}_{Z_i})$  form a dextral orthonormal coordinate frame on the  $i$ -th vehicle's body.
- $c_i, \vec{r}_{ci}$   $i$ -th vehicle's center of mass, the vector from  $O$  to  $c_i$ . (see Figure 4.1)
- $d_i, \vec{r}_{di}$   $i$ -th vehicle's reference point on  $\mathcal{L}$ , the vector from  $O$  to  $d_i$ . (see Figure 4.1)
- $\vec{t}(d_i), \vec{n}(d_i)$  unit tangent vector at the point  $d_i$  on  $\mathcal{L}$ , unit inward normal at the point  $d_i$  on  $\mathcal{L}$ .

- $\epsilon_i, \epsilon_{di}$  the angle between the  $Ox$ -axis and the  $i$ -th vehicle's longitudinal axis, the angle between the  $Ox$ -axis and  $\vec{t}(d_i)$ .
- $\Delta_{i,lat}$  lateral deviation of the  $i$ -th vehicle's center of mass from the lane center.
- $A_i, B_i$  the midpoint on the  $i$ -th vehicle's front bumper, the midpoint on the  $i$ -th vehicle's rear bumper.
- $\vec{r}_{i-1,i}$  the vector from  $A_i$  to  $B_{i-1}$ . (see Figure 4.2)
- $\theta_{i-1,i}$  the angle between the  $Ox$ -axis and  $\vec{r}_{i-1,i}$ .
- $\Delta_{desired}$  the desired length of vector  $\vec{r}_{i-1,i}$ .
- $\Delta_{i-1,i}$  deviation of the length of vector  $\vec{r}_{i-1,i}$  from its desired value  $\Delta_{desired}$ .
- $l_{F_i}, l_{R_i}$  the distance between the  $i$ -th vehicle's center of mass and its front axle, the distance between the  $i$ -th vehicle's center of mass and its rear axle. (see Figure 4.3)
- $\bar{l}_{F_i}, \bar{l}_{R_i}$  the distance between the  $i$ -th vehicle's center of mass and its front bumper (point  $A_i$ ), the distance between the  $i$ -th vehicle's center of mass and its rear bumper (point  $B_i$ ). (see Figure 4.3)
- $m_i$  mass of the  $i$ -th vehicle.
- $I_{Zi}$  moment of inertia of the  $i$ -th vehicle about the vertical axis through its center of mass.
- $C_{Fi}, C_{Ri}$  sum of the front tires' cornering stiffnesses for the  $i$ -th vehicle, sum of the rear tires' cornering stiffnesses for the  $i$ -th vehicle in ( $N/rad$ ).
- $\tau_i$   $i$ -th vehicle's engine time lag.
- $F_{ei}$  driving force produced by the  $i$ -th vehicle's engine along the longitudinal axis of the  $i$ -th vehicle. (see Figure 4.4)
- $\vec{F}_{Fi}, \vec{F}_{Ri}$  force exerted by the road on the front tires of the  $i$ -th vehicle, force exerted by the road on the rear tires of the  $i$ -th vehicle. (see Figure 4.4)

- $v_{F_i}, v_{S_i}$  component of the velocity of the center of mass of the  $i$ -th vehicle along its longitudinal axis, component of the velocity of the center of mass of the  $i$ -th vehicle along its transversal axis.
- $a_{F_i}, a_{S_i}$  component of the acceleration of the center of mass of the  $i$ -th vehicle along  $\hat{e}_{F_i}$ , component of the acceleration of the center of mass of the  $i$ -th vehicle along  $\hat{e}_{S_i}$ .
- $u_i$  throttle command input to the  $i$ -th vehicle's engine.
- $\delta_{F_i}, \delta_{command,i}$   $i$ -th vehicle's front steering angle,  $i$ -th vehicle's steering angle command input.
- $d_{m_i}$   $i$ -th vehicle's mechanical drag.
- $K_{d_i}$   $i$ -th vehicle's aerodynamic drag coefficient.
- $\tau_{a_i}$   $i$ -th vehicle's steering actuator time constant.
- $s_{d_i}$  arc length traversed by the  $i$ -th vehicle's reference point on the lane center  $\mathcal{L}$ .
- $\kappa = \frac{1}{\rho}$  where  $\rho$  is radius of curvature of lane center line.
- $\hat{e}_{r_{i-1,i}}, \hat{e}_{\theta_{i-1,i}}$  unit vector along  $\vec{r}_{i-1,i}$ , unit vector normal to  $\vec{r}_{i-1,i}$  and in the direction of increasing  $\theta_{i-1,i}$  (i.e., counter-clockwise direction).
- $\tilde{c}_i$  exogenous input to the  $i$ -th vehicle's longitudinal dynamics.

### 4.3 Kinematics

In this section, we summarize the derivation of kinematic equations for the  $i$ -th vehicle ( $i = 1, 2, \dots, N$ ) in a platoon.

Figure 4.1 shows the relevant quantities for the lateral dynamics of the  $i$ -th vehicle in a platoon ( $i = 1, 2, \dots, N$ ).

**Definition [reference point  $d_i$ ]-** Given the location of the  $i$ -th vehicle's center of mass ( $\vec{r}_{ci}$ ), we draw the osculating circle to  $\mathcal{L}$  centered at point  $c_i$ ; this circle is tangent to the road at a *reference point*, called  $d_i$ . Thus, by definition of  $d_i$ ,  $(\vec{r}_{ci} - \vec{r}_{di})$  is parallel to  $\vec{n}(d_i)$ .  $\Delta_{i,lat}$  denotes the radius of the osculating circle. Hence,

$$\Delta_{i,lat} := (\vec{r}_{ci} - \vec{r}_{di}) \cdot \vec{n}(d_i). \quad (4.1)$$

Writing the Frenet formulas for  $\dot{\vec{n}}(d_i)$  and  $\dot{\vec{t}}(d_i)$ , we get

$$\dot{\vec{n}}(d_i) = -\kappa(s_{di})\dot{s}_{di}\vec{t}(d_i) \quad (4.2)$$

$$\dot{\vec{t}}(d_i) = \kappa(s_{di})\dot{s}_{di}\vec{n}(d_i). \quad (4.3)$$

Noting that  $\dot{\vec{t}}(d_i) = \dot{\epsilon}_{di}\vec{n}(d_i)$ , from (4.3) we get

$$\dot{\epsilon}_{di} = \kappa(s_{di})\dot{s}_{di}. \quad (4.4)$$

Taking derivatives of both sides of (4.1) with respect to t, we get

$$\dot{\Delta}_{i,lat} = (\dot{\vec{r}}_{ci} - \dot{\vec{r}}_{di}) \cdot \vec{n}(d_i) + (\vec{r}_{ci} - \vec{r}_{di}) \cdot \dot{\vec{n}}(d_i). \quad (4.5)$$

By definition of  $\vec{t}(d_i)$ ,  $\dot{\vec{r}}_{di}$  is parallel to  $\vec{t}(d_i)$ . Hence,  $\dot{\vec{r}}_{di} \cdot \vec{n}(d_i) = 0$  in (4.5). Furthermore,  $(\vec{r}_{ci} - \vec{r}_{di})$  is parallel to  $\vec{n}(d_i)$ . Hence, using (4.2) in the right hand side of (4.5), we get

$$\dot{\Delta}_{i,lat} = \dot{\vec{r}}_{ci} \cdot \vec{n}(d_i). \quad (4.6)$$

Exhibiting the components of the velocity, see Figure 4.1,  $\dot{\vec{r}}_{ci} := v_{F;i}\hat{e}_{F;i} + v_{S;i}\hat{e}_{S;i}$ , so from (4.6) we get

$$\dot{\Delta}_{i,lat} = v_{F;i} \sin(\epsilon_i - \epsilon_{di}) + v_{S;i} \cos(\epsilon_i - \epsilon_{di}). \quad (4.7)$$

Taking derivatives of both sides of (4.6) with respect to t, we get

$$\ddot{\Delta}_{i,lat} = \ddot{\vec{r}}_{ci} \cdot \vec{n}(d_i) + \dot{\vec{r}}_{ci} \cdot \dot{\vec{n}}(d_i). \quad (4.8)$$

Noting that  $\ddot{\vec{r}}_{ci} := a_{F;i}\hat{e}_{F;i} + a_{S;i}\hat{e}_{S;i}$ ,  $\dot{\vec{r}}_{ci} := v_{F;i}\hat{e}_{F;i} + v_{S;i}\hat{e}_{S;i}$ , and using (4.2), we get

$$\begin{aligned} \ddot{\Delta}_{i,lat} &= (a_{F;i} + \kappa(s_{di})\dot{s}_{di}v_{S;i}) \sin(\epsilon_i - \epsilon_{di}) \\ &+ (a_{S;i} - \kappa(s_{di})\dot{s}_{di}v_{F;i}) \cos(\epsilon_i - \epsilon_{di}). \end{aligned} \quad (4.9)$$

Using (4.4), we can simplify this expression to

$$\ddot{\Delta}_{i,lat} = (a_{F;i} + v_{S;i}\dot{\epsilon}_{di}) \sin(\epsilon_i - \epsilon_{di}) + (a_{S;i} - v_{F;i}\dot{\epsilon}_{di}) \cos(\epsilon_i - \epsilon_{di}). \quad (4.10)$$

Comparing the expression for  $\ddot{\Delta}_{i,lat}$  obtained by differentiating both sides of (4.7), with respect to t, with the expression in the right hand side of (4.10) we get

$$\dot{v}_{F;i} = a_{F;i} + v_{S;i}\dot{\epsilon}_i \quad (4.11)$$

$$\dot{v}_{S;i} = a_{S;i} - v_{F;i}\dot{\epsilon}_i. \quad (4.12)$$

Differentiating both sides of (4.10) with respect to  $t$ , we get after some straightforward calculations

$$\begin{aligned}\ddot{\Delta}_{i,\text{lat}} &= (\dot{a}_{F_i} + \dot{v}_{S_i} \dot{\epsilon}_{d_i} + v_{S_i} \ddot{\epsilon}_{d_i}) \sin(\epsilon_i - \epsilon_{d_i}) \\ &+ (a_{F_i} + v_{S_i} \dot{\epsilon}_{d_i})(\dot{\epsilon}_i - \dot{\epsilon}_{d_i}) \cos(\epsilon_i - \epsilon_{d_i}) \\ &+ (\dot{a}_{S_i} - \dot{v}_{F_i} \dot{\epsilon}_{d_i} - v_{F_i} \ddot{\epsilon}_{d_i}) \cos(\epsilon_i - \epsilon_{d_i}) \\ &- (a_{S_i} - v_{F_i} \dot{\epsilon}_{d_i})(\dot{\epsilon}_i - \dot{\epsilon}_{d_i}) \sin(\epsilon_i - \epsilon_{d_i}).\end{aligned}\quad (4.13)$$

In section 4.5, we use the kinematic equation (4.13) and propose a lateral control law for the  $i$ -th vehicle.

Figures 4.2 and 4.3 show the relevant quantities for the longitudinal dynamics of the  $(i-1)$ -th and the  $i$ -th vehicles in a platoon (for  $i = 1, 2, \dots, N$ ). From Figure 4.2 and by definition of  $\Delta_{i-1,i}$ , we have

$$\Delta_{i-1,i} := \vec{r}_{i-1,i} \cdot \hat{e}_{r_{i-1,i}} - \Delta_{\text{desired}}; \quad (4.14)$$

and by definition of  $\hat{e}_{r_{i-1,i}}$  and  $\hat{e}_{\theta_{i-1,i}}$  (see Figure 4.2), we have

$$\dot{\hat{e}}_{r_{i-1,i}} = \dot{\theta}_{i-1,i} \hat{e}_{\theta_{i-1,i}} \quad (4.15)$$

$$\dot{\hat{e}}_{\theta_{i-1,i}} = -\dot{\theta}_{i-1,i} \hat{e}_{r_{i-1,i}}. \quad (4.16)$$

Differentiating both sides of (4.14) with respect to  $t$ , we get

$$\dot{\Delta}_{i-1,i} = \dot{\vec{r}}_{i-1,i} \cdot \hat{e}_{r_{i-1,i}} + \vec{r}_{i-1,i} \cdot \dot{\hat{e}}_{r_{i-1,i}}. \quad (4.17)$$

By definition,  $\vec{r}_{i-1,i}$  is parallel to  $\hat{e}_{r_{i-1,i}}$ . Hence, using the expression for  $\dot{\hat{e}}_{r_{i-1,i}}$  from (4.15), we get

$$\vec{r}_{i-1,i} \cdot \dot{\hat{e}}_{r_{i-1,i}} = 0. \quad (4.18)$$

Let  $\vec{v}_{A_i}, \vec{v}_{B_i}$  denote the velocity vectors of points  $A_i, B_i$ , respectively. Then, for  $i = 1, 2, \dots, N$ , we have

$$\dot{\vec{r}}_{i-1,i} = \vec{v}_{B_{i-1}} - \vec{v}_{A_i}. \quad (4.19)$$

By definition of  $\hat{e}_{F_i}$  and  $\hat{e}_{S_i}$  (see Figure 4.1), we have

$$\dot{\hat{e}}_{F_i} = \dot{\epsilon}_i \hat{e}_{S_i} \quad (4.20)$$

$$\dot{\hat{e}}_{S_i} = -\dot{\epsilon}_i \hat{e}_{F_i}. \quad (4.21)$$

From Figures 4.2 and 4.3, we note that

$$\vec{r}_{Ai} - \vec{r}_{ci} = \tilde{l}_{Fi}\hat{e}_{Fi} \quad (4.22)$$

$$\vec{r}_{ci} - \vec{r}_{Bi} = \tilde{l}_{Ri}\hat{e}_{Fi}. \quad (4.23)$$

Differentiating both sides of (4.22), (4.23) with respect to t, using the expression for  $\dot{\hat{e}}_{Fi}$  from (4.20), and noting that  $\vec{r}_{ci} := v_{Fi}\hat{e}_{Fi} + v_{Si}\hat{e}_{Si}$ , we get

$$\vec{v}_{Ai} = v_{Fi}\hat{e}_{Fi} + (v_{Si} + \tilde{l}_{Fi}\dot{\epsilon}_i)\hat{e}_{Si} \quad (4.24)$$

$$\vec{v}_{Bi} = v_{Fi}\hat{e}_{Fi} + (v_{Si} - \tilde{l}_{Ri}\dot{\epsilon}_i)\hat{e}_{Si}. \quad (4.25)$$

Substituting the expressions for  $\vec{v}_{Bi-1}$ ,  $\vec{v}_{Ai}$  from (4.24)-(4.25) in (4.19) and using (4.18), we can simplify (4.17) to

$$\begin{aligned} \dot{\Delta}_{i-1,i} &= v_{Fi-1}\cos(\theta_{i-1,i} - \epsilon_{i-1}) + (v_{Si-1} - \tilde{l}_{Ri-1}\dot{\epsilon}_{i-1})\sin(\theta_{i-1,i} - \epsilon_{i-1}) \\ &\quad - v_{Fi}\cos(\theta_{i-1,i} - \epsilon_i) - (v_{Si} + \tilde{l}_{Fi}\dot{\epsilon}_i)\sin(\theta_{i-1,i} - \epsilon_i). \end{aligned} \quad (4.26)$$

Successively differentiating both sides of (4.26) with respect to t and using the expressions for  $\dot{v}_{Fi-1}$ ,  $\dot{v}_{Si-1}$ ,  $\dot{v}_{Fi}$ , and  $\dot{v}_{Si}$  from (4.11)-(4.12), we get

$$\begin{aligned} \ddot{\Delta}_{i-1,i} &= [a_{Fi-1} + \tilde{l}_{Ri-1}\dot{\epsilon}_{i-1}^2 + (v_{Si-1} - \tilde{l}_{Ri-1}\dot{\epsilon}_{i-1})\dot{\theta}_{i-1,i}] \cos(\theta_{i-1,i} - \epsilon_{i-1}) \\ &\quad + [-(a_{Fi} - \tilde{l}_{Fi}\dot{\epsilon}_i^2) - (v_{Si} + \tilde{l}_{Fi}\dot{\epsilon}_i)\dot{\theta}_{i-1,i}] \cos(\theta_{i-1,i} - \epsilon_i) \\ &\quad + [a_{Si-1} - \tilde{l}_{Ri-1}\ddot{\epsilon}_{i-1} - v_{Fi-1}\dot{\theta}_{i-1,i}] \sin(\theta_{i-1,i} - \epsilon_{i-1}) \\ &\quad + [-(a_{Si} + \tilde{l}_{Fi}\ddot{\epsilon}_i) + v_{Fi}\dot{\theta}_{i-1,i}] \sin(\theta_{i-1,i} - \epsilon_i). \end{aligned} \quad (4.27)$$

$$\begin{aligned} \dddot{\Delta}_{i-1,i} &= [(\dot{a}_{Fi-1} - a_{Si-1}\dot{\epsilon}_{i-1} + 3\tilde{l}_{Ri-1}\dot{\epsilon}_{i-1}\ddot{\epsilon}_{i-1}) + 2\dot{\theta}_{i-1,i}(a_{Si-1} - \tilde{l}_{Ri-1}\ddot{\epsilon}_{i-1})] \cos(\theta_{i-1,i} - \epsilon_{i-1}) \\ &\quad + [\ddot{\theta}_{i-1,i}(v_{Si-1} - \tilde{l}_{Ri-1}\dot{\epsilon}_{i-1}) - \dot{\theta}_{i-1,i}^2 v_{Fi-1}] \cos(\theta_{i-1,i} - \epsilon_{i-1}) \\ &\quad + [-(\dot{a}_{Fi} - a_{Si}\dot{\epsilon}_i - 3\tilde{l}_{Fi}\dot{\epsilon}_i\ddot{\epsilon}_i) - 2\dot{\theta}_{i-1,i}(a_{Si} + \tilde{l}_{Fi}\ddot{\epsilon}_i)] \cos(\theta_{i-1,i} - \epsilon_i) \\ &\quad + [-\ddot{\theta}_{i-1,i}(v_{Si} + \tilde{l}_{Fi}\dot{\epsilon}_i) + \dot{\theta}_{i-1,i}^2 v_{Fi}] \cos(\theta_{i-1,i} - \epsilon_i) \\ &\quad + [\dot{a}_{Si-1} + a_{Fi-1}\dot{\epsilon}_{i-1} + \tilde{l}_{Ri-1}\dot{\epsilon}_{i-1}^3 - \tilde{l}_{Ri-1}\ddot{\epsilon}_{i-1}] \sin(\theta_{i-1,i} - \epsilon_{i-1}) \\ &\quad + [-2\dot{\theta}_{i-1,i}(a_{Fi-1} + \tilde{l}_{Ri-1}\dot{\epsilon}_{i-1}^2)] \sin(\theta_{i-1,i} - \epsilon_{i-1}) \\ &\quad + [-\ddot{\theta}_{i-1,i} v_{Fi-1} - \dot{\theta}_{i-1,i}^2(v_{Si-1} - \tilde{l}_{Ri-1}\dot{\epsilon}_{i-1})] \sin(\theta_{i-1,i} - \epsilon_{i-1}) \\ &\quad + [-(\dot{a}_{Si} + a_{Fi}\dot{\epsilon}_i - \tilde{l}_{Fi}\dot{\epsilon}_i^3 + \tilde{l}_{Fi}\ddot{\epsilon}_i) + 2\dot{\theta}_{i-1,i}(a_{Fi} - \tilde{l}_{Fi}\dot{\epsilon}_i^2)] \sin(\theta_{i-1,i} - \epsilon_i) \\ &\quad + [\ddot{\theta}_{i-1,i} v_{Fi} + \dot{\theta}_{i-1,i}^2(v_{Si} + \tilde{l}_{Fi}\dot{\epsilon}_i)] \sin(\theta_{i-1,i} - \epsilon_i). \end{aligned} \quad (4.28)$$

In section 4.5, we use the kinematic equation (4.28) and propose longitudinal control laws for a platoon of vehicles.

## 4.4 Dynamics

In this section, we describe the dynamic equations representing the  $i$ -th vehicle's engine and steering actuator dynamics (for  $i = 1, 2, \dots, N$ ); then, we derive the equations of motion for the  $i$ -th vehicle's center of mass. These dynamic equations are suitable for a system-level study of the combined longitudinal and lateral dynamics of a platoon of vehicles, traveling on a curved lane of a highway, with sufficiently large radius of curvature, under nominal operation.

In this system-level study, we model each vehicle in the platoon as a rigid body. We write Newton's second law for the  $i$ -th vehicle's center of mass and the dynamics of the angular momentum of the  $i$ -th vehicle about the vertical axis through its center of mass. The external forces acting on the  $i$ -th vehicle are driving force produced by the  $i$ -th vehicle's engine, drag forces due to aerodynamic and mechanical drags, and tire forces exerted by the road on the  $i$ -th vehicle's tires.

**Engine dynamics** We use a *nonlinear* differential equation to represent the  $i$ -th vehicle's engine dynamics

$$\dot{F}_{ei} = -\frac{F_{ei}}{\tau_i(v_{Fi}, v_{Si})} + \frac{u_i}{\tau_i(v_{Fi}, v_{Si})}. \quad (4.29)$$

The simple model used to describe the engine dynamics is useful for preliminary system-level studies in longitudinal control of a platoon of vehicles [41],[51]. As a consequence, we do not use complex engine models which take into account factors such as ambient temperature, engine temperature, altitude, condition of spark plugs, transmission dynamics, etc... (for a more detailed model of engine dynamics refer to [13]).

**Steering actuator dynamics** The steering actuator used is modelled as a first order lag

$$\dot{\delta}_{Fi} = -\frac{\delta_{Fi}}{\tau_{ai}} + \frac{\delta_{command,i}}{\tau_{ai}}. \quad (4.30)$$

**Equations of motion for the  $i$ -th vehicle ( $i = 1, 2, \dots, N$ )** Writing Newton's second law for the  $i$ -th vehicle's center of mass, we get

$$m_i \ddot{\vec{r}}_{ci} = \vec{F}_{ei} + \vec{F}_{drag,i} + \vec{F}_{tires,i} \quad (4.31)$$

where

$$\vec{F}_{ci} := F_{ci}\hat{e}_{Fi} \quad (4.32)$$

$$\begin{aligned} \vec{F}_{drag,i} &:= \vec{F}_{aerodynamic,i} + \vec{F}_{mechanical,i} \\ &:= -K_{di}v_{Fi}^2\hat{e}_{Fi} - d_{mi}\hat{e}_{Fi} \end{aligned} \quad (4.33)$$

$$\vec{F}_{tires,i} := \vec{F}_{Fi} + \vec{F}_{Ri}. \quad (4.34)$$

Note that (4.31) does not include the effect of wind gusts nor the slope of the highway.

We use a bicycle model (also called half-car model) to represent the lateral dynamics of the  $i$ -th vehicle [1],[24],[30] (see Figure 4.4): magnitude of the force exerted by the road on a tire is modelled as proportional to the angle between the tire patch and the direction of the velocity vector of the tire [34]; the constant of proportionality is called the tire's *cornering stiffness*; the direction of the force exerted by the road on a tire is orthogonal to the axis of the tire patch. (see Figure 4.4) In this study, we consider only vehicles with front-wheel steering. For the  $i$ -th vehicle,  $\alpha_{Fi}$  denotes the angle between front tire patches and the direction of the velocity vector of the front tires; similarly,  $\alpha_{Ri}$  denotes the angle between rear tire patches and the direction of the velocity vector of the rear tires;  $\vec{v}_{Fi}$  denotes the velocity vector of the front tires; and  $\vec{v}_{Ri}$  denotes the velocity vector of the rear tires. Using these definitions, we have

$$|\vec{F}_{Fi}| = C_{Fi}\alpha_{Fi} \quad (4.35)$$

$$|\vec{F}_{Ri}| = C_{Ri}\alpha_{Ri}. \quad (4.36)$$

Projecting  $\vec{F}_{Fi}$ ,  $\vec{F}_{Ri}$  on the  $\hat{e}_{Fi}$ ,  $\hat{e}_{Si}$  -axes, we get

$$\vec{F}_{Fi} = C_{Fi}\alpha_{Fi}\sin\delta_{Fi}\hat{e}_{Fi} - C_{Fi}\alpha_{Fi}\cos\delta_{Fi}\hat{e}_{Si} \quad (4.37)$$

$$\vec{F}_{Ri} = -C_{Ri}\alpha_{Ri}\hat{e}_{Si}. \quad (4.38)$$

From Figure 4.4, we note

$$\vec{r}_{Fi} - \vec{r}_{ci} = l_{Fi}\hat{e}_{Fi}. \quad (4.39)$$

Differentiating both sides of (4.39) with respect to  $t$ , substituting the expression for  $\dot{\vec{e}}_{Fi}$  from (4.20), and noting  $\dot{\vec{r}}_{ci} := v_{Fi}\hat{e}_{Fi} + v_{Si}\hat{e}_{Si}$ , we get

$$\vec{v}_{Fi} := \dot{\vec{r}}_{Fi} = v_{Fi}\hat{e}_{Fi} + (v_{Si} + l_{Fi}\dot{\epsilon}_i)\hat{e}_{Si}. \quad (4.40)$$

Similarly, we get

$$\ddot{\vec{v}}_{Ri} := \dot{\vec{r}}_{Ri} = v_{Fi}\hat{e}_{Fi} + (v_{Si} - l_{Ri}\dot{\epsilon}_i)\hat{e}_{Si}. \quad (4.41)$$

From (4.40), (4.41), and Figure 4.4, we note

$$\alpha_{Fi} = \arctan\left(\frac{v_{Si} + l_{Fi}\dot{\epsilon}_i}{v_{Fi}}\right) - \delta_{Fi} \quad (4.42)$$

$$\alpha_{Ri} = \arctan\left(\frac{v_{Si} - l_{Ri}\dot{\epsilon}_i}{v_{Fi}}\right). \quad (4.43)$$

Substituting the expressions for  $\vec{F}_{ei}$  (equation (4.32)),  $\vec{F}_{drag,i}$  (equation (4.33)), and  $\vec{F}_{tires,i}$  (equations (4.34), (4.37), (4.38), (4.42), (4.43)), and noting that  $\ddot{\vec{r}}_{ci} := a_{Fi}\hat{e}_{Fi} + a_{Si}\hat{e}_{Si}$ , we get

$$m_i a_{Fi} = (F_{ei} - K_{di}v_{Fi}^2 - d_{mi}) + C_{Fi} \left[ \arctan\left(\frac{v_{Si} + l_{Fi}\dot{\epsilon}_i}{v_{Fi}}\right) - \delta_{Fi} \right] \sin \delta_{Fi} \quad (4.44)$$

$$m_i a_{Si} = -C_{Fi} \left[ \arctan\left(\frac{v_{Si} + l_{Fi}\dot{\epsilon}_i}{v_{Fi}}\right) - \delta_{Fi} \right] \cos \delta_{Fi} - C_{Ri} \arctan\left(\frac{v_{Si} - l_{Ri}\dot{\epsilon}_i}{v_{Fi}}\right). \quad (4.45)$$

Considering the rate of change of the angular momentum of the  $i$ -th vehicle about the vertical axis through its center of mass (i.e., the  $\hat{e}_{Zi}$ -axis), we get

$$I_{Zi}\ddot{\epsilon}_i\hat{e}_{Zi} = \vec{\tau}_{ei} + \vec{\tau}_{drag,i} + \vec{\tau}_{tires,i} \quad (4.46)$$

where  $\vec{\tau}_{ei}$  denotes the torque produced by the driving force of the  $i$ -th vehicle's engine ( $\vec{F}_{ei}$ ) about the  $\hat{e}_{Zi}$ -axis;  $\vec{\tau}_{drag,i}$  denotes the torque produced by the  $i$ -th vehicle's drag forces ( $\vec{F}_{drag,i}$ ) about the  $\hat{e}_{Zi}$ -axis; and  $\vec{\tau}_{tires,i}$  denotes the torque produced by the external forces on the  $i$ -th vehicle's tires ( $\vec{F}_{tires,i}$ ).

We assume that  $\vec{F}_{drag,i}$  is applied to the  $i$ -th vehicle's center of mass ( $c_i$ ) and that the supporting line of  $\vec{F}_{ei}$  goes through  $c_i$ , hence

$$\vec{\tau}_{ei} = \vec{\tau}_{drag,i} = \vec{0}. \quad (4.47)$$

Hence, from (4.46), (4.47), and Figure 4.4, we note

$$I_{Zi}\ddot{\epsilon}_i\hat{e}_{Zi} := \vec{\tau}_{tires,i} := \vec{\tau}_{Fi} + \vec{\tau}_{Ri} \quad (4.48)$$

where  $\vec{\tau}_{Fi}$  denotes the torque produced by the external forces on the  $i$ -th vehicle's front tires ( $\vec{F}_{Fi}$ ); and  $\vec{\tau}_{Ri}$  denotes the torque produced by the external forces on the  $i$ -th vehicle's rear tires ( $\vec{F}_{Ri}$ ). Hence, we have

$$\vec{\tau}_{Fi} = l_{Fi}\hat{e}_{Fi} \times \vec{F}_{Fi} \quad (4.49)$$

$$\vec{\tau}_{Ri} = -l_{Ri}\hat{e}_{Fi} \times \vec{F}_{Ri}. \quad (4.50)$$

In (4.49)-(4.50), we have used  $\times$  to denote cross-product of two vectors in  $R^3$ . Using the expressions for  $\vec{F}_{Fi}$ ,  $\vec{F}_{Ri}$  (equations (4.37)-(4.38)),  $\alpha_{Fi}$ ,  $\alpha_{Ri}$  (equations (4.42)-(4.43)), and noting that  $\hat{e}_{Zi} := \hat{e}_{Fi} \times \hat{e}_{Si}$ , we get

$$\vec{\tau}_{Fi} = -C_{Fi}l_{Fi} \left[ \arctan\left(\frac{v_{Si} + l_{Fi}\dot{\epsilon}_i}{v_{Fi}}\right) - \delta_{Fi} \right] \cos \delta_{Fi} \quad \hat{e}_{Zi} \quad (4.51)$$

$$\vec{\tau}_{Ri} = C_{Ri}l_{Ri} \arctan\left(\frac{v_{Si} - l_{Ri}\dot{\epsilon}_i}{v_{Fi}}\right) \quad \hat{e}_{Zi}. \quad (4.52)$$

Substituting the expressions for  $\vec{\tau}_{Fi}$ ,  $\vec{\tau}_{Ri}$  from (4.51)-(4.52) into (4.48), we get

$$I_{Zi}\ddot{\epsilon}_i = -C_{Fi}l_{Fi} \left[ \arctan\left(\frac{v_{Si} + l_{Fi}\dot{\epsilon}_i}{v_{Fi}}\right) - \delta_{Fi} \right] \cos \delta_{Fi} + C_{Ri}l_{Ri} \arctan\left(\frac{v_{Si} - l_{Ri}\dot{\epsilon}_i}{v_{Fi}}\right). \quad (4.53)$$

Equations (4.29), (4.30), (4.44), (4.45), and (4.53) represent the *combined* longitudinal and lateral dynamics: the control inputs are  $u_i$ , throttle command input to the  $i$ -th vehicle's engine, and  $\delta_{command,i}$ ,  $i$ -th vehicle's steering command input. In the next section, we use these equations to propose control laws for a platoon of vehicles accelerating on a *curved* lane of a highway.

## 4.5 Control laws

Given a platoon of  $N$  vehicles following a lead vehicle on a curved lane of a highway, we would like to design control laws which, at all times, maintain a close-spacing between successive vehicles in the platoon and keep all the vehicles close to the center of this lane. More precisely, for  $i = 1, 2, \dots, N$ , we wish to design control laws for the throttle input to the  $i$ -th vehicle's engine,  $u_i$ , and the steering command input,  $\delta_{command,i}$ , such that when the lead vehicle accelerates (or decelerates), over some interval say  $[0, T]$ , then a)  $\Delta_{i-1,i}(t) \rightarrow 0$  as  $t \rightarrow \infty$ , b)  $\Delta_{i,lat}(t) \rightarrow 0$  as  $t \rightarrow \infty$ , and c)  $\max_t |\Delta_{i,lat}(t)|$  and  $\max_t |\Delta_{i-1,i}(t)|$  are small.

To achieve these control objectives, we use the kinematic equations (4.13) and the dynamic equations (4.29), (4.30), (4.44), (4.45), and (4.53) to design a lateral control law for the  $i$ -th vehicle ( $i = 1, 2, \dots, N$ ); furthermore, we use the kinematic equation (4.28) and the dynamic equations (4.29), (4.30), (4.44), (4.45), and (4.53) to design longitudinal control laws for the platoon.

**Lateral control law for the  $i$ -th vehicle ( $i = 1, 2, \dots, N$ )** Substituting the expressions for  $\dot{a}_{Fi}$  and  $\dot{a}_{Si}$ , obtained by differentiating both sides of (4.44) and (4.45), into (4.13) and

rearranging terms, we get

$$\begin{aligned}
\ddot{\Delta}_{i,lat} = & \left\{ \frac{\dot{F}_{ei} - 2K_{di}v_{Fi}\dot{v}_{Fi}}{m_i} + \dot{v}_{Si}\dot{\epsilon}_{di} + v_{Si}\ddot{\epsilon}_{di} \right\} \sin(\epsilon_i - \epsilon_{di}) \\
& + \left\{ \left[ \frac{C_{Ri}}{m_i} \arctan\left(\frac{v_{Si} - l_{Ri}\dot{\epsilon}_i}{v_{Fi}}\right) + v_{Fi}\dot{\epsilon}_{di} \right] (\dot{\epsilon}_i - \dot{\epsilon}_{di}) \right\} \sin(\epsilon_i - \epsilon_{di}) \\
& + \left\{ \left[ \frac{F_{ei} - K_{di}v_{Fi}^2 - d_{mi}}{m_i} + v_{Si}\dot{\epsilon}_{di} \right] (\dot{\epsilon}_i - \dot{\epsilon}_{di}) \right\} \cos(\epsilon_i - \epsilon_{di}) \\
& + \left\{ -\frac{C_{Ri}}{m_i} \frac{(\dot{v}_{Si} - l_{Ri}\ddot{\epsilon}_i)v_{Fi} - (v_{Si} - l_{Ri}\dot{\epsilon}_i)\dot{v}_{Fi}}{v_{Fi}^2 + (v_{Si} - l_{Ri}\dot{\epsilon}_i)^2} \right\} \cos(\epsilon_i - \epsilon_{di}) \\
& + \left\{ -\dot{v}_{Fi}\dot{\epsilon}_{di} - v_{Fi}\ddot{\epsilon}_{di} \right\} \cos(\epsilon_i - \epsilon_{di}) \\
& + \left\{ \frac{C_{Fi}}{m_i} \left[ \arctan\left(\frac{v_{Si} + l_{Fi}\dot{\epsilon}_i}{v_{Fi}}\right) - \delta_{Fi} \right] (\dot{\delta}_{Fi} + \dot{\epsilon}_i - \dot{\epsilon}_{di}) \right\} \sin(\delta_{Fi} + \epsilon_i - \epsilon_{di}) \\
& + \left\{ -\frac{C_{Fi}}{m_i} \frac{(\dot{v}_{Si} + l_{Fi}\ddot{\epsilon}_i)v_{Fi} - (v_{Si} + l_{Fi}\dot{\epsilon}_i)\dot{v}_{Fi}}{v_{Fi}^2 + (v_{Si} + l_{Fi}\dot{\epsilon}_i)^2} + \frac{C_{Fi}}{m_i} \dot{\delta}_{Fi} \right\} \cos(\delta_{Fi} + \epsilon_i - \epsilon_{di}).
\end{aligned} \tag{4.54}$$

Substituting the expression for  $\dot{\delta}_{Fi}$  from (4.30) into (4.54) and approximating

(Lat 1)  $\sin(\epsilon_i - \epsilon_{di}) \approx 0, \cos(\epsilon_i - \epsilon_{di}) \approx 1,$

(Lat 2)  $\sin(\delta_{Fi} + \epsilon_i - \epsilon_{di}) \approx 0, \cos(\delta_{Fi} + \epsilon_i - \epsilon_{di}) \approx 1,$

we get

$$\begin{aligned}
\ddot{\Delta}_{i,lat} \approx & \left[ \frac{F_{ei} - K_{di}v_{Fi}^2 - d_{mi}}{m_i} + v_{Si}\dot{\epsilon}_{di} \right] (\dot{\epsilon}_i - \dot{\epsilon}_{di}) - \frac{C_{Ri}}{m_i} \frac{(\dot{v}_{Si} - l_{Ri}\ddot{\epsilon}_i)v_{Fi} - (v_{Si} - l_{Ri}\dot{\epsilon}_i)\dot{v}_{Fi}}{v_{Fi}^2 + (v_{Si} - l_{Ri}\dot{\epsilon}_i)^2} \\
& - \dot{v}_{Fi}\dot{\epsilon}_{di} - v_{Fi}\ddot{\epsilon}_{di} - \frac{C_{Fi}}{m_i} \frac{(\dot{v}_{Si} + l_{Fi}\ddot{\epsilon}_i)v_{Fi} - (v_{Si} + l_{Fi}\dot{\epsilon}_i)\dot{v}_{Fi}}{v_{Fi}^2 + (v_{Si} + l_{Fi}\dot{\epsilon}_i)^2} \\
& - \frac{C_{Fi}}{m_i \tau_{ai}} \delta_{Fi} + \frac{C_{Fi}}{m_i \tau_{ai}} \delta_{command,i}.
\end{aligned} \tag{4.55}$$

Using (4.55) we propose the following lateral control law  $\delta_{command,i}$  for the  $i$ -th vehicle:

$$\begin{aligned}
\delta_{command,i} = & \frac{m_i \tau_{ai}}{C_{Fi}} \left\{ - \left[ \frac{F_{ei} - K_{di}v_{Fi}^2 - d_{mi}}{m_i} + v_{Si}\dot{\epsilon}_{di} \right] (\dot{\epsilon}_i - \dot{\epsilon}_{di}) \right\} \\
& + \frac{m_i \tau_{ai}}{C_{Fi}} \left\{ \frac{C_{Ri}}{m_i} \frac{(\dot{v}_{Si} - l_{Ri}\ddot{\epsilon}_i)v_{Fi} - (v_{Si} - l_{Ri}\dot{\epsilon}_i)\dot{v}_{Fi}}{v_{Fi}^2 + (v_{Si} - l_{Ri}\dot{\epsilon}_i)^2} + \dot{v}_{Fi}\dot{\epsilon}_{di} + v_{Fi}\ddot{\epsilon}_{di} \right\} \\
& + \frac{m_i \tau_{ai}}{C_{Fi}} \left\{ \frac{C_{Fi}}{m_i} \frac{(\dot{v}_{Si} + l_{Fi}\ddot{\epsilon}_i)v_{Fi} - (v_{Si} + l_{Fi}\dot{\epsilon}_i)\dot{v}_{Fi}}{v_{Fi}^2 + (v_{Si} + l_{Fi}\dot{\epsilon}_i)^2} + \frac{C_{Fi}}{m_i \tau_{ai}} \dot{\delta}_{Fi} \right\} \\
& + \frac{m_i \tau_{ai}}{C_{Fi}} \left\{ -c_{\bar{\Delta},lat}\ddot{\Delta}_{i,lat} - c_{\dot{\Delta},lat}\dot{\Delta}_{i,lat} - c_{\Delta,lat}\Delta_{i,lat} \right\}
\end{aligned} \tag{4.56}$$

where  $c_{\bar{\Delta},lat}$ ,  $c_{\dot{\Delta},lat}$ , and  $c_{\Delta,lat}$  are design constants chosen so as to make  $s^3 + c_{\bar{\Delta},lat}s^2 + c_{\dot{\Delta},lat}s + c_{\Delta,lat}$  a Hurwitz polynomial giving rise to appropriate time constants.

Similar to computed-torque control laws in robotics, control law (4.56) cancels the nonlinearities in (4.55) due to road geometry, engine dynamics, and longitudinal and lateral dynamics: substituting the expression for  $\delta_{command,i}$  from (4.56) into (4.55), we get

$$\ddot{\Delta}_{i,lat} \approx -c_{\bar{\Delta},lat}\ddot{\Delta}_{i,lat} - c_{\dot{\Delta},lat}\dot{\Delta}_{i,lat} - c_{\Delta,lat}\Delta_{lat}. \quad (4.57)$$

Hence, the closed-loop dynamics of (4.55) under control law (4.56) is exponentially stable.

To implement this control law, we need to either estimate or measure the nonlinearities in (4.55). At the present time, some of these measurements are done by sensors and we propose to estimate the others by appropriate estimators. (refer to the next section for a discussion on implementation issues.)

Approximations (Lat 1) and (Lat 2) have proved useful in simplifying the lateral dynamics, for roads with large radius of curvature, under nominal operation.

**Longitudinal control laws for a platoon of vehicles** In this system-level study, we have assumed that longitudinal dynamics of a platoon of closely-spaced vehicles on a road with suitably large radius of curvature is approximately the same as the longitudinal dynamics of this platoon on a straight road. More specifically, we have made the following approximations:

(Long 1)  $\cos(\theta_{i-1,i} - \epsilon_{i-1}) \approx 1$  for  $i = 1, 2, \dots, N$ ;

(Long 2)  $\sin(\theta_{i-1,i} - \epsilon_{i-1}) \approx 0$  for  $i = 1, 2, \dots, N$ ;

(Long 3)  $\cos(\theta_{i-1,i} - \epsilon_i) \approx 1$  for  $i = 1, 2, \dots, N$ ;

(Long 4)  $\sin(\theta_{i-1,i} - \epsilon_i) \approx 0$  for  $i = 1, 2, \dots, N$ ;

(Long 5)  $\dot{\epsilon}_i \approx 0$  for  $i = 0, 1, \dots, N$ ;

(Long 6)  $\dot{\theta}_{i-1,i} \approx 0$  for  $i = 1, 2, \dots, N$ ;

(Long 7)  $\ddot{\theta}_{i-1,i} \approx 0$  for  $i = 1, 2, \dots, N$ ;

(Long 8)  $\sin \delta_{F,i} \approx 0$  for  $i = 1, 2, \dots, N$ .

Under the approximations (Long 1)-(Long 7), equation (4.28) reduces to:

$$\ddot{\Delta}_{i-1,i} \approx \dot{a}_{F_{i-1}} - \dot{a}_{F_i} \quad (4.58)$$

for the  $i$ -th vehicle ( $i = 1, 2, \dots, N$ ) in the platoon.

From (4.44) and (Long 8) we get, for  $i = 1, 2, \dots, N$ ,

$$m_i a_{F_i} \approx F_{ei} - K_{di} v_{F_i}^2 - d_{mi}. \quad (4.59)$$

Differentiating both sides of (4.59) with respect to  $t$ , substituting the expressions for  $F_{ei}$  from (4.59) and  $\dot{F}_{ei}$  from (4.29), and noting that under assumption (Long 5) equation (4.11) reduces to  $\dot{v}_{F_i} \approx a_{F_i}$ , we get, for  $i = 1, 2, \dots, N$ ,

$$m_i \ddot{a}_{F_i} \approx -2K_{di} v_{F_i} a_{F_i} - \frac{1}{\tau_i(v_{F_i}, v_{Si})} \left[ m_i a_{F_i} + K_{di} v_{F_i}^2 + d_{mi} \right] + \frac{u_i}{\tau_i(v_{F_i}, v_{Si})}. \quad (4.60)$$

Based on (4.60), we use the following nonlinear control law for the  $i$ -th vehicle in the platoon ( $i = 1, 2, \dots, N$ )

$$u_i = m_i \tau_i(v_{F_i}, v_{Si}) \left\{ \tilde{c}_i + 2 \frac{K_{di} v_{F_i} a_{F_i}}{m_i} + \frac{1}{\tau_i(v_{F_i}, v_{Si})} \left[ a_{F_i} + \frac{K_{di} v_{F_i}^2}{m_i} + \frac{d_{mi}}{m_i} \right] \right\} \quad (4.61)$$

where for  $i = 1, 2, \dots, N$ ,  $\tilde{c}_i$  is an exogenous input to the  $i$ -th vehicle's longitudinal dynamics.

Substituting the expression for  $u_i$  from (4.61) into (4.60) we get, for  $i = 1, 2, \dots, N$ ,

$$\dot{a}_{F_i} \approx \tilde{c}_i. \quad (4.62)$$

Similar to our previous work on longitudinal control of a platoon of vehicles on a straight lane of a highway in chapter 2, [41],[47], we propose the following control laws  $\tilde{c}_i$  ( $i = 1, 2, \dots, N$ ):

$$\tilde{c}_1 := c_{p1} \Delta_{0,1} + c_{v1} \dot{\Delta}_{0,1} + c_{a1} \ddot{\Delta}_{0,1} + k_{v1} [v_{F0} - v_{F0}(0-)] + k_{a1} a_{F0} \quad (4.63)$$

for the first vehicle, and

$$\tilde{c}_i := c_p \Delta_{i-1,i} + c_v \dot{\Delta}_{i-1,i} + c_a \ddot{\Delta}_{i-1,i} + k_v [v_{F0} - v_{F_i}] + k_a [a_{F0} - a_{F_i}] \quad (4.64)$$

for the  $i$ -th vehicle ( $i = 2, 3, \dots, N$ ). In (4.63),  $\Delta_{0,1}$  denotes the deviation of the first vehicle's position from its desired value  $\Delta_{desired}$ .

In (4.63) and (4.64), constants  $c_{p1}, c_{v1}, c_{a1}, k_{v1}$ ,  $k_{a1}, c_p, c_v, c_a, k_v$ , and  $k_a$  are chosen based on design considerations for longitudinal control of a platoon (see chapter 2, [41],[47] for a thorough discussion).

In the next section, we discuss some of the implementation issues for using longitudinal control laws (4.61), with  $\tilde{c}_i$  as in (4.63)- (4.64).

## 4.6 Implementation issues

In this section, we discuss sensors, estimators, the guidance system, and the communication link needed to implement the lateral control law (4.56) and longitudinal control laws (4.61), (4.63)-(4.64). In addition, we briefly discuss some alternative methods for implementing these control laws.

We need sensors to measure both velocity components  $v_{F_i}$  and  $v_{S_i}$ , both acceleration components  $a_{F_i}$  and  $a_{S_i}$ , the yaw rate  $\dot{\epsilon}_i$ , the front steering angle  $\delta_{F_i}$ , the lateral deviation  $\Delta_{i,lat}$ , and the deviation of the  $i$ -th vehicle's position from its desired value ( $\Delta_{i-1,i}$ ). Using the measured values of  $v_{F_i}$ ,  $v_{S_i}$ ,  $a_{F_i}$ ,  $a_{S_i}$ , and  $\dot{\epsilon}_i$ , we can use (4.11)-(4.12) to estimate the values of  $\dot{v}_{F_i}$  and  $\dot{v}_{S_i}$ . We assume that we know the vehicle's mass  $m_i$ , the drag coefficient  $K_{di}$ , the mechanical drag  $d_{mi}$ , the moment of inertia about the  $\hat{e}_{Z_i}$ -axis ( $I_{Z_i}$ ), the distances  $l_{Fi}$ ,  $l_{Ri}$ ,  $\tilde{l}_{Fi}$ , and  $\tilde{l}_{Ri}$  (see Figure 4.3), and the  $i$ -th vehicle's engine time-lag as a function of its speed ( $\tau_i(\cdot)$ ). We assume the steering actuator's time-lag ( $\tau_{ai}$ ) is known. By integrating the measured value of  $\dot{\epsilon}_i$  and knowing the initial values of the  $i$ -th vehicle's yaw angle ( $\epsilon_i(0-)$ ), we can estimate  $\epsilon_i$ . We can estimate the value of  $\ddot{\epsilon}_i$  by two different methods: a) by appropriately averaging the finite differences of the measured values of  $\dot{\epsilon}_i$ , and b) by computing the expression for  $\ddot{\epsilon}_i$  from (4.53). Similarly, by appropriately averaging the finite differences of the measured values of  $\Delta_{i,lat}$  and  $\Delta_{i-1,i}$ , we can estimate  $\dot{\Delta}_{i,lat}$ ,  $\ddot{\Delta}_{i,lat}$ ,  $\dot{\Delta}_{i-1,i}$ , and  $\ddot{\Delta}_{i-1,i}$ . We need parameter identifiers to estimate the  $i$ -th vehicle's cornering stiffnesses ( $C_{Fi}$  and  $C_{Ri}$ ). Using (4.44), we can estimate the values of the driving force produced by the  $i$ -th vehicle's engine ( $F_{ei}$ ).

We assume that each vehicle in the platoon has a road map

$$\vec{r}_d = \vec{\phi}(s_d), \quad (4.65)$$

where  $\vec{r}_d$  denotes the  $(x, y)$ -coordinates of a point on the lane center and  $\vec{\phi}(\cdot)$  is a parameterization of the lane-center line  $\mathcal{L}$  as a function of arc length  $s_d$ . Given this road map (4.65), we can obtain unit tangent and unit normal vectors ( $\vec{t}$  and  $\vec{n}$ , respectively) at any point on  $\mathcal{L}$  as functions of arc length. We can also compute the radius of curvature at any point. Given the location of the  $i$ -th vehicle's center of mass ( $\vec{r}_{ci}$ ), the initial value of  $s_{di}(0-)$ , the measured values of  $\dot{\epsilon}_i$ ,  $v_{F_i}$ , and  $v_{S_i}$  (or alternatively, the measured values of  $a_{F_i}$  and  $a_{S_i}$ ), and the measured values of  $\Delta_{i,lat}$  and its time derivatives, we can estimate  $s_{di}$ . (See Appendix.) Thus, we can compute the values of  $\epsilon_{di}$ ,  $\dot{\epsilon}_{di}$ , and  $\ddot{\epsilon}_{di}$ .

Components of the velocity of the center of mass of the lead vehicle ( $v_{F0}$ ) and acceleration ( $a_{F0}$ ), used in the  $i$ -th vehicle's longitudinal control laws (4.63)-(4.64), are transmitted to the  $i$ -th vehicle via a communication link [48]. At the present time, system designers view such a communication link indispensable for safety, merging, and demerging maneuvers [14]. For a discussion on longitudinal control laws on a straight lane which do not use a communication link refer to [46].

## 4.7 Simulation Results

To check the performance of the proposed control laws, we ran simulations for a platoon of 5 vehicles following a lead vehicle (i.e.,  $N = 5$ ) consisting of three *different types* of vehicles. In all simulations conducted, all the vehicles were initially traveling at a speed of 20 m/s (i.e., about 45 m.p.h.) on a straight lane of highway; lateral deviation of all vehicles' center of masses from the lane center  $\mathcal{L}$  was zero (i.e., for  $i = 1, 2, \dots, 5$ ,  $\Delta_{i,lat}(0-) = 0$ ) and all vehicles were traveling at their allotted slot on the lane (i.e., for  $i = 1, 2, \dots, 5$ ,  $\Delta_{i-1,i}(0-) = 0$ ).

**Lane description** Figure 4.5 shows the lane center  $\mathcal{L}$  (a curve in  $R^2$  specified by the map  $x \mapsto \hat{y}(x)$ ) and its derivatives as functions of  $x$ . The lane center consists of three sections: the beginning and the end sections are straight and the middle section is a slalom curve. More specifically, the lane center  $\mathcal{L}$  is described as follows (SI units throughout)

$$\hat{y}(x) = \begin{cases} 0 & x < 20 \\ \left[2 - 2 \cos\left(\frac{\pi x}{90} - \frac{2\pi}{9}\right)\right] \left[\tanh\left(\frac{x-20}{18}\right)\right]^3 & 20 < x < 290 \\ \left[2 - 2 \cos\left(\frac{\pi x}{90} - \frac{2\pi}{9}\right)\right] \left[\tanh\left(\frac{560-x}{18}\right)\right]^3 & 290 < x < 560 \\ 0 & x > 560, \end{cases} \quad (4.66)$$

hence this choice of  $\mathcal{L}$  is at least three times continuously differentiable. (See also Figure 4.5.) Hence, the lateral control law (4.56) does not contain any discontinuities due to non-smooth road geometry. In addition, from the plots of  $\hat{y}''(\cdot)$  and  $\hat{y}'(\cdot)$  in Figure 4.5, we note that the radius of curvature of  $\mathcal{L}$  is larger than 250 m.

**Vehicle parameters** In all simulations, the platoon consisted of three different types of vehicles: the lead vehicle, the first, and the fourth vehicles were of the same type; the second and the fifth vehicles were of the same type. Table 4.1 shows the vehicle parameters used in the simulations: some of the parameters of the lead vehicle, the first vehicle, and

vehicle $i$	0	1	2	3	4	5
curb mass (kg)	1175	1175	1760	1550	1175	1760
passengers' and luggage mass (kg)	270	270	200	250	270	200
$m_i$ (kg)	1445	1445	1960	1800	1445	1960
$\tau_i$ (s)	0.2	0.2	0.25	0.2	0.2	0.25
$K_{di}$ (kg/m)	0.44	0.44	0.49	0.51	0.44	0.49
$d_{mi}$ (N)	352	352	392	408	352	392
$F_{ci}(0-)$ (N)	528	528	588	612	528	588
$C_{Fi}$ (N/rad)	135200	135200	90000	84000	135200	90000
$C_{Ri}$ (N/rad)	135200	135200	80000	84000	135200	80000
$I_{Zi}$ (kg.m <sup>2</sup> )	2094	2094	2820	3100	2094	2820
$l_{Fi}$ (m)	1.54	1.54	1.97	1.82	1.54	1.97
$l_{Ri}$ (m)	2.46	2.46	2.03	2.18	2.46	2.03
$l_{F_i}$ (m)	0.88	0.88	1.37	1.15	0.88	1.37
$l_{R_i}$ (m)	1.79	1.79	1.43	1.51	1.79	1.43

Table 4.1: Vehicle parameters used in simulations

the fourth vehicle correspond to a vehicle in [56]; some of the parameters of the second and the fifth vehicles correspond to a vehicle in [24]; some of the parameters of the third vehicle correspond to a vehicle in [30].

The steering actuator's time lag was 30 ms for all the vehicles. (i.e., for  $i = 1, 2, \dots, 5$ ,  $\tau_{ai} = 0.030$  s)

**Controller parameters** In all simulations, the lateral controller parameters in (4.56) were chosen as follows:  $c_{\Delta,lat} = 30$ ,  $c_{\dot{\Delta},lat} = 300$ , and  $c_{\Delta,lat} = 1000$ . Under this choice of parameters, the closed-loop dynamics of  $\Delta_{i,lat}$ , for  $i = 1, 2, \dots, 5$ , were governed by the transfer function  $\frac{1}{(s+10)^3}$ .

The longitudinal parameters in (4.63)-(4.64) were chosen as follows:  $c_{a1} = 15$ ,  $c_{v1} = 74$ ,  $c_{p1} = 120$ ,  $k_{a1} = -3.03$ ,  $k_{v1} = -0.05$ ,  $c_a = 5$ ,  $c_v = 49$ ,  $c_p = 120$ ,  $k_a = 10$ , and  $k_v = 25$ . This choice of parameters was suggested to us by our previous studies in longitudinal control of a platoon of vehicles on a straight lane of a highway. (see chapter 2, [41],[47])

**Maneuver description** When the lead vehicle arrives at the curved section of the lane shown in Figure 4.5, its throttle command input increases linearly from its initial value of 528 N, at a rate of 736 N/s, until it reaches its maximum value of 2000 N after 2 seconds; then, it remains constant at 2000 N for 7 seconds; finally, the throttle input decreases

linearly, at a rate of  $-736 \text{ N/s}$ , until it reaches its final value of  $528 \text{ N}$  in 2 seconds; see Figure 4.6. During the first 11 seconds, the lead vehicle accelerates until its speed reaches the maximum value of  $28.5 \text{ m/s}$  (i.e., about 64 m.p.h.). During this part of the maneuver, the magnitude of acceleration of the lead vehicle is less than  $1 \text{ m/s}^2$  and its jerk is less than  $0.5 \text{ m/s}^3$ . After reaching its maximum speed in the first 11 seconds, the lead vehicle gradually decelerates due to aerodynamic drag and mechanical drag.

Figure 4.7 shows the longitudinal and transversal components of the  $i$ -th vehicle's acceleration, in this maneuver, for  $i = 1, 2, \dots, 5$ . As shown in Figure 4.7, the longitudinal components of the  $i$ -th vehicle's acceleration ( $a_{F_i}$ , for  $i = 1, 2, \dots, 5$ ) closely follow the longitudinal component of the lead vehicle's acceleration ( $a_{F_0}$ ); moreover, the transversal components of the  $i$ -th vehicle's acceleration ( $a_{S_i}$ , for  $i = 1, 2, \dots, 5$ ) closely resemble the transversal component of the lead vehicle's acceleration ( $a_{S_0}$ ) delayed in time. Both the longitudinal and transversal components of the  $i$ -th vehicle's acceleration, for  $i = 1, 2, \dots, 5$ , are within acceptable comfort limits.

Figure 4.8 shows the yaw angle  $\epsilon_i$  and  $\epsilon_{di}$  (for  $i = 1, 5$ ) in this maneuver. Under the above control laws, the value of  $\epsilon_i$  closely follows  $\epsilon_{di}$ , for  $i = 1, 2, \dots, 5$ . The difference between  $\epsilon_i$  and  $\epsilon_{di}$  depends on the  $i$ -th vehicle's parameters (e.g., moment of inertia of the  $i$ -th vehicle about  $\hat{e}_{Z_i}$ -axis,  $I_{Z_i}$ , tires' cornering stiffnesses,  $C_{F_i}$  and  $C_{R_i}$ , etc...) For all the vehicles in this study,  $\max_t |\epsilon_i(t) - \epsilon_{di}(t)| \leq 0.032 \text{ rad}$ .

Lateral deviation of the  $i$ -th vehicle's center of mass from the lane center ( $\Delta_{i,lat}$ , for  $i = 1, 2, \dots, 5$ ) is shown in Figure 4.9. For this maneuver, the magnitude of the lateral deviation of the  $i$ -th vehicle, for  $i = 1, 2, \dots, 5$ , was much less than  $0.01 \text{ m}$  (i.e.,  $\max_t |\Delta_{i,lat}(t)| \leq 0.01 \text{ m}$ , for  $i = 1, 2, \dots, 5$ ).

Figure 4.10 shows the longitudinal deviation of the  $i$ -th vehicle from its assigned slot ( $\Delta_{i-1,i}$ , for  $i = 1, 2, \dots, 5$ ): this magnitude is less than  $0.1 \text{ m}$  (i.e.,  $\max_t |\Delta_{i-1,i}(t)| \leq 0.1 \text{ m}$ , for  $i = 1, 2, \dots, 5$ ). Note that, for  $i \geq 2$ ,  $\max_t |\Delta_{i-1,i}(t)|$  gets larger as one goes down the platoon. We believe that this drift in magnitude of  $\Delta_{i-1,i}$  is mainly due to numerical errors in successively integrating  $\ddot{\Delta}_{i-1,i}$  to obtain  $\Delta_{i-1,i}$ .

Based on these simulations, we conclude that the proposed combined longitudinal and lateral control laws perform well for roads with suitably large radius of curvature *under nominal operation*.

## 4.8 Conclusions

We have considered the problem of combined longitudinal and lateral control of a platoon of vehicles accelerating on a curved lane of a highway. Based on nonlinear models of vehicles' combined longitudinal and lateral dynamics, we have proposed lateral control laws for each vehicle in the platoon and longitudinal control laws for a platoon of vehicles. For the  $i$ -th vehicle in the platoon ( $i = 1, 2, \dots, N$ ), we proposed a *nonlinear* lateral control law which cancels the nonlinearities due to road geometry, engine dynamics, and longitudinal and lateral dynamics, and results in a closed-loop dynamics for  $\Delta_{i,lat}$  which is exponentially stable with appropriate time constants. In the case of longitudinal control of a platoon of vehicles, we assumed that longitudinal dynamics of a platoon of closely-spaced vehicles on a road with suitably large radius of curvature is approximately the same as the longitudinal dynamics of this platoon on a straight road. Thus, we proposed longitudinal control laws similar to the longitudinal control laws for a platoon of vehicles on a straight lane of a highway as in chapter 2,[41],[47].

Simulation results show that the proposed control laws perform well, for roads with suitably large radius of curvature, under nominal operation. More specifically, these simulations show that when the lead vehicle accelerates from  $20 \text{ m/s}$  to  $28 \text{ m/s}$ , at a maximum rate of  $1 \text{ m/s}^2$ , the magnitude of the lateral deviation of each vehicle in the platoon remains well below  $0.01 \text{ m}$ ; furthermore, the magnitude of the longitudinal deviation of each vehicle from its assigned slot is less than  $0.1 \text{ m}$ .

The performance shown in Figures 4.7, 4.8, 4.9, and 4.10 is based on the assumption that the following measurements are available in the  $i$ -th vehicle:  $v_{F_i}$ ,  $v_{S_i}$ ,  $a_{F_i}$ ,  $a_{S_i}$ ,  $\dot{\epsilon}_i$ ,  $\Delta_{i,lat}$ , and  $\Delta_{i-1,i}$ . Hence, the longitudinal and lateral control laws for each vehicle in the platoon are *decentralized* in that these control laws use local measurements on each vehicle to compute the control input for the vehicle.

## 4.9 Appendix

In this section, we present three different methods for computing the arc length traversed by point  $d_i$  on  $\mathcal{L}$  (for  $i = 1, 2, \dots, N$ ). Then, we describe the required measurements for applying each method.

**Problem** Consider the  $i$ -th vehicle in a platoon ( $i = 1, 2, \dots, N$ ). For any fixed time  $t$ ,

the location of the  $i$ -th vehicle's center of mass ( $c_i$ ) is specified by  $\vec{r}_{ci}(t)$ . (See Figure 4.1) The center lane is a curve  $\mathcal{L}$  specified by the road map

$$\vec{r}_d = \vec{\phi}(s_d), \quad (4.67)$$

where  $s_d$  is the arc length. Given  $\vec{r}_{ci}(t)$ , we draw the osculating circle to  $\mathcal{L}$  centered at point  $c_i$ ; this circle is tangent to  $\mathcal{L}$  at a well-defined point  $d_i$  which we call reference point. We want to estimate  $s_{di}$  (i.e., the arc length traversed by the point  $d_i$  on  $\mathcal{L}$ ).

**Methods for estimating  $s_{di}$**  By definition of  $d_i$ , the function  $s \mapsto \|\vec{r}_{ci}(t) - \vec{\phi}(s)\|^2$  is minimized at  $s = s_{di}$  (i.e.,  $\|\vec{r}_{ci}(t) - \vec{\phi}(s_{di})\|^2 = \min_s \|\vec{r}_{ci}(t) - \vec{\phi}(s)\|^2$ ). Thus, we have

$$\frac{d}{ds} \|\vec{r}_{ci}(t) - \vec{\phi}(s_{di})\|^2 = 0. \quad (4.68)$$

From (4.68), we get

$$f_i(t, s_{di}) = 0, \quad (4.69)$$

where  $\tilde{s} \mapsto f_i(t, \tilde{s}) := \vec{t}(\tilde{s}) \cdot [\vec{r}_{ci}(t) - \vec{\phi}(\tilde{s})]$ .

**Method 1** Solve (4.69), say by Newton-Raphson. Equation (4.69) implicitly defines  $s_{di}$ : in order to estimate  $s_{di}$  from (4.69), we need to know  $\vec{r}_{ci}(t)$  (i.e., the location of the  $i$ -th vehicle's center of mass with respect to a fixed inertial reference frame,  $(O, x, y)$  in Figure 4.1) and the map (4.67).

**Method 2** Differentiating both sides of (4.69) with respect to  $t$ , we get

$$D_1 f_i(t, s_{di}) + D_2 f_i(t, s_{di}) \dot{s}_{di} = 0 \quad (4.70)$$

where  $D_k f_i$  denotes derivative of  $f_i$  with respect to the  $k$ -th variable ( $k = 1, 2$ ).

Computing the expressions for  $D_1 f_i(t, s_{di})$  and  $D_2 f_i(t, s_{di})$ , and using (4.70), we get

$$\dot{s}_{di} = \frac{v_{Fi}(t) \cos(\epsilon_i(t) - \epsilon_{di}(s_{di})) - v_{Si}(t) \sin(\epsilon_i(t) - \epsilon_{di}(s_{di}))}{1 - \kappa(s_{di}) \Delta_{i, lat}(t)}. \quad (4.71)$$

To obtain  $s_{di}$  by integrating (4.71), we need to measure  $v_{Fi}(t)$ ,  $v_{Si}(t)$ ,  $\epsilon_i(t)$ , and  $\Delta_{i, lat}(t)$ , and to know the initial condition  $s_{di}(0-)$ .

**Method 3** Differentiating both sides of (4.70) with respect to  $t$ , we get

$$D_1^2 f_i(t, s_{di}) + 2D_1 D_2 f_i(t, s_{di}) + D_2^2 f_i(t, s_{di}) \dot{s}_{di}^2 + D_2 f_i(t, s_{di}) \ddot{s}_{di} = 0. \quad (4.72)$$

Computing the expressions for  $D_1^2 f_i(t, s_{di})$ ,  $D_1 D_2 f_i(t, s_{di})$ ,  $D_2^2 f_i(t, s_{di})$ , and  $D_2 f_i(t, s_{di})$ , and using (4.72), we get

$$\ddot{s}_{di} = \frac{a_{Fi}(t) \cos(\epsilon_i(t) - \epsilon_{di}(s_{di})) - a_{Si}(t) \sin(\epsilon_i(t) - \epsilon_{di}(s_{di}))}{1 - \kappa(s_{di}) \Delta_{i, lat}(t)}$$

$$+ \frac{2\kappa(s_{di})\dot{\Delta}_{i,lat}(t)\dot{s}_{di} + \kappa'(s_{di})\Delta_{i,lat}(t)\dot{s}_{di}^2}{1 - \kappa(s_{di})\Delta_{i,lat}(t)}. \quad (4.73)$$

To obtain  $s_{di}$  by integrating (4.73), we need to measure  $a_{F_i}(t)$ ,  $a_{S_i}(t)$ ,  $\epsilon_i(t)$ ,  $\Delta_{i,lat}(t)$ , and  $\dot{\Delta}_{i,lat}(t)$ , and to know the initial conditions  $s_{di}(0-)$ ,  $\dot{s}_{di}(0-)$ .

**Practical considerations** Using (4.71) or (4.73), we can estimate  $s_{di}$  given appropriate sensors on board the  $i$ -th vehicle, a road map, and appropriate sensors on the road; however, using (4.69), we need to estimate the location of the  $i$ -th vehicle's center of mass with respect to a fixed inertial frame. The estimates of  $s_{di}$  obtained from numerically integrating the expressions in (4.71) or (4.73), are sensitive to measurement noise and errors in initial conditions. Hence, we need to update the value of  $s_{di}$  at appropriate intervals of time when using (4.71) or (4.73).

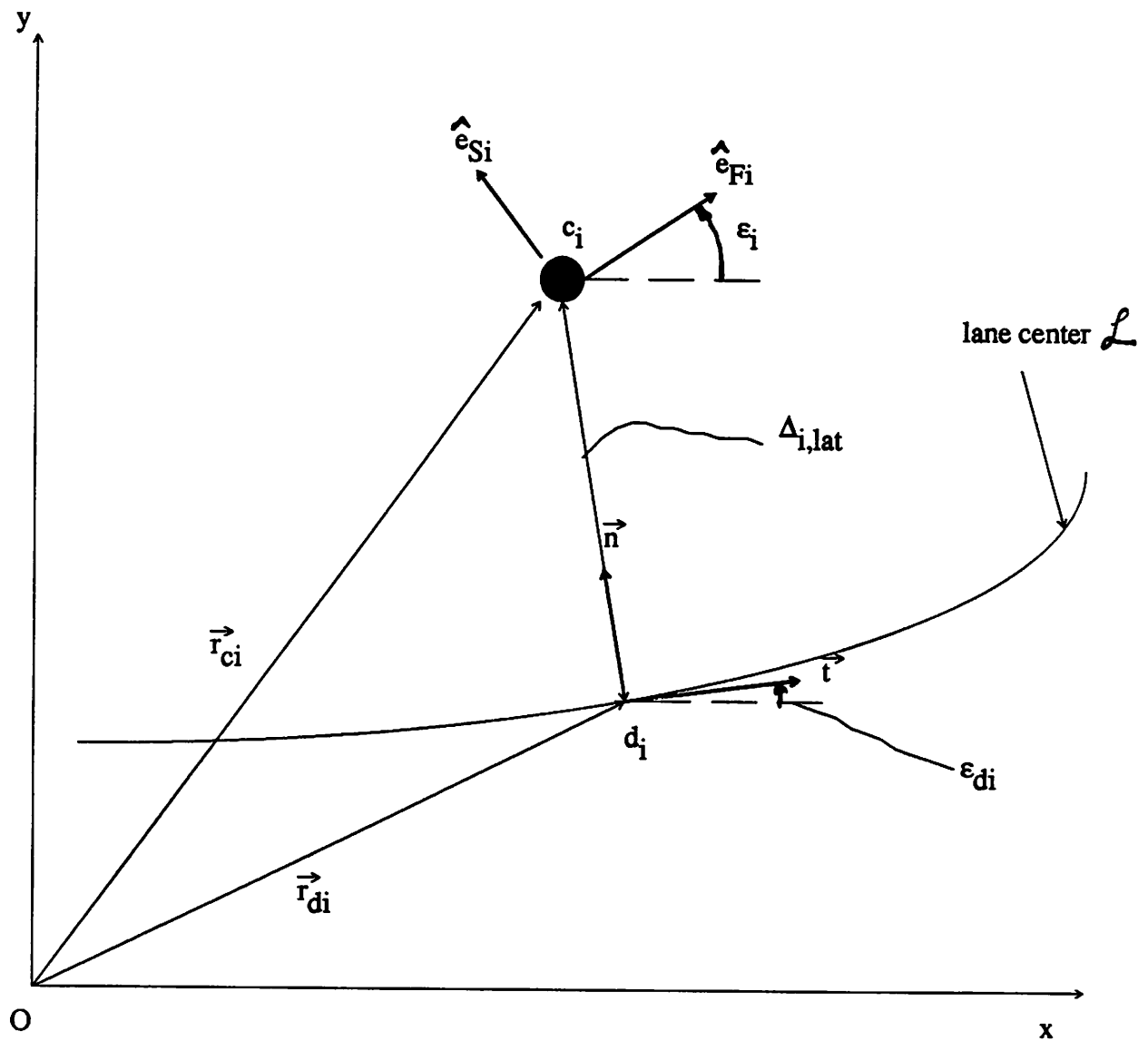


Figure 4.1: relevant quantities for the lateral dynamics of the  $i$ -th vehicle.

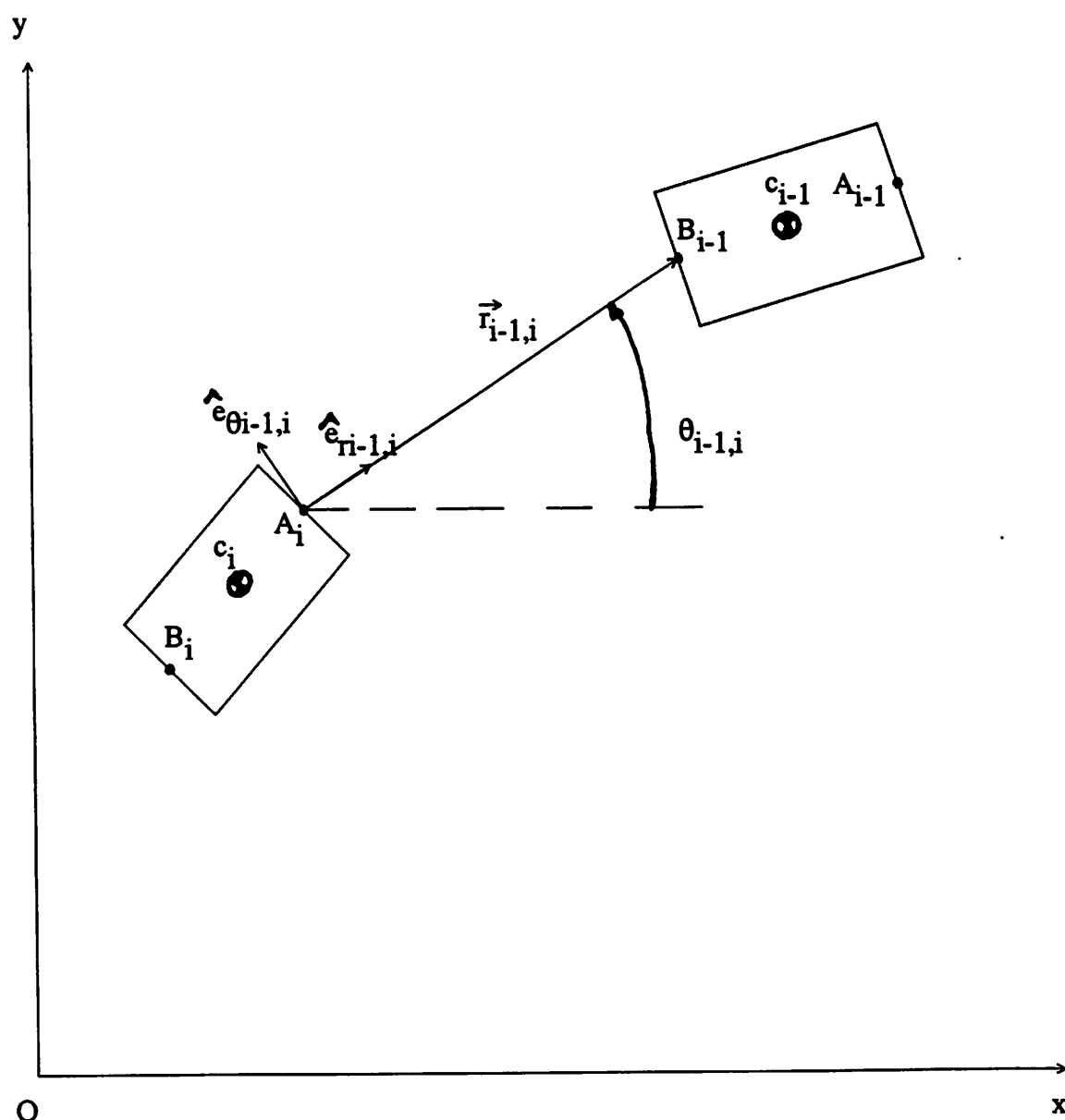


Figure 4.2: relevant quantities for the longitudinal dynamics of the  $(i - 1)$ -th and the  $i$ -th vehicles in a platoon:  $i = 1, 2, \dots, N$ .

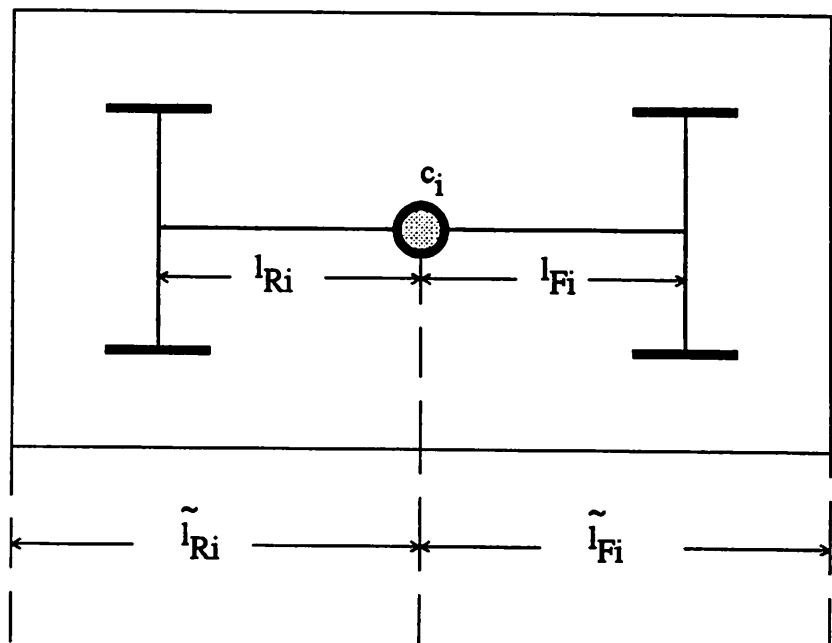


Figure 4.3: The body frame of the  $i$ -th vehicle.

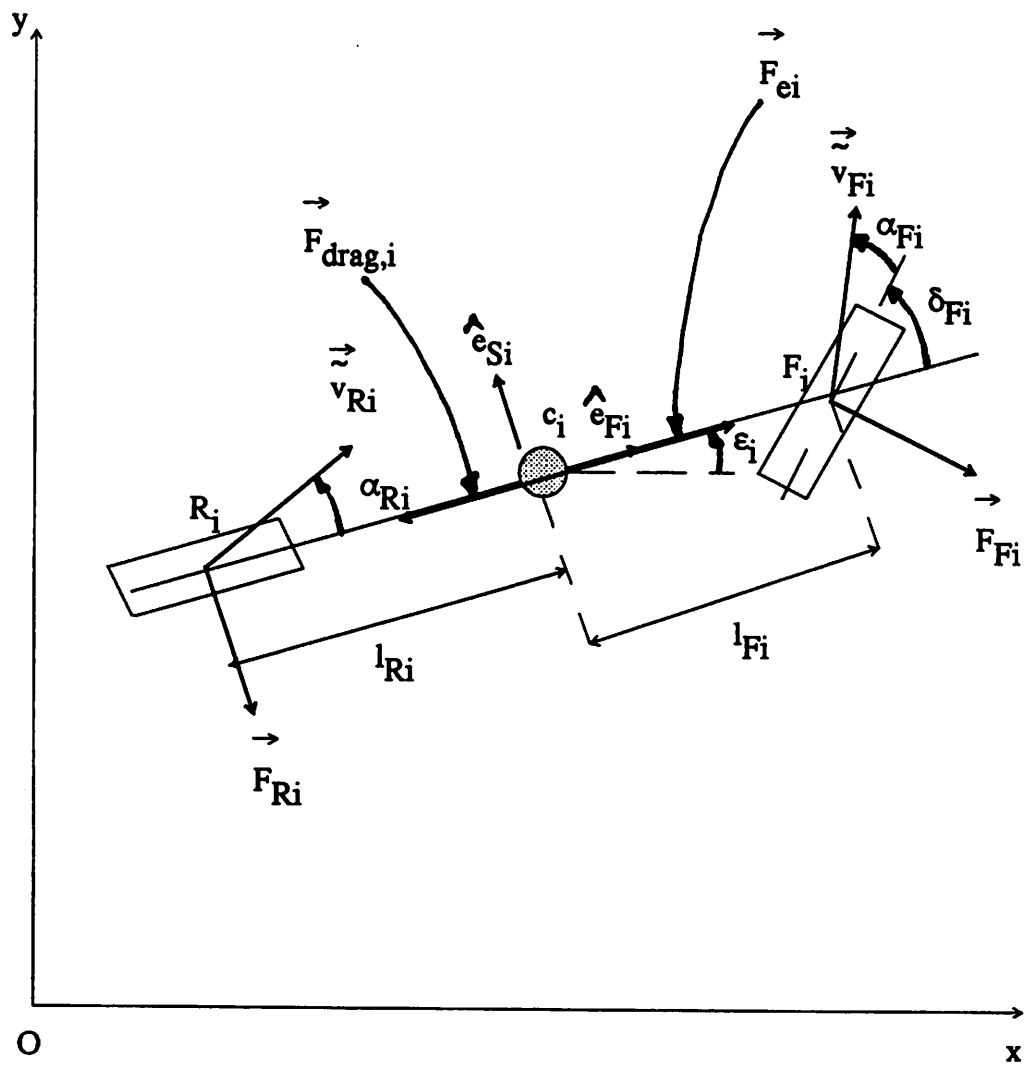


Figure 4.4: Bicycle model for the  $i$ -th vehicle in a platoon:  $i = 1, 2, \dots, N$ .

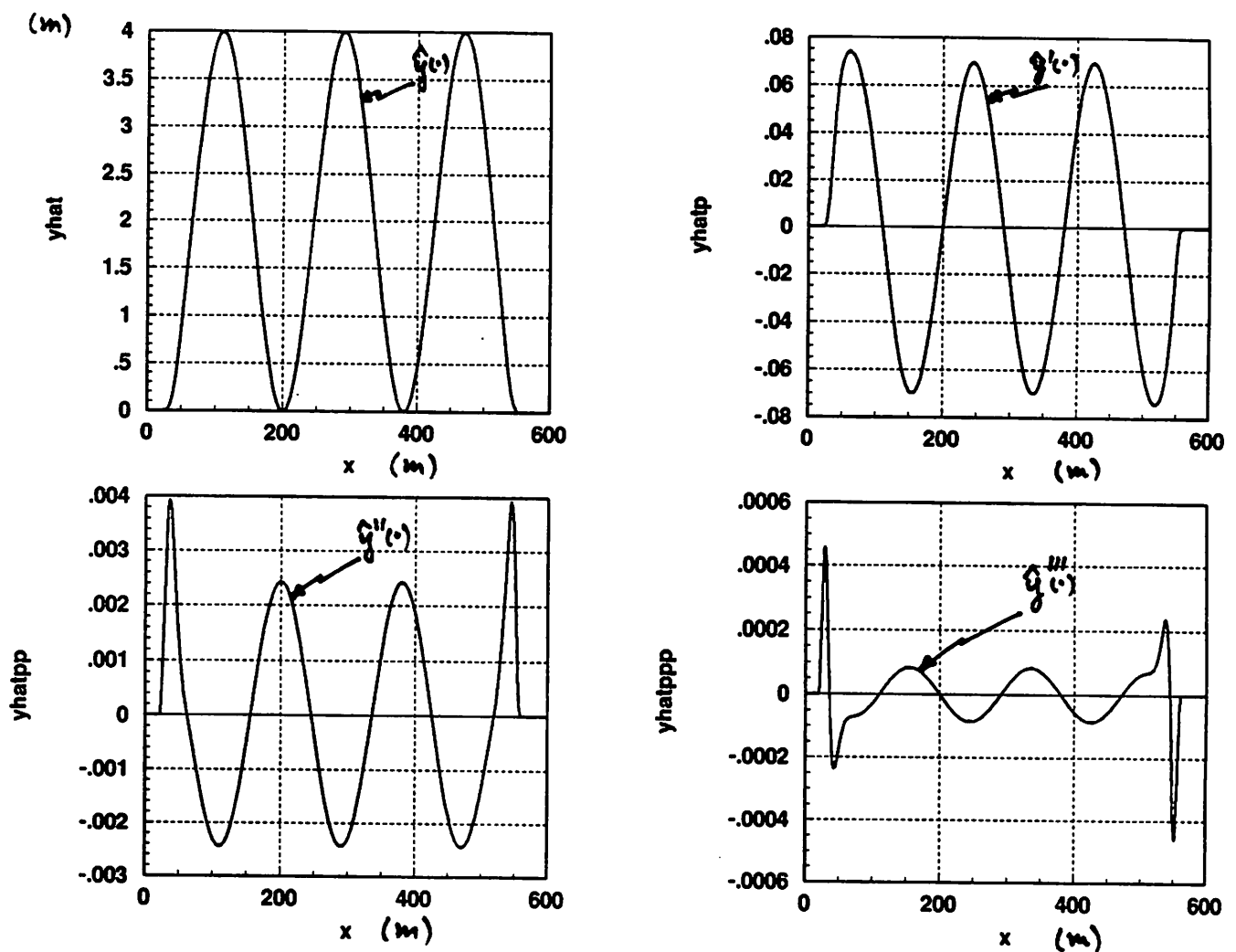


Figure 4.5: plot of the lane center  $\mathcal{L}$  and its derivatives:  $\hat{y}(\cdot)$ ,  $\hat{y}'(\cdot)$ ,  $\hat{y}''(\cdot)$ , and  $\hat{y}'''(\cdot)$  vs.  $x$ .

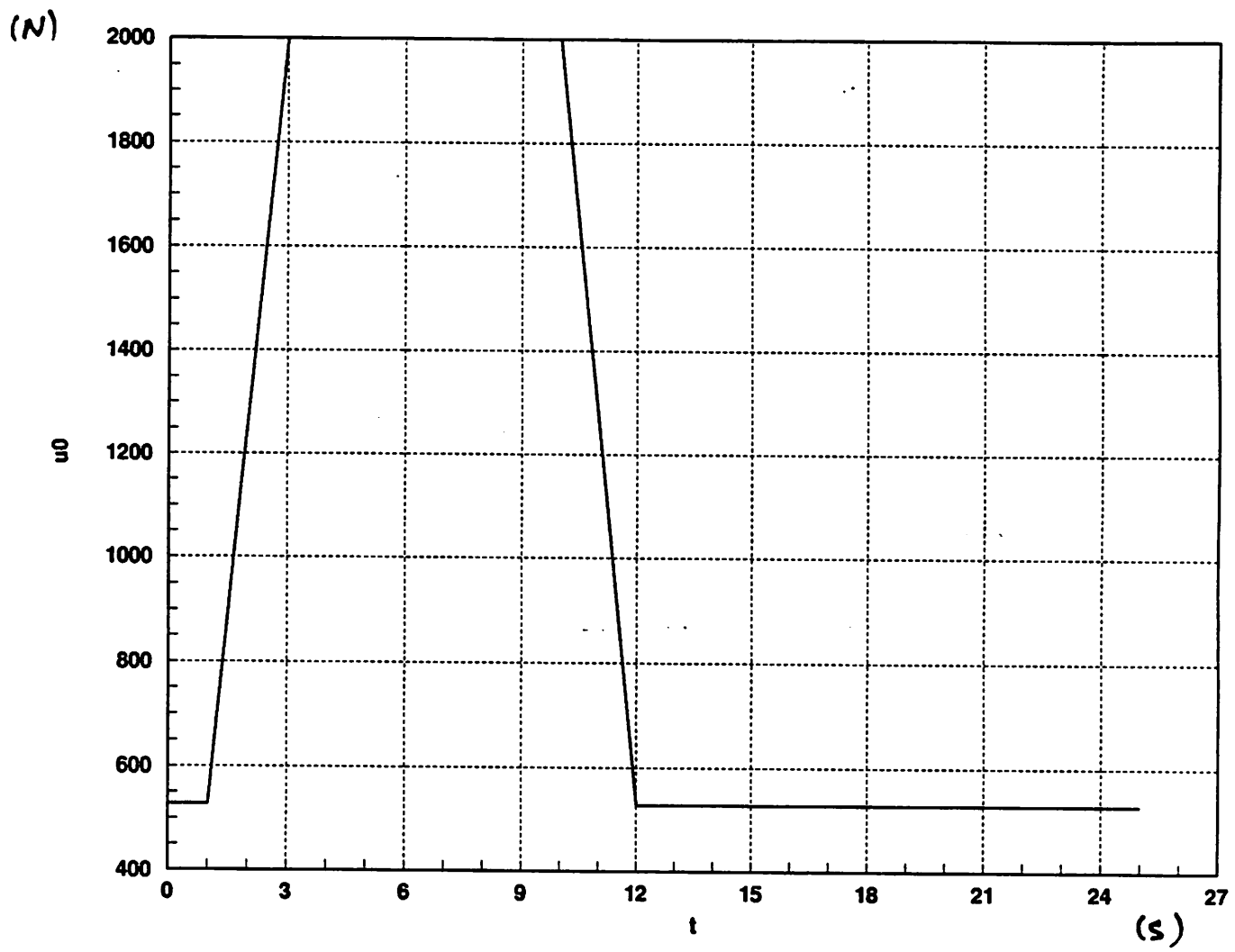


Figure 4.6: the lead vehicle's throttle input:  $u_0$  vs.  $t$ .

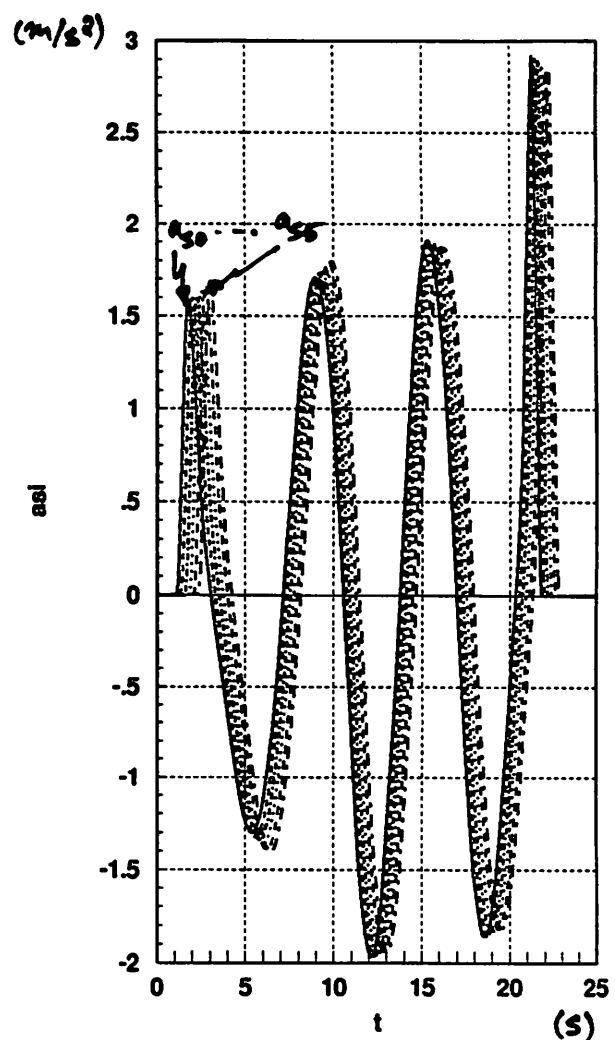
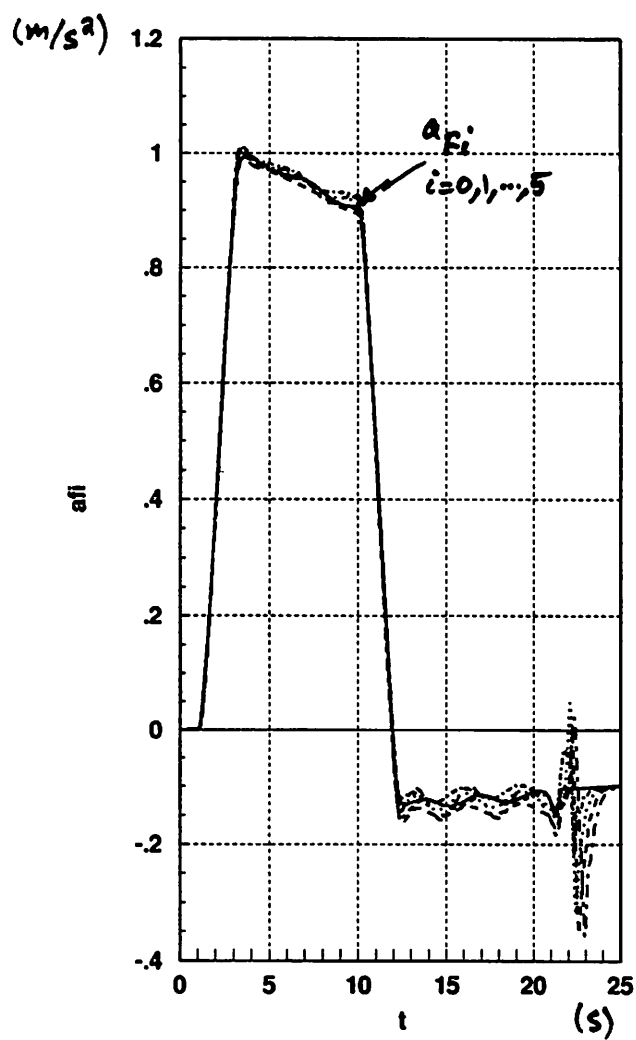


Figure 4.7: components of acceleration of the  $i$ -th vehicle:  $a_{F_i}$  vs.  $t$  and  $a_{S_i}$  vs.  $t$ , for  $i = 0, 1, \dots, 5$ ; the solid curves represent  $a_{F_0}$  and  $a_{S_0}$ , respectively. (SI units)

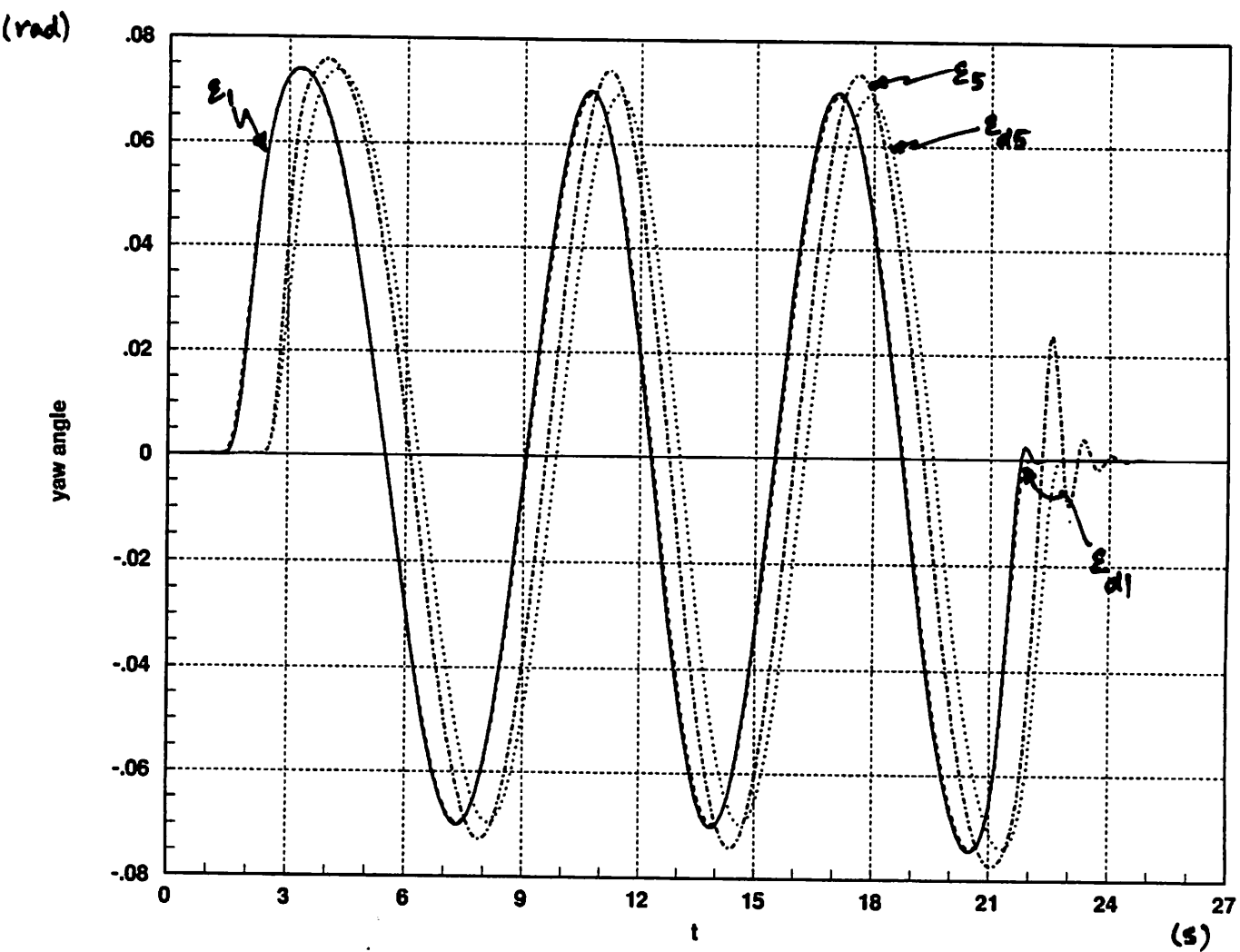


Figure 4.8: yaw angle of the  $i$ -th vehicle and the corresponding angle on the lane center:  $\epsilon_i$  vs.  $t$  and  $\epsilon_{di}$  vs.  $t$ , for  $i = 1, 5$ ; the solid curve represents  $\epsilon_1$ .

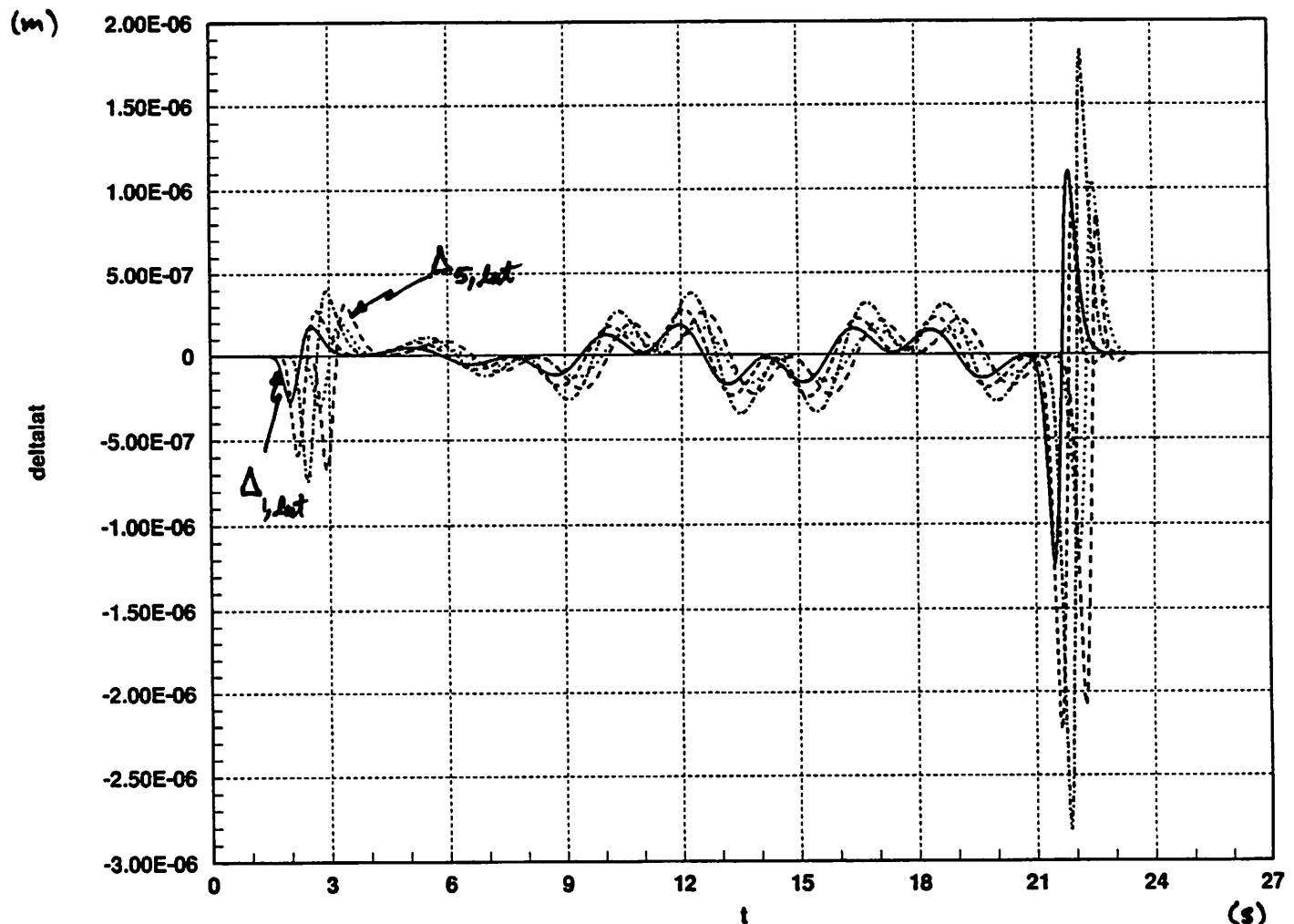


Figure 4.9:  $\Delta_{i,\text{lat}}$  vs.  $t$ , for  $i = 1, 2, \dots, 5$ .

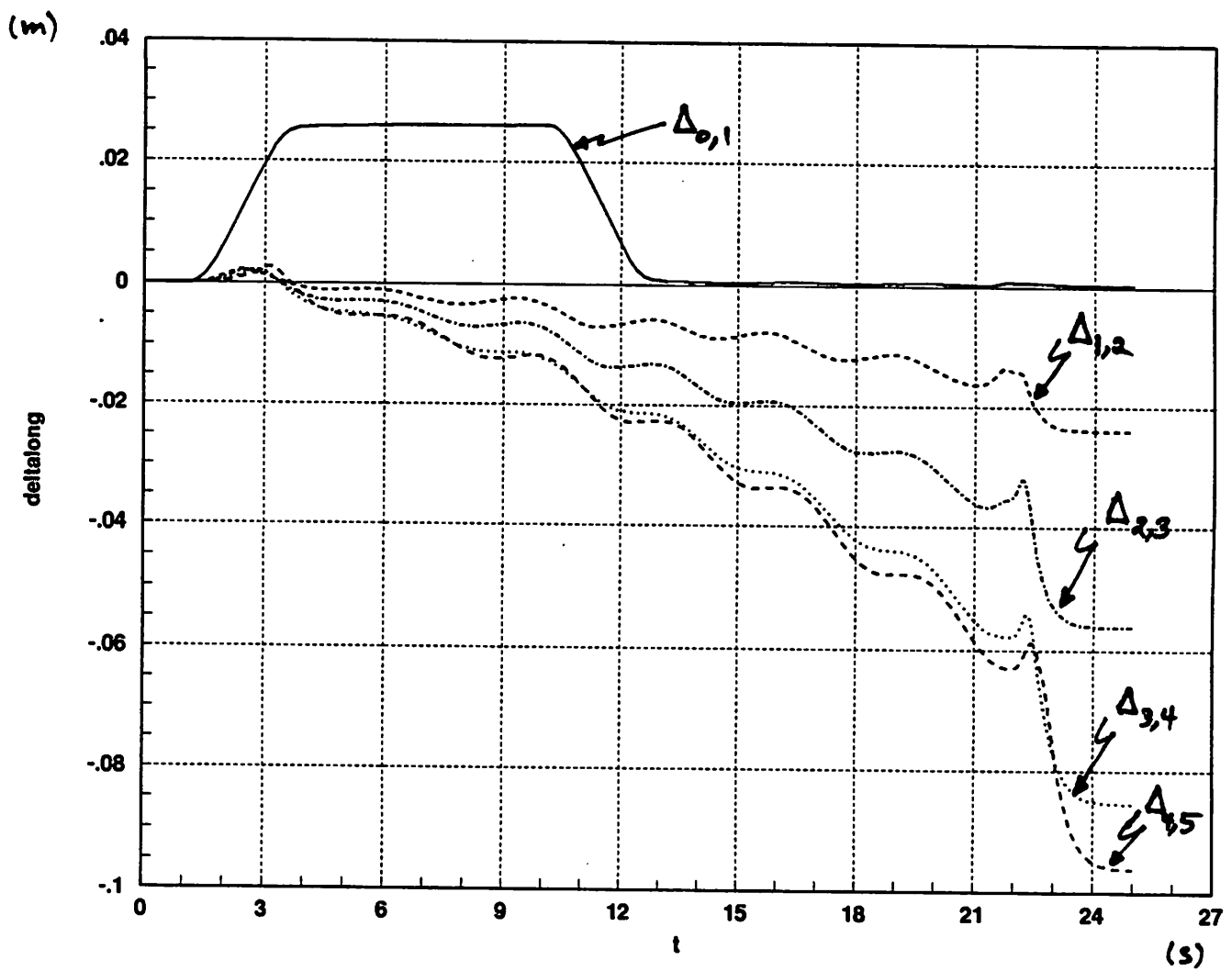


Figure 4.10:  $\Delta_{i-1,i}$  vs.  $t$ , for  $i = 1, 2, \dots, 5$ .

## Part II

# Decentralized Control of a Class of Interconnected Nonlinear Dynamical Systems

## Chapter 5

# Control of Interconnected Nonlinear Dynamical Systems:the platoon problem

The problem in this chapter is motivated by the highway automation project described in chapters 2, 3, and 4. The overall system consists of  $N$  vehicles,(the platoon); each vehicle is driven by the same input  $u$  and the state of the  $k$ -th vehicle affects the dynamics of the  $(k + 1)$ -th vehicle; furthermore, the dynamics of each vehicle is affected by its (local) state-feedback controller. Under very general conditions, it is shown that for sufficiently slowly varying inputs, *decentralized controllers* can be designed so that the platoon maintains its cohesion.

### 5.1 Introduction

In previous chapters, using a *simplified* model of vehicle dynamics we studied the platoon control problem: a *decentralized* control law has been developed for this model and the platoon performance evaluated. Certain specific properties of the model greatly simplified the decentralized controller design. The platoon concept with the assumed pattern leads to a special interconnection of dynamical subsystems each one representing a vehicle.

The purpose of this chapter is to demonstrate that *under general qualitative conditions imposed on the nonlinear dynamical subsystems* interconnected as above, it is possible

to obtain appropriate dynamical behavior for the overall system *using only decentralized control*.

The study of interconnections of dynamical systems has a long history usually under the heading of "Large Scale Systems". Some of the main results are to be found in [26] and [58]. The treatise in [21] on singular perturbations is an excellent reference on the concepts and techniques associated with the notions of slow and fast dynamics. From a system design point of view these studies show that two aspects are very important: a) the graph of the interconnection [58] and b) the time-scale separation of dynamics [21].

The system under study has a special interconnection which is dictated by the platoon concept: the system consists of  $N$  nonlinear subsystems, each one representing a vehicle. To maintain the cohesion of the platoon, the lead vehicle's velocity and acceleration is transmitted to each vehicle of the platoon, and vehicle  $k$  measures the distance  $\Delta_k$  between it and the preceding vehicle. As an approximation we may view the dynamics of the sensors and actuators and that of the engine as fast with respect to that of the vehicle. We show that by suitable design of each controller in each vehicle it is possible to achieve the following: given that the platoon is operating in the steady state at constant velocity,  $v$ , at  $t = t_0$ , and that the lead vehicle accelerates to reach a constant velocity  $v_1$  at some later time  $T$ , decentralized control laws can be designed so that for all  $k \geq 1$ ,  $\Delta_k(t)$  is bounded on  $[t_0, \infty)$  and, for some  $\alpha < 1$ ,  $\|\Delta_k(\cdot)\|_\infty \leq \alpha \|\Delta_{k-1}(\cdot)\|_\infty + \|\phi_k(\cdot)\|_\infty$  where  $\phi_k(t) \rightarrow 0$  exponentially as  $t \rightarrow \infty$  at a rate controlled by the choice of the control laws; here  $\|\cdot\|_\infty$  denotes the sup norm over  $[T, \infty)$ .

## 5.2 Problem motivation

Consider a "platoon" of  $N + 1$  vehicles traveling in the same lane of a straight stretch of highway and following closely one another. Initially, all vehicles travel at the same constant velocity, say  $v$ . The lead vehicle is labelled " $l$ ", the next one is labelled " $1$ ", and the last one " $N$ ":  $x_k$  denotes the abscissa of the rear bumper of the  $k$ -th vehicle and  $x_l$  that of the lead vehicle; each vehicle is allotted a slot of length  $L$ ; let  $\Delta_k$  be defined by

$$\Delta_k := x_{k-1} - (x_k + L);$$

$\Delta_k$  measures the deviation in the assigned distance between vehicle  $k - 1$  and vehicle  $k$ .

Each vehicle is equipped with sensors that measure  $\dot{x}_k, \ddot{x}_k, \Delta_k, \dot{\Delta}_k$ , and  $\ddot{\Delta}_k$  as well as  $\dot{x}_l$  and  $\ddot{x}_l$  (the last two measurements are obtained by a communication link). Using a nonlinear first order model of the engine, equation (2.4), and Newton's law, equation (2.3), for the  $k$ -th vehicle we obtain the following dynamical model in terms of the state  $\zeta_k := (\Delta_k, \dot{x}_k - v, \ddot{x}_k)$  and the engine input  $u_k$ , (say, the throttle input)

$$\dot{\zeta}_k = f_k(\zeta_k, \zeta_{k-1}) + g_k(\zeta_k)u_k \quad (5.1)$$

for  $k \geq 2$ , [41],[42].

As shown, for example in chapter 2, it turns out that these equations have such a form that a suitable nonlinear control will lead to the following equation for the  $k$ -th vehicle

$$\dot{\zeta}_k = f(\zeta_k, \zeta_{k-1}, u) \quad (5.2)$$

for  $k = 2, 3, \dots, N$ , where  $u(t) = (\dot{x}_l(t), \ddot{x}_l(t))$ , the velocity and acceleration of the lead vehicle.

Note that in (5.2), the function  $f(., ., .)$  depends only on the state of the  $k$ -th and  $(k-1)$ -th vehicle and the "input"  $u$ : the dependence on the vehicle characteristics (mass  $m_k$ , cross section  $A_k$ , aerodynamic coefficient  $C_k$ , and engine characteristic  $\tau(\dot{x}_k)$ ) have been eliminated by the nonlinear feedback law [41]; hence,  $f(., ., .)$  does not depend on  $k$  for  $k \geq 2$ . For the first vehicle, the control law leads to an equation of the form

$$\dot{\zeta}_1 = f_1(\zeta_1, u). \quad (5.3)$$

The above discussion suggests the following problem: suppose the platoon of  $N+1$  vehicles is initialized as above and suppose that at  $t = t_0$  the lead vehicle accelerates from the velocity  $v$  to some other constant velocity, say  $v_1$ , which it reaches at some time  $T$ . Is it possible to choose a *decentralized* controller in each vehicle such that, for such increases in velocity, for  $k = 1, 2, \dots, N$ ,  $\Delta_k(.)$  is bounded,  $\Delta_k(t) \rightarrow 0$  as  $t \rightarrow \infty$  and, for  $t'$  sufficiently large,  $\max_{t \geq T+t'} |\Delta_k(t)|$  is a decreasing function of  $k$ ? This is a new control problem in that not only are the  $\Delta_k$ 's required to go to zero but also, for  $t'$  sufficiently large,  $\tilde{m}_k := \max_{t \geq T+t'} |\Delta_k(t)|$  is such that  $k \mapsto \tilde{m}_k$  is a decreasing function of  $k$ .

### 5.3 Problem formulation

With the above application in mind, we formulate the platoon problem in a more general setting as follows: we are given an interconnection of nonlinear time-invariant dynamical systems described by the following differential equations:

$$\begin{aligned}\dot{\zeta}_1 &= f_1(\zeta_1, u) \\ \dot{\zeta}_2 &= f(\zeta_2, \zeta_1, u) \\ \dot{\zeta}_3 &= f(\zeta_3, \zeta_2, u) \\ &\vdots \\ \dot{\zeta}_N &= f(\zeta_N, \zeta_{N-1}, u)\end{aligned}\tag{5.4}$$

where the exogeneous control  $u$  belongs to an open set  $U \subset R^m$  and for  $k = 1, 2, \dots, N$ ,  $\zeta_k$  belongs to an open set  $P_U \subset R^n$ ;  $f_1$  and  $f$  are  $C^2$  functions of their arguments;  $\zeta_k$  includes  $x_k, \dot{x}_k$ , and  $\ddot{x}_k$  as components.

Consider the situation where all vehicles travel at the same constant velocity, say  $v$  (i.e.,  $\dot{x}_k = v$ ) and are at their assigned positions (i.e.,  $\Delta_k = 0$  for  $k = 1, 2, \dots, N$ ). Call  $u_0$  the corresponding input  $u_0 = (v, 0)$ : then by the nature of the vehicle dynamics we have  $f_1(\zeta_e, u_0) = 0$ , and  $f(\zeta_e, \zeta_e, u_0) = 0$ , where the *equilibrium state*  $\zeta_e$  is a function of  $u_0$ . We assume that, by clever design of the control law within each vehicle, the dynamical system (5.4) has a whole set of such equilibrium points for appropriate values of  $u_0$  and that about each such equilibrium of (5.4) there is a suitable basin of attraction.

Theorem 5.1 considers a special case of (5.4) and gives precise conditions under which a slowly varying input  $u$  will cause  $\zeta$  to vary slowly and remain within the basin of attraction of the corresponding equilibrium point. Theorem 5.2 considers the interconnection of nonlinear dynamical systems described by (5.4) and gives precise conditions under which the deviations of  $\zeta_k$  ( $k = 1, 2, \dots, N$ ) from the equilibrium state  $\zeta_e$  remain bounded for a slowly varying input  $u$ ; furthermore, if after some time  $T$ ,  $u(t)$  becomes constant, then the peak value of these deviations decreases as  $k$  increases.

Consider some dynamical system described as follows:

$$\dot{\zeta} = f(\zeta, \zeta_p, u) \quad (5.5)$$

where  $\zeta$  and  $\zeta_p$  belong to  $P_U$ , an open set of  $R^n$ , and  $u$  belongs to  $U$ , an open set of  $R^m$ ;  $f$  is a  $C^2$  function.

**Definition** A point  $\zeta_0$  in  $P_U$  is called a *sink* of (5.5) corresponding to the constant state-input  $\zeta_{p0}$  in  $P_U$  and constant input  $w_0$  in  $U$  if  $f(\zeta_0, \zeta_{p0}, w_0) = 0$  and  $\text{Re}\sigma[D_1f(\zeta_0, \zeta_{p0}, w_0)] < 0$ ; where  $D_1f(., ., .)$  denotes the Jacobian matrix of  $f(., ., .)$  with respect to the first variable and  $\sigma[.]$  denotes the spectrum of a matrix.

It is well known that if  $\zeta_0$  is a sink corresponding to  $(\zeta_{p0}, w_0)$ , then there is a ball  $B(\zeta_0; r)$ , centered on  $\zeta_0$ , such that for all  $\zeta(t_0) \in B(\zeta_0, r)$ , the solution of  $\dot{\zeta} = f(\zeta, \zeta_{p0}, w_0)$  is bounded and decays exponentially to  $\zeta_0$  (see e.g. [57], [10]).

We also assume that by suitable design of the control law in (5.5) we may move the spectrum of  $D_1f(\zeta_e, \zeta_e, u)$  further into the left half plane.

**Theorem 5.1** Suppose that  $P_U \subset R^n$  is open and convex, and  $U \subset R^m$  is open; let  $f : P_U \times P_U \times U \rightarrow R^n$  be a  $C^2$  function such that

$$M_U := \left\{ (\tilde{\zeta}_e, \zeta_p, u) \in P_U \times P_U \times U \mid \tilde{\zeta}_e \text{ is a sink of (5.5) corresponding to } (\zeta_p, u) \right\}$$

has a non-empty interior. Let  $\bar{Q}_U$  be a compact, connected subset of  $M_U$ , with a non-empty interior  $Q_U$ . Let  $u : [t_0, \infty) \rightarrow U$ , with  $u(t_0) = u_0$ ,  $\zeta_p : [t_0, \infty) \rightarrow P_U$ , and  $\tilde{\zeta}_e : [t_0, \infty) \rightarrow P_U$  be three given  $C^1$  functions such that  $(\tilde{\zeta}_e(t), \zeta_p(t), u(t)) \in Q_U$  for all  $t \geq t_0$ . Let  $\zeta(.)$  be the solution of (5.5) with the  $(\zeta_p(.), u(.))$  defined above and with initial condition  $\zeta(t_0)$ .

Then, for any  $\rho > 0$ , there exist  $\delta_0 > 0$ ,  $\delta_u > 0$ ,  $\delta_\zeta > 0$  independent of  $t_0$ , such that for all  $u(.), \zeta_p(.)$ , and  $\zeta_e(.)$  as defined above and satisfying  $|\zeta(t_0) - \tilde{\zeta}_e(t_0)| \leq \delta_0$ ,  $\max_{t \geq t_0} |\dot{u}(t)| \leq \delta_u$  and  $\max_{t \geq t_0} |\dot{\zeta}_p(t)| \leq \delta_\zeta$  we have:

- i)  $|\zeta(t) - \tilde{\zeta}_e(t)| < \rho$  for all  $t \geq t_0$ ,
- ii) if, in addition,  $\rho$  is sufficiently small, then for all  $t \geq t_0$ ,  $\zeta(t)$  belongs to the basin of attraction of the sink  $\tilde{\zeta}_e(t)$  with respect to  $(\zeta_p(t), u(t))$ .

There are two methods for proving this theorem: 1) estimation in the time domain (see [19], with improvements [39]); 2) using Lyapunov functions (the existence follows from lemma 2 of Hoppensteadt [17], the technique is detailed by Khalil and Kokotovic [20]).

Since  $\overline{Q}_U$  is compact, from i) of theorem 5.1, there exists a compact set  $Z_U$  such that for all  $t \geq t_0$ ,  $\zeta(t) \in Z_U$ .

## 5.4 Main result

We consider now the composite dynamical system described by (5.4). Let  $f$  satisfy the assumptions of theorem 5.1; consider some slowly varying  $u(t)$  and the corresponding  $\zeta_e(t)$ .

With respect to the first equation of (5.4):

$$\dot{\zeta}_1 = f_1(\zeta_1, u), \quad (5.6)$$

we assume that  $f_1 : P_U \times U \rightarrow R^n$  is a  $C^2$  function such that

$$M_U^1 := \{(\zeta_e, u) \in P_U \times U \mid \zeta_e \text{ is a sink of (5.6) corresponding to } u\}$$

has a non-empty interior. Let  $\overline{Q}_U^1$  be a compact, connected subset of  $M_U^1$ , with a non-empty interior  $Q_U^1$ . Let  $u : [t_0, \infty) \rightarrow U$  and  $\zeta_e : [t_0, \infty) \rightarrow P_U$  be two given  $C^1$  functions such that  $(\zeta_e(t), u(t)) \in Q_U^1$  for all  $t \geq t_0$ .

Consider (5.6). It is a well known result (e.g. [19],[20]) that given these assumptions on  $f_1$ , for any  $\rho > 0$ , there exist  $\delta_0^1 > 0$  and  $\delta_u^1 > 0$  such that if  $|\zeta_1(t_0) - \zeta_e(t_0)| \leq \delta_0^1$  and  $\max_{t \geq t_0} |\dot{u}(t)| < \delta_u^1$  then for all  $t \geq t_0$ ,  $\zeta_1(t) \in Z_U$  and  $|\zeta_1(t) - \zeta_e(t)| < \rho$ .

**Lemma 5.1** Consider the nonlinear dynamical system described by (5.4) keeping in mind the above considerations. Under the conditions stated above, by suitable design of the control laws, if  $\rho$  is chosen sufficiently small, then for  $k = 1, 2, \dots, N$ : 1) for all  $t \geq t_0$ ,  $\zeta_k(t) \in Z_U$ , and 2) for all  $t \geq t_0$ ,  $\max_{t \geq t_0} |\dot{\zeta}_k(t)| \leq \delta_\zeta$ .

**Proof** We use induction.

Writing the Taylor expansion of (5.6) about  $(\zeta_e, u)$  and noting that  $f_1(\zeta_e, u) = 0$  we obtain

$$\dot{\zeta}_1 = H_1(\zeta_e, u, \zeta_1)(\zeta_1 - \zeta_e) \quad (5.7)$$

where  $H_1(\zeta_e, u, \zeta_1) := \int_0^1 D_1 f_1[\zeta_e + \lambda(\zeta_1 - \zeta_e), u] d\lambda$ ; note that  $H_1(\cdot, \cdot, \cdot)$  is continuous.

Since for all  $t \geq t_0$ ,  $(\zeta_e(t), u(t), \zeta_1(t)) \in \overline{Q}_U^1 \times Z_U$ , a compact set, and  $H_1(\cdot, \cdot, \cdot)$  is continuous, there exists a constant,  $h_1 \geq 0$ , such that

$$h_1 = \max_{t \geq t_0} |H_1(\zeta_e(t), u(t), \zeta_1(t))|. \quad (5.8)$$

From (5.7) and (5.8) we obtain

$$\max_{t \geq t_0} |\dot{\zeta}_1(t)| \leq h_1 \rho \quad (5.9)$$

hence,

$$\text{If } \rho \leq \frac{\delta_\zeta}{h_1} \text{ then } \max_{t \geq t_0} |\dot{\zeta}_1(t)| \leq \delta_\zeta. \quad (5.10)$$

**Induction step** We use the notations of theorem 5.1. Assume that for some  $k \geq 1$ ,  $|\zeta_{k+1}(t_0) - \zeta_e(t_0)| \leq \delta_0$ ,  $\max_{t \geq t_0} |\dot{u}(t)| \leq \delta_u$ , and for all  $t \geq t_0$ ,  $\zeta_k(t) \in Z_U$  and  $\max_{t \geq t_0} |\dot{\zeta}_k(t)| \leq \delta_\zeta$ ; we will show that for all  $t \geq t_0$ ,  $\zeta_{k+1}(t) \in Z_U$  and  $\max_{t \geq t_0} |\dot{\zeta}_{k+1}(t)| \leq \delta_\zeta$ .

Consider the following dynamical system

$$\dot{\zeta}_{k+1} = f(\zeta_{k+1}, \zeta_k, u). \quad (5.11)$$

Since the assumptions of theorem 5.1 are satisfied for (5.11), we have for all  $t \geq t_0$ ,  $\zeta_{k+1}(t) \in Z_U$  and  $|\zeta_{k+1}(t) - \zeta_e(t)| < \rho$ .

Writing the Taylor expansion of (5.11) about  $(\zeta_e, \zeta_e, u)$  and noting that  $f(\zeta_e, \zeta_e, u) = 0$  we obtain

$$\begin{aligned} \dot{\zeta}_{k+1} &= \int_0^1 D_1 f[\zeta_e + \lambda(\zeta_{k+1} - \zeta_e), \zeta_e + \lambda(\zeta_k - \zeta_e), u] d\lambda (\zeta_{k+1} - \zeta_e) \\ &\quad + \int_0^1 D_2 f[\zeta_e + \lambda(\zeta_{k+1} - \zeta_e), \zeta_e + \lambda(\zeta_k - \zeta_e), u] d\lambda (\zeta_k - \zeta_e). \end{aligned} \quad (5.12)$$

Here  $D_k f(., ., .)$  denotes the Frechet derivative of  $f(., ., .)$  with respect to its  $k$ -th argument.

We can write (5.12) as follows

$$\dot{\zeta}_k = G_1(\zeta_e, u, \zeta_k, \zeta_{k+1})(\zeta_{k+1} - \zeta_e) + G_2(\zeta_e, u, \zeta_k, \zeta_{k+1})(\zeta_k - \zeta_e) \quad (5.13)$$

where  $G_1(\zeta_e, u, \zeta_k, \zeta_{k+1})$  and  $G_2(\zeta_e, u, \zeta_k, \zeta_{k+1})$  denote the first and the second integrals in the right hand side of (5.12), respectively.

Let  $P_{Q_U, U} := \{(\zeta_e, u) | (\zeta_e, \zeta_p, u) \in Q_U\}$ . Now, for all  $t \geq t_0$ ,  $(\zeta_e(t), u(t), \zeta_k(t), \zeta_{k+1}(t)) \in \overline{P}_{Q_U, U} \times Z_U \times Z_U := Y_U$ , a compact set;  $G_1(., ., ., .) \in C^1$ , and  $G_2(., ., ., .) \in C^1$ . Hence  $G_1(., ., ., .)$  and  $G_2(., ., ., .)$  are bounded on  $Y_U$ , say by  $g_1 \geq 0$  and  $g_2 \geq 0$ , respectively.

Using these bounds and (5.13), and noting that by the induction hypothesis for all  $t \geq t_0$ ,  $|\zeta_k(t) - \zeta_e(t)| < \rho$  we obtain

$$\max_{t \geq t_0} |\dot{\zeta}_{k+1}(t)| \leq (g_1 + g_2)\rho \quad (5.14)$$

hence,

$$\text{If } \rho \leq \frac{\delta_\zeta}{g_1 + g_2} \text{ then } \max_{t \geq t_0} |\dot{\zeta}_{k+1}(t)| \leq \delta_\zeta. \quad (5.15)$$

From (5.10) and (5.15) we note that for  $k = 1, 2, \dots, N$ , if  $\rho \leq \min\left\{\frac{\delta_\zeta}{h_1}, \frac{\delta_\zeta}{g_1 + g_2}\right\}$  then  $\max_{t \geq t_0} |\dot{\zeta}_k(t)| \leq \delta_\zeta$ .  $\blacksquare$

Again, let  $f$  satisfy the assumptions of theorem 5.1; consider some slowly varying  $u(t)$  and the corresponding  $\zeta_e(t)$ . Let for  $k \geq 2$ ,  $d_k(t) + \zeta_e(t) = \zeta_k(t)$  and assume  $d_k(t_0) = 0$  for all  $k$ .

**Theorem 5.2** Under these conditions,

1. if (a)  $\rho$  is sufficiently small so that lemma 5.1 holds, (b) for some sufficiently small  $\delta_u > 0$  as in the statement of theorem 5.1,  $\max_{t \geq t_0} |\dot{u}(t)| < \delta_u$ , and (c) for some sufficiently small  $\delta_\zeta > 0$  as in the statement of theorem 5.1,  $\max_{t \geq t_0} |\dot{\zeta}_e(t)| < \delta_\zeta$ , then, by suitable design of control laws, there exist some constants  $\alpha$  and  $\beta$  such that  $0 \leq \alpha < 1$ ,  $0 < \beta < \infty$ , and for  $k \geq 2$ ,

$$\|d_{k+1}\|_\infty \leq \alpha \|d_k\|_\infty + \beta \|\dot{\zeta}_e\|_\infty \quad (5.16)$$

hence, for large  $k$ ,

$$\|d_k\|_\infty \leq \frac{\beta}{1 - \alpha} \|\dot{\zeta}_e\|_\infty + O(\alpha^{k-1}); \quad (5.17)$$

i.e., there is a uniform bound on  $\|\zeta_k - \zeta_e\|_\infty$ :

2. if, in addition, after some time  $T$ ,  $u(t)$  and (consequently)  $\zeta_e(t)$  become constant, then by local control law design, we can obtain

$$\|d_{k+1}\|_\infty \leq \alpha \|d_k\|_\infty + \|\phi_k\|_\infty \quad (5.18)$$

where, as in (5.16),  $\alpha < 1$ ; here  $\phi_k(t) \rightarrow 0$  exponentially as  $t \rightarrow \infty$ , and  $\|\cdot\|_\infty$  denotes the sup norm on  $[T, \infty)$ .

In other words, in case of a change in  $u$  in the lead vehicle from the initial steady-state value  $u_0$  to the final steady-state value  $u_f$ , the peak disturbances down the platoon, i.e.,  $d_2(\cdot), d_3(\cdot), \dots$  decrease as  $k$  increases (after sufficiently long time).

**Proof(theorem 5.2, part 1)** Adding and subtracting  $D_1 f(\zeta_e, \zeta_e, u) d_{k+1}$  to the right hand side of (5.12) and noting that  $\dot{\zeta}_{k+1} = \dot{\zeta}_e + \dot{d}_{k+1}$  we obtain

$$\dot{d}_{k+1} = A(t)d_{k+1} + R(t)d_{k+1} + B(t)d_k - \dot{\zeta}_e \quad (5.19)$$

where

$$A(t) := D_1 f(\zeta_e(t), \zeta_e(t), u(t)) \quad (5.20)$$

$$R(t) := \int_0^1 \{D_1 f[\zeta_e(t) + \lambda d_{k+1}(t), \zeta_e(t) + \lambda d_k(t), u(t)] - D_1 f(\zeta_e(t), \zeta_e(t), u(t))\} d\lambda \quad (5.21)$$

and

$$B(t) := \int_0^1 D_2 f[\zeta_e(t) + \lambda d_{k+1}(t), \zeta_e(t) + \lambda d_k(t), u(t)] d\lambda. \quad (5.22)$$

Let  $\Phi(t, \tau)$  be the state transition matrix of  $\dot{z} = A(t)z$ . Then from (5.19) we obtain

$$\begin{aligned} d_{k+1}(t) &= \Phi(t, t_0) d_{k+1}(t_0) \\ &+ \int_{t_0}^t \Phi(t, \tau) R(\tau) d_{k+1}(\tau) d\tau \\ &+ \int_{t_0}^t \Phi(t, \tau) [B(\tau) d_k(\tau) - \dot{\zeta}_e(\tau)] d\tau; \end{aligned} \quad (5.23)$$

here the first term in the right hand side of (5.23) is zero since  $d_{k+1}(t_0) = 0$ .

Note that for all  $t \geq t_0$ ,  $(\zeta_e(t), u(t)) \in \overline{P}_{Q_U, U}$ , a compact set, and  $D_1 f(., ., .)$  is continuous; hence,

$$A(.) \text{ is bounded on } [t_0, \infty). \quad (5.24)$$

Since  $\sigma[A(t)] = \sigma[D_1 f(\zeta_e(t), \zeta_e(t), u(t))]$  is a continuous function of its entries and for all  $t \geq t_0$ ,  $(\zeta_e(t), u(t)) \in \overline{Q}_U$  with  $\zeta_e(t)$  being a sink of (5.11) corresponding to  $(\zeta_e(t), u(t))$ , there exists a constant  $\mu < 0$  such that

$$\text{for all } t \geq t_0, \operatorname{Re}\sigma[A(t)] \leq \mu. \quad (5.25)$$

From (5.24) and (5.25) we note [57, Cor.41 and Thm.6, sec.5.6 with Thm.27, sec.5.3] or [3, Thm. 2, sec.32] that there exists a constant  $\epsilon > 0$  such that if  $|\dot{A}(t)| \leq \epsilon$  then

for some  $\tilde{k} \geq 1$  and some  $\eta > 0$  and for all  $t \geq s \geq t_0$ ,  $|\Phi(t, s)| \leq \tilde{k} \exp[-\eta(t-s)]$ . (5.26)

Differentiating the right hand side of (5.20) with respect to  $t$  and using the chain rule we obtain

$$\begin{aligned} \dot{A}(t) &= \{D_1 D_1 f(\zeta_e(t), \zeta_e(t), u(t)) + D_2 D_1 f(\zeta_e(t), \zeta_e(t), u(t))\} \dot{\zeta}_e(t) \\ &+ D_3 D_1 f(\zeta_e(t), \zeta_e(t), u(t)) \dot{u}(t). \end{aligned} \quad (5.27)$$

Since  $D_1 D_1 f(., ., .)$ ,  $D_2 D_1 f(., ., .)$ , and  $D_3 D_1 f(., ., .)$  are continuous and for all  $t \geq t_0$ ,  $(\zeta_e(t), u(t)) \in \overline{Q}_U$ , a compact set,  $D_1 D_1 f(., ., .)$ ,  $D_2 D_1 f(., ., .)$ , and  $D_3 D_1 f(., ., .)$  are bounded on  $\overline{Q}_U$ . Let

$$a_1 := \max \left\{ |D_1 D_1 f(\zeta_e, \zeta_e, u) + D_2 D_1 f(\zeta_e, \zeta_e, u)| : (\zeta_e, u) \in \overline{Q}_U \right\}$$

and

$$a_2 := \max \left\{ |D_3 D_1 f(\zeta_e, \zeta_e, u)| : (\zeta_e, \zeta_e, u) \in \bar{Q}_U \right\}.$$

If  $\max_{t \geq t_0} |\dot{u}(t)| < \delta_u \leq \frac{\epsilon}{2a_2}$  and  $\max_{t \geq t_0} |\dot{\zeta}_e(t)| < \delta_\zeta \leq \frac{\epsilon}{2a_1}$  then from (5.27) we obtain  $|\dot{A}(t)| \leq \epsilon$  and (5.26) is satisfied.

Now, from lemma 5.1, for all  $t \geq t_0$ ,  $(\zeta_e(t), u(t), \zeta_k(t), \zeta_{k+1}(t)) \in Y_U$ , a compact set, and  $B(\cdot, \cdot, \cdot, \cdot)$  is continuous; hence, there exists a constant  $b \geq 0$  such that

$$b = \max_{t \geq t_0} |B(t)|. \quad (5.28)$$

Similarly,  $R(\cdot, \cdot, \cdot, \cdot)$  is continuous and bounded on  $Y_U$ ; hence, by compactness, for some constant  $\gamma \geq 0$  we have

$$\gamma = \max_{t \geq t_0} |R(t)|. \quad (5.29)$$

From (5.23), (5.26), (5.28), and (5.29) we obtain

$$\begin{aligned} |d_{k+1}(t)| &\leq \int_{t_0}^t \tilde{k}\gamma \exp[-\eta(t-\tau)]|d_{k+1}(\tau)|d\tau \\ &+ \int_{t_0}^t \tilde{k} \exp[-\eta(t-\tau)][b|d_k(\tau)| + |\dot{\zeta}_e(\tau)|]d\tau. \end{aligned} \quad (5.30)$$

Applying a form of Gronwall lemma to (5.30), [23, Corollary 1.9.1], we obtain

$$\begin{aligned} |d_{k+1}(t)| &\leq \int_{t_0}^t \tilde{k} \exp[(-\eta + \tilde{k}\gamma)(t-\tau)][b|d_k(\tau)| + |\dot{\zeta}_e(\tau)|]d\tau \\ &\leq \int_{t_0}^t \tilde{k} \exp[(-\eta + \tilde{k}\gamma)(t-\tau)]d\tau [b||d_k||_\infty + ||\dot{\zeta}_e||_\infty]. \end{aligned} \quad (5.31)$$

By suitable design of the control law, we can increase  $\eta$  sufficiently beyond  $\tilde{k}\gamma$  so that  $0 \leq \alpha := \frac{b\tilde{k}}{\eta - \tilde{k}\gamma} < 1$ ; let  $\beta := \frac{\tilde{k}}{\eta - \tilde{k}\gamma}$ . Then, from (5.31), for all  $t \geq t_0$ ,

$$|d_{k+1}(t)| \leq \alpha||d_k||_\infty + \beta||\dot{\zeta}_e||_\infty \quad (5.32)$$

hence,

$$||d_{k+1}||_\infty \leq \alpha||d_k||_\infty + \beta||\dot{\zeta}_e||_\infty. \quad (5.33)$$

By recurrence, noting that  $\alpha < 1$ , we see that for all  $k \geq 2$ ,

$$||d_k||_\infty \leq \frac{\beta}{1-\alpha}||\dot{\zeta}_e||_\infty + O(\alpha^{k-1}). \quad (5.34)$$

■

**Proof(theorem 5.2, part 2)** From (5.19) we note that for  $t \geq T$ ,

$$\begin{aligned} d_{k+1}(t) &= \Phi(t, T)d_{k+1}(T) \\ &+ \int_T^t \Phi(t, \tau)R(\tau)d_{k+1}(\tau)d\tau \\ &+ \int_T^t \Phi(t, \tau)[B(\tau)d_k(\tau) - \dot{\zeta}_e(\tau)]d\tau. \end{aligned} \quad (5.35)$$

Hence, noting that for  $t \geq T, \dot{\zeta}_e(t) = 0$ , from (5.35), (5.26),(5.28), and (5.29) we obtain

$$\begin{aligned} |d_{k+1}(t)| &\leq \tilde{k} \exp[-\eta(t-T)]|d_{k+1}(T)| \\ &+ \int_T^t \tilde{k}\gamma \exp[-\eta(t-\tau)]|d_{k+1}(\tau)|d\tau \\ &+ \int_T^t \tilde{k}b \exp[-\eta(t-\tau)]|d_k(\tau)|d\tau. \end{aligned} \quad (5.36)$$

Applying a form of Gronwall lemma [23, Corollary 1.9.1] to (5.36) and using the previously defined  $\alpha$ , we obtain for all  $t \geq T$ ,

$$\begin{aligned} |d_{k+1}(t)| &\leq \tilde{k} \exp[(-\eta + \tilde{k}\gamma)(t-T)]|d_{k+1}(T)| \\ &+ \int_T^t \tilde{k}b \exp[(-\eta + \tilde{k}\gamma)(t-\tau)]|d_k(\tau)|d\tau \end{aligned} \quad (5.37)$$

$$\begin{aligned} &\leq \tilde{k} \exp[(-\eta + \tilde{k}\gamma)(t-T)]|d_{k+1}(T)| \\ &+ \alpha\|d_k\|_\infty. \end{aligned} \quad (5.38)$$

By design,  $\eta > \tilde{k}\gamma$  can be increased so that  $\alpha := \frac{\tilde{k}b}{\eta - \tilde{k}\gamma} < 1$  and we have  $|d_{k+1}(t)| \leq \alpha\|d_k\|_\infty + \|\phi_k\|_\infty$  where  $\phi_k(t) \rightarrow 0$  exponentially as  $t \rightarrow \infty$ , and  $\|\cdot\|_\infty$  denotes the sup norm on  $[T, \infty)$ . ■

**Conclusion** These theorems establish that, under some general qualitative conditions on the dynamics of vehicle models, decentralized controllers (using only  $v_i, a_i, \Delta_k$ , and the vehicle state) can achieve the design goals of the platoon concept:  $N$  vehicles traveling down the highway at high speed and maintaining tight formation. Simulations based on simple vehicle models and decentralized controllers in chapters 2 and 3 support these conclusions.

## Chapter 6

# Indirect Adaptive Control of a Class of Interconnected Nonlinear Dynamical Systems

In this chapter, we consider the class of interconnected nonlinear dynamical systems suggested by the problem of longitudinal and lateral control of a platoon of vehicles on automated highways. After describing the physical setting from which the control problem arises, we propose a local indirect adaptive control scheme for this class of interconnected nonlinear systems. Then, we state precise conditions on the inputs, on the uncertain parameters, and on the dynamics of the nonlinear plants under which it is possible to attain the design objectives by using *local, nonlinear, adaptive* control laws.

### 6.1 Introduction

Motivated by the highway automation project presented in chapters 2, 3, and 4, we propose *local adaptive nonlinear* control laws which are suitable for a class of interconnected nonlinear dynamical systems. These control laws have two main advantages: a) since they use *local* measurements of the relevant signals, the computational and measurement costs are reduced while the reliability and the flexibility of the control system as a whole are increased; b) since they are *adaptive* by design, the robustness of the control system with respect to uncertain parameters is increased. The purpose of this chapter is to state precise

conditions on the inputs, on the uncertain parameters, and on the dynamics of the nonlinear plants under which we can design suitable *local* control laws for a class of interconnected nonlinear systems.

The organization of the chapter is as follows: in section 6.2, we describe the physical setting from which the control problem arises; motivated by the application discussed in section 6.2, in section 6.3, we propose an indirect adaptive control scheme for a general class of interconnected nonlinear dynamical systems; in section 6.4, we state precise conditions on the inputs and parameter errors, under which we can apply the adaptive control scheme in section 6.3 to design suitable control laws for the class of interconnected nonlinear systems under consideration; finally, in section 6.5, we provide concluding remarks regarding the proposed control scheme. The proofs of the theorems together with the proof of stability of proposed identifiers are included in the appendix at the end of the chapter.

## 6.2 Problem Description

In this section, using the dynamic equations in chapters 2 and 4 representing the longitudinal and lateral dynamics of a platoon of vehicles, we motivate the form of the equations representing the dynamics of the class of interconnected nonlinear dynamical systems under study.

### 6.2.1 Longitudinal Dynamics of a Platoon

Longitudinal dynamics of a platoon of *non-identical* vehicles using simple *nonlinear* engine models were reported in chapter 2; these studies considered only a *straight* highway.

For the  $k$ -th vehicle ( $k = 2, 3, \dots, N$ ), the form of the differential equations representing the  $k$ -th vehicle's longitudinal dynamics is as follows: (suppressing the explicit dependence on  $t$ ),

$$\dot{\zeta}_k = f_k(\zeta_k, \zeta_{k-1}) + g_k(\zeta_k)u_k \quad (6.1)$$

where  $\zeta_k \in \mathbb{R}^3$ ,  $\zeta_{k-1} \in \mathbb{R}^3$ ,  $f_k : \mathbb{R}^3 \times \mathbb{R}^3 \rightarrow \mathbb{R}^3$ ,  $g_k : \mathbb{R}^3 \rightarrow \mathbb{R}^3$ , and  $u_k \in \mathbb{R}$ ; the components of  $\zeta_k$  are  $\Delta_k$  (the headway),  $v_{Fk}$  (the velocity of the center of mass of the  $k$ -th vehicle along its longitudinal body axis), and  $a_{Fk}$  (the acceleration of the center of mass of the  $k$ -th vehicle along its longitudinal body axis);  $u_k$  denotes the throttle input to the  $k$ -th vehicle's engine. Equation (6.1) is derived from equations (2.3)-(2.4).

To explicitly show the dependence of the  $k$ -th vehicle's longitudinal dynamics ( $k = 2, 3, \dots, N$ ) on the  $k$ -th vehicle's characteristics (e.g., engine time constant, mass of the vehicle, drag coefficient, and mechanical drag), we write (6.1) as

$$\dot{\zeta}_k = W_k(\zeta_k, \zeta_{k-1}, u_k) \theta_k^* \quad (6.2)$$

where  $\theta_k^*$  is a column vector of the known parameters of the  $k$ -th vehicle and  $W_k(., ., .)$  is a matrix function of appropriate dimensions. For the first vehicle ( $k = 1$ ), equation (6.2) takes the form

$$\dot{\zeta}_1 = W_1(\zeta_1, u_1, u) \theta_1^* \quad (6.3)$$

where  $u_1$  denotes the throttle input;  $u$  denotes the vector  $(v_F, a_F)$ ;  $\theta_1^*$  denotes a column vector of the known parameters of the first vehicle; and  $W_1(., ., .)$  is a matrix function with appropriate dimensions.

### 6.2.2 Lateral Dynamics of a Vehicle

In chapter 4, we have used a *nonlinear* model to represent the lateral vehicle dynamics (equations (4.7), (4.9), (4.11), (4.12), (4.44), (4.45), and (4.53))

$$\dot{\xi} = \tilde{W}(\xi, \delta, u_{road}) \tilde{\theta}^* \quad (6.4)$$

where  $\xi \in R^6$ ,  $\delta \in R$ ,  $u_{road} \in R^2$ ; the components of  $\xi$  are the lateral deviation of the vehicle's center of mass from the lane center ( $\Delta_{lat}$ ) and its time-derivative ( $\dot{\Delta}_{lat}$ ), the components of the velocity of the vehicle's center of mass along its longitudinal and transversal axes ( $v_F$  and  $v_S$ , respectively), and the vehicle's yaw angle ( $\epsilon$ ) and its time-derivative ( $\dot{\epsilon}$ );  $\delta$  denotes the steering angle command input;  $u_{road}$  denotes the input to the vehicle's lateral dynamics due to the road geometry;  $\tilde{\theta}^*$  denotes a column vector of the known parameters for the vehicle's lateral dynamics (these parameters depend on the vehicle's mass, the vehicle tires' cornering stiffnesses, the moment of inertia of the vehicle about the vertical axis through its center of mass, etc...); and  $\tilde{W}(., ., .)$  is a matrix function of appropriate dimensions.

### 6.2.3 Control Laws

Note that the differential equations representing the longitudinal dynamics of one vehicle (6.2)-(6.3) and those representing the lateral dynamics of one vehicle (6.4) depend *linearly*

on the parameters. If these parameters are known, we can design suitable control laws for the longitudinal control of a platoon of vehicles ([41],[47]) and the lateral control of each vehicle ([43]): in the case of the longitudinal control of a platoon, we can design *local nonlinear* control laws  $u_1 = \bar{u}_1(\zeta_1, u, \theta_1^*)$  and  $u_k = \bar{u}_k(\zeta_k, \zeta_{k-1}, u, \theta_k^*)$  (for  $k = 2, 3, \dots, N$ ) such that the differential equations (6.2)-(6.3), under these control laws, have the following form

$$\dot{\zeta}_1 = f_1(\zeta_1, u) \quad (6.5)$$

for  $k = 2, 3, \dots, N$ ,

$$\dot{\zeta}_k = f(\zeta_k, \zeta_{k-1}, u). \quad (6.6)$$

Figure 6.1 shows the interconnection of nonlinear systems with no parameter uncertainties (6.5)-(6.6). From (6.6) we note that (for  $k = 2, 3, \dots, N$ ) the control laws  $u_k = \bar{u}_k(\zeta_k, \zeta_{k-1}, u, \theta_k^*)$  have resulted in longitudinal dynamics for the  $k$ -th vehicle which are *independent* of its particular characteristics. We have shown that it is possible to design the above control laws ([45],[44],[40]) so that in the case of a sufficiently slow change in the lead vehicle's velocity ( $v_{FL}$ ) from its steady-state value: a) for  $k = 1, 2, \dots, N$ ,  $t \mapsto \Delta_k(t)$  is bounded, b) for  $k = 1, 2, \dots, N$ ,  $\Delta_k(t) \rightarrow 0$  as  $t \rightarrow \infty$ , and c) for  $k = 2, 3, \dots, N$ , the peak deviation of the  $k$ -th vehicle from its assigned position monotonically decreases as  $k$  increases.

In the case of the lateral control of a vehicle, we can design *nonlinear* control laws  $\delta = \bar{\delta}(\xi, u_{road}, \bar{\theta}^*)$  such that the differential equations (6.4), under these control laws, have the form

$$\dot{\xi} = \tilde{f}(\xi, u_{road}). \quad (6.7)$$

Subsequently, applying the results from [45],[44],[40] to (6.7), under sufficiently slowly-varying  $u_{road}$  and by the suitable design of lateral control laws  $\delta = \bar{\delta}(\xi, u_{road}, \bar{\theta}^*)$  we have: a)  $t \mapsto \Delta_{lat}(t)$  is bounded, and b)  $\Delta_{lat}(t) \rightarrow 0$  as  $t \rightarrow \infty$ .

In the discussion above, the control laws depended on the exact knowledge of the parameters in the differential equations describing the longitudinal or the lateral dynamics. In the next section, we take a more realistic point of view and propose *local* indirect adaptive control laws when the parameters are not known exactly. Motivated by the above application, we propose an indirect adaptive control scheme for the class of interconnected nonlinear dynamical systems depicted in Figure 6.1. In fact, in section 6.4, we will show that under sufficiently small parameter errors and sufficiently slowly-varying inputs, we can

design suitable control laws such that: a) for  $k = 1, 2, \dots, N$ ,  $t \mapsto \Delta_k(t)$  is bounded, b) for  $k = 1, 2, \dots, N$ ,  $\Delta_k(t) \rightarrow 0$  as  $t \rightarrow \infty$ , c) for  $k = 2, 3, \dots, N$ , the peak deviation of the  $k$ -th vehicle from its assigned position due to a change in the lead vehicle's velocity monotonically decreases as  $k$  increases, d) for  $k = 1, 2, \dots, N$ ,  $t \mapsto \Delta_{k,\text{lat}}(t)$  is bounded ( $\Delta_{k,\text{lat}}(t)$  denotes the lateral deviation of the  $k$ -th vehicle's center of mass from the center of the lane), and e)  $\Delta_{k,\text{lat}}(t) \rightarrow 0$  as  $t \rightarrow \infty$ .

### 6.3 Problem Formulation

Throughout the chapter we suppress the explicit dependence on  $t$ ;  $|x|$ ,  $|W|$  denote the max norm of vector  $x$  and the corresponding induced max norm of matrix  $W$ .

Motivated by the above discussion, we consider the following nonlinear, time-invariant differential equations representing a class of interconnected nonlinear dynamical systems:

$$\begin{aligned}\dot{\zeta}_1 &= W_1(\zeta_1, u_1, u)\theta_1^* \\ \dot{\zeta}_2 &= W_2(\zeta_2, \zeta_1, u_2)\theta_2^* \\ \dot{\zeta}_3 &= W_3(\zeta_3, \zeta_2, u_3)\theta_3^* \\ &\vdots \\ \dot{\zeta}_N &= W_N(\zeta_N, \zeta_{N-1}, u_N)\theta_N^*\end{aligned}\tag{6.8}$$

where the exogenous input  $u$  belongs to an open set  $U \subset R^m$  ( $u = (v_{Fl}, a_{Fl})$  in the longitudinal control problem above and  $u = u_{road}$  in the lateral control problem above); for  $k = 1, 2, \dots, N$ ,  $\zeta_k$  belongs to an open and convex set  $P_U \subset R^n$ , the control input to the  $k$ -th dynamical system  $u_k$  belongs to an open set  $U_k \subset R^q$ , the parameter vector of the  $k$ -th dynamical system  $\theta_k^*$  belongs to  $R^p$ , and  $W_k(\cdot, \cdot, \cdot)$  is an  $n \times p$  matrix function.

Note that the differential equations representing the  $k$ -th dynamical system in (6.8) depend *linearly* on the parameters. If these parameters are known, we assume that we can design suitable *local nonlinear* control laws  $u_1 = \bar{u}_1(\zeta_1, u, \theta_1^*)$  and  $u_k = \bar{u}_k(\zeta_k, \zeta_{k-1}, u, \theta_k^*)$  (for  $k = 2, 3, \dots, N$ ) such that, under these control laws, the closed loop dynamics of the interconnection of nonlinear dynamical systems has the following form:

$$\begin{aligned}\dot{\zeta}_1 &= f_1(\zeta_1, u) \\ \dot{\zeta}_2 &= f(\zeta_2, \zeta_1, u)\end{aligned}$$

$$\begin{aligned}
\dot{\zeta}_3 &= f(\zeta_3, \zeta_2, u) \\
&\vdots \\
\dot{\zeta}_N &= f(\zeta_N, \zeta_{N-1}, u).
\end{aligned} \tag{6.9}$$

Note that, for  $k = 2, 3, \dots, N$ , these control laws have resulted in dynamics for the  $k$ -th dynamical system which are *independent* of its particular characteristics (i.e., the function  $f(., ., .)$  in (6.9) does not depend on  $k$ , for  $k \geq 2$ ). Thus, we make the following assumption:

**Assumption [certainty equivalence condition] ([55],[22],[35]):** We assume that we can design control laws  $\bar{u}_k$  ( $k = 1, 2, \dots, N$ ) with  $\bar{u}_1 : P_U \times U \times R^p \rightarrow R^q$ , and for  $k = 2, 3, \dots, N$ ,  $\bar{u}_k : P_U \times P_U \times U \times R^p \rightarrow R^q$  such that under these control laws:

$$W_1(\zeta_1, \bar{u}_1(\zeta_1, u, \theta), u)\theta = f_1(\zeta_1, u)$$

and for  $k \geq 2$ ,

$$W_k(\zeta_k, \zeta_{k-1}, \bar{u}_k(\zeta_k, \zeta_{k-1}, u, \theta))\theta = f(\zeta_k, \zeta_{k-1}, u)$$

for all  $u \in U$ , for all  $\zeta_k \in P_U$  ( $k = 1, 2, \dots, N$ ), and for all  $\theta \in R^p$ .

### 6.3.1 Interconnection of the Nonlinear Dynamical Systems with Parameter Uncertainty

In case the parameters  $\theta_k^*$  in (6.8) are unknown, we use estimates of the parameters (denoted by  $\hat{\theta}_k$  for  $k = 1, 2, \dots, N$ ) for computing the control input to the  $k$ -th dynamical system: for the first dynamical system,

$$u_1 = \bar{u}_1(\zeta_1, u, \hat{\theta}_1) \tag{6.10}$$

and for  $k = 2, 3, \dots, N$ ,

$$u_k = \bar{u}_k(\zeta_k, \zeta_{k-1}, u, \hat{\theta}_k). \tag{6.11}$$

Substituting the expressions for  $u_k$  from (6.10)-(6.11) into (6.8) we obtain

$$\begin{aligned}
\dot{\zeta}_1 &= W_1(\zeta_1, \bar{u}_1(\zeta_1, u, \hat{\theta}_1), u)\theta_1^* \\
\dot{\zeta}_2 &= W_2(\zeta_2, \zeta_1, \bar{u}_2(\zeta_2, \zeta_1, u, \hat{\theta}_2))\theta_2^* \\
\dot{\zeta}_3 &= W_3(\zeta_3, \zeta_2, \bar{u}_3(\zeta_3, \zeta_2, u, \hat{\theta}_3))\theta_3^* \\
&\vdots \\
\dot{\zeta}_N &= W_N(\zeta_N, \zeta_{N-1}, \bar{u}_N(\zeta_N, \zeta_{N-1}, u, \hat{\theta}_N))\theta_N^*.
\end{aligned} \tag{6.12}$$

Adding and subtracting  $W_1(\zeta_1, \bar{u}_1(\zeta_1, u, \hat{\theta}_1), u)\hat{\theta}_1$  to the right hand side of the first equation in (6.12) and noting the certainty equivalence condition for the first dynamical system, we obtain

$$\dot{\zeta}_1 = f_1(\zeta_1, u) + W_1(\zeta_1, \bar{u}_1(\zeta_1, u, \hat{\theta}_1), u)(\theta_1^* - \hat{\theta}_1). \quad (6.13)$$

Similarly, adding and subtracting  $W_k(\zeta_k, \zeta_{k-1}, \bar{u}_k(\zeta_k, \zeta_{k-1}, u, \hat{\theta}_k))\hat{\theta}_k$  to the right hand side of the  $k$ -th equation ( $k = 2, 3, \dots, N$ ) in (6.12) and noting the certainty equivalence condition for the  $k$ -th dynamical system, we obtain (for  $k = 2, 3, \dots, N$ )

$$\dot{\zeta}_k = f(\zeta_k, \zeta_{k-1}, u) + W_k(\zeta_k, \zeta_{k-1}, \bar{u}_k(\zeta_k, \zeta_{k-1}, u, \hat{\theta}_k))(\theta_k^* - \hat{\theta}_k). \quad (6.14)$$

Denote the parameter error by  $\phi_k := \hat{\theta}_k - \theta_k^*$  ( $k = 1, 2, \dots, N$ ). Then from (6.13)-(6.14) we note

$$\begin{aligned} \dot{\zeta}_1 &= f_1(\zeta_1, u) - W_1(\zeta_1, \bar{u}_1(\zeta_1, u, \hat{\theta}_1), u)\phi_1 \\ \dot{\zeta}_2 &= f_2(\zeta_2, \zeta_1, u) - W_2(\zeta_2, \zeta_1, \bar{u}_2(\zeta_2, \zeta_1, u, \hat{\theta}_2))\phi_2 \\ \dot{\zeta}_3 &= f_3(\zeta_3, \zeta_2, u) - W_3(\zeta_3, \zeta_2, \bar{u}_3(\zeta_3, \zeta_2, u, \hat{\theta}_3))\phi_3 \\ &\vdots \\ \dot{\zeta}_N &= f_N(\zeta_N, \zeta_{N-1}, u) - W_N(\zeta_N, \zeta_{N-1}, \bar{u}_N(\zeta_N, \zeta_{N-1}, u, \hat{\theta}_N))\phi_N. \end{aligned} \quad (6.15)$$

Figure 6.2 shows the interconnection of nonlinear dynamical systems with parameter uncertainties described by (6.15). Note that, for  $k = 1, 2, \dots, N$ , the *local* control laws  $\bar{u}_k$  in (6.10)-(6.11) have resulted in closed loop dynamics for the  $k$ -th dynamical system which differs from the respective closed loop dynamics in (6.9) in that the dynamics of the  $k$ -th dynamical system in (6.15) are affected by nonlinear perturbations  $W_k\phi_k$ .

### 6.3.2 Indirect Adaptive Control of the Interconnection

In this subsection, we propose *local* indirect adaptive control laws ([55, and references therein]) for the interconnection of nonlinear dynamical systems in (6.8). The control laws for the  $k$ -th dynamical system in (6.8) ( $k = 1, 2, \dots, N$ ) use parameter estimates,  $\hat{\theta}_k$ , obtained from an identifier for the  $k$ -th dynamical system, to compute the control input to the  $k$ -th dynamical system in (6.8).

**Identifier Structure:** We propose a standard identifier structure for nonlinear systems with dynamics which depend linearly on the unknown parameters ([55],[22],[4],[32]): let

$A \in R^{n \times n}$  be a Hurwitz matrix and let  $Q \in R^{n \times n}$  be a given symmetric, positive definite matrix; let  $P \in R^{n \times n}$  denote the symmetric positive definite matrix solution of the Lyapunov equation  $A^T P + PA = -Q$ ; for the first dynamical system in (6.8) the identifier is:

$$\begin{aligned}\dot{\hat{\zeta}}_1 &= A(\hat{\zeta}_1 - \zeta_1) + W_1(\zeta_1, u_1, u)\hat{\theta}_1 \\ \dot{\hat{\theta}}_1 &= -W_1^T(\zeta_1, u_1, u)P(\hat{\zeta}_1 - \zeta_1);\end{aligned}\quad (6.16)$$

for the  $k$ -th dynamical system ( $k = 2, 3, \dots, N$ ) in (6.8) the identifier is:

$$\begin{aligned}\dot{\hat{\zeta}}_k &= A(\hat{\zeta}_k - \zeta_k) + W_k(\zeta_k, \zeta_{k-1}, u_k)\hat{\theta}_k \\ \dot{\hat{\theta}}_k &= -W_k^T(\zeta_k, \zeta_{k-1}, u_k)P(\hat{\zeta}_k - \zeta_k).\end{aligned}\quad (6.17)$$

We assume that for  $k = 1, 2, \dots, N$ ,  $W_k$  is bounded. Then, using a standard Lyapunov argument, we can show that for  $k = 1, 2, \dots, N$ ,  $\phi_k \in L_\infty$  and  $(\hat{\zeta}_k - \zeta_k)(t) \rightarrow 0$  as  $t \rightarrow \infty$ . Furthermore, if  $W_k$  (for  $k = 1, 2, \dots, N$ ) is sufficiently rich (see [35, page 72]), then  $\phi_k(t) \rightarrow 0$  as  $t \rightarrow \infty$  (i.e., parameter convergence is established as in [27]). The proof of stability of the proposed identifiers is given in the Appendix.

**Indirect Adaptive Control Laws:** We propose the control laws (6.10)-(6.11) for the interconnection of nonlinear dynamical systems in (6.8). These control laws use the parameter estimates,  $\hat{\theta}_k$  (for  $k = 1, 2, \dots, N$ ), obtained from the above identifiers to compute the control input to the  $k$ -th dynamical system in (6.8). As shown in subsection 6.3.1, the resulting closed loop dynamics of the interconnection of nonlinear dynamical systems under these control laws has the form given in (6.15). Figures 6.3 and 6.4 show the diagrams of the indirect adaptive control of the  $k$ -th dynamical system in (6.8).

The question arises as to how parameter errors  $\phi_k$ , for  $k = 1, 2, \dots, N$ , will affect the closed loop performance of the interconnection of dynamical systems (6.15). In the next section, we give precise conditions on the inputs,  $u$ , and parameter errors,  $\phi_k$ , for  $k = 1, 2, \dots, N$ , under which we can design suitable control laws,  $\bar{u}_k$ , for  $k = 1, 2, \dots, N$ , for the interconnection of nonlinear dynamical systems (6.8).

## 6.4 Main Results

In this section, we state two theorems regarding the closed loop performance of the interconnection of dynamical systems (6.15). Theorem 6.1 considers a single dynamical

system in (6.15) (e.g., the first dynamical system in (6.15)) and states precise conditions on the inputs,  $u$ , and the parameter errors,  $\phi_1$ , under which we can design suitable control laws. Theorem 6.2 considers the interconnection of dynamical systems (6.15) and states precise conditions on the inputs,  $u$ , and the parameter errors,  $\phi_k$ , for  $k = 1, 2, \dots, N$ , under which we can design suitable *local* control laws for each dynamical subsystem in (6.15).

#### 6.4.1 Stability of a nonlinear dynamical system with slowly- varying inputs and small parameter errors

We start with a crucial definition.

**Definition [sink] ([19])** Consider a dynamical system described as follows:

$$\dot{\zeta}_1 = f_1(\zeta_1, u) \quad (6.18)$$

where  $u \in U$ , open in  $R^m$ , and  $\zeta_1 \in P_U$ , open in  $R^n$ , and  $f_1$  is  $C^2$ .

A point  $\zeta_1^0$  in  $P_U$  is called a *sink* of (6.18) corresponding to the constant input  $w_0$  in  $U$  if  $f_1(\zeta_1^0, w_0) = 0$  and  $\text{Re}\sigma[D_1 f_1(\zeta_1^0, w_0)] < 0$ ; where  $D_1 f_1(.,.)$  denotes the Jacobian matrix of  $f_1(.,.)$  with respect to the first variable and  $\sigma[.]$  denotes the spectrum of a matrix.

It is well known that if  $\zeta_1^0$  is a sink corresponding to  $w_0$ , then there is a ball  $B(\zeta_1^0, r)$ , centered on  $\zeta_1^0$ , such that for all  $\zeta_1(t_0) \in B(\zeta_1^0, r)$ , the solution of  $\dot{\zeta}_1 = f_1(\zeta_1, w_0)$  is bounded and decays exponentially to  $\zeta_1^0$  (see e.g., [57],[10]). By suitable design of the control laws, we *assume* that we can move the spectrum of  $D_1 f_1(\zeta_1^0, w_0)$  further into the left half plane.

**Theorem 6.1** Consider the dynamical system described as follows:

$$\dot{\zeta}_1 = f_1(\zeta_1, u) - W_1(\zeta_1, \bar{u}_1(\zeta_1, u, \hat{\theta}_1), u)\phi_1. \quad (6.19)$$

Suppose that  $P_U$  is an open and convex subset of  $R^n$ ;  $U$  is an open subset of  $R^m$ ; and,  $U_1$  is an open subset of  $R^q$ . We assume that  $f_1 : P_U \times U \rightarrow R^n$  is a  $C^2$  function such that

$$M_U^1 := \{(\zeta_e, u) \in P_U \times U | \zeta_e \text{ is a sink of (6.18) corresponding to } u\}$$

has a non-empty arcwise-connected interior  $Q_U^1$ . Let  $\overline{Q}_U^1$  be compact. Let  $u : [t_0, \infty) \rightarrow U$  and  $\zeta_e : [t_0, \infty) \rightarrow P_U$  be two given  $C^1$  functions such that  $(\zeta_e(t), u(t)) \in \overline{Q}_U^1$  for all  $t \geq t_0$ . Let  $\zeta_1(.)$  be the solution of (6.19) with the  $u(.)$  defined above and with initial condition

$\zeta_1(t_0)$ . Let  $\phi_1 \in R^p$ .

We assume that  $W_1 : P_U \times U_1 \times U \rightarrow R^{n \times p}$  is an  $n \times p$  matrix which is bounded, more precisely, for some  $0 < b_{w1} < \infty$  and for all  $(\zeta, \bar{u}, u) \in P_U \times U_1 \times U$ , we have

$$|W_1(\zeta, \bar{u}, u)| \leq b_{w1}.$$

Let  $P_{Q_U^1} := \{q \in P_U | (q, u) \in Q_U^1\}$ . Let  $Z_U$  be a compact set with interior  $Z_U^0$  such that  $\overline{P}_{Q_U^1} \subset Z_U^0 \subset Z_U \subset P_U$ . (Such a  $Z_U$  exists because  $\overline{P}_{Q_U^1}$  is a compact subset of the open set  $P_U$ .)

Then, for any  $\rho > 0$ , there exist  $\delta_0^1 := \delta_0^1(\rho, f_1, Q_U^1) > 0$ ,  $\delta_u^1 := \delta_u^1(\rho, f_1, Q_U^1) > 0$ , and  $\delta_{\phi_1} := \delta_{\phi_1}(\rho, f_1, Q_U^1) > 0$  such that for all  $u(\cdot)$  and  $\zeta_e(\cdot)$  as defined above and satisfying  $|\zeta_1(t_0) - \zeta_e(t_0)| \leq \delta_0^1$ ,  $\max_{t \geq t_0} |\dot{u}(t)| \leq \delta_u^1$ , and  $\max_{t \geq t_0} |\phi_1(t)| \leq \delta_{\phi_1}$  we have:

- (i) for all  $t \geq t_0$ ,  $\zeta_1(t) \in Z_U$ ,
- (ii) for all  $t \geq t_0$ ,  $|\zeta_1(t) - \zeta_e(t)| < \rho$ , and
- (iii) if  $\rho$  is sufficiently small, then for all  $t \geq t_0$ ,  $\zeta_1(t)$  belongs to the basin of attraction of the sink  $\zeta_e(t)$  with respect to  $u(t)$ .

#### Comments-

- (i) If the parameters of the first dynamical system in (6.8) are known (i.e.,  $\phi_1 \equiv 0$ ) then (6.19) will reduce to (6.18). In this case, there are two methods for proving the above theorem: 1) estimation in the time domain (see [19], with improvements [39]); 2) using Lyapunov functions (the existence follows from lemma 6.2 of [17], the technique is detailed by Khalil and Kokotovic [20]). For completeness, we give the proof of Theorem 6.1 when  $\phi_1$  is not identically zero. We use a method similar to that in [19] and [39].
- (ii) Applying the results of Theorem 6.1 to the longitudinal and lateral control problems discussed in section 6.2, we note that: in the case of longitudinal control of the first vehicle in the platoon, we can design suitable control laws such that under sufficiently slow changes in the lead vehicle's velocity,  $v_{F1}$ , and sufficiently small parameter errors for the first vehicle,  $\phi_1, t \mapsto \Delta_1(t)$  is bounded, and  $\Delta_1(t) \rightarrow 0$  as  $t \rightarrow \infty$ ; in the case of lateral control of each vehicle in the platoon, we can design suitable control laws such that under sufficiently slow changes in the road curvature and slope and sufficiently small parameter errors for each vehicle, for  $k = 1, 2, \dots, N$ ,  $t \mapsto \Delta_{k,lat}(t)$  is bounded, and  $\Delta_{k,lat}(t) \rightarrow 0$  as  $t \rightarrow \infty$ .

- (iii) The proof of Theorem 6.1 consists of three main steps: 1) writing the Taylor expansion of  $f_1(\zeta_1, u)$  about  $(\zeta_e, u)$  in the right hand side of (6.19) and deriving a linear time-varying differential equation representing the dynamics of  $(\zeta_1 - \zeta_e)$ ; 2) using a special form of Bellman-Gronwall lemma (see [9, Ch.I,lemma I.6,consequence 1]) to bound  $|\zeta_1(t) - \zeta_e(t)|$ ; and 3) showing that under suitable design of control laws, together with sufficiently slowly-varying inputs,  $u$ , and small parameter errors,  $\phi_1$ , the bound on  $|\zeta_1(t) - \zeta_e(t)|$  holds for all  $t \geq t_0$ .

The proof of Theorem 6.1 is in the Appendix.

#### 6.4.2 Control of an interconnection of nonlinear dynamical systems with slowly-varying inputs and small parameter errors

In this subsection, we consider the interconnection of nonlinear dynamical systems (6.15). Let  $u : [t_0, \infty) \rightarrow U$  and  $\zeta_e : [t_0, \infty) \rightarrow P_U$  be two given  $C^1$  functions such that for all  $t \geq t_0$ ,  $\zeta_e(t)$  is a sink of  $\dot{\zeta}_1 = f_1(\zeta_1, u(t))$  corresponding to  $u(t)$  and the same  $\zeta_e(t)$  is a sink of  $\dot{\zeta}_k = f_k(\zeta_k, \zeta_e(t), u(t))$  (for  $k = 2, 3, \dots, N$ ) corresponding to  $(\zeta_e(t), u(t))$ .

By suitable design of the control laws, there exists a  $\tilde{\mu} < 0$  such that for all  $t \geq t_0$ ,  $\text{Re}\sigma[D_1f(\zeta_e(t), \zeta_e(t), u(t))] \leq \tilde{\mu} < 0$ . Thus, there exists an  $\tilde{\epsilon} > 0$  such that if  $|\frac{d}{dt}D_1f(\zeta_e(t), \zeta_e(t), u(t))| \leq \tilde{\epsilon}$  then for some  $\tilde{k} \geq 1$ , some  $\tilde{\eta} > 0$ , and for all  $t \geq s \geq t_0$ ,  $|\tilde{\Phi}(t, s)| \leq \tilde{k}e^{-\tilde{\eta}(t-s)}$ , (here  $\tilde{\Phi}(., .)$  denotes the state transition matrix of  $\dot{z} = D_1f(\zeta_e(t), \zeta_e(t), u(t))z$  ([3],[57])).

Furthermore, we assume that for all  $t \geq t_0$ ,  $(\zeta_e(t), \zeta_e(t), u(t))$  belongs to a compact set and  $f$  is a  $C^2$  function. Thus, there exists a finite number  $\tilde{b} > 0$  such that

$\max_{t \geq t_0} |D_2f(\zeta_e(t), \zeta_e(t), u(t))| = \tilde{b}$ ; furthermore, by suitable design of control laws, the size of  $\tilde{b}$  can be reduced.

Let  $d_k := \zeta_k - \zeta_e$  (for  $k = 1, 2, \dots, N$ ) where  $\zeta_k(.)$  is the solution of the differential equations representing the  $k$ -th dynamical system in (6.15) with initial condition  $\zeta_k(t_0)$ .

**Theorem 6.2** Consider the interconnection of nonlinear dynamical systems (6.15). Suppose that  $P_U$  is an open and convex subset of  $R^n$ ;  $U$  is an open subset of  $R^m$ ; and  $U_1$  is an open subset of  $R^q$ . We assume that  $f_1 : P_U \times U \rightarrow R^n$  is a  $C^2$  function such that

$$M_U^1 := \{(q, u) \in P_U \times U \mid q \text{ is a sink of } \dot{\zeta}_1 = f_1(\zeta_1, u) \text{ corresponding to } u\}$$

has a non-empty interior. We assume that  $f : P_U \times P_U \times U \rightarrow R^n$  is a  $C^2$  function such that

$$M_U := \{(q, \zeta_e, u) \in P_U \times P_U \times U \mid q \text{ is a sink of } \dot{\zeta} = f(\zeta, \zeta_e, u) \text{ corresponding to } (\zeta_e, u)\}$$

has a non-empty interior (in the relative topology of  $M_U$ ). Let  $\overline{Q}_U^1$  and  $\overline{Q}_U$  be compact, arcwise-connected subsets of  $M_U^1$  and  $M_U$ , respectively. Let  $\overline{Q}_U^1$  and  $\overline{Q}_U$  have non-empty interiors  $Q_U^1$  and  $Q_U$ , respectively. Let  $u : [t_0, \infty) \rightarrow U$  and  $\zeta_e : [t_0, \infty) \rightarrow P_U$  be two given  $C^1$  functions such that for all  $t \geq t_0$ ,  $(\zeta_e(t), u(t)) \in Q_U^1$  and  $(\zeta_e(t), \zeta_e(t), u(t)) \in Q_U$ . Let  $\zeta_k(\cdot)$  (for  $k = 1, 2, \dots, N$ ) be the solution to the  $k$ -th equation in (6.15) with the  $u(\cdot)$  defined above and with initial condition  $\zeta_k(t_0)$ . For  $k = 1, 2, \dots, N$ , let  $\phi_k \in R^p$ .

We assume that  $W_1 : P_U \times U_1 \times U \rightarrow R^{n \times p}$  is an  $n \times p$  matrix which is bounded, more precisely, for some  $0 < b_{w1} < \infty$  and for all  $(\zeta, \bar{u}, u) \in P_U \times U_1 \times U$ , we have

$$|W_1(\zeta, \bar{u}, u)| \leq b_{w1}.$$

Furthermore, we assume that for  $k = 2, 3, \dots, N$ ,  $W_k : P_U \times P_U \times U \rightarrow R^{n \times p}$  is an  $n \times p$  matrix which is bounded, more precisely, for some  $0 < b_w < \infty$  and for all  $(\zeta, \zeta_p, u) \in P_U \times P_U \times U$ , we have

$$|W_k(\zeta, \zeta_p, u)| \leq b_w.$$

Let  $P_{Q_U^1} := \{q \in P_U \mid (q, u) \in Q_U^1\}$  and  $P_{Q_U} := \{q \in P_U \mid (q, \zeta_e, u) \in Q_U\}$ . Let  $Z_U$  be a compact set such that  $\overline{P}_{Q_U^1} \cup \overline{P}_{Q_U} \subset Z_U^0 \subset Z_U \subset P_U$ . (Such a  $Z_U$  exists because  $\overline{P}_{Q_U^1} \cup \overline{P}_{Q_U}$  is a compact subset of the open set  $P_U$ .)

We assume that by suitable design of control laws we can increase the value of  $\tilde{\eta}$  so that it is much larger than the values of  $\tilde{k}$  and  $\tilde{b}$ . ( $\tilde{\eta}, \tilde{k}$ , and  $\tilde{b}$  were defined before the statement of Theorem 6.2.)

Then, there exists a  $\rho_0 := \rho_0(f, Q_U, Z_U) > 0$  such that for any  $0 < \rho < \rho_0$ , there exists  $\delta_0^1 := \delta_0^1(\rho, f_1, Q_U^1) > 0$ ,  $\tilde{\delta}_0 := \tilde{\delta}_0(\rho, f, Q_U, Z_U) > 0$ ,  $\tilde{\delta}_u := \tilde{\delta}_u(\rho, f_1, f, Q_U^1, Q_U) > 0$ ,  $\tilde{\delta}_\zeta := \tilde{\delta}_\zeta(\rho, f, Q_U, Z_U) > 0$ , and  $\tilde{\delta}_\phi := \tilde{\delta}_\phi(\rho, f_1, f, Q_U^1, Q_U, Z_U) > 0$  such that for all  $u(\cdot)$  and  $\zeta_e(\cdot)$  as defined above and satisfying:

- (a)  $|\zeta_1(t_0) - \zeta_e(t_0)| \leq \delta_0^1$ ,
- (b) for  $k = 2, 3, \dots, N$ ,  $|\zeta_k(t_0) - \zeta_e(t_0)| \leq \tilde{\delta}_0$ ,
- (c)  $\max_{t \geq t_0} |\dot{u}(t)| \leq \tilde{\delta}_u$ ,

(d)  $\max_{t \geq t_0} \max \{|\phi_1(t)|, \dots, |\phi_N(t)|\} \leq \tilde{\delta}_\phi$ ,

(e)  $\max_{t \geq t_0} |\dot{\zeta}_e(t)| \leq \tilde{\delta}_\zeta$ ,

we have :

(i) for all  $k = 1, 2, \dots, N$ , for all  $t \geq t_0$ ,  $\zeta_k(t) \in Z_U$ ,

(ii)  $\|d_1(\cdot)\|_\infty < \rho$ , and with  $d_k := \zeta_k - \zeta_e$

(iii) if, in addition, for all  $k = 1, 2, \dots, N$ ,  $d_k(t_0) = 0$ , then there exist constants  $0 \leq \alpha := \alpha(f, Q_U) < 1$ ,  $0 \leq \beta_\phi := \beta_\phi(f, Q_U) < \infty$ , and  $0 \leq \beta_\zeta := \beta_\zeta(f, Q_U) < \infty$  such that for  $k \geq 1$ ,  $\|d_{k+1}(\cdot)\|_\infty \leq \alpha \|d_k(\cdot)\|_\infty + \beta_\phi \|\phi_k(\cdot)\|_\infty + \beta_\zeta \|\dot{\zeta}_e(\cdot)\|_\infty$ .

### Comments-

- (i) Applying the results of Theorem 6.2 to the longitudinal control problem of a platoon of vehicles discussed in section 6.2, we note that we can design suitable control laws such that in the case of a sufficiently slow change in the lead vehicle's velocity,  $v_{Fl}$ , from its steady-state value and under sufficiently small parameter errors we have: 1) for  $k = 1, 2, \dots, N$ ,  $t \mapsto \Delta_k(t)$  is bounded, 2) for  $k = 2, 3, \dots, N$ ,  $\Delta_k(t) \rightarrow 0$  as  $t \rightarrow \infty$ , and 3) for  $k = 2, 3, \dots, N$ , the peak deviation of the  $k$ -th vehicle position from its assigned position monotonically decreases as  $k$  increases.
- (ii) The proof of Theorem 6.2 consists of three main steps: 1) writing the Taylor expansion of  $f(\zeta_k, \zeta_{k-1}, u)$  about  $(\zeta_e, \zeta_e, u)$  in the right hand side of the  $k$ -th differential equation in (6.15) and deriving a linear time-varying differential equation representing the dynamics of  $d_k := \zeta_k - \zeta_e$ ; 2) using a special form of Bellman-Gronwall lemma (see [9, Ch.I, lemma I.6, consequence 1]) to bound  $|d_k(t)|$ ; 3) using an induction argument on  $k$  to show that, under suitable design of the control laws together with sufficiently slowly-varying inputs,  $u$ , and small parameter errors,  $\phi_k$ , for  $k = 1, 2, \dots, N$ , the bound on  $|d_k(t)|$  holds for all  $t \geq t_0$ .
- (iii) The above theorems establish sufficient conditions on the inputs,  $u$ , and the parameter errors,  $\phi_k$ , for  $k = 1, 2, \dots, N$ , under which we can design suitable *local nonlinear adaptive* control laws for the general class of interconnected nonlinear dynamical systems (6.8), shown in Figure 6.2.

The proof of Theorem 6.2 is in the Appendix.

## 6.5 Conclusion

In this chapter, we have initiated a theoretical investigation in *local adaptive* control laws for a class of interconnected nonlinear dynamical systems. More precisely, we have stated sufficient conditions on the inputs and the parameter errors under which we can design suitable *local* control laws for the interconnection of nonlinear dynamical systems under consideration. The class of interconnected nonlinear dynamical systems has been suggested by the problem of longitudinal and lateral control of a platoon of vehicles on automated highways.

This study makes both theoretical and practical contributions to the design of control laws for interconnected nonlinear dynamical systems. From a theoretical point, it shows that, for a class of interconnected nonlinear dynamical systems, it is possible to attain the design objectives by using *local, nonlinear, adaptive* control laws. From a control designer's view point, the *local* nature of the proposed control laws reduces the computational costs while increasing the reliability and the flexibility of the control system as a whole; furthermore, the *adaptive* nature of these control laws increases the *robustness* of the control system with respect to uncertain parameters.

## 6.6 Appendix

**Stability of Identifiers:** For  $k = 1, 2, \dots, N$ , let  $e_k := \hat{\zeta}_k - \zeta_k$ . Then from (6.8), (6.16), and (6.17) we obtain: for the first dynamical system in (6.8)

$$\begin{aligned}\dot{e}_1 &= Ae_1 + W_1(\zeta_1, u_1, u)\phi_1 \\ \dot{\phi}_1 &= -W_1^T(\zeta_1, u_1, u)Pe_1;\end{aligned}\tag{6.20}$$

for the  $k$ -th dynamical system ( $k = 2, 3, \dots, N$ ) in (6.8)

$$\begin{aligned}\dot{e}_k &= Ae_k + W_k(\zeta_k, \zeta_{k-1}, u_k)\phi_k \\ \dot{\phi}_k &= -W_k^T(\zeta_k, \zeta_{k-1}, u_k)Pe_k.\end{aligned}\tag{6.21}$$

We assume that for  $k = 1, 2, \dots, N$ ,  $W_k$  is bounded. Then, as in [35, sec. 2.4], using a standard Lyapunov argument with  $V_k(e_k, \phi_k) := e_k^T Pe_k + \phi_k^T \phi_k$  ( $k = 1, 2, \dots, N$ ), we can show that for  $k = 1, 2, \dots, N$ ,  $\phi_k \in L_\infty$ ,  $e_k \in L_2 \cap L_\infty$ , and  $\dot{e}_k \in L_\infty$ . The last two relations imply  $e_k(t) \rightarrow 0$  as  $t \rightarrow \infty$ . Furthermore, if  $W_k$  ( $k = 1, 2, \dots, N$ ) is sufficiently

rich (see [35, page 72]), then  $\phi_k(t) \rightarrow 0$  as  $t \rightarrow \infty$  (i.e., parameter convergence is established as in [27]).  $\blacksquare$

### Proof of Theorem 6.1:

[Step 1- Analysis] To simplify notation, we let  $W_1(\hat{\theta}_1) := W_1(\zeta_1, \bar{u}_1(\zeta_1, u, \hat{\theta}_1), u)$  in (6.19). Writing the Taylor expansion of  $f_1(\zeta_1, u)$  about  $(\zeta_e, u)$  in the right hand side of (6.19) and noting that  $f_1(\zeta_e, u) = 0$  we obtain

$$\dot{\zeta}_1 = \int_0^1 D_1 f_1 [\zeta_e + \lambda(\zeta_1 - \zeta_e), u] d\lambda(\zeta_1 - \zeta_e) - W_1(\hat{\theta}_1) \phi_1. \quad (6.22)$$

Differentiating both sides of  $f_1(\zeta_e, u) = 0$  with respect to time and using chain rule we get

$$D_1 f_1(\zeta_e, u) \dot{\zeta}_e + D_2 f_1(\zeta_e, u) \dot{u} = 0. \quad (6.23)$$

Since  $\text{Re}\sigma[D_1 f_1(\zeta_e, u)] < 0$ ,  $D_1 f_1(\zeta_e, u)$  is invertible and from (6.23) we get

$$\dot{\zeta}_e = -[D_1 f_1(\zeta_e, u)]^{-1} D_2 f_1(\zeta_e, u) \dot{u}. \quad (6.24)$$

Subtracting (6.24) from (6.22) we get

$$\begin{aligned} \dot{\zeta}_1 - \dot{\zeta}_e &= \int_0^1 D_1 f_1 [\zeta_e + \lambda(\zeta_1 - \zeta_e), u] d\lambda(\zeta_1 - \zeta_e) \\ &\quad + [D_1 f_1(\zeta_e, u)]^{-1} D_2 f_1(\zeta_e, u) \dot{u} - W_1(\hat{\theta}_1) \phi_1. \end{aligned} \quad (6.25)$$

Adding and subtracting  $D_1 f_1(\zeta_e, u)(\zeta_1 - \zeta_e)$  to the right hand side of (6.25) we get

$$\begin{aligned} \dot{\zeta}_1 - \dot{\zeta}_e &= D_1 f_1(\zeta_e, u)(\zeta_1 - \zeta_e) \\ &\quad + \int_0^1 \{D_1 f_1 [\zeta_e + \lambda(\zeta_1 - \zeta_e), u] - D_1 f_1(\zeta_e, u)\} d\lambda(\zeta_1 - \zeta_e) \\ &\quad + [D_1 f_1(\zeta_e, u)]^{-1} D_2 f_1(\zeta_e, u) \dot{u} - W_1(\hat{\theta}_1) \phi_1. \end{aligned} \quad (6.26)$$

To simplify the notation, we let

$$A(t) := A(\zeta_e(t), u(t)) := D_1 f_1(\zeta_e(t), u(t)), \quad (6.27)$$

$$\begin{aligned} R(t) &:= R(\zeta_e(t), u(t), \zeta_1(t)) \\ &:= \int_0^1 \{D_1 f_1 [\zeta_e(t) + \lambda(\zeta_1(t) - \zeta_e(t)), u(t)] - D_1 f_1(\zeta_e(t), u(t))\} d\lambda, \end{aligned} \quad (6.28)$$

$$B(t) := B(\zeta_e(t), u(t)) := [D_1 f_1(\zeta_e(t), u(t))]^{-1} D_2 f_1(\zeta_e(t), u(t)), \quad (6.29)$$

$$W_1(t) := W_1(\hat{\theta}_1(t)). \quad (6.30)$$

Using (6.27)-(6.30), we can write (6.26) as follows

$$\dot{\zeta}_1 - \dot{\zeta}_e = A(t)(\zeta_1 - \zeta_e) + R(t)(\zeta_1 - \zeta_e) + B(t)\dot{u} - W_1(t)\phi_1. \quad (6.31)$$

Solving (6.31) we get

$$\begin{aligned} (\zeta_1 - \zeta_e)(t) &= \Phi(t, t_0)(\zeta_1 - \zeta_e)(t_0) \\ &+ \int_{t_0}^t \Phi(t, s) \{R(s)(\zeta_1 - \zeta_e)(s) + B(s)\dot{u}(s) - W_1(s)\phi_1(s)\} ds \end{aligned} \quad (6.32)$$

where  $\Phi(t, t_0)$  denotes the state transition matrix of  $\dot{y} = A(t)y$ .

Since  $(\zeta_e(t), u(t)) \in \overline{Q}_U^1$ ,  $\overline{Q}_U^1$  is compact, and  $D_1 f_1(., .)$  is continuous ( $f_1 \in C^2$ ),

$$A(.) \text{ is bounded on } [t_0, \infty). \quad (6.33)$$

Since  $\sigma[A(., .)]$  is a continuous function of its entries,  $(\zeta_e(t), u(t)) \in \overline{Q}_U^1$ ,  $\overline{Q}_U^1$  is compact, and  $\zeta_e(t)$  is a sink of (6.18) corresponding to  $u(t)$ , for all  $t \geq t_0$ ,

$$\text{there exists a } \mu < 0 \text{ such that } \operatorname{Re}\sigma[A(t)] \leq \mu < 0. \quad (6.34)$$

Note that by suitable design of control laws, we can move the spectrum of  $D_1 f_1(\zeta_e(t), u(t))$  further into the left half plane for all  $t \geq t_0$ .

From (6.33)-(6.34) and using the results in [3, Thm.2, sec. 32] we know that there exists an  $\epsilon > 0$  such that

$$\text{if } |\dot{A}(t)| \leq \epsilon \text{ then for some } k \geq 1 \text{ and some } \eta > 0 \text{ and for all } t \geq s \geq t_0, |\Phi(t, s)| \leq ke^{-\eta(t-s)}. \quad (6.35)$$

Differentiating both sides of (6.27) with respect to time and using chain rule we get

$$\dot{A}(t) = D_1^2 f_1(\zeta_e(t), u(t))\dot{\zeta}_e(t) + D_2 D_1 f_1(\zeta_e(t), u(t))\dot{u}(t). \quad (6.36)$$

Substituting the expression for  $\dot{\zeta}_e(t)$  from (6.24) into (6.36) and noting (6.29) we get

$$\dot{A}(t) = E(\zeta_e(t), u(t))\dot{u}(t) \quad (6.37)$$

where

$$E(\zeta_e(t), u(t)) := -D_1^2 f_1(\zeta_e(t), u(t))B(t) + D_2 D_1 f_1(\zeta_e(t), u(t)). \quad (6.38)$$

Since  $(\zeta_e(t), u(t)) \in \overline{Q}_U^1$ ,  $\overline{Q}_U^1$  is compact,  $E(., .)$  is continuous ( $f_1 \in C^2$ ),  $E(., .)$  is bounded on  $Q_U^1$ . Let  $a := \max_{Q_U^1} |E(\zeta_e, u)|$  with  $a < \infty$ . Thus if

$$\max_{t \geq t_0} |\dot{u}(t)| \leq \delta'_u := \frac{\epsilon}{a} \quad (6.39)$$

then  $|\dot{A}(t)| \leq \epsilon$  and (6.35) is satisfied.

[Step 2- Topology] Let  $W_U^1 := \overline{Q}_U^1 \times Z_U$ ;  $W_U^1$  is compact. Since  $f_1 \in C^2$ , the integrand in (6.28) is  $C^1$ , so  $R(.,.,.)$  is  $C^1$  on  $W_U^1$ . If, in (6.28),  $\zeta_1(t) = \zeta_e(t)$ , then  $R(t) = 0$ . By assumption,  $\zeta_e(t) \in P_{Q_U^1} \subset Z_U$ , hence by uniform continuity of  $R(.,.,.)$  on  $W_U^1$ , we conclude that, for any  $c > 0$ , there exists a  $\delta' := \delta'(c) > 0$  such that for all  $t \geq t_0$ ,

$$\text{if } \zeta_1(t) \in Z_U \text{ and } |\zeta_1(t) - \zeta_e(t)| \leq \delta' \text{ then } |R(t)| \leq c. \quad (6.40)$$

From (6.32),(6.35), and (6.40) we note that if a)  $\max_{t \geq t_0} |\dot{u}(t)| \leq \delta'_u$ , b) for all  $t \geq t_0$ ,  $\zeta_1(t) \in Z_U$ , and c) for all  $t \geq t_0$ ,  $|\zeta_1(t) - \zeta_e(t)| \leq \delta'$  then for all  $t \geq t_0$ ,

$$\begin{aligned} |\zeta_1(t) - \zeta_e(t)| &\leq ke^{-\eta(t-t_0)}|\zeta_1(t_0) - \zeta_e(t_0)| \\ &+ k \int_{t_0}^t e^{-\eta(t-s)} [|B(s)||\dot{u}(s)| + |W_1(s)||\phi_1(s)|] ds \\ &+ kc \int_{t_0}^t e^{-\eta(t-s)}|\zeta_1(s) - \zeta_e(s)| ds. \end{aligned} \quad (6.41)$$

Using Bellman-Gronwall inequality [9, Ch.I,lemma I.6,consequence1] if a),b), and c) are satisfied we obtain, for all  $t \geq t_0$ ,

$$\begin{aligned} |\zeta_1(t) - \zeta_e(t)| &\leq ke^{(-\eta+kc)(t-t_0)}|\zeta_1(t_0) - \zeta_e(t_0)| \\ &+ k \int_{t_0}^t e^{(-\eta+kc)(t-s)} [|B(s)||\dot{u}(s)| + |W_1(s)||\phi_1(s)|] ds. \end{aligned} \quad (6.42)$$

Let  $d$  denote the distance between  $\overline{P}_{Q_U^1}$  and  $\partial Z_U$  (boundary of  $Z_U$ ). Since  $\overline{P}_{Q_U^1}$  is a proper subset of  $Z_U$ ,  $d > 0$ . Let  $b := \max_{Q_U^1} |B(\zeta_e, u)|$ , where  $B(.,.)$  is defined in (6.29). Since  $\overline{Q}_U^1$  is compact,  $B(.,.)$  is continuous ( $f_1 \in C^2$  and (6.33)- (6.34) hold),  $b < \infty$ . Choose  $c > 0$  such that  $-\eta + kc < 0$ . Choose  $\delta' := \delta'(c) > 0$  such that (6.40) is satisfied. Let  $\delta := \min \{\delta'(c), d\}$  and choose constants  $l, r, \gamma_u$ , and  $\gamma_\phi$  such that  $0 < l < 1$ ,  $0 \leq r \leq 1$ ,  $0 < \gamma_u < 1$ ,  $0 < \gamma_\phi < 1$ , and  $\gamma_u + \gamma_\phi \leq 1$ . Denote  $\delta_0^1 := \frac{l\delta r}{k}$ ,  $\delta_u^1 := \min \left\{ \delta'_u, -\gamma_u \frac{(-\eta+kc)(1-r)\delta}{kb} \right\}$ , and  $\delta_{\phi 1} := -\gamma_\phi \frac{(-\eta+kc)(1-r)\delta}{kb\omega_1}$ .

**Lemma 6.1** *If  $c, \delta, \delta_0^1, \delta_u^1$ , and  $\delta_{\phi 1}$  are chosen as above and if  $\zeta_1(t_0), u(.),$  and  $\phi_1(.)$  are such that  $|\zeta_1(t_0) - \zeta_e(t_0)| \leq \delta_0^1$ ,  $\max_{t \geq t_0} |\dot{u}(t)| \leq \delta_u^1$ , and  $\max_{t \geq t_0} |\phi_1(t)| \leq \delta_{\phi 1}$  then the hypotheses a),b), and c) required for (6.41) and (6.42) are satisfied.*

**Proof of Lemma 6.1:** Since  $\max_{t \geq t_0} |\dot{u}(t)| \leq \delta_u^1 \leq \delta'_u$ , a) is satisfied.

Next we show that c) is satisfied:

$$\text{for all } t \geq t_0, |\zeta_1(t) - \zeta_e(t)| \leq \delta'. \quad (6.43)$$

Suppose (6.43) is false. Then there exists a  $t_2 \in (t_0, \infty)$  such that

$$|\zeta_1(t) - \zeta_e(t)| < \delta' \text{ for all } t \in [t_0, t_2) \text{ and } |\zeta_1(t_2) - \zeta_e(t_2)| = \delta'. \quad (6.44)$$

**Claim:**

$$\text{for all } t \in [t_0, t_2], \zeta_1(t) \in Z_U. \quad (6.45)$$

Suppose (6.45) is false. Then there exists a  $t_3 \in (t_0, t_2)$  such that

$$\text{for all } t \in [t_0, t_3], \zeta_1(t) \in Z_U \text{ and } \zeta_1(t_3) \in \partial Z_U. \quad (6.46)$$

From (6.44) and (6.46) we note that for all  $t \in [t_0, t_3]$  the hypotheses of (6.42) are satisfied. Thus, from (6.42) we get, for all  $t \in [t_0, t_3]$ ,

$$\begin{aligned} |\zeta_1(t) - \zeta_e(t)| &< k\delta_0^1 + k[b\delta_u^1 + b_{w1}\delta_{\phi1}] \frac{1}{-(-\eta + kc)} \\ &\leq l\delta r + (\gamma_u + \gamma_\phi)(1 - r)l\delta \\ &\leq l\delta. \end{aligned} \quad (6.47)$$

By continuity of  $(\zeta_1(\cdot) - \zeta_e(\cdot))$  and (6.47) we get  $|\zeta_1(t_3) - \zeta_e(t_3)| \leq l\delta < \delta \leq d$  which is in contradiction to (6.46) in that  $\zeta_1(t_3) \in \partial Z_U$  but  $|\zeta_1(t_3) - \zeta_e(t_3)| < d$ . Hence, (6.45) is true and claim is proved. Thus, from (6.44) and (6.45) we note that for all  $t \in [t_0, t_2]$  the hypotheses of (6.42) are satisfied. Hence, from (6.42) we get, for all  $t \in [t_0, t_2]$ ,  $|\zeta_1(t) - \zeta_e(t)| \leq l\delta$ . In particular,  $|\zeta_1(t_2) - \zeta_e(t_2)| \leq l\delta < \delta \leq \delta'$  which contradicts (6.44). Hence, (6.43) is true and c) is satisfied.

Finally, to complete the proof of Lemma 6.1 we will show that:

$$\text{for all } t \geq t_0, \zeta_1(t) \in Z_U^0. \quad (6.48)$$

Suppose (6.48) is false. Then there exists a  $t_1 \in (t_0, \infty)$  such that

$$\text{for all } t \in [t_0, t_1], \zeta_1(t) \in Z_U^0 \text{ and } \zeta_1(t_1) \in \partial Z_U. \quad (6.49)$$

So from (6.43) and (6.49) we note that for all  $t \in [t_0, t_1)$  the hypotheses of (6.42) are satisfied. Thus, from (6.42) we get, for all  $t \in [t_0, t_1)$ ,  $|\zeta_1(t) - \zeta_e(t)| \leq l\delta$ . By continuity of  $(\zeta_1(\cdot) - \zeta_e(\cdot))$ , we obtain  $|\zeta_1(t_1) - \zeta_e(t_1)| \leq l\delta < \delta \leq d$  which contradicts (6.49) in that  $\zeta_1(t_1) \in \partial Z_U$ . Hence, (6.48) is true and b) is satisfied. This completes the proof of Lemma 6.1.

**Theorem 6.1 (part (i)):** Under the hypotheses of Lemma 6.1, (6.48) holds. Hence, Part (i) of Theorem 6.1 follows from (6.48).

**Theorem 6.1 (part (ii)):** Given  $\rho > 0$ , choose  $c > 0, \delta_0^1 > 0, \delta_u^1 \geq 0, \delta_{\phi 1} \geq 0$ , and  $0 < l < \min\{1, \frac{\rho}{\delta}\}$  so that hypotheses of Lemma 6.1 are satisfied. Then, using (6.42) we get, for all  $t \in [t_0, \infty)$ ,  $|\zeta_1(t) - \zeta_e(t)| \leq l\delta < \rho$ .

**Theorem 6.1 (part (iii)):** If  $\rho \leq \frac{\delta}{k}$  (let  $r = 1$  and  $0 < l < 1$ ), then  $\delta_0^1 = \frac{l\delta}{k} < \frac{\delta}{k}$ . Hence,  $|\zeta_1(t_0) - \zeta_e(t_0)| < \frac{\delta}{k}$ . Since  $r = 1, \delta_u^1 = \delta_{\phi 1} = 0$  and for all  $t \geq t_0, \dot{u}(t) = \phi_1(t) = 0$ . Hence, from (6.42) we get, for all  $t \geq t_0, |\zeta_1(t) - \zeta_e(t)| < \delta e^{(-\eta+kc)(t-t_0)}$  and  $|\zeta_1(t) - \zeta_e(t)| \leq \delta \leq d$ . (i.e., for all  $t \geq t_0, \zeta_1(t)$  belongs to the basin of attraction of the sink  $\zeta_e(t)$  with respect to  $u(t)$ ).  $\blacksquare$

**Proof of Theorem 6.2:** The proof is broken into several steps.

[Step 1- Preliminary Analysis]- Consider the  $k$ -th equation in (6.15) ( $k \geq 2$ ):

$$\dot{\zeta}_k = f(\zeta_k, \zeta_{k-1}, u) - W_k(\hat{\theta}_k)\phi_k \quad (6.50)$$

where we abuse notation and write  $W_k(\hat{\theta}_k)$  to denote  $W_k(\zeta_k, \zeta_{k-1}, \bar{u}_k(\zeta_k, \zeta_{k-1}, u, \hat{\theta}_k))$ .

Writing the Taylor expansion of  $f(\zeta_k, \zeta_{k-1}, u)$  about  $(\zeta_e, \zeta_e, u)$  and noting  $f(\zeta_e, \zeta_e, u) = 0$ , from (6.50), we obtain

$$\begin{aligned} \dot{\zeta}_k &= \int_0^1 D_1 f[\zeta_e + \lambda d_k, \zeta_e + \lambda d_{k-1}, u] d\lambda d_k \\ &+ \int_0^1 D_2 f[\zeta_e + \lambda d_k, \zeta_e + \lambda d_{k-1}, u] d\lambda d_{k-1} \\ &- W_k(\hat{\theta}_k)\phi_k. \end{aligned} \quad (6.51)$$

Subtracting  $\dot{\zeta}_e$  from both sides of (6.51) and noting  $d_k := \zeta_k - \zeta_e$ , we get

$$\begin{aligned} \dot{d}_k &= \int_0^1 D_1 f[\zeta_e + \lambda d_k, \zeta_e + \lambda d_{k-1}, u] d\lambda d_k \\ &+ \int_0^1 D_2 f[\zeta_e + \lambda d_k, \zeta_e + \lambda d_{k-1}, u] d\lambda d_{k-1} \\ &- W_k(\hat{\theta}_k)\phi_k - \dot{\zeta}_e. \end{aligned} \quad (6.52)$$

Adding and subtracting  $D_1 f(\zeta_e, \zeta_e, u) d_k$  to the right hand side of (6.52) we get

$$\dot{d}_k = \tilde{A}(t)d_k + \tilde{R}(t)d_k + \tilde{B}(t)d_{k-1} - W_k(t)\phi_k - \dot{\zeta}_e \quad (6.53)$$

where

$$\begin{aligned} \tilde{A}(t) &:= \tilde{A}(\zeta_e(t), \zeta_e(t), u(t)) \\ &:= D_1 f(\zeta_e(t), \zeta_e(t), u(t)), \end{aligned} \quad (6.54)$$

$$\begin{aligned}
\tilde{R}(t) &:= \tilde{R}(\zeta_e(t), \zeta_e(t), u(t), \zeta_k(t), \zeta_{k-1}(t)) \\
&:= \int_0^1 \{D_1 f[\zeta_e(t) + \lambda d_k(t), \zeta_e(t) + \lambda d_{k-1}(t), u(t)] - D_1 f(\zeta_e(t), \zeta_e(t), u(t))\} d\lambda,
\end{aligned} \tag{6.55}$$

$$\begin{aligned}
\tilde{B}(t) &:= \tilde{B}(\zeta_e(t), \zeta_e(t), u(t), \zeta_k(t), \zeta_{k-1}(t)) \\
&:= \int_0^1 D_2 f[\zeta_e(t) + \lambda d_k(t), \zeta_e(t) + \lambda d_{k-1}(t), u(t)] d\lambda,
\end{aligned} \tag{6.56}$$

$$W_k(t) := W_k(\hat{\theta}_k(t)). \tag{6.57}$$

From (6.53) we get

$$\begin{aligned}
d_k(t) &= \tilde{\Phi}(t, t_0) d_k(t_0) \\
&+ \int_{t_0}^t \tilde{\Phi}(t, s) \tilde{R}(s) d_k(s) ds \\
&+ \int_{t_0}^t \tilde{\Phi}(t, s) \tilde{B}(s) d_{k-1}(s) ds \\
&- \int_{t_0}^t \tilde{\Phi}(t, s) [W_k(s) \phi_k(s) + \dot{\zeta}_e(s)] ds
\end{aligned} \tag{6.58}$$

where  $\tilde{\Phi}(\cdot, \cdot)$  is the state transition matrix of  $\dot{z} = \tilde{A}(t)z$ .

Since for all  $t \geq t_0$ ,  $(\zeta_e(t), \zeta_e(t), u(t)) \in \overline{Q}_U$ ,  $\overline{Q}_U$  is compact,  $D_1 f(\cdot, \cdot, \cdot)$  is continuous ( $f \in C^2$ ),  $\sigma[\tilde{A}(\cdot, \cdot, \cdot)]$  is continuous, and by design  $\sigma[\tilde{A}(\cdot, \cdot, \cdot)] \subset \overset{\circ}{C}_-$ , we conclude that there exists a  $\tilde{\mu} < 0$  such that for all  $t \geq t_0$ ,  $\operatorname{Re}\sigma[\tilde{A}(t)] \leq \tilde{\mu} < 0$ . Thus, there exists an  $\tilde{\epsilon} := \tilde{\epsilon}(f, Q_U) > 0$  such that

$$\begin{aligned}
\text{if } |\tilde{A}(t)| \leq \tilde{\epsilon} \text{ then for some } \tilde{k} := \tilde{k}(f, Q_U) \geq 1 \text{ and some } \tilde{\eta} := \tilde{\eta}(f, Q_U) > 0 \\
\text{and for all } t \geq s \geq t_0, |\tilde{\Phi}(t, s)| \leq \tilde{k} e^{-\tilde{\eta}(t-s)}. \tag{6.59}
\end{aligned}$$

Differentiating the right hand side of (6.54) with respect to time and using chain rule we get

$$\begin{aligned}
\dot{\tilde{A}}(t) &= \{D_1^2 f(\zeta_e(t), \zeta_e(t), u(t)) + D_2 D_1 f(\zeta_e(t), \zeta_e(t), u(t))\} \dot{\zeta}_e(t) \\
&+ D_3 D_1 f(\zeta_e(t), \zeta_e(t), u(t)) \dot{u}(t).
\end{aligned} \tag{6.60}$$

Since for all  $t \geq t_0$ ,  $(\zeta_e(t), \zeta_e(t), u(t)) \in \overline{Q}_U$ ,  $\overline{Q}_U$  is compact,  $D_1^2 f(\cdot, \cdot, \cdot)$ ,  $D_2 D_1 f(\cdot, \cdot, \cdot)$ , and  $D_3 D_1 f(\cdot, \cdot, \cdot)$  are continuous ( $f \in C^2$ ), there exist constants  $a_1 \geq 0$  and  $a_2 \geq 0$  such that

$$a_1 := \max_{t \geq t_0} |D_1^2 f(\zeta_e(t), \zeta_e(t), u(t)) + D_2 D_1 f(\zeta_e(t), \zeta_e(t), u(t))|$$

and

$$a_2 := \max_{t \geq t_0} |D_3 D_1 f(\zeta_e(t), \zeta_e(t), u(t))|.$$

Hence, if  $\max_{t \geq t_0} |\dot{\zeta}_e(t)| \leq \tilde{\delta}'_\zeta := \tilde{\delta}'_\zeta(f, Q_U) := \frac{\tilde{\epsilon}}{2a_1}$  and  $\max_{t \geq t_0} |\dot{u}(t)| \leq \tilde{\delta}'_u := \tilde{\delta}'_u(f, Q_U) := \frac{\tilde{\epsilon}}{2a_2}$  then  $|\dot{A}(t)| \leq \tilde{\epsilon}$  and the conclusion of (6.59) is true. From (6.55)-(6.56) we note that when  $d_k(t) = d_{k-1}(t) = 0$  (i.e.,  $\zeta_k(t) = \zeta_{k-1}(t) = \zeta_e(t)$ ),  $\tilde{R}(t) = 0$  and  $\tilde{B}(t) = D_2 f(\zeta_e(t), \zeta_e(t), u(t))$ .

Let  $\tilde{W}_U := \overline{Q}_U \times Z_U \times Z_U$ . From (6.55)-(6.56) we note that since  $\tilde{R}(\cdot, \cdot, \cdot, \cdot, \cdot)$  and  $\tilde{B}(\cdot, \cdot, \cdot, \cdot, \cdot)$  are continuous ( $f \in C^2$ ) on  $\tilde{W}_U$  (a compact set),  $\tilde{R}(\cdot, \cdot, \cdot, \cdot, \cdot)$  and  $\tilde{B}(\cdot, \cdot, \cdot, \cdot, \cdot)$  are uniformly continuous on  $\tilde{W}_U$ . Thus, given  $\tilde{c} > 0$ , there exists a  $\tilde{\delta}' := \tilde{\delta}'(\tilde{c}, f, Q_U, Z_U) > 0$  such that for all  $t \geq t_0$ ,

$$\begin{aligned} &\text{if } (\zeta_k(t), \zeta_{k-1}(t)) \in Z_U \times Z_U \text{ and } |(d_k(t), d_{k-1}(t))| \leq \tilde{\delta}' \\ &\text{then } |\tilde{R}(t)| \leq \tilde{c} \text{ and } |\tilde{B}(t) - D_2 f(\zeta_e(t), \zeta_e(t), u(t))| \leq \tilde{c}. \end{aligned} \quad (6.61)$$

Since for all  $t \geq t_0$ ,  $(\zeta_e(t), \zeta_e(t), u(t)) \in \overline{Q}_U$  (a compact set) and  $D_2 f(\cdot, \cdot, \cdot)$  is continuous ( $f \in C^2$ ), there exists a constant  $\tilde{b} := \tilde{b}(f, Q_U)$  such that  $\tilde{b} := \max_{t \geq t_0} |D_2 f(\zeta_e(t), \zeta_e(t), u(t))|$ . Thus, from (6.61) we get for  $t \geq t_0$ ,

$$\begin{aligned} &\text{if } (\zeta_k(t), \zeta_{k-1}(t)) \in Z_U \times Z_U \text{ and } |(d_k(t), d_{k-1}(t))| \leq \tilde{\delta}' \text{ then } |\tilde{R}(t)| \leq \tilde{c} \text{ and } |\tilde{B}(t)| \leq \tilde{b} + \tilde{c}. \end{aligned} \quad (6.62)$$

Summarizing to this point, if 1)  $\max_{t \geq t_0} |\dot{u}(t)| \leq \tilde{\delta}'_u$ , 2)  $\max_{t \geq t_0} |\dot{\zeta}_e(t)| \leq \tilde{\delta}'_\zeta$ , 3) for all  $t \geq t_0$ ,  $(\zeta_k(t), \zeta_{k-1}(t)) \in Z_U \times Z_U$ , and 4) for all  $t \geq t_0$ ,  $|(d_k(t), d_{k-1}(t))| \leq \tilde{\delta}'$  then from (6.58), (6.59), and (6.62) we get: for all  $t \geq t_0$ ,

$$\begin{aligned} |d_k(t)| &\leq \tilde{k} e^{-\tilde{\eta}(t-t_0)} |d_k(t_0)| \\ &+ \tilde{k} \tilde{c} \int_{t_0}^t e^{-\tilde{\eta}(t-s)} |d_k(s)| ds \\ &+ \tilde{k} \int_{t_0}^t e^{-\tilde{\eta}(t-s)} [(\tilde{b} + \tilde{c}) |d_{k-1}(s)| + |W_k(s)| |\phi_k(s)| + |\dot{\zeta}_e(s)|] ds. \end{aligned} \quad (6.63)$$

Applying a form of Bellman-Gronwall inequality [9] to (6.63) we get

$$\begin{aligned} |d_k(t)| &\leq \tilde{k} e^{(-\tilde{\eta} + \tilde{k}\tilde{c})(t-t_0)} |d_k(t_0)| \\ &+ \tilde{k} \int_{t_0}^t e^{(-\tilde{\eta} + \tilde{k}\tilde{c})(t-s)} [(\tilde{b} + \tilde{c}) |d_{k-1}(s)| + |W_k(s)| |\phi_k(s)| + |\dot{\zeta}_e(s)|] ds. \end{aligned} \quad (6.64)$$

[Step 2- Topology]- Let  $\tilde{d} := \tilde{d}(f, Q_U, Z_U)$  denote the distance between  $\overline{P}_{Q_U}$  and  $\partial Z_U$ . Then  $\tilde{d} > 0$  because  $\overline{P}_{Q_U}$  is a proper subset of  $Z_U$ . Choose  $\tilde{c} := \tilde{c}(f, Q_U) > 0$

such that  $-\tilde{\eta} + \tilde{k}\tilde{c} < 0$ . Given this  $\tilde{c}$ , choose  $\tilde{\delta}' := \tilde{\delta}'(\tilde{c}, f, Q_U, Z_U) > 0$  such that (6.61) and (6.62) are true. Let  $\tilde{\delta} := \tilde{\delta}(\tilde{c}, f, Q_U, Z_U) := \min\left\{\frac{\tilde{\delta}'}{2}, \tilde{d}\right\} > 0$ . Choose constants  $\tilde{l}, \tilde{r}, \tilde{\gamma}_\zeta, \tilde{\gamma}_\phi$ , and  $\tilde{\gamma}_\rho$  such that  $0 < \tilde{l} < 1, 0 \leq \tilde{r} < 1, \tilde{\gamma}_\zeta > 0, \tilde{\gamma}_\phi > 0, \tilde{\gamma}_\rho > 0$ , and  $\tilde{\gamma}_\zeta + \tilde{\gamma}_\phi + \tilde{\gamma}_\rho \leq 1$ . Let  $\tilde{\delta}'_0 := \tilde{\delta}'_0(\tilde{c}, f, Q_U, Z_U) := \frac{\tilde{l}\tilde{r}}{\tilde{k}}, \tilde{\delta}''_\zeta := \tilde{\delta}''_\zeta(\tilde{c}, f, Q_U, Z_U) := \min\left\{\tilde{\delta}'_\zeta, -\tilde{\gamma}_\zeta \frac{(-\tilde{\eta} + \tilde{k}\tilde{c})(1 - \tilde{r})\tilde{l}\tilde{\delta}}{\tilde{k}}\right\}$ ,  $\tilde{\delta}'_\phi := \tilde{\delta}'_\phi(\tilde{c}, f, Q_U, Z_U) := -\tilde{\gamma}_\phi \frac{(-\tilde{\eta} + \tilde{k}\tilde{c})(1 - \tilde{r})\tilde{l}\tilde{\delta}}{\tilde{k}b_w}$ , and  $\rho_0 := \rho_0(f, Q_U, Z_U) := \min\left\{\frac{\tilde{\delta}'}{2}, -\tilde{\gamma}_\rho \frac{(-\tilde{\eta} + \tilde{k}\tilde{c})(1 - \tilde{r})\tilde{l}\tilde{\delta}}{\tilde{k}(b + \tilde{c})}\right\}$ .

**Lemma 6.2** *Let  $\tilde{c}, \tilde{\delta}'_0, \tilde{\delta}'_u, \tilde{\delta}''_\zeta, \tilde{\delta}'_\phi$ , and  $\rho_0$  be defined as above. Let  $\rho$  be any real number with  $0 < \rho < \rho_0$ . If  $\zeta_k(t_0), u(\cdot), \zeta_e(\cdot), \phi_k(\cdot)$ , and  $\zeta_{k-1}(\cdot)$  are such that  $|\zeta_k(t_0) - \zeta_e(t_0)| \leq \tilde{\delta}'_0$ ;  $\max_{t \geq t_0} |\dot{u}(t)| \leq \tilde{\delta}'_u$ ;  $\max_{t \geq t_0} |\dot{\zeta}_e(t)| \leq \tilde{\delta}''_\zeta$ ;  $\max_{t \geq t_0} |\phi_k(t)| \leq \tilde{\delta}'_\phi$ ; for all  $t \geq t_0$ ,  $\zeta_{k-1}(t) \in Z_U$  and  $|\zeta_{k-1}(t) - \zeta_e(t)| \leq \rho$  then the hypotheses 1)-4) required for (6.63) and (6.64) are satisfied.*

**Proof of Lemma 6.2:** Since  $\max_{t \geq t_0} |\dot{u}(t)| \leq \tilde{\delta}'_u$  and  $\max_{t \geq t_0} |\dot{\zeta}_e(t)| \leq \tilde{\delta}''_\zeta \leq \tilde{\delta}'_\zeta$ , hypotheses 1) and 2) required for (6.63) and (6.64) are satisfied.

Next we show that

$$\text{for all } t \geq t_0, |\zeta_k(t) - \zeta_e(t)| \leq \tilde{\delta}'. \quad (6.65)$$

Suppose (6.65) is false: Then there exists a  $t_2 \in (t_0, \infty)$  such that

$$\text{for all } t \in [t_0, t_2], |\zeta_k(t) - \zeta_e(t)| < \tilde{\delta}' \text{ and } |\zeta_k(t_2) - \zeta_e(t_2)| = \tilde{\delta}'. \quad (6.66)$$

**Claim:**

$$\text{for all } t \in [t_0, t_2], \zeta_k(t) \in Z_U. \quad (6.67)$$

Suppose (6.67) is false. Then there exists a  $t_3 \in (t_0, t_2)$  such that

$$\text{for all } t \in [t_0, t_3], \zeta_k(t) \in Z_U \text{ and } \zeta_k(t_3) \in \partial Z_U. \quad (6.68)$$

From (6.66) and (6.68) we note that for all  $t \in [t_0, t_3]$  the hypotheses of (6.63) and (6.64) are satisfied. Thus, from (6.64) we get, for all  $t \in [t_0, t_3]$ ,

$$\begin{aligned} |d_k(t)| &< \tilde{k}\tilde{\delta}'_0 + \tilde{k} \left[ (\tilde{b} + \tilde{c})\rho + b_w\tilde{\delta}'_\phi + \tilde{\delta}''_\zeta \right] \frac{1}{-(-\tilde{\eta} + \tilde{k}\tilde{c})} \\ &\leq \tilde{l}\tilde{\delta}\tilde{r} + (\tilde{\gamma}_\rho + \tilde{\gamma}_\phi + \tilde{\gamma}_\zeta)(1 - \tilde{r})\tilde{l}\tilde{\delta} \\ &\leq \tilde{l}\tilde{\delta}. \end{aligned} \quad (6.69)$$

By continuity of  $d_k(\cdot)$  and (6.69) we get  $|d_k(t_3)| \leq \tilde{l}\delta < \tilde{\delta} \leq \tilde{d}$  which is a contradiction to (6.68) in that  $\zeta_k(t_3) \in \partial Z_U$  but  $|\zeta_k(t_3) - \zeta_e(t_3)| < \tilde{d}$ . Hence, (6.67) is true and the claim is proved. Thus, from (6.66) and (6.67) we note that for all  $t \in [t_0, t_2]$  the hypotheses of (6.64) are satisfied. Thus, from (6.64) we get, for all  $t \in [t_0, t_2]$ ,  $|d_k(t)| \leq \tilde{l}\delta$ . In particular,  $|\zeta_k(t_2) - \zeta_e(t_2)| \leq \tilde{l}\delta < \tilde{\delta} \leq \frac{\tilde{\delta}'}{2}$  which contradicts (6.66). Hence, (6.65) is true and since for all  $t \geq t_0$ ,  $|d_{k-1}(t)| \leq \rho < \rho_0 \leq \frac{\tilde{\delta}'}{2}$ , hypothesis 4) required for (6.63) and (6.64) is satisfied. Finally, to complete the proof of Lemma 6.2, we will show that:

$$\text{for all } t \geq t_0, \zeta_k(t) \in Z_U^0. \quad (6.70)$$

Suppose (6.70) is false. Then, there exists a  $t_1 \in (t_0, \infty)$  such that

$$\text{for all } t \in [t_0, t_1], \zeta_k(t) \in Z_U^0 \text{ and } \zeta_k(t_1) \in \partial Z_U. \quad (6.71)$$

So from (6.71) we note that for all  $t \in [t_0, t_1]$  the hypotheses of (6.64) are satisfied. Thus, from (6.64) we get, for all  $t \in [t_0, t_1]$ ,  $|d_k(t)| \leq \tilde{l}\delta$ . By continuity of  $d_k(\cdot)$ , we obtain  $|d_k(t_1)| \leq \tilde{l}\delta < \tilde{\delta} \leq \tilde{d}$  which contradicts (6.71) in that  $\zeta_k(t_1) \in \partial Z_U$ . Hence, (6.70) is true and hypothesis 3) required for (6.63) and (6.64) is satisfied. This completes the proof of Lemma 6.2.

**[Step 3- Choosing Bounds]-** Let  $\tilde{\delta}'_0, \tilde{\delta}'_u, \tilde{\delta}''_\zeta, \tilde{\delta}'_\phi$ , and  $\rho_0$  be as defined before. For any  $0 < \rho < \rho_0$ , choose  $\delta_0^1 := \delta_0^1(\rho, f_1, Q_U^1) > 0$ ,  $\delta_u^1 := \delta_u^1(\rho, f_1, Q_U^1) > 0$ , and  $\delta_{\phi 1} := \delta_{\phi 1}(\rho, f_1, Q_U^1) > 0$  as in the statement of Theorem 6.1; choose  $\tilde{\delta}_0 := \tilde{\delta}_0(\rho, f, Q_U, Z_U) := \min \left\{ \rho, \frac{\rho}{-(\tilde{\eta} + \tilde{k}\tilde{c})}, \tilde{\delta}'_0 \right\}$ ,  $\tilde{\delta}_u := \tilde{\delta}_u(\rho, f_1, f, Q_U^1, Q_U) := \min \left\{ \delta_u^1, \tilde{\delta}'_u \right\}$ ,  $\tilde{\delta}_\zeta := \tilde{\delta}_\zeta(\rho, f, Q_U, Z_U) := \min \left\{ \rho, \tilde{\delta}''_\zeta \right\}$ , and  $\tilde{\delta}_\phi := \tilde{\delta}_\phi(\rho, f_1, f, Q_U^1, Q_U, Z_U) := \min \left\{ \rho, \delta_{\phi 1}, \tilde{\delta}'_\phi \right\}$ .

**[Step 4- Theorem 6.2, part (i)]-** We use induction to prove part (i).

**Initial Case  $k = 1$ :** Since  $|\zeta_1(t_0) - \zeta_e(t_0)| \leq \delta_0^1$ ,  $\max_{t \geq t_0} |\dot{u}(t)| \leq \tilde{\delta}_u \leq \delta_u^1$ , and  $\max_{t \geq t_0} |\phi_1(t)| \leq \tilde{\delta}_\phi \leq \delta_{\phi 1}$ , by Theorem 6.1, we have for all  $t \geq t_0$ ,  $\zeta_1(t) \in Z_U$ , and  $|\zeta_1(t) - \zeta_e(t)| < \rho$ .

**Induction Step:** Assume that for all  $i = 1, 2, \dots, k$ , for all  $t \geq t_0$ ,  $\zeta_i(t) \in Z_U$ , and  $|\zeta_i(t) - \zeta_e(t)| < \rho$ . We will show that for all  $t \geq t_0$ ,  $\zeta_{k+1}(t) \in Z_U$ , and  $|\zeta_{k+1}(t) - \zeta_e(t)| < \rho$ . Since  $|\zeta_{k+1}(t_0) - \zeta_e(t_0)| \leq \tilde{\delta}_0 \leq \tilde{\delta}'_0$ ;  $\max_{t \geq t_0} |\dot{u}(t)| \leq \tilde{\delta}_u \leq \tilde{\delta}'_u$ ;  $\max_{t \geq t_0} |\dot{\zeta}_e(t)| \leq \tilde{\delta}_\zeta \leq \tilde{\delta}''_\zeta$ ;  $\max_{t \geq t_0} |\phi_{k+1}(t)| \leq \tilde{\delta}_\phi \leq \tilde{\delta}'_\phi$ ; for all  $t \geq t_0$ ,  $\zeta_k(t) \in Z_U$  and  $|\zeta_k(t) - \zeta_e(t)| < \rho$ , by Lemma 6.2, we have for  $t \geq t_0$ ,  $\zeta_{k+1}(t) \in Z_U$  and applying the inequality (6.64) to  $d_{k+1}(\cdot)$  we get

$$|d_{k+1}(t)| < \tilde{k}\tilde{\delta}_0 + \tilde{k}[(\tilde{b} + \tilde{c})\rho + b_w\tilde{\delta}_\phi + \tilde{\delta}_\zeta] \frac{1}{-(\tilde{\eta} + \tilde{k}\tilde{c})}$$

$$\begin{aligned}
&\leq \frac{\tilde{k}\rho + \tilde{k}(\tilde{b} + \tilde{c})\rho + \tilde{k}b_w\rho + \tilde{k}\rho}{-(-\tilde{\eta} + \tilde{k}\tilde{c})} \\
&= \left[ \frac{\tilde{k}(2 + \tilde{b} + \tilde{c} + b_w)}{-(-\tilde{\eta} + \tilde{k}\tilde{c})} \right] \rho. \tag{6.72}
\end{aligned}$$

By design of the control laws, we can increase  $\tilde{\eta}$  so that  $\tilde{\eta}$  is sufficiently larger than  $\tilde{b}$  and  $\tilde{k}$  and  $\frac{\tilde{k}(2 + \tilde{b} + \tilde{c} + b_w)}{-(-\tilde{\eta} + \tilde{k}\tilde{c})} < 1$ . Hence, from (6.72) with this choice of  $\tilde{\eta}$  we get  $|d_{k+1}(t)| < \rho$  and part (i) of Theorem 6.2 is proved.

[Step 5- Theorem 6.2, part (ii)]- From the proof of the initial case  $k = 1$  in part (i) of Theorem 6.2, we note that  $\max_{t \geq t_0} |\zeta_1(t) - \zeta_e(t)| := \max_{t \geq t_0} |d_1(t)| < \rho$ . Thus, part (ii) of Theorem 6.2 is proved.

[Step 6- Theorem 6.2, part (iii)]- Similar to the argument of the induction step in part (i) of Theorem 6.2, for  $k \geq 2$ , Lemma 6.2 holds. Hence, applying the inequality (6.64) to  $d_{k+1}(\cdot)$  assuming that  $d_{k+1}(t_0) = 0$ , we get, for  $t \geq t_0$ ,

$$|d_{k+1}(t)| \leq \frac{\tilde{k}(\tilde{b} + \tilde{c})}{-(-\tilde{\eta} + \tilde{k}\tilde{c})} \|d_k(\cdot)\|_\infty + \frac{\tilde{k}b_w}{-(-\tilde{\eta} + \tilde{k}\tilde{c})} \|\phi_k(\cdot)\|_\infty + \frac{\tilde{k}}{-(-\tilde{\eta} + \tilde{k}\tilde{c})} \|\dot{\zeta}_e(\cdot)\|_\infty. \tag{6.73}$$

Denoting  $\alpha := \alpha(f, Q_U) := \frac{\tilde{k}(\tilde{b} + \tilde{c})}{-(-\tilde{\eta} + \tilde{k}\tilde{c})}$ ,  $\beta_\phi := \beta_\phi(f, Q_U) := \frac{\tilde{k}b_w}{-(-\tilde{\eta} + \tilde{k}\tilde{c})}$ , and  $\beta_\zeta := \beta_\zeta(f, Q_U) := \frac{\tilde{k}}{-(-\tilde{\eta} + \tilde{k}\tilde{c})}$ , from (6.73) we get

$$\|d_{k+1}(\cdot)\|_\infty \leq \alpha \|d_k(\cdot)\|_\infty + \beta_\phi \|\phi_k(\cdot)\|_\infty + \beta_\zeta \|\dot{\zeta}_e(\cdot)\|_\infty. \tag{6.74}$$

By suitable design of the control laws we can increase  $\tilde{\eta}$  so that  $\alpha < 1$ . This completes the proof of Theorem 6.2. ■

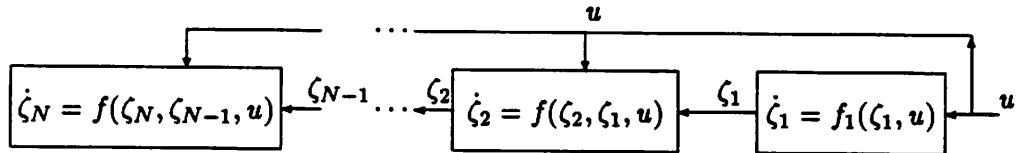


Figure 6.1: The interconnection of nonlinear dynamical systems with no parameter uncertainties

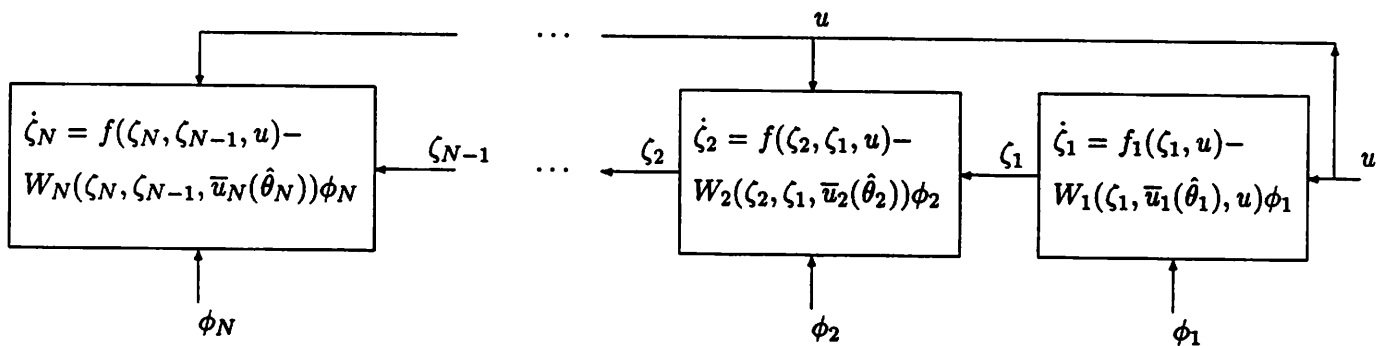


Figure 6.2: The interconnection of nonlinear dynamical systems with parameter uncertainties; each dynamical system is *locally* controlled by an indirect adaptive controller. For brevity, we have used  $\bar{u}_1(\hat{\theta}_1) := \bar{u}_1(\zeta_1, u, \hat{\theta}_1)$  and for  $k = 2, 3, \dots, N$ ,  $\bar{u}_k(\hat{\theta}_k) := \bar{u}_k(\zeta_k, \zeta_{k-1}, u, \hat{\theta}_k)$ .

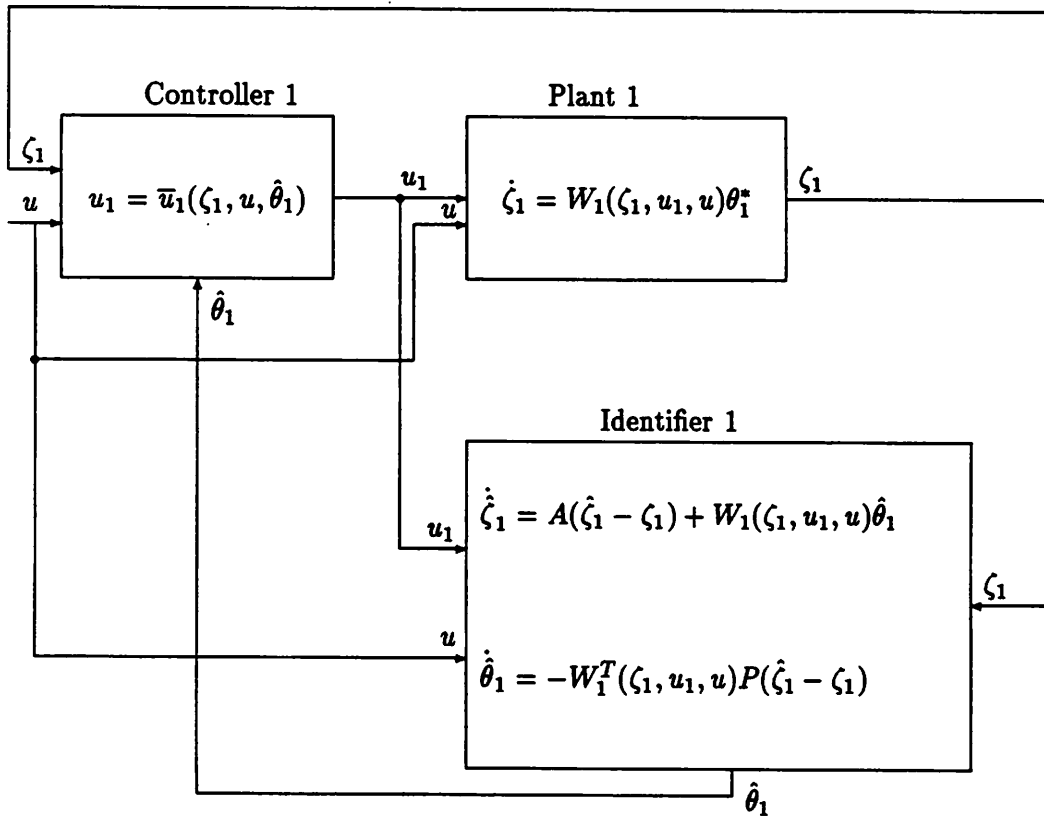


Figure 6.3: Indirect adaptive control of the first dynamical system

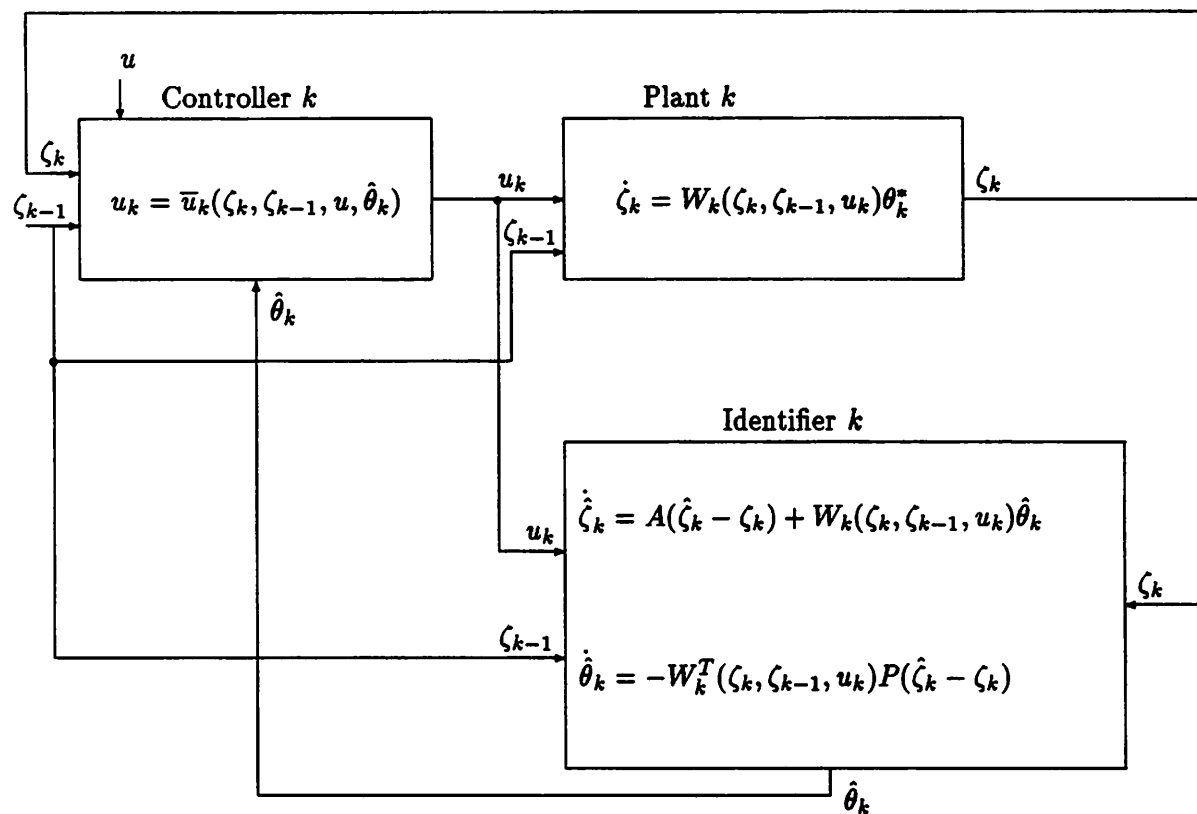


Figure 6.4: Indirect adaptive control of the  $k$ -th dynamical system ( $k = 2, 3, \dots, N$ )

## Chapter 7

### Conclusion

In this dissertation we have studied the problem of controlling a platoon of closely-spaced *non-identical* vehicles traveling at high speeds on automated highways. We have proposed *decentralized nonlinear* control laws, for each vehicle in the platoon, which maintain close spacing between successive vehicles and keep all the vehicles in the platoon close to the lane center. The longitudinal control laws take advantage of communication possibilities not available in the recent past.

Motivated by this platoon control problem, we carried out a feasibility study for designing *local* controllers for a class of interconnected nonlinear dynamical systems. We have given precise conditions on inputs to the dynamical subsystems and the dynamical behavior of the subsystems in the interconnection which allow such *local* controller design. Furthermore, we have proposed a *local, nonlinear, adaptive* control scheme for this class of interconnected nonlinear dynamical systems.

These studies make both practical and theoretical contributions to the design of control laws for interconnected nonlinear dynamical systems. From a control designer's view point, the *local* nature of the proposed control laws reduces the computational costs while increasing the reliability and the flexibility of the control system as a whole. From a theoretical point, these studies show that, for a class of interconnected nonlinear dynamical systems, it is possible to attain the design objectives by using *local, nonlinear, adaptive* control laws; furthermore, the *adaptive* nature of these control laws increases the *robustness* of the control system with respect to uncertain parameters.

Much work remains to implement longitudinal and lateral control laws for a platoon of vehicles. In addition to work on sensors (accelerometers, velocity sensors, etc...),

actuators, communication system, road tests, safety considerations, and socio-economic studies, a number of systems engineering concepts have to be addressed: studies are needed for analyzing and controlling platoons of vehicles on a *network* of highways. The control system hierarchy from the regulation level of controlling one platoon on one lane to the network level of controlling the flow of traffic on several highways has to be studied. At this time, a major obstacle for higher level control of platoons is the lack of good models for describing the flow of traffic.

At the regulation level, we have initiated a system-level study for controlling a platoon of vehicles traveling on a lane of highway. For the proposed combined longitudinal and lateral control laws, we have an additional problem that needs to be addressed: investigate the use of adaptive control methods to improve the robustness of these control laws to unknown parameters; in addition, we need to check the robustness of these control laws to measurement noise and communication delays. Furthermore, we need to incorporate more realistic engine models, tire dynamics, wind gusts, road irregularities, etc...

From the theoretical stand point, we have originated methods for analysis and design of decentralized adaptive controllers for a class of interconnected nonlinear dynamical systems. Future research can improve on these methods and apply them to other classes of interconnected nonlinear systems. Furthermore, theoretical research is needed to design fault-tolerant controllers which can reconfigure themselves in case of failures. Investigating the possibility of using decentralized controls for improved fault-tolerance will yield benefit in a number of applications where safety and reliability are major cost factors.

# References

- [1] J. Ackermann and W. Sienel. Robust Control for Automatic Steering. In *Proceedings of the American Control Conference*, volume 1, pages 795–800, May 1990.
- [2] L. Armijo. Minimization of functions having Lipschitz continuous first partial derivatives. *Pacific Journal of Mathematics*, 16:1–3, 1966.
- [3] R.W. Brockett. *Finite Dimensional Linear Systems*. Wiley, New York, 1970.
- [4] G. Campion and G. Bastin. Indirect Adaptive State Feedback Control of Linearly Parameterized Nonlinear Systems. Technical Report AP 89.09, Laboratoire D'Automatique, Dynamique et Analyse des Systèmes, Université Catholique de Louvain, 1989.
- [5] R.J. Caudill and W.L. Garrard. Vehicle-Follower Longitudinal Control for Automated Transit Vehicles. *Journal of Dynamic Systems, Measurement and Control*, 99(4):241–248, December 1977.
- [6] H.Y. Chiu, G.B. Stupp, Jr., and S.J. Brown, Jr. Vehicle-Follower Control with Variable-Gains for Short Headway Automated Guideway Transit Systems. *Journal of Dynamic Systems, Measurement and Control*, 99(3):183–189, September 1977.
- [7] W.H. Cormier and R.E. Fenton. On the Steering of Automated Vehicles- A Velocity-Adaptive Controller. *IEEE Transactions on Vehicular Technology*, VT-29:375–385, 1980.
- [8] R.E. Fenton and R.J. Mayhan. Automated Highway Studies at the Ohio State University- An Overview. *IEEE Transactions on Vehicular Technology*, VT-40(1):100–113, February 1991.

- [9] A. Halanay. *Differential Equations: Stability, Oscillations, Time Lags*. Academic, New York, 1974.
- [10] J.K. Hale. *Ordinary Differential Equations*. Wiley-Interscience, New York, 1969.
- [11] A.S. Hauksdottir and R.E. Fenton. On the Design of a Vehicle Longitudinal Controller. *IEEE Transactions on Vehicular Technology*, VT-34(4):182–187, November 1985.
- [12] A.S. Hauksdottir and R.E. Fenton. On Vehicle Longitudinal Controller Design. In *1988 IEEE Workshop on Automotive Applications of Electronics*, pages 77–83, 1988.
- [13] J.K. Hedrick, D. McMahon, V. Narendran, and D. Swaroop. Longitudinal Vehicle Controller Design for IVHS System. In *Proceedings of the American Control Conference*, volume 3, pages 3107–3112, June 1991.
- [14] A. Hitchcock, 1990. Private Communication at UC Berkeley.
- [15] L.L. Hoberock. A Survey of Longitudinal Acceleration Comfort Studies in Ground Transportation Vehicles. *Journal of Dynamic Systems, Measurement and Control*, 99:76–84, June 1977.
- [16] L.L. Hoberock and R.J. Rouse, Jr. Emergency Control of Vehicle Platoons: System Operation and Platoon Leader Control. *Journal of Dynamic Systems, Measurement and Control*, 98(3):245–251, September 1976.
- [17] F.C. Hoppensteadt. Singular perturbations on the infinite interval. *Transactions of the American Mathematical Society*, 123:521–535, 1966.
- [18] A. Isidori. *Nonlinear Control Systems*. Springer-Verlag, 2nd. edition, 1989.
- [19] M. Kelemen. A Stability Property. *IEEE Transactions on Automatic Control*, AC-31(8):766–768, August 1986.
- [20] H.K. Khalil and P.V. Kokotovic. On Stability Properties of Nonlinear Systems with Slowly-Varying inputs. *IEEE Transactions on Automatic Control*, AC-36:229, 1991.
- [21] P. Kokotovic, H.K. Khalil, and J. O'Reilly. *Singular Perturbation Methods in Control: Analysis and design*. Academic Press, 1986.

- [22] G. Kreisselmeier. Adaptive Observers with Exponential Rate of Convergence. *IEEE Transactions on Automatic Control*, AC-22:2-8, 1977.
- [23] V. Lakshmikantham and S. Leela. *Differential and Integral Inequalities*, volume 1. Academic Press, New York, 1969.
- [24] P. Luger. Horizontal Motion of Automobiles: Theoretical and Practical Investigations. In *Dynamics of High Speed Vehicles*, pages 83–146. Springer-Verlag, Wien-New York, 1982.
- [25] D.H. McMahon and J.K. Hedrick. Vehicle Modelling and Control for Automated Highway Systems. In *Proceedings of the American Control Conference*, pages 297–303, May 1990.
- [26] A.N. Michel and R.K. Miller. *Qualitative Analysis of Large Scale Dynamical Systems*. Academic Press, 1977.
- [27] A.P. Morgan and K.S. Narendra. On the Stability of Nonautonomous Differential Equations  $\dot{x} = [A(t) + B(t)]x$ , with Skew Symmetric matrix  $B(t)$ . *SIAM Journal of Control and Optimization*, 15:163–176, 1977.
- [28] H. Nijmeijer and A. Van der Schaft. *Nonlinear Dynamical Control Systems*. Springer-Verlag, New York, 1990.
- [29] Program on Advanced Technology for the Highways. Proceedings of Test-Vehicle Definition Workshop. Workshop report, University of California, Berkeley, November 1990.
- [30] H. Peng and M. Tomizuka. Vehicle Lateral Control for Highway Automation. In *Proceedings of the American Control Conference*, volume 1, pages 788–794, May 1990.
- [31] E. Polak. On the mathematical foundations of nondifferentiable optimization in engineering design. *SIAM Review*, 29(1):21–90, March 1987.
- [32] J. Pomet and L. Praly. Indirect Adaptive Nonlinear Control. In *Proceedings of the Conference on Decision and Control*, pages 2414–2415, 1988.
- [33] R.J. Rouse, Jr. and L.L. Hoberock. Emergency Control of Vehicle Platoons:Control of Following-Law Vehicles. *Journal of Dynamic Systems, Measurement and Control*, 98(3):239–244, September 1976.

- [34] H. Sakai. Theoretical and experimental studies on the dynamic properties of tyres Part 1: Review of theories of rubber friction. *International Journal of Vehicle Design*, 2(1):78–110, 1981.
- [35] S.S. Sastry and M. Bodson. *Adaptive Control: Stability, Convergence, and Robustness*. Prentice Hall, 1st. edition, 1989.
- [36] S.S. Sastry and A. Isidori. Adaptive Control of Linearizable Systems. *IEEE Transactions on Automatic Control*, 34(11):1123–1131, November 1989.
- [37] S. Sheikholeslam. Reduced Order Observer Based Identifier for Identifying the Mass of a Vehicle. term paper, December 1990.
- [38] S. Sheikholeslam and C.A. Desoer. Longitudinal Control of a Platoon of Vehicles I:Linear Model. PATH Research Report UCB-ITS-PRR-89-3 and UCB/ERL Memorandum M89/106, University of California, Berkeley, August 1989.
- [39] S. Sheikholeslam and C.A. Desoer. A Stability Result. Technical Memorandum UCB/ERL memo M89/124, University of California, Berkeley, November 1989.
- [40] S. Sheikholeslam and C.A. Desoer. Control of an Interconnection of Nonlinear Dynamical Systems. In *Proceedings of the Conference on Decision and Control*, volume 6, pages 3615–3616, 1990.
- [41] S. Sheikholeslam and C.A. Desoer. Longitudinal Control of a Platoon of Vehicles. In *Proceedings of the American Control Conference*, volume 1, pages 291–297, May 1990.
- [42] S. Sheikholeslam and C.A. Desoer. Longitudinal Control of a Platoon of Vehicles III:Nonlinear Model. PATH Research Report UCB-ITS-PRR-89-6, University of California, Berkeley, April 1990.
- [43] S. Sheikholeslam and C.A. Desoer. Combined Longitudinal and Lateral Control of a Platoon of Vehicles: A system-level study. Path technical memorandum 91-3, University of California, Berkeley, September 1991.
- [44] S. Sheikholeslam and C.A. Desoer. Control of a String of Nonlinear Systems. to appear in Proceedings of the Symposium on Mathematical Theory of Networks and Systems, 1991.

- [45] S. Sheikholeslam and C.A. Desoer. Control of Interconnected Nonlinear Dynamical Systems: The Platoon Problem. to appear in *IEEE Transactions on Automatic Control*, 1991.
- [46] S. Sheikholeslam and C.A. Desoer. Longitudinal Control of a Platoon of Vehicles with no Communication of Lead Vehicle Information. In *Proceedings of the American Control Conference*, volume 3, pages 3102–3107, June 1991.
- [47] S. Sheikholeslam and C.A. Desoer. A System-Level Study of the Longitudinal Control of a Platoon of Vehicles. to appear in ASME Journal on Dynamic Systems, Measurement and Control, June 1992.
- [48] S. Shladover, C.A. Desoer, J.K. Hedrick, M. Tomizuka, J. Walrand, W.B. Zhang, D. McMahon, H. Peng, S. Sheikholeslam, and N. McKeown. Automatic Vehicle Control Developments in the PATH Program. *IEEE Transactions on Vehicular Technology*, VT-40(1):114–130, February 1991.
- [49] S.E. Shladover. Operation of automated guideway transit vehicles in dynamically reconfigured trains and platoons. Technical Report UMTA-MA-06-00855-79-1, Automated Guideway Transit Technology Program, April 1979.
- [50] S.E. Shladover. Longitudinal Control of Automotive Vehicles in Close-Formation Platoons, December 1989. 1989 ASME Winter Annual Meeting.
- [51] S.E. Shladover. Longitudinal Control of Automotive Vehicles in Close-Formation Platoons. *ASME Journal on Dynamic Systems, Measurement and Control*, 113(2):231–241, June 1991.
- [52] S.E. Shladover, D.N. Wormley, H.H. Richardson, and R. Fish. Steering Controller Design for Automated Guideway Transit Vehicles. *ASME Journal on Dynamic Systems, Measurement, and Control*, 100:1–8, 1978.
- [53] G.M. Takasaki and R.E. Fenton. On the Identification of Vehicle Longitudinal Dynamics. *IEEE Transactions on Automatic Control*, 22(4):610–615, August 1977.
- [54] A. Teel, R. Kadiyala, P. Kokotovic, and S.S. Sastry. Indirect Techniques for Adaptive Input Output Linearization of Nonlinear Systems. Technical Memorandum(revised) UCB/ERL memo M89/93, University of California, Berkeley, March 1990.

- [55] A. Teel, R. Kadiyala, P. Kokotovic, and S.S. Sastry. Indirect Techniques for Adaptive Input-Output Linearization of Nonlinear Systems. *International Journal of Control*, 53:193–222, 1991.
- [56] J.D. Trom, M.J. Vanderploeg, and J.E. Bernard. Application of Inverse Models to Vehicle Optimization Problems. *Vehicle System Dynamics*, pages 97–110, 1990.
- [57] M. Vidyasagar. *Nonlinear Systems Analysis*. Prentice-Hall, Englewood Cliffs, New Jersey, 1978.
- [58] M. Vidyasagar. *Input-Output Analysis of Large Scale Interconnected Systems*, volume 29 of *Lecture Notes in Control and Information Sciences*. Springer-Verlag, 1981.
- [59] J.C. Walrand, March-August 1989. Private Communication at UC Berkeley.